Univerzita Karlova v Praha
3. lékařská fakulta
Ústav anatomie

Studijní program: Neurovědy

Volumetrie a lateralita struktur CNS v experimentu na zvířeti a u člověka (ve zdraví a nemoci)

Volumetry and laterality of CNS structures in animal experiments and in human (in health and disease)

Dizertační práce
Komentovaný soubor vlastních původních prací

Bc. MUDr. Jana Mrzílková

Školitel: doc. MUDr. Petr Zach, CSc.

Praha, 2015

Prohlášení:

Prohlašuji, že jsem závěrečnou práci zpracovala samostatně a že jsem řádně uvedla a citovala všechny použité prameny a literaturu. Současně prohlašuji, že práce nebyla využita k získání jiného nebo stejného titulu

Souhlasím s trvalým uložením elektronické verze mé práce v databázi systému meziuniverzitního projektu Theses.cz za účelem soustavné kontroly podobnosti kvalifikačních prací.

V Praze dne 15. 6. 2015 Bc. MUDr. Jana Mrzílková

Identifikační záznam:

MRZÍLKOVÁ, Jana. *Volumetrie a lateralita struktur CNS v experimentu na zvířeti a u člověka (ve zdraví a nemoci). [Volumetry and laterality of CNS structures in animal experiments and in human (in health and disease]*. Praha, 2015. 138 s. Dizertační práce. Univerzita Karlova v Praze, 3. lékařská fakulta, Ústav anatomie 3. LF UK 2015. Školitel doc. MUDr. Petr Zach, CSc.

Klíčová slova:

lateralita; volumetrie; Alzheimerova nemoc; stres; hipokampus; traktografie

Keywords:

laterality; volumetry; Alzheimer's disease; stress; hippocampus; tractography

OBSAH

1 ÚVOD DO PROBLÉMU 5

2 SEZNAM POUŽITÝCH ZKRATEK 6

3 VĚDECKÁ OTÁZKA A CÍLE PRÁCE 7

4 HYPOTÉZA 9

5 PŘEHLED POUŽITÝCH METODIK 10

5.1 Metodiky používané při práci s mozkem laboratorního potkana 10

5.1.2 Volumetrie CNS u potkana 10

5.2 Metodiky používané při práci s mozkem člověka 10

5.2.1 Magnetická rezonance 11

5.2.2 Autopsie mozkové tkáně 12

5.2.3 Volumetrie CNS 12

5.2.4 Použití polysiloxanové pryskyřice pro měření plochy planum temporale 12

5.2.5 FreeSurfer (FS) analýza 13

5.2.6 Traktografie bílé hmoty (MedINRIA, SPM8) 13

5.3 Statistická analýza 14

6 ZPŮSOB ORGANIZACE SBĚRU A ZÍSKÁVÁNÍ EXPERIMENTÁLNÍCH DAT 15

6.1 Spolupráce s Poradnou pro poruchy paměti - AD centrem a přístup do databáze snímků MR pacientů s AD a kontrol 15

6.2 Laboratorní potkani pro volumetrické studie 15

6.4 Autoptický materiál pro morfologii planum temporale 16

7 VYUŽITÍ A PŘÍNOS VÝSLEDKŮ 17

7.1 Shrnutí využití a výsledků u člověka 17

7.1.2 Kvantifikace volumetrických změn hipokampu bez reorientace MR snímků . 17

7.1.3 Planum temporale a jeho asymetrie 17

7.1.4 Změny ve velikosti pyramidových neuronů ze třetí vrstvy PT 18

7.1.5 Rekonstrukce struktur CNS pomocí FS u podkorových a korových struktur . 18

7.1.6 Traktografie bílé hmoty 19

7.2 Shrnutí využití a výsledků u laboratorního potkana 20

7.2.1 Volumetrie hipokampu u laboratorního potkana ve stresu. *20*
7.2.2 Podávání kortikoidů a CTA *20*
7.2.3 Využití neuroprotektiva při vaskulárních změnách v CNS *21*
8 ČASOVÝ HARMONOGRAM POSTUPU EXPERIMENTÁLNÍ PRÁCE **22**
9 DISKUZE **23**
9.1 Planum temporale a změny jeho velikosti u AD *23*
9.2 Planum temporale jako marker stranovosti u mozkové tkáně post mortem *24*
9.3 Změny ve velikosti neuronů ve III. korové vrstvě PT u AD a kontrol *24*
9.4 Volumetrická analýza hipokampu, pontu a mozečku u AD a kontrol na MR *25*
9.5 Evaluace pozice hipokampu na MRI pro kliniku a experiment *27*
9.6 Vliv chronického stresu na hipokampus u laboratorního potkana *28*
9.7 Vliv chronického podávání kortikoidů na CTA *31*
9.8 Automatická analýza objemu struktur CNS na FS *32*
9.9 Traktografie komisurálních vláken u AD pacientů *34*
10 ZÁVĚR **36**
11 OBRAZOVÁ DOKUMENTACE **39**
12 POUŽITÁ LITERATURA **45**
13 PŘEHLED PUBLIKACÍ AUTORA **52**
13.1 Publikace autora, vztahující se k tématu *52*
13.2 Ostatní publikace autora *54*
14 PLNÉ ZNĚNÍ VÝZNAMNĚJŠÍCH PRACÍ AUTORA, VZTAHUJÍCÍCH SE K TÉMATU **55**

Poděkování

Ráda bych na tomto místě poděkovala svému školiteli doc. MUDr. Petru Zachovi, CSc., za trpělivost a kreativitu při vedení mého studia a možnost spolupráce na výzkumu. Svému klinickému školiteli doc. MUDr. Aleši Bartošovi, Ph.D., děkuji za podnětnou klinickou spolupráci a jeho nadšení pro vědu. Také bych ráda velmi poděkovala svému velkému učiteli a anatomickému a lidskému vzoru prof. MUDr. Josefu Stinglovi, CSc., za umožnění mého doktorského studia v oboru Neurověd.

V neposlední řadě děkuji všem spoluautorům našich společných prací, zvláště pak jmenovitě RNDr. Karlu Valešovi, Ph.D., Mgr. Ibrahimu Ibrahimovi, Ph.D., RNDr. Aleši Stuchlíkovi, Ph.D., Ing. Zdeně Krištofikové, Ph.D., a ing. Jaroslavu Tintěrovi, Ph.D.

Také děkuji všem svým spolupracovníkům, zvláště pak PhDr. Vladimíru Musilovi, Ivance Žížalové, MUC. Matějovi Patzeltovi, RNDr. Jitce Riedlové a Zdeňku Wurstovi.

Velký dík také patří Ondřejovi, Anežce a Jeníkovi a celé rodině i všem přátelům za podporu, pomoc a trpělivost, kterou mi nezištně po celou dobu studia poskytovali.

1 Úvod do problému

Úbytek šedé či bílé hmoty CNS je předmětem zájmu i multidisciplinárního výzkumu biologických, lékařských a technicky zaměřených oborů, zejména v souvislosti s psychiatrickými onemocněními, jako je např. skupina demencí. Málo pozornosti je však věnováno stranovosti těchto úbytků hmoty, neboli asymetrii, nebo také lateralitě. Přitom lateralita hemisfér, jader a bílé hmoty mozku je přítomna nejenom u člověka a vyšších savců, ale také u obojživelníků, plazů, ptáků a bezobratlých živočichů. Termíny asymetrie, lateralita nebo lateralizace jsou v literatuře používány jako synonyma, ačkoliv asymetrie je většinou používána pro morfologický popis, zatímco lateralita nebo lateralizace více pro funkci.

V naší práci jsme studovali objemové změny a asymetrii zejména hipokampu jak u laboratorního potkana, tak u člověka, se zaměřením na nalezení rozdílu mezi pravou a levou stranou volumetricky. U laboratorního potkana jsme asymetrii studovali jak u kontrol, tak u farmakologického modelu chronického stresu, u kterého je řadu let známo zmenšení objemu hipokampu. U dospělého člověka jsme in vivo sledovali změny ve velikosti hipokampu, pontu a mozečku u kontrol a u pacientů s klinicky diagnostikovanou Alzheimerovou demencí, u které je v literatuře také popisováno zmenšení objemu hipokampu. Na autoptické tkáni jsme pak sledovali u zemřelých pacientů s klinicky i post mortem ověřenou diagnózou Alzheimerovy nemoci asymetrii planum temporale, struktury CNS s výraznou pravo-levou asymetrií, které se využívá k nepřímému určování levorukosti nebo pravorukosti. Ze snímků z magnetické rezonance jsme pak prováděli virtuální rekonstrukce CNS pomocí software FreeSurfer s cílem zmapování úbytku šedé i bílé hmoty na dalších strukturách CNS (korové oblasti, podkorové oblasti, bílá hmota hemisfér a mozečku apod.) a jejich případnou asymetrii. Nakonec jsme prováděli programem MedINRIA traktografie bílé hmoty s cílem zjištění úbytku v pravé či levé hemisféře v návaznosti na Alzheimerovu nemoc. Na získání vzorků mozkové tkáně se podílely tyto instituce: vzorky tkáně mozku člověka z Ústavu patologie v Psychiatrickém centru Praha a z Patologického oddělení Nemocnice na Bulovce, magnetické rezonance mozku z IKEM Praha a Neurologické kliniky 3. LF UK a FNKV a vzorky mozkové tkáně laboratorních potkanů z Fyziologického ústavu AV ČR v Krči.

Plné znění původních studií je uvedeno na konci práce, počínaje kapitolou 14.

2 Seznam použitých zkratek

AD - Alzheimerova nemoc

ACTH - adrenokortikotropní hormon

AX – axiální koeficient

CA1, CA2, CA3 – podoblasti hipokampu, corna ammonis

CA-CP osa - osa procházející předozadně přes commissura anterior - commissura posterior

CC – corpus callosum

CNS – centrální nervový systém

CTA – conditioned taste aversion (reakce podmíněné chuťové averze)

DTI – diffusion tensor imaging (difúzní tenzorové zobrazení)

DWI – diffusion weight images (difúzní vážené snímky) na MR

EPI – echo planar imaging (rozlišení na MR)

FA – frakční anizotropie

FLAIR – fluid attenuated inversion recovery (sekvence na MR)

FgÚ AV ČR v.v.i. – Fyziologický ústav Akademie věd České republiky

FOV – field of view (na MR)

FS - software FreeSurfer pro převod MR snímků do tetrahedronové matrice

GC – gyrus cinguli

hippo osa - dlouhá osa hipokampu předozadně

HPA osa - hypothalamo-hypofyzeo-adrenální osa neuroendokrinní regulace

IKEM – Institut Klinické a Experimentální Medicíny

MedINRIA – volná kolekce software pro zobrazení a analýzu snímků z MR, vyvinutá v rámci výzkumného programu Asclepios

MMSE – minimental state exam (test kognitivních funkcí)

MPRAGE – magnetization for rapid acquisition gradient echo (sekvence na MR)

MR – magnetická rezonance

MRIcro – volně distribuované software k analýze snímků z MR

NNE – neonatal novelty exposure (vystavení novým podnětům)

PCP – Psychiatrické Centrum Praha

RD – radiální koeficient

ROI – region of interest (oblast zájmu)

3 Vědecká otázka a cíle práce

Alzheimerova choroba je vedle demence frontotemporální jednou z nejčastějších demencí nejen u stárnoucí populace, ale i ve středním věku. Nástup tohoto onemocnění je morfologicky pozorovatelný zmenšením paměťové struktury hipokampu ve spánkovém laloku. Proces atrofie nervové tkáně zřejmě začíná v poblíž se nacházejícím gyrus collateralis a postupuje dále do mediotemporálních struktur, mozečku, mozkového kmene a do dalších částí mozkové kůry. Objemové zmenšení hipokampu u AD začíná být klinicky jedním z důležitých diagnostických nástrojů in vivo na magnetické rezonanci. Zejména pak korelace baterie neuropsychiatrických vyšetření v kombinaci s volumetrií hipokampu, popřípadě likvorologické vyšetření je vodítkem k diagnóze. Naše studie se zaměřily na otázku, zdali je možné morfologická data zpřesnit, popřípadě zavést další struktury, které by bylo možno přiřadit jako AD specifické. Jedním z důležitých aspektů naší práce bylo sledování asymetrie změn ve velikosti struktur – tzv. laterality, která je ve většině prací opomíjená, ačkoliv může být velice důležitým klíčem ke sledování rozvoje AD.

Chronický stres je považován za jednu z možných příčin nástupu či rozvoje Alzheimerovy demence (Obr. 1). Je známo, že dlouhodobý stres vede právě k atrofii hipokampu. Přesná korelace není mezi chronickým stresem a AD ještě plně objasněna. Není jasné, zdali dochází spíše k postižení dendritů, nebo těl neuronů, případně neuroglie. V pokusu na zvířeti jsme se proto pokusili zjistit, zdali chronický stres vyvolaný farmakologicky vede ke zmenšení objemu hipokampu a hlavně, zdali je toto zmenšení asymetrické. Dle údajů z literatury nebylo v té době jednoznačně jasné, jestli neurodegenerace vlivem kortikoidů vede k postižení neuronů, zmenšení jejich objemu, nebo jaderné struktury jako celku, i s mezibuněčnou tekutinou, případně jedná-li se o úbytek počtu neuronů. Dále jsme pak uvažovali, jestli je zmenšení struktury hipokampu u člověka doprovázeno u Alzheimerovy demence zmenšením dalších struktur CNS, jako je Varolův most nebo mozeček. Poté následovalo zaměření se na další struktury CNS – gyri, sulci, podkorové oblasti, komorový systém, bílou hmotu s cílem zjištění, zdali u Alzheimerovy demence dochází i zde k jednoznačně morfologicky odlišitelné změně objemu rekonstrukcí a počítačovou analýzou v programu FreeSurfer

(http://freesurfer.net/). U fornixů, commissura anterior, corpus callosum a gyrus cinguli jsme pak stanovovali, zdali dochází k specifickému úbytku vláken bílé hmoty, nebo její dezorganizace, popř. strukturálních změn mikrotubulů či myelinu axonů s cílem potvrzení poškození vláken podílejících se na konsolidaci paměti, která spojují zejména spánkové laloky a asociační oblasti kůry. Použili jsme traktografický software MedINRIA (http://www-sop.inria.fr/asclepios/software/MedINRIA/) a DTI studio (https://www.mristudio.org/). Shrnuto, naší otázkou bylo, jestli postižení vybraných struktur CNS u AD je asymetrické a jestli je v experimentu na zvířeti tato asymetrie vázána na dlouhodobé podávání kortikoidů. Za tímto účelem jsme volili různé zobrazovací techniky a metodologie in vivo a post mortem.

4 Hypotéza

Vycházeli jsme ze situace, kdy dlouhodobě a opakovaně zvýšená hladina stresových hormonů může způsobit nevratné změny ve velikosti citlivých struktur CNS (hipokampus, prefrontální kůra, gasální ganglia apod.). Pakliže by vliv stresových hormonů měl efekt zvýšeně pouze na pravou nebo levou strukturu CNS (např. hipokampus) mohlo by to znamenat, že tento efekt má lateralizovaný charakter a postihne tedy např. dominantní strukturu z hlediska její funkce (např. u hipokampu pokud bychom uvažovali o dominanci pravého či levého ve vztahu k rukovosti, nebo řečového centra). Na počátku Alzheimerovy demence může stát chronicky zvýšená hladina stresových hormonů (kromě dalších hypotéz o vzniku AD jako je cholinergní hypotéza, amyloidní hypotéza a další), protože je prokázáno, že vede k neurodegeneraci. Dále nás zajímalo, jestli je známé zmenšení objemu hipokampu v případě AD následováno podobným zmenšením Varolova mostu či mozečku, tedy struktur, u kterých by se to dalo předpokládat vzhledem k jejich zapojení a účasti na kognitivních a motorických funkcích. Mezi dalšími strukturami nás zajímala oblast v sousedství hipokampu – planum temporale na horní části spánkového laloku, která má pravo-levý vztah k rukovosti a to dokonce i ve vztahu k pohlaví. Zde jsme předpokládali, že asymetrické změny velikosti planum temporale by mohly sloužit jako další morfologicko-diagnostický nástroj u Alzheimerovy demence. Poté se náš zájem obrátil na další struktury CNS kde jsme předpokládali změny u AD, jako je nucleus acumbens, amygdala, mozkový kmen jako celek, kůra mozečku, velkosti hemisfér mozečku, basální ganglia a další. Náš předpoklad byl podobný jako u předchozích struktur – očekávali jsme asymetrické zmenšení oproti kontrolám více méně u všech sledovaných struktur. Další hypotézou bylo snížení objemu, případně změna průběhu či tvaru, vláken fornixu a commissura anterior (zejména části spojující oba spánkové laloky), corpus callosum a gyrus cinguli. Zde jsme očekávali snížení objemu a počtu vláken bílé hmoty a dalších charakteristik axonů (neuspořádanost vláken, kontinuita mikrofilament a kvalita myelinu) mezi skupinou AD pacientů a skupinou kontrolní a to opět jak symetricky, tak asymetricky v obou hemisférách CNS. Poslední zkoumanou hypotézou byl vztah mezi úbytkem počtu neuronů v korových i podkorových oblastech CNS a snížením neuspořádanosti a objemu či počtu vláken bílé hmoty propojujících tyto oblasti postižené degenerací.

5 Přehled použitých metodik

5.1 Metodiky používané při práci s mozkem laboratorního potkana

5.1.2 Volumetrie CNS u potkana

Mozky potkanů kmene Long Evans byly perfundovány intrakardiálně 10% pufrovaným roztokem paraformaldehydu, vyjmuty z lebky a uloženy do roztoku 5% sacharózy do klesnutí. Následně byly zamrazeny kryosprejem (Bamed, ČR) a uloženy do -70 °C do zpracování. Na zmrazovacím mikrotomu Leica CM 1850 byly pořízeny sériové řezy o tloušťce 20 μm a nataženy na podložní sklíčka potažená 10% roztokem želatiny. Po zaschnutí byly řezy obarveny kresylvioletí dle Nissla a uchovány pro další analýzu. Velikost hipokampů byla stanovena pomocí světelného mikroskopu Leica. Objemy granulární vrstvy a pyramidové vrstvy neuronů v rozmezí polí CA1 - CA3 a subiculum (bez podoblastí presubiculum a parasubiculum) byly stanoveny podle Cavalieriho principu (Gundersen a kol., 1988). Velikost celého mozku laboratorního potkana byla stanovena z řezů mozkem pod světelným mikroskopem (bez bulbus olfactorius, chiasma opticum a cerebellum – mozkový kmen byl odříznut těsně nad colliculi superiores), které byly převedeny do standardního PC, kde byly plochy každého řezu ručně ohraničeny a změřeny pomocí volně distribuovaného software Image J (http://rsbweb.nih.gov/ij/). V případě chybějících nebo poškozených řezů (< 8 řezů v průměru na každý mozek) byla chybějící data kalkulována jako průměrná plocha z předchozího a následného řezu.

5.2 Metodiky používané při práci s mozkem člověka

Všichni pacienti s diagnózou AD splňovali kritéria NINCDS-ADRDA (McKhann a kol., 1984). Pacienti i věkově odpovídající normální senioři byli testováni následujícími neuropsychologickými testy: Mini-Mental State Examination (MMSE), Mattis Dementia Rating Scale, Trail Making Test version A a B, Disability Assessment in Dementia, 7-Minute Screen, test verbální fluence a Edinburgh Handedness Inventory. Podle vylepšené verze vědeckých kritérií pro diagnostiku AD (Dubois a kol., 2007) jsme přidali skóre mediální temporální atrofie (Scheltens a kol., 1992), zvlášť pro levou a pravou hemisféru.

5.2.1 Magnetická rezonance

1.5T Siemens přístroj

MR snímky byly pořízeny na 1.5T Siemens Vision MR skeneru se standardní hlavicí podle následujícího protokolu:

T1-vážené snímky (T1W) 3D magnetizace pro rapid acquisition gradient echo (MPRAGE) s parametry: velikost voxelu 1x1x1x mm^3, 160 sagitálních řezů, echo time (TE) 7 ms, opakovací čas (TR) 2010 ms, flip úhel 10°, FOV 256 mm.

Difúzní vážené snímky (DWI) sekvence SE-EPI s parametry: TR = 6 s, TE = 110 ms, velikost voxelu 2,5x2,5x2,5 mm^3, 27 axiálních řezů, 3 průměry, FOV = 320 mm, 6 difúzních směrů, dvě b-hodnoty: 0 a 1000 s/mm^2

3T Siemens přístroj

3T MR skener (Siemens Magnetom Trio, Erlangen, Germany) pomocí 12 kanálů, phased-array head coil s protokolem:

T1-vážené 3D MPRAGE s následujícími parametry:

Velikost voxelu 0,85×0,85×0,85 mm^3, 192 sagitálních řezů, echo time (TE) 4,73 ms, opakovací čas (TR) 2000 ms, flip úhel 10°, FOV 326 mm.

3D T2-vážené FLAIR s parametry: velikost voxelu 1×1×1 mm^3, 176 sagitálních řezů, TE 422 ms, TR 6000 ms a FOV 256 mm.

Difúzní vážené snímky s SE EPI sekvencí s parametry:

Velikost voxelu 2×2×2 mm^3, TR 6000 ms, TE 93 ms, 44 axiálních snímků, tři průměry, FOV=256 mm, počet difúzních směrů 20, dvě b hodnoty: 0 a 1000 s/mm^2

DTI protokol

Pro měření DTI byla použita sekvence dvojitého spinového echa (SE) EPI (spin-echo, echo-planar imaging) se dvěma páry bipolárních gradientních pulzů, které vytvářejí celkový b faktor b = 1000 s/mm^2 . Dva různé protokoly pro měření difúze, které byly použity na přístroji Siemens Trio 3T (s 12 kanálovou cívkou), lokalizer (min:s) (0:10), počet vrstev 44, orientace transversální, FOV (mm) = 256x256, rozlišení (mm) = 2x2x2, TR (ms) = 6000, TE (ms) = 93, počet opakování = 3, b-faktor (s/mm^2) = 0 a 1000, počet difúzních směrů = 20, čas měření (min/s) = 6:38, PAT faktor = 2.

5.2.2 Autopsie mozkové tkáně

Vzorky mozkové tkáně byly získávány v průběhu let 2008-2010 z Patologického oddělení Nemocnice na Bulovce a původního Ústavu patologie PCP. Celé mozky po zvážení byly umístěny do 10% roztoku paraformaldehydu s 5% roztokem alkoholu. Po 30 denní fixaci byly z mozků odděleny sledované struktury (planum temporale, hipokampus) a dále zpracovány.

5.2.3 Volumetrie CNS

Objem hipokampu, Varolova mostu a mozečku byl měřen volumetricky ze snímků magnetické rezonance. Tyto snímky byly nejprve převedeny do jednoho souboru pomocí volně distribuovaného programu MRIcro. Dále byly převedeny ve frontální rovině do stereologického volně distribuovaného programu Image J, ve kterém byly měřeny plochy, jejichž součtem byl stanoven objem struktury. Všechny měřené struktury byly normalizovány vzhledem k velikosti mozkové tkáně na řezu ve frontální rovině v místě commissura anterior. Pro statistická měření byl použit program Statistica v. 10. Objemy struktur v normě a v patologii byly hodnoceny 2-way ANOVA, pro vyloučení nulové hypotézy pak t-testem.

5.2.4 Použití polysiloxanové pryskyřice pro měření plochy planum temporale

Omyté vzorky PT jsme umístili na Petriho misky a štětečkem pokryli celý povrch vzorků, tj. Heschlovy gyri, část gyrus temporalis superior, přechod do insuly a dorzální raménko, tekutou fází kondenzační polysiloxanové pryskyřice (STOMAFLEX CRÈME (SC)), látky která se běžně používá v dentální medicíně. Důraz jsme přitom kladli na to, aby se tekutina dostala do všech nerovností a záhybů na povrchu PT. SC během pěti minut zpolymerizovala a vytvořila tenkou otiskovou vrstvu (masku) na vzorcích, kterou jsme opatrně sňali pinzetou. Touto cestou vytvořené masky povrchu PT již měly výraznou 3D strukturu. V místě otisků zářezů mezi gyri jsme masky rozdělili do více částí tak, abychom dostali několik vzorků téměř ideálního 2D povrchu. Všechny 2D vzorky z jednoho PT jsme z důvodu vytvoření jednolitých ploch umístili mezi skleněná podložní sklíčka o velikosti 50x50 mm, běžně používaná v mikroskopii. Takto připravené vzorky řezů jsme pak digitalizovali pomocí kamery Olympus 5050 připojené ke standardnímu PC a následně je pak použili pro volumetrickou analýzu pomocí Image J software (Zach a kol., 2006).

5.2.5 FreeSurfer (FS) analýza

Analýza byla provedena na speciálně konfigurovaném PC (Debian Linux 3.2.46-1 x86_64 operating system) s dvěma paralelními instalacemi FreeSurfer v5.2.0 a v5.3.0 (http://surfer.nmr.mgh.harvard.edu/). DICOM MR snímky z 3T skeneru skupin AD pacientů a kontrol byly převedeny do FS programu do formátu *.mgz souborů pomocí příkazu mri_convert. Celková rekonstrukce tetrahedronové matice obrazů (korové a podkorové oblasti, mozkový kmen, mozkomíšní mok, komory, bílá hmota) byla provedena příkazem recon –all ve formátu recon-all –vw256 –s jménopacienta –all –hippo-subfields. Recon –all procedura selhala u 2 kontrolních MRI – tyto byly z další analýzy odstraněny. Datové výstupní volumetrické soubory pro statistickou analýzu byly použity z adresáře /stats (aseg.stats, lh aparc.stats atd.) z programu FS a převedeny do software Statistica 10.

5.2.6 Traktografie bílé hmoty (MedINRIA, SPM8)

DTI sken zachycuje Brownův pohyb molekul vody podél axonů a určí tak difúzní tenzor, který pro daný voxel určí směr a orientaci vláken. Program MedINRIA i DTI studio po označení sledovaných struktur (commisura anterior, oboustranně fornix, corpus callosum a gyrus cinguli) zobrazí a vypočítá soubory vláken a jejich vlastnosti (délka, počet a další charakteristiky axonů). DTI data byla upravena kvůli možné distorzi a zpětným proudům pomocí programu FSL (www.fmrib.ox.ac.uk/fsl/index.html). EPI obrazy z DTI sady snímků byly adaptovány podle T1-vážených 3D MPRAGE snímků pro získání koregistrační matrice, která byla následně využita pro další EPI difúzní obrazy. EPI a T1W 3D MPRAGE koregistrované obrazy pak byly normalizovány k T1 templátům. Koregistrace a prostorová normalizace byla provedena programem SPM8 (http://www.fil.ion.ucl.ac.uk/spm/ software/spm8). Normalizované DTI indexy (FA, MD, λax, a λrad) byly vypočítány pomocí software MedINRIA (Asclepios Research Project—INRIA Sophia Antipolis, http://wwwsop.inria.fr/asclepios/software/MedINRIA) a DTI studio (https://www.mristudio.org/). Oblasti zájmu (dále ROI), tedy fornix a commissura anterior, byly manuálně ohraničeny v sagitální a axiální projekci na T1W 3D MPRAGE normalizovaném obrazu (Obr. 2). Corpus callosum i gyrus cinguli byly parcelovány automatickou sekvenací v programu DTI studio na 5 podčástí v případě corpus callosum - CC anterior, CC mid-anterior, CC centralis, CC mid-posterior a

CC posterior (Witelson, 1989), a 2 podčásti gyrus cinguli - GC anterior a GC posterior. Program následně vyhodnotil v ROI parametry délka, počet a objem vláken bílé hmoty, frakční anizotropii (FA) – (míra neuspořádanosti vláken), axiální koeficient (AX, svědčí o stavu mikrofilament) a radiální koeficient (RD, stav myelinu). Všechny parametry jsme porovnali mezi skupinou AD pacientů a kontrol s přihlédnutím k lateralitě.

5.3 Statistická analýza

Ve všech případech byl použit statistický program Statistica 10 (StatSoft, Česká republika). Pro porovnání dat u pacientů s AD a kontrol (vpravo-vlevo) byla použita ANOVA s opakovaným měřením. Pro post hoc byla využita Neuwman-Keuls analýza. Pro ověření nenulové hypotézy byl použit párový nebo jednotlivý studentův t-test. Pro ověření kvality hypotézy a validity výsledků byla použita ROC curve analýza (http://www.rad.jhmi.edu/jeng/javarad/roc/JROCFITi.html).

6 Způsob organizace sběru a získávání experimentálních dat

6.1 Spolupráce s Poradnou pro poruchy paměti - AD centrem a přístup do databáze snímků MR pacientů s AD a kontrol

MR snímky jsme získávali v rámci výzkumného programu doc. MUDr. Aleše Bartoše, Ph.D., Poradna pro poruchy paměti - AD centrum (dále AD Centrum Praha) (projekt MŠMT (1M0002375201) Centrum neuropsychiatrických studií Neurobiologie v klinické aplikaci v letech 2005–2011), které byly pořizovány na Pracovišti diagnostiky a intervenční radiologie IKEM a to od roku 2007 1,5T a od roku 2008 3T. Zpracovaná data z MR jsme ukládali do zálohované Excelové databáze (sdílení souborů s AD Centrem Praha, kde se uchovávala všechna diagnostická vyšetření, baterie neuropsychologických testů, biochemické parametry, kognitivní funkce, likvorologická vyšetření apod.) jak pro skupinu pacientů s AD, tak pro skupinu kontrol. Data při provádění analýzy byla dvojitě slepě označena pro vyloučení subjektivní bias. Zpracování snímků MR probíhalo manuálně i automaticky pomocí speciálních software (viz 5.2) na Ústavu anatomie 3. LF UK. Celkem bylo zpracováno a archivováno v Excelové databázi od více než 250 pacientů s AD a kontrol.

6.2 Laboratorní potkani pro volumetrické studie

Byli použiti potkani z chovu Fyziologického ústavu AV ČR v.v.i., kmeny Long Evans a Wistar, kde na ústavu Neurofyziologie paměti proběhla experimentální část stresové reakce a chuťové averze. Pro provedení fyziologické části pokusů byly jejich mozky dále neurohistologicky zpracovány na Ústavu anatomie 3. LF UK a tamtéž proběhlo histologické zpracování materiálu, volumetrická a stereologická měření.

6.3 Spolupráce s IKEM Praha, MR jednotka

Snímky magnetické rezonance s DTI sekvencí byly pořízeny na Pracovišti radiodiagnostiky a intervenční radiologie IKEM. Traktografická obrazová data pacientů s AD a kontrol byla exportována na datové nosiče nebo přenosem počítačovou sítí. Pacienti s AD i kontroly byli opět ukládáni do Excelové databáze sdílené s AD Centrem Praha (obsahující podrobná vyšetření obou skupin, viz 6.1).

Data byla po konverzi do PC na Ústavu anatomie normalizována pro zpracování na dvou počítačích s programy MedINRIA a SMP8. Numerická i obrazová data pak byla vyhodnocována nezávisle po sobě dvěma výzkumníky.

6.4 Autoptický materiál pro morfologii planum temporale

Autoptický materiál byl získán z původního Oddělení patologie při Psychiatrickém centru Praha v Bohnicích a dále z Patologického oddělení Nemocnice na Bulovce – zdravé kontroly a pacienti s diagnózou AD. Patolog odebírající vzorky autoptického materiálu byl podrobně seznámem s detaily umístění a ohraničení planum temporale ve spánkovém laloku mozku oproti ostatním korovým strukturám. Odebrané vzorky byly následně zpracovány na Ústavu anatomie 3. LF UK. Veškerý autoptický materiál byl pořízen se souhlasem Etické komise 3. LF UK dle znění předpisů v témže roce (2005).

7 Využití a přínos výsledků

7.1 Shrnutí využití a výsledků u člověka

Post mortem studie i in vivo MR studie na člověku rozšiřují možnosti stávajících zobrazovacích diagnostických postupů v mnoha směrech.

7.1.1 Volumetrická analýza struktur mozku člověka na MR

Analýza ukázala statisticky významné oboustranné snížení objemu hipokampu, přičemž u pacientů s AD je významnější na pravé straně. V obou hemisférách mozečku i v celé struktuře měřeného úseku pontu v mozkovém kmeni ke statisticky významnému úbytku hmoty u pacientů s AD nedošlo. Pro účely včasné diagnostiky a stadia progrese AD onemocnění tedy doporučujeme pouze měření změn objemu hipokampu, volumetrie mozečku a pontu není pro skórování závažnost onemocnění využitelná.

7.1.2 Kvantifikace volumetrických změn hipokampu bez reorientace MR snímků

Ačkoliv je kvantifikace volumetrických změn v hipokampu platným diagnostickým markerem onemocnění AD, sama pozice hipokampu na MR může být ovlivněna vlivem natočení hlavy, velikosti lebky, rotace mozkové tkáně uvnitř lebky a dalšími faktory. Naproti tomu jsme zjistili, že reorientace hipokampu do některých ze standardně užívaných rovin (osy commissura anterius a commissura posterius a dlouhé osy hipokampu) není nutná pro validní volumetrická data a je možné pracovat s nativním MR snímkem hipokampu (Obr. 3).

Hlavní praktické využití tohoto nálezu je možnost analýzy jednoho specifického snímku hipokampu na MR, tzv. optimálního řezu nacházejícího se v místě přechodu alevus hipokampu do těla hipokampu, bez nutnosti složité reorientace a tedy snažší využití ve skórování progrese AD v běžné klinické praxi.

7.1.3 Planum temporale a jeho asymetrie

Celková velikost této struktury a tloušťka její korové vrstvy může sloužit jako další vhodný parametr pro stanovování morfologických rozdílů mezi AD pacienty a kontrolami. U kontrol převládala pravo-levá asymetrie, zatímco u AD pacientů došlo k obrácení této asymetrie do levo-pravé. Bylo by tedy možné využít asymetrie

planum temporale na mozcích pacientů post mortem s využitím naší originální metodiky (potažení struktury polysiloxanovou dentální pryskyřicí a měření její velikosti). Současně je ale možné využít zjištěných asymetrií PT pro zobrazovací techniky jako je MR a následné FreeSurfer analýzy.

7.1.4 Změny ve velikosti pyramidových neuronů ze třetí vrstvy PT

Na základě zjištěné reverze asymetrie velikosti planum temporale jsme dále sledovali změny ve velikosti pyramidových neuronů ve třetí vrstvě kůry PT. Konkrétně jsme zjišťovali délku pyramidových neuronů ve čtyřech marginálních zónách planum temporale (přechod do gyrus temporalis superior, Heschlovy gyri, přechod do insulární kůry a přechod do Sylviovy rýhy) u kontrol a pacientů s AD. Předpokládali jsme, že délka pyramidových neuronů bude celkově menší u pacientů s AD v porovnání s kontrolami a že bude přítomna pravo-levá asymetrie u kontrol a její reverze u pacientů s AD, podobně jako u měření plochy a tloušťky kůry planum temporale. Výsledky ukázaly asymetrii délky neuronů pouze u kontrol a to pouze v případě přechodu do Sylviovy rýhy. Ostatní zóny planum temporale byly bez asymetrie u pacientů obou skupin. Detailní porovnání rozdílů mezi kontrolami a pacienty s AD dále ukázaly: a) absenci rozdílů v délce neuronů v přechodu do gyrus temporalis superior, b) významně menší délku neuronů u AD skupiny než u kontrol na přechodu do insulární kůry vlevo, c) vpravo i vlevo významně menší délku neuronů na přechodu do Heschlových gyrů u AD versus kontroly a d) vpravo na přechodu do Sylviovy rýhy významně menší délku neuronů u AD skupiny v porovnání s kontrolami. Na základě těchto výsledků můžeme doporučit tuto metodiku stanovování délky pyramidových neuronů v planum temporale jako doplňující metodiku k již existujícím neuropatologickým diagnostikám AD.

7.1.5 Rekonstrukce struktur CNS pomocí FS u podkorových a korových struktur

Měření velikosti a asymetrie podkorových oblastí CNS ukázalo kromě standardně uznávaného snížení objemu hipokampu u AD versus kontroly důležitost volumetrie u dalších dvou struktur – nucleus accumbens a amygdalárního komplexu (Obr. 4). V obou případech rekonstruce odhalila významné zmenšení velikosti u AD. Asymetrické zvětšení celého objemu postranní komory vpravo FS analýzou ukázalo, že se netýká temporálního rohu komory, ačkoliv jsme očekávali jeho zvětšení kvůli prokázané atrofii hipokampu, jehož volný povrch vyčnívá právě do prostoru

temporálního rohu komory. Z toho vyplývá, že se zvětšení postranních komor musí týkat některé ze zbývajících částí – frontálního rohu, centrální části nebo okcipitálního rohu. U řady dalších měřených struktur, putamen, pallidum, šedá kůra mozečku, počet korových defektů koncového mozku, byly očekávané výraznější změny u AD skupiny v porovnání s kontrolami, ale bez statistické významnosti. Pouze u několika dalších měřených struktur jsme zjistili následující statisticky významné rozdíly: celkový povrch šedé kůry koncového mozku větší u kontrol, velikost čtvrté komory větší u kontrol a objem mozkomíšního moku vyšší u AD, zřejmě kvůli většímu prostoru komory.

Pravo-levé asymetrie byly rozloženy jinak u AD než u kontrol. V případě AD skupiny jsme zjistili významnou asymetrii v počtu korových defektů koncového mozku (vpravo méně než vlevo) a objemu postranní komory (vpravo menší než vlevo) a amygdalárního komplexu (vpravo větší než vlevo). Naproti tomu jsme u kontrolní skupiny zjistili významnou asymetrii v objemu bílé hmoty mozečku (vpravo větší než vlevo), ale bez statistické významnosti u mozečkové kůry (vpravo větší než vlevo).

Automatická analýza nabízí v porovnání s manuální analýzou rychlejší, standardní a reprodukovatelná data pro klinická pracoviště.

7.1.6 Traktografie bílé hmoty

Měření počtu bílých vláken ukázalo jejich statisticky významný úbytek pouze v pravém fornixu u pacientů s AD. Tento nález dobře koresponduje s výraznějším pravostranným úbytkem hmoty hipokampu v pravém spánkovém laloku v porovnání s levou stranou. V případě commisura anterior jsme nezjistili rozídly mezi skupinou AD a kontrolami. Corpus callosum vykazuje statisticky významnou změnu počtu vláken v námi sledovaných podčástech corpus callosum (CC anterior, CC mid-anterior, CC centralis a CC posterior (Obr. 5)), mimo CC mid-posterior části. Stejně tak obě podčásti gyrus cinguli (GC anterior a GC posterior) snážení počtu vláken neukázaly. U pacientů s AD jsme však v celé oblasti CC a GC nalezli statisticky významný posun ve všech sledovaných parametrech traktografického zobrazení: frakční anizotropie (FA), axiálního koeficientu (AX) a radiálního koeficientu (RD). Tato data svědčící pro upořádání vláken, stavu mikrofilament uvnitř axonu a stavu myelinu jsou dobře využitelná pro časnou diagnostiku choroby, neboť reflektují jak intracelulární změny v ukládání tau proteinu, tak i vazbu mezi extracelulární

akumulací β-amyloidu a stavem myelinu. Tyto výsledky byly publikovány na Morphology 2014 v Brně a v roce 2015 budou prezentovány na Morphology 2015 v Olomouci a předpokládáme jejich zveřejnění v časopise s IF v následujícím roce.

7.2 Shrnutí využití a výsledků u laboratorního potkana

7.2.1 Volumetrie hipokampu u laboratorního potkana ve stresu.

Studie vlivu chronického podávání kortikoidů potkanovi měla objasnit, zdali dochází ke zmenšování velikosti neuronů v hipokampu, jejich počtu, případně celkového objemu hipokampu. Tento model chronického stresu tvoří jednu z možných hypotéz rozvoje AD u člověka – stresový model vzniku a rozvoje AD. Zjistili jsme významné změny objemu a zvláště v asymetrii podčástí hipokampu mezi kontrolami a skupinou potkanů s podávanými kortikoidy. Levý hipokampus měl signifikantně větší objem než pravý u skupiny s kortikoidy, nikoliv u kontrol. U kontrolní skupiny byl naopak objem pravého hipokampu větší než levého. Závěrem studie bylo pozorování, že zmenšení objemu není vázáno specificky na neurony, ale také na ostatní složky (glie, extracelulární prostor) a že zmenšení objemu je výraznější vpravo než vlevo.

Na tyto naše pokusy navazovalo experimentální podávání nootropik a sledování vývoje degenerace nebo regenerace neuronů v hipokampu (gyrus dentatus) a také asymetrie těchto změn u skupiny s chronicky podávanými kortikoidy a kontrolami. Na model asymetrického ovlivnění hipokampu chronickým stresem mohou navazovat různé farmakologické studie ovlivňující regeneraci neuronů v této oblasti.

7.2.2 Podávání kortikoidů a CTA

Podobně jako v případě bodu *7.2.1* podávání kortikoidů vedlo k narušení formování podmíněné reakce chuťové averze, vývojově jednoho z nejstarších reflexních systémů. Také v tomto modelu jsme nepozorovali morfologické změny na neuronech (nucleus parabrachialis, amygdalárního komplexu a mediální frontální kůry), jejich subcelulární degeneraci, nebo snižování jejich celkového počtu a to ani na úrovni glie či extracelulárního prostoru.

Zde mohou navazovat další experimenty zaměřené na studium systému neuroglie a kvality složení extracelulárního prostoru.

7.2.3 Využití neuroprotektiva při vaskulárních změnách v CNS

Ve spolupráci s FgÚ AV ČR jsme dopravovali po experimentálních ischemiích neuroprotektivum (modifikace pregnenolon sulfátu) do poškozené mozkové tkáně. Cílem byla minimalizace či zamezení poškození CNS ischemickými změnami. Výsledky by byly využitelné pro vývoj nových neuroprotektiv.

8 Časový harmonogram postupu experimentální práce

2008 naučení se odběru vzorku planum temporale, dokončení sběru materiálu a analýza planum temporale, práce s polysiloxanovou pryskyřicí, zvládnutí práce s volumetrickým software na PC Image J, zvládnutí základních statistických postupů (program Statistica, ANOVA, t-test, post hoc analýzy);

2009 publikace článku na téma planum temporale;

2009 podávání kortikoidů laboratornímu potkanovi, analýza dat, zvládnutí techniky řezání na kryomikrotomu, barvení řezů CNS podle Nissla, digitalizace řezů mozkem potkana pro PC analýzu, práce s volumetrickým software;

2010 publikace článku na téma vliv kortikoidů na hipokampus u potkana;

2010 podávání kortikoidů laboratornímu potkanovi a analýza vlivu na podmíněnou chuťovou averzi;

2011 publikace článku na téma vliv kortikoidů a chuťová averze;

2011 sběr magnetických rezonancí pacientů s AD a volumetrická analýza, hipokampu, pontu a mozečku, analýza pozice hipokampu na magnetické rezonanci, zvládnutí ohraničování struktur CNS v software Image J, účast při tvorbě skórovacího systému ve vazbě na Neurologickou kliniku 3. LF UK a FNKV;

2012 publikace článku na téma volumetrie hipokampu, pontu a mozečku, zvládnutí práce se software FreeSurfer, MedINRIA pro rekonstrukce a traktografie;

2013 neurohistologická analýza planum temporale u člověka, pyramidové neurony a měření jejich délky zobrazovacím systémem Leica;

2014 publikace článku na téma změn ve velikosti pyramidových neuronů planum temporale u AD;

2014 publikace článku na téma pozice hipokampu na magnetické rezonanci;

2014 prezentace výsledků traktografií Morphology 2014 v Brně;

2015 podání článku na téma automatické volumetrie podkorových struktur u AD a kontrol na FreeSurferu;

2015 prezentace výsledků traktografií na Morphology 2015 v Olomouci;

2015 v přípravě je CLARITY systém pro zobrazení mozku potkana při experimentálních ischemiích v kombinaci se zobrazením v mikro CT.

9 Diskuze

9.1 Planum temporale a změny jeho velikosti u AD.

Nová volumetrická metoda potažení povrchu mozku polysiloxanovou pryskyřicí je založena na vlastnosti této pryskyřice, která, pokud je v tekuté fázi, může kopírovat povrch planum temporale, včetně zářezů, zakřivení a dalších nerovností. Po zatvrdnutí pak vytváří gumový odlitek povrchu. Po sejmutí je možno odlitek upravit do požadovaného tvaru, přesně ohraničit okraje vzorku a uzpůsobit je pro zasazení mezi dvě podložní sklíčka do 2D pozice. Takto mohou být snadněji hodnoceny volumetrické změny v případě nerovností a nepravidelností tvaru povrchu planum temporale, v porovnání s jinými komplikovanějšími metodami post mortem evaluace změn v mozku (např. Harasty a kol., 1999). Otisky pryskyřice by bylo možné teoreticky použít nejenom v případě plochy planum temporale, ale také dalších korových oblastí CNS, jejichž plocha je post mortem jinak obtížně měřitelná. Jiným příkladem využití může být situace, kdy není na zobrazovacích technikách dostatečně viditelné ohraničení cytoarchitektonicky definovaných oblastí mozkové kůry, např. přechod mezi senzorimotorickou kůrou a premotorickými oblastmi čelního laloku.

U kontrol jsme zjistili mírnou pravo-levou asymetrii jak v ploše, tak v tloušťce kůry a objemu planum temporale. Takovýto nález není v souladu s údaji v literatuře, kde se uvádí opačná, tedy levo-pravá asymetrie (např. Geschwind a kol., 1968; Galaburda a kol., 1987). Vysvětlení je možné kvůli rozdílným popisům hranic planum temporale oproti ostatním strukturám (gyrus temporalis superior, zadní a přední vzestupné raménko u Sylviovy rýhy) (Obr. 6). V případě AD jsme pozorovali posun od pravo-levé asymetrie k levo-pravé asymetrii v případě plochy, tloušťky kůry a objemu PT. Detailnější analýza PT ukázala mírný pokles v uvedených parametrech vpravo a nárůst vlevo u AD v porovnání s kontrolami (Obr. 7). Je možné, že pravá strana PT bude více poškozena v důsledku neurodegenerace. Takovýto nález je v rozporu s pracemi uvádějícími výraznější postižení dominantní, tedy levé hemisféry ve většině případů (Toga a Thompson, 2003). Pokud bude levá strana PT více postižena zánětem nebo gliózou vedoucí k zvětšení plochy a objemu (Miller, 2004), v takovém případě budou obě strany PT postiženy s podobnou intenzitou. K projevům změn pak bude docházet v druhostranné hemisféře.

Histologická analýza nepotvrdila významnou asymetrii v denzitě plaků v hipokampu nebo v korových oblastech, nicméně, v některých případech byla levá hemisféra postižena výrazněji.

9.2 Planum temporale jako marker stranovosti u mozkové tkáně post mortem

Levá hemisféra je u většiny populace dominantní z hlediska řečových center (přibližně 96 % praváků a 73 % leváků vykazuje levostrannou lokalizaci řečového centra). V případě lidské autoptické tkáně nejsou potřebná data o rukovosti často k dispozici. V takovémto případě se ukazuje, že data z volumetrických asymetrií PT by mohla sloužit jako marker, jelikož stupeň asymetrie je vyšší u praváků, než u leváků (Toga a Thompson, 2003).

9.3 Změny ve velikosti neuronů ve III. korové vrstvě PT u AD a kontrol

Pro zjištění povahy změn velikosti PT u AD jsme dále měřili velikost pyramidových neuronů ve III. vrstvě PT (v místech přechodu PT do gyrus temporalis superior, přechodu PT do insuly, přechodu PT do Sylviovy rýhy a v místě Heschlových závitů). Ačkoliv jsme netřídili v experimentu neurony dle velikosti, jejich délka se nacházela vždy v rozmezí 15 až 25 mikrometrů, bez ohledu skupinu. Naše výsledky ukázaly, že pouze oblast přechodu do Sylviovy rýhy měla větší objem těl neuronů (vpravo více vyjádřen než vlevo) a to pouze u kontrol. Tato část PT není součástí auditorní kůry, ale účastní se senzorimotorických integrací při provádění vokalizace v hrtanu (Hickok a Saberi, 2012). U AD skupiny jsme nenašli v žádné podoblasti PT signifikantní pravo-levou asymetrii v délce neuronů. V místě přechodu PT do insuly jsme nalezli levo-pravou asymetrii v délce neuronů, ale v případě přechodu do Sylviovy rýhy byla délka neuronů téměř identická. To je v kontrastu se studií uvádějící jednoznačnou levo-pravou asymetrii u kontrol (sledovány byly buňky v auditorní nebo řečové oblasti, ale pouze magnopyramidální tpy, čítající pouze10 % ze všech buněk) (Hutsler, 2003). Námi pozorovaná absence pravo-levé asymetrie u AD skupiny může být hodnocena jako pokles pravé dominance, která je u kontrol přítomna. Podobně jako v případě, kdy dojde k vymizení běžně přítomné asymetrie u pacientů s AD v objemu hipokampu a navíc až k reverzi této asymetrie (Mrzílková a kol., 2012). Zadní část PT tedy může být další oblastí specificky postiženou při AD onemocnění, kromě již známých oblastí jako je gyrus collateralis, entorhinální kůra, hipokampus a mozkový kmen. Vzhledem k účasti temporoparietální kůry ve

zpracování řečové informace a zmenšení velikosti pyramidových neuronů ze III. vrstvy PT, předpokládáme možnou souvislost mezi vokalizačními potížemi a postižením deklarativní paměti u pacientů s AD. To by mělo platit pouze u populace s pravostranným umístěním řečového a sluchového centra, jelikož jsme nenalezli zmenšení délky těl neuronů na straně levé. Kromě námi pozorovaných změn u AD bylo zmenšení velikosti neuronů ve III. vrstvě PT také popsáno u bipolární poruchy, nikoliv však u schizofrenie nebo depresivní poruchy. Při měření velikosti neuronů ze všech vrstev kůry PT (nikoliv pouze z vrstvy III), se ale úbytek jejich délky neprojevil (Beasley a kol., 2005). Redukce objemu těl neuronů byla také popsána ve III. pyramidové vrstvě spánkové asociační kůry u pacientů se schizofrenií (Sweet a kol., 2003). Námi pozorované zkrácení délky neuronů ve III. vrstvě PT u pacientů s AD by mohlo být v budoucnu obdobně nalezeno v sousedních korových asociačních oblastech. Námi pozorovaná obrácená asymetrie (vymizení pravo-levé a posun k levo-pravé) v přechodu PT do gyrus temporalis superior, je opakem k běžně pozorované asymetrii u schizofrenie (pravo-levá) (Shapleske a kol., 1999). Ve III. vrstvě kůry PT většinou nalézáme jak malé a středně veliké pyramidové neurony, tak i ostatní typy neuronů. Ačkoliv pyramidové neurony jsou hlavním cílem interhemisférických kortiko-kortikálních aferentů a také primárním zdrojem kortiko-kortikálních eferentů, není jasné, zdali byly ostatní typy neuronů (interneurony, granulární buňky apod.) postiženy také. Pravostranná asymetrie délky neuronů u pacientů s AD se nemusí nutně omezovat pouze na III. vrstvu PT a tak studie měření velikosti neuronů v dalších vrstvách by mohla být cílem dalších experimentů.

9.4 Volumetrická analýza hipokampu, pontu a mozečku u AD a kontrol na MR

Skupina AD pacientů i kontrol byla věkově spárovaná, ale nezohlednili jsme rozdíly mezi pohlavími, a to kvůli rozdílnému počtu mužů a žen v obou skupinách. U AD skupiny s MMSE dichotomií a bez ní jsme nalezli oboustranné snížení objemu hipokampu v porovnání s kontrolami. Nenalezli jsme signifikantní asymetrii v žádné z měřených struktur jak u AD, tak u kontrol s výjimkou hipokampu (pravo-levá asymetrie u kontrol a levo-pravá asymetrie u AD skupiny s MMSE nad 18). Normalizace objemu struktur k velikosti mozku nebo lebky mělo pouze malý efekt na výše uvedené výsledky a to pouze v pontu mozkového kmene. Nečekaným nálezem bylo snížení objemu pravého hipokampu u AD skupiny v porovnání s kontrolami s $p < 0{,}01$ s normalizací i bez normalizace k mozku nebo lebce.

Objemové snížení levého hipokampu u AD skupiny bylo významné pouze při porovnání s kontrolní skupinou jak s normalizací, tak bez normalizace k velikosti mozku. Nenalezli jsme významné snížení objemu obou mozečkových hemisfér ani pontu mozkového kmene u AD skupiny v porovnání s kontrolní skupinou. To lze vysvětlit relativní stabilitou objemu mozkového kmene během procesu stárnutí (Luft a kol., 1999). Na druhou stranu auditorní asymetrie na úrovni mesencephalon jsou známy, ale jejich propagace do pontu mozkového kmene není popsána (Schönwiesner a kol., 2007). Při pohledu na MR skeny pouhým okem jsme zjistili, že mozkový kmen zdaleka nemá v sagitální rovině rovný tvar, ale je vychýlený lehce vlevo nebo vpravo, zvláště pak u starších pacientů. V takovém případě nemůže být pons mozkového kmene považován za rotačně symetrickou strukturu. Abychom zhodnotili vliv „skoliózy“ mozkového kmene na levostranou volumetrickou asymetrii, vybrali jsme šest pacientů s AD s výrazným zakřivením průběhu a měřili pontinní asymetrii zvlášť. Ačkoliv jsme u těchto pacientů zjistili výraznější pravostrannou asymetrii, t-test neodhalil významný rozdíl v porovnání s celou AD skupinou. Metodologicky jsme čelili problému, jak ohraničit anatomicky dorzální a laterální stranu pontu. Rozhodli jsme se nepoužívat běžně zavedenou trigeminofaciální čáru ohraničující laterálně přechod z pontu do mozečkových pediklů, jelikož v sagitální projekci není tato linie na MR zřetelná. Naproti tomu jsme využili velmi dobře viditelný přechod (mezi pons dorsálně a tegmentum) na snímcích v blízkosti střední čáry, zobrazený jako kontrastní šedobílá linie ve tvaru eplipsoidu, která laterálně postupně vymizí. Takto jsme definovali laterální ohraničení měřené struktury (Obr. 8). Pro diagnózu AD jsme využili stará kritéria (Khan a kol., 1994), ale zavzali jsme i skóre mediální temporální atrofie jako moderní marker AD hodnocení. Nevyužili jsme markery mozkomíšního moku u AD, jelikož v době odběru vzorků nebyly běžně k dispozici. Výběr pacientů s MMSE skóre pod 18 nevedl k výrazně odlišným výsledkům v porovnání s objemem a asymetrií AD skupiny s MMSE skóre nad 18. Očekávali jsme, že AD skupina s MMSE skóre pod 18 bude vykazovat vyšší změny v objemu a asymetrii struktur vzhledem k závažnějšímu postižení. Vysvětlení tohoto jevu může být v relativně malém počtu pacientů s AD a MMSE nižším než 18 (n=11). Nepodařilo se nám prokázat, že by zmenšení objemu hipokampu bylo na MR snímcích doprovázeno podobným snížením objemu mozkového kmene (pons) nebo mozečku. To neznamená, že by imunohistochemické nebo molekulárně biologické změny

nemohly v budoucnu odhalit počátek AD změn právě zde. Ve shodě s literaturou jsme potvrdili významné objemové zmenšení pouze pravého hipokampu u AD skupiny. Pro další studie se zdá být vhodné provádět manuální volumetrická měření hipokampu, zejména pak z hlediska odlišení AD versus MCI (Teipel a kol., 2010).

9.5 Evaluace pozice hipokampu na MRI pro kliniku a experiment

Hodnotili jsme vliv rotace hlavy v sagitální rovině na manuální měření plochy řezu hipokampu, která by mohla vést k nesourodým výsledkům tam, kde se využívají jednotlivé řezy při manuálním ohraničení struktur CNS. Celkově jsme nezjistili žádný statisticky významný rozdíl mezi plochou hipokampu (AC-PC vs nat), měřenou na MR snímcích ve frontální rovině (v místě přechodu alveus hipokampu do těla hipokampu – námi definovaného jako tzv. ideální řez (Obr. 9)). To je v rozporu s jednoduchým pozorováním okem, kde se tvar hipokampu a temporálního rohu postranní komory mozku zdá být odlišný ve třech různých natočeních mozku (AC-PC osa, dlouhá osa hipokampu a nativní snímek bez reorientace). Kromě toho hipokampus ani temporální roh postranní komory nejsou rotačně symetrické v žádné z geometrických projekcí (frontální, sagitální, horizontální). Také jsme zjistili drobné rozdíly v natočení mezi plochou samotného hipokampu a plochou hipokampu s temporálním rohem postranní komory. Vysvětlení je možné kvůli vlivu větší celkové plochy na pozici mozku. Do měření jsme zahrnuli bez rozlišení kontroly i AD pacienty, různé věkové kategorie a obě hemisféry mozku, protože naším cílem bylo zjištění vlivu místní geometrie na plošnou míru (což je případ většiny MR volumetrických studií). Pokud přihlédneme k rozdílům v těchto kategoriích, AD pacienti většinou mají větší objemy temporálního rohu postranní komory v porovnání s kontrolami (Scheltens a kol., 1992). Takto by více pacientů s diagnózou AD mohlo mít falešně pozitivně větší plochy a tím odlišné výsledky. Nepokoušeli jsme se měřit objem celého hipokampu nebo společně hipokampu a temporálního rohu postranní komory, jelikož součet plochy řezů celé struktury (objem) by se neměl lišit v žádné rovině natočení. Technicky platí, že poloha hlavy a její laterální rotace je vyloučena fixací nástavcem během snímání, zatímco poloha hlavy v předozadním směru takto zabezpečena není.

Pokud zohledňujeme při měření pouze jeden z řezů, není jisté, zdali je možné vypočíst, nakolik si můžeme dovolit rotovat mozek uvnitř stereologického software, aniž bychom významně změnili výsledky měření plochy dané struktury. Jinými

slovy, není jisté, jak je veliký úhlový interval, v rámci kterého můžeme manipulovat s rotací mozku, aniž bychom získali odlišné výsledky. Zodpovězení této otázky by mělo velký vliv na vnitřní porovnatelnost různých studií volumetrie hipokampu, bez ohledu na odlišné úhly zobrazení při měření.

Mezi neočekávané nálezy patřila vysoká individuální variabilita v rotaci mozku a lebky na MR (až 35°). V případě rotace lebky jsme využili spolehlivou antropologickou míru pro její evaluaci (Frankfurtskou horizontálu - ta je považována za jednu z nejspolehlivějších antropologických rovin). Porovnání natočení mozku v námi sledovaných rovinách (AC-PC osa vs. nat osa, hipp osa vs, nat osa) a rotace lebky ukazovaly podobně individuální variabilitu. Měření plochy v tzv. ideálním řezu hipokampu ve všech třech námi sledovaných rovinách pak ukázalo, že reorientace do AC-PC osy nebo nat osy vykazuje stejné výsledky. Naproti tomu reorientace do hip osy a měření plochy dává výsledky výrazně odlišné. Ukázali jsme, že reorientace do AC-PC osy, která je rutinně využívána při volumetrických měřeních, není nutná, lze použít přímo nativní rovinu zobrazení.

V případě porovnání hipp osy vs. nat osy se ukázalo snížení rozsahu dorzální rotace hlavy, nebo alespoň jejího temporálního laloku, u AD pacientů a to zejména na levé straně. Tento nález je konzistentní s celkovým snížením objemu hipokampu u AD pacientů. Zdá se, že zmenšení objemu hipokampu může mít zvláštní efekt na pozici celého mozku uvnitř lebky, zvláště pak ve fossa cerebri media, kde se spánkový lalok nachází. Je otázkou, co přesně zodpovídá za variabilitu pozice mozku uvnitř lebky u AD pacientů a zdali je možné ji připsat rozdílům v pozici lebky uvnitř MR, nebo geometricky specifické atrofii mozkové tkáně. Pokud by atrofie byla příčinou variability pozice, pak jakékoliv normalizace nejsou validní z důvodu torze tkáně, její elongace a možná dosud nerozpoznané variabilitě vnitřní geometrie mozkové tkáně při atrofii. V dostupné literatuře jsme nenalezli srovnatelné údaje popisující efekt atrofie CNS na jeho specifickou pozici uvnitř lebky.

9.6 Vliv chronického stresu na hipokampus u laboratorního potkana

Studovali jsme opožděný vliv zvýšených hladin kortikosteronu na volumetrii, počet neuronů a hrubé znaky neurodegenerace hipokampální formace u laboratorního potkana kmene Long-Evans. Zvířata byla vystavena kortikosteronu po tři týdny technikou podkožních pelet (kontrolní skupina dostávala cholesterol). Měření počtu neuronů, hrubé známky degenerace a objemy byly stanoveny za sedm týdnů po

ukončení podávání kortikosteronu. Během podávání kortikosteronu jsme pozorovali snížení plasmatické hladiny ACTH. To lze vysvětlit přímou inhibicí uvolňování ACTH kortikosteronem z adenohypofýzy a nepřímou inhibicí uvolňování ACTH přes CRH regulaci (Parker a Rainey, 2004). Protože jsme se zaměřili na dlouhodobé účinky, spíše než na krátkodobé, neprovedli jsme stereologické měření v momentě suprese vrcholu ACTH. Změny, ke kterým mělo dojít v období mezi maximální redukcí ACTH (třetí týden) a stereologickými měřeními (desátý týden) by zahrnovaly: pokles plazmatické hladiny kortikosteronu, obnovení normální funkce HPA osy a vznik neuronální a gliové reparativní jizvy. U kontrol byl objem pravého hipokampu významně větší v porovnání s levým k velikosti mozku a to i po normalizaci. Nenalezli jsme však významný rozdíl v objemu mezi levou a pravou hemisférou u kontrolní skupiny. Větší levou hemisféru v porovnání s pravou uvádí (Sahin a kol., 2001), ale na vyšší hladině významnosti v porovnání s našimi výsledky. Jiná studia na samcích kmene Long-Evans ukázala opak - pravá hemisféra byla větší než levá. Detailní analýza pak ukázala rozdíl mezi tloušťkou neokortexu (vpravo silnější než vlevo), ačkoliv měření průřezu hemisférami, hipokampy, mozečkem, thalamem a mozkovým kmenem neprokázaly spolehlivé rozdíly (Kolb a kol., 1982). Nejvýznamějším výsledkem naší studie bylo zmenšení absolutního objemu pravého hipokampu u skupiny s podávaným kortikosteronem. Jelikož normalizace objemu hipokampu neměla vliv na toto snížení objemu ani na levostrannou asymetrii, je možné vysvětlit objemové zmenšení pravé hemisféry zmenšením objemu pravého hipokampu. Podobné výsledky jsou ve studii, kdy krátkodobá a přechodná stimulace na počátku života vedla k posílení pravostranné hipokampální volumetrické dominance v dospělosti u kmene Long-Evans (Vesrstynen a kol., 2001). Podobně, vystavení novým podnětům (neonatal novelty exposure, NNE) a následná krátkodobá i dlouhodobá potenciace (dvě formy synaptické plasticity mající dlouhodobé trvání), byly nalezeny pouze v pravém hipokampu (Tang a kol., 2008). Kromě toho senzitivita synaptické plasticity pravého hipokampu při dlouhodobém podávání kortikosteronu, měřeno dlouhodobou potenciací *in vitro,* byla významně zvýšena po vystavení novým podnětům (NNE) v porovnání s kontrolami (Tang a Zhou, 2002). To je v souladu s našimi výsledky, kde byl zmenšen objem pouze pravého hipokampu vlivem podávání kortikosteronu. Ačkoliv stres většinou redukuje objem hipokampu, přínos naší studie je ve zjištění, že k této redukci dochází pouze na pravé straně. To potvrzuje naši hypotézu, že

neonatální vystavení novému podnětu (NNE) zvyšuje asymetricky objem pravého hipokampu, zatímco podávání kortikosteronu má účinek opačný, zvláště pak v subiculum a méně v gyrus dentatus a podčástech CA1-CA3. Zmenšení objemu hipokampu vpravo u skupiny s podávaným kortikosteronem může být způsobeno snížením počtu neuronů. Významné snížení počtu neuronů v gyrus dentatus a CA3 podoblasti hipokampu bylo ale nalezeno pouze u laboratorního potkana exponovaného glukokortikoidům v neonatálním období, ne v dospělosti (Sousa a kol., 1998). Podobně, naše data ukázala pouze malé (CA1 a CA2 podoblasti) nebo žádné změny (gyrus dentatus a CA3) v počtu neuronů. Subiculum jsme do měření počtu neuronů nezahrnuli. Ačkoliv subikulární pyramidové neurony mají morfologicky uniformní tvar, existují kontroverze ohledně jejich laminární a kolumnární organizace a sublaminace (Ishizuka, 2001), což komplikuje jejich měření. Uspořádání neuronů v pyramidální vrstvě subiculum je volnější v porovnání s podoblastí CA1 a také elektrofyziologicky můžeme unikátně dělit tyto neurony na „bursting“ a „spiking“ neurony v porovnání s ostatními oblastmi hipokampu (Witter, 2006). Ačkoliv jsme subiculum nezahrnuli do našich měření, jedná se o důležitou podoblast hipokampu, kterou by bylo vhodné v dalších studiích zohlednit.

V druhé části experimentu jsme sledovali, zda objemové změny hipokampu mohou být výsledkem probíhající neurodegenerace a proto jsme k volumetrii přidali ještě měření počtu neuronů a hrubé známky neurodegenerace. Nezjistili jsme ale významné změny mezi kontrolami a skupinou, které byl podáván kortikosteron. Počty neuronů ani sledování neurodegenerace tedy nevysvětlují snížení objemu hipokampu vpravo. Neurodegenerace hraje roli pouze ve specifickém krátkodobém intervalu a pozorované objemové změny tedy nemohou být důsledkem dlouhodobě probíhající neurodegenerace. Významné změny v počtu degenerujících neuronů jsme nepozorovali, jelikož byly pravděpodobně odstraněny imunitním procesem (neuroglie) nebo dalšími reparativními procesy v CNS. Změny v hladinách kortikosteronu ale vedou ke změnám v mikrostruktuře neuronů, k hrubým známkám neurodegenerace a poškození kognitivních funkcí (Schubert a kol., 2008). Většina těchto změn je zřejmě reverzibilní a později je obtížné prokázat je morfologicky (Sousa a kol., 1999; Joëls, 2008). Permanentní zmenšení objemu pravého hipokampu u skupiny s podávaným kortikosteronem může být vysvětleno neuroplasticitou (zmenšením objemu cytoplasmy neuronu, ztrátou synapsí apod.), nebo změnami na úrovni molekulární biologie. Např. funkční asymetrie vysoce

afinitního vychytávání cholinu (HACU) bylo nalezeno pouze v levém hipokampu u Wistar potkanů a to pouze u dospělých samců, nikoliv samic (Krištofiková a kol., 2004). Není také jasné, jestli snížení objemu pravého hipokampu následkem podávání kortikosteronu je anebo není specifické pro kmen Long-Evans, nebo pro laboratorního potkana vůbec.

9.7 Vliv chronického podávání kortikoidů na CTA

Chuťová averze je integrální součástí potravního chování. Je to biologicky důležitý fenomén, jelikož přežití organismu závisí na schopnosti účelně získávat a zpracovávat potravu a vyhýbat se možným jedům. Potravní chování a dlouhodobá regulace váhy společně s regulací příjmu potravy je synchronizována složitými interakcemi mezi CNS a periferními orgány (regulace se účastní dále, mimo jiné, leptiny, glukokortikoidy, insulin, hormony GIT) (Dostálová a kol., 2007; Zach a kol., 2006; Papežová a kol., 2005). Naše výsledky ukazují na poškození utváření CTA vlivem chronického podávání kortikosteronu. Podmíněná chuťová averze je dobře zavedené behaviorální paradigma učení se a paměti, a představuje užitečný nástroj ke studiu neuronální plasticity (mezi výhody patří dobře anatomicky definované struktury, známé fyziologické buněčné mechanismy a jednoduchá měřitelnost) (Bureš, 1998). Regulace je řízena z hypotalamu, prefrontální kůry mozku, amygdaly, striata a z mezencefalonu. Vliv stresu a kortikosteronu na učení a paměť je v popředí zájmu vědeckých debat, jelikož se účastní řady neuropsychiatrických onemocnění. Morfologické studie ukázaly, že dlouhodobé vystavení stresu nebo nadměrným dávkám glukokortikoidů vede k časově závislému poškození neuronů, rozsahem od počáteční vratné atrofie dendritických výběžků (Woolley a kol., 1990; Watanabe a kol., 1992a; Magarinos a kol., 1995) po nevratnou ztrátu hipokampálních pyramidových neuronů (Landfield, 1987; Sapolsky a kol., 1985). Toto stresem nebo glukokortikoidy vyvolané strukturální postižení se zdá spojené s deficitem v učení se, a v uchovávání informací v paměti. Posilování tvorby CTA vlivem akutního podávání kortikosteronu bylo popsáno dříve (Tenk a kol., 2006). Efekt akutního a chronického podávání kortikosteronu na kognitivní schopnosti se strukturálně i funkčně velmi liší (Sousa a kol., 1999). Mozková atrofie doprovázející poruchy příjmu potravy je časně detekovatelná. Strukturální morfometrie mozku ukázala, že objem jak bílé, tak šedé hmoty, je v případě akutní anorexie výrazně snížen. Po úspěšné realimentaci má ale bílá hmota tendenci

k návratu do původního objemu, zatímco šedá hmota ne. To je možné částečně vysvětlit trvalou ztrátou neuronů nebo glie způsobené např. vysokými hladinami kortizolu. Mezi alternativní vysvětlení můžeme uvést, že ztráta neuronů není následkem anorexie, ale abnormálního vývoje nervového systému. Výsledky ukazují na dlouhodobé změny neschopnosti zvířete reagovat adekvátně na různé kognitivní úlohy, což může být spojeno se strukturálními změnami v CNS (Bureš, 1998). Nenalezli jsme signifikantní zvýšení/snížení počtu neuronů a hrubých známek neurodegenerace v prefrontální kůře, amygdale, nebo hipokampu na řezech mozku barvených podle Nissla v experimentu na zvířeti. Takovýto nález je ve shodě s Tata a kol. (2006), kde jsou popsány u experimentálního zvířete subcelulární změny po aplikaci kortikoidů. Dřívější studie detekovaly pouze hrubé morfologické změny těl neuronů a dendritů (Sapolsky a kol., 1985; Wolley a kol., 1990), což je možné částečně vysvětlit odlišnou metodologií. Drobné ztráty počtu neuronů v laterální části parabrachiálního jádra (nepřevyšující 2 % z celkového počtu neuronů) je třeba dále verifikovat imunohistochemicky pro zpřesnění nálezu. Poškození parabrachiálního komplexu lze očekávat kvůli jeho zapojení v okruhu CTA reakce. Tato poškození nevykazovala asymetrické změny.

9.8 Automatická analýza objemu struktur CNS na FS

Pro automatickou volumetrii hlavních podkorových struktur CNS u člověka jsme zvolili software FreeSurfer, který je často využíván v teoretických studiích pro měření úbytku hmoty mozku u AD. Naší hypotézou bylo snížení objemu všech měřených struktur, zvláště pak amygdalárního komplexu, ale opačně zvýšeného objemu komor u AD pacientů v porovnání s kontrolami. Dle očekávání naše výsledky byly v souladu s obecně přijímaným konceptem snížení objemu CNS u AD (de Jong a kol., 2008; Philippi a kol., 2012). Pro vyloučení artefaktů matematického zpracování jsme použili dvě verze programu FS – v5.2.0 a v5.3.0 a obě verze vedly ke shodným výsledkům. Po diskuzi s tvůrci programu FA (MGH/HST Athinoula A. Martinos Center for Biomedical Imaging) jsme došli k závěru, že některé anatomické hranice oblastí CNS je potřeba v budoucnu zpřesnit v software pro lepší výsledky (např. podoblasti hipokampu). První pokus o neurohistologickou kolokalizaci podoblastí hipokampu na MR s vysokým rozlišením již vedl k znatelnému vylepšení ohraničení v prostředí FS (Adler a kol., 2012). Přesto však v některých případech těžšího postižení mozkové tkáně při AD atrofii mohou být

hranice struktur těžko rozlišitelné. Na druhou stranu manuální a automatická segmentace mediotemporálních struktur CNS u AD, MCI a kontrol, zaměřená převážně na korové oblasti (entorhinální, perirhinální a parahipokampální kůra a hipokampus) se od sebe výrazně nelišila (Insausti a kol., 2011). Podobně porovnání manuální a automatické volumetrie hipokampu u MCI a AD ukázalo, že obě metody korelují výsledky s vysokou shodou, za předpokladu zohlednění věku, pohlaví a normalizace k intrakraniálnímu objemu lebky (Shen a kol., 2010).

Analýza strukturální asymetrie ukázala na rozdíly mezi AD a kontrolní skupinou. Úbytek hmoty nucleus accumbens byl oboustranně významně snížený u AD skupiny v porovnání s kontrolami, podobně jako u Pievani a kol. (2013) a pouze lehce snížený v nucleus caudatus na straně pravé. Tyto dvě sousedící struktury mají rozdílnou funkci. Obě náleží k bazálním gangliím, nucleus accumbens je však zapojen v systému odměny a nucleus caudatus je součástí okruhů motorické regulace.

V případě kontrolní skupiny jsme nalezli statisticky významné asymetrické změny objemu pouze u bílé hmoty mozečku, u mozečkové kůry byla asymetrie hemisfér statisticky nevýznamná. V případě AD skupiny jsme zjistili významnou asymetrickou distribuci v počtu telencefalických korových defektů vlevo a vpravo a významné asymetrické změny v objemu postranních komor a amygdalárního komplexu. Objemovou asymetrii bílé hmoty mozečku i korových objemů koncového mozku v případě AD skupiny lze vysvětlit asymetrickou ztrátou obou objemů v procesu progrese AD onemocnění (Colloby a kol., 2014). Ve skupině pacientů s AD jsme nalezli větší objem levé postranní komory v porovnání s pravou. Analýza spánkového rohu postranní komory asymetrické změny objemu nezachytila, ačkoliv byl přítomen lehce zvýšený objem levé komory oproti pravé. To naznačuje, že objem spánkového rohu postranní komory nehraje zásadní roli v asymetrii objemu postranních komor jako celku u AD, což považujeme za významný nález. Znamená to, že ostatní části postranního komorového systému hrají v této asymetrii větší roli. Není zatím možné touto metodou upřesnit, které podčásti komorového systému se na tomto zvětšení podílejí, zda čelní roh, centrální část, nebo týlní roh postranní komory. Dle očekávání jsme nalezli výraznou pravostrannou asymetrii amygdalárního komplexu u AD skupiny, zatímco u kontrolní skupiny jsme žádnou asymetrii nepozorovali. Předpokládáme, že asymetrie amygdalárního komplexu

doprovází podobnou distribuci asymetrie, objemovou ztrátu a pravostrannou asymetrii hipokampu u AD pacientů (Mrzílková a kol., 2012).

9.9 Traktografie komisurálních vláken u AD pacientů

Úbytek neuronů v šedé hmotě AD pacientů lze pozorovat nepřímo traktografickým zobrazením a měřením komisurálních vláken především temporálního laloku, který se nejvíce podílí na konsolidaci paměti. Přes počet vláken komisurálních spojení temporálního laloku a jejich dalších charakteristik můžeme přesněji vyhodnotit difúzní úbytek neuronů. Paměťová spojení probíhají cestou obou fornixů a rovněž významné interhemisferické spojení jde cestou commisura anterior. Corpus callosum, zvláště pak část CC mid-posterior (Witelson a kol., 1989) propojující parietální asociační kůru s gyrus cinguli, se významně podílejí na konzolidaci paměťových okruhů (Papez, 1995).

Z DTI skenů 3T MRI z Pracoviště radiodiagnostiky a intervenční radiologie IKEM pacientů i kontrolních osob jsme vytvořili traktografické mapy, ze kterých jsme vyhodnotili počty vláken a další charakteristiky axonů (neuspořádanost vláken, kontinuita mikrofilament a kvalita myelinu) daných oblastí. Pomocí 3D rekonstrukce z T1 vážených řezů (MPR) jsme provedli vizuální kontrolu v 3D zobrazení vláken v námi sledovaných oblastech.

Statisticky jsme nejprve porovnali výsledky měření počtu vláken fornixů a commisura anterior, přičemž statisticky významný posun jsme zaznamenali u pravého fornixu, kdy u AD pacientů došlo k poklesu počtu vláken. U levého fornixu AD pacientů jsme statisticky významný pokles počtu vláken nezaznamenali a stejně tak tomu bylo i u commisura anterior.

Pomocí traktografického zobrazení komisur a jejich kvantifikace jsme zjistili, že nedochází k úbytku vláken v commisura anterior, a tak předpokládáme, že k difúznímu úbytku neuronů v jí propojených oblastech (spánkový lalok) také nedochází. Počet vláken pravého a levého fornixu propojujících hipokampus s dalšími strukturami CNS signifikantně klesá jen na pravé straně, a to přičítáme lateralizovanému úbytku neuronů mezi pravým a levým hippokampem (Mrzílková a kol., 2012).

Počet vláken u pacientů s AD v porovnání s kontrolami je signifikantně snížen u všech podčástí corpus callosum (mimo CC mid-posterior). U gyrus cinguli a jeho podčástí počet vláken mezi oběma skupinami neklesl. V ostatních charakteristikách

jako je FA, AX a RD byl signifikantně významný rozdíl ve všech částech corpus callosum i gyrus cinguli u pacientů s AD v porovnání s kontrolami (Wang a kol., 2014). Z těchto výsledků usuzujeme, že změny na subcelulární úrovni axonu (stav mikrofilament, myelinu a míra neuspořádanosti FA, AX, RD) začínají u AD dříve, než dojde k reálnému úbytku vláken bílé hmoty a snížení jejich počtu. Překvapivým nálezem bylo, že v oblasti CC mid-posterior, kde jsme očekávali kvůli propojení asociační kůry parietálních laloků signifikantní úbytek, se paradoxně změny neprojevily. Je možné, že právě asociační oblast parietální kůry kompenzuje u pacientů s AD deficit kognitivních funkcí způsobený poškozením mediotemporální oblasti.

10 Závěr

V experimentu na laboratorním potkanovi i u člověka jsme se pokusili kvantifikovat změny struktur CNS potižené chronickým stresem a nemocí AD.

Naše nová volumetrická metodika využívající polysiloxanovou dentální pryskyřici je, v porovnání se zobrazovacími metodami, relativně jednoduchá a levná. Je také dostatečně přesná, ale nelze využít v experimentu *in vivo*. Kromě potvrzení alterace planum temporale u pacientů se schizofrenií již popsané v literatuře (Obr. 10) (Hirayashu a kol., 2000) naše výsledky ukazují poprvé změny v lateralitě planum temporale u pacientů s demencí, statisticky významné zvláště u AD skupiny. Informace ohledně stupně laterality planum temporale mohou být využity jako doplňkový materiál v situacích, kdy informace o rukovosti chybí, jako je tomu např. u zemřelých pacientů.

Neurohistologická evaluace změn ve třetí vrstvě pyramidových neuronů planum temporale (zvláště pak podčástí přechodu do insuly, do Sylviovy rýhy a do gyrus temporalis superior) u pacientů s AD navazuje na předchozí výsledky volumetrické metodologie měření planum temporale polysiloxanovou pryskyřicí. Data ze studie PT sledující hrubé morfologické změny ukázala pravo-levý posun v asymetrii korové tloušťky, plochy a objemu u kontrol a obrácení této asymetrie do levo-pravé u AD skupiny. V neurohistologické evaluaci změn jsme nalezli podobnou pravo-levou asymetrii u kontrolní skupiny a pokles, vymizení, nebo obrat této asymetrie u AD skupiny. Takto lze tedy hrubé morfologické změny v planum temporale u AD částečně vysvětlit neurohistologickými změnami ve třetí vrstvě pyramidových neuronů. Navrhujeme, že by metoda měření délky pyramidových neuronů šla využít klinicky jako další diagnostické, neuropatologické vyšetření AD post mortem.

Evaluace volumetrie hmoty mozečku nebo pontu mozkového kmene ukázala, že na MR tyto změny, ačkoliv jistě existující, nedávají statisticky signifikantní výsledky, využitelné klinicky podobně jako je tomu v případě volumetrie hipokampu. Pacienti s AD tedy na MR vykazují dobře měřitelné objemové změny hipokampu (a to i asymetricky), ale ne mozečku nebo pontu mozkového kmene.

Reorientace nativních snímků z magnetické rezonance mozku do AC-PC osy nevede k významným změnám ve velikosti plochy řezu hipokampem. Předpokládáme, že nevyhnutelná drobná sagitální rotace hlavy pacienta (např. kvůli velikosti zádových

svalů, abnormálnímu zakřivení páteře, tvaru lebky) nemá významný vliv na měření plochy mediotemporálních struktur. Proto tedy pro rutinní měření plochy hipokampu v klinice můžeme použít pouze nativní snímky, jelikož jejich reorientace do standardizované AC-PC osy není nezbytná. Vliv ale může mít asymetrická atrofie mozkové tkáně. Také množství a objem mozkomíšního moku v komorách nebo subarachnoidálním prostoru může přispět ke změnám v objemu nebo tvaru. Úpon dura mater na periostu lebky je variabilní a může ovlivnit objem subdurálního nebo epidurálního prostoru. To pak může vést k ventrální nebo dorzální torzi čelního laloku (Yakovlevská torze), která může vést k většímu natočení AC-PC osy, v porovnání s natočením dlouhé osy hipokampu nebo naopak. V případě atrofie temporálního laloku bude větší natočení úhlu mezi AC-PC vs. hipokampem vzhledem k poklesu pozice celého spánkového laloku společně s hipokampem do střední lební jámy. Shrnuto, došli jsme k závěru, že je obtížné vymezit všechny možné efekty mající vliv na pozici mozku uvnitř lebky, takže je otázkou, zdali jsou reorientace v literatuře skutečně validní. Zjistili jsme ale, že plocha řezu hipokampu v námi definovaném optimálním řezu na nativním snímku je srovnatelná s plochou po reorientaci hipokampu do AC-PC osy, což je dle literatury standardní procedura. Pro kliniku je tato reorientace relativně časově náročná, takže vidíme význam našich výsledků ve zjednodušení této praxe. Pro časnou diagnostiku v klinické praxi není tedy nutná reorientace.

Měření vlivu dlouhodobého podávání kortikosteronu na morfologii hipokampu u laboratorního potkana objevilo dvě zásadní skutečnosti. První z nich byla významná objemová asymetrie hipokampu vpravo – vlevo. U kontrolní skupiny byl objem pravého hipokampu výrazně vyšší v porovnání s ostatními měřenými objemy: s levým hipokampem u kontrol a levým i pravým hipokampem u zvířat s podáváným kortikosteronem. Objem levého hipokampu se mezi skupinami nelišil. Druhou skutečností pak byl efekt dlouhodobého podávání kortikosteronu na pravý hipokampus, kde jsme zjistili významný rozdíl v objemu a zvláště v asymetrii podčástí hipokampu mezi kontrolami a zvířaty s podávaným kortikosteronem. Řada studií popisuje vliv kortikosteronu na objem hipokampu. Výsledky však nejsou jednoznačné. Vliv kortikosteronu na asymetrii hipokampu je málokdy sledován. V tomto je naše studie unikátní.

Narušení CTA reakce podle našich exprimentů nevedlo k asymetrickým morfologickým změnám v žádné ze sledovaných struktur (prefrontální kůra,

amygdalární komplex, nucleus parabrachialis). Je možné, že dlouhodobější časové období po narušení CTA reakce by tyto změny mohlo zachytit.

Při automatické rekonstrukci snímků MR v programu FS jsme pozorovali levo-pravou asymetrii v počtu korových defektů, objemu celé postranní komory a pravo-levou asymetrii v objemu amygdalárního komplexu u AD skupiny. To se ale nepřekrývá s asymetriemi u kontrolní skupiny. Dalším důležitým nálezem byl vysoce významný pokles objemu nucleus accumbens a amygdalárního komplexu u AD skupiny v porovnání s kontrolami. Kromě toho jsme pozorovali vymizení pravo-levé asymetrie bílé hmoty mozečku u AD skupiny. Nepodařilo se nám prokázat nárůst pravo-levé asymetrie nebo významné zmenšení objemu u dalších měřených struktur u obou skupin (např. bazální ganglia, bílá hmota koncového mozku).

Pomocí traktografického zobrazení komisurálních vláken a jejich kvantifikací jsme zjistili významné snížení počtu vláken probíhajících pravým fornixem u pacientů s AD. V případě levého fornixu jsme zjistili nevýznamný úbytek vláken, stejně tak jsme nepozorovali ani rozdíl v počtu vláken probíhajících v commissura anterior u pacientů s AD.

Corpus callosum i gyrus cinguli v charakteristikách neuspořádanosti vláken (FA), stavu myelinu (RD) a integrity mikrofilament (AX) vykazovaly statisticky významné změny u skupiny AD v porovnání s kontrolami ve všech sledovaných podčástech. Snížení počtu vláken jsme u pacientů s AD nalezli pouze v oblastech CC anterior, CC mid anterior, CC centralis a CC posterior. V gyrus cinguli, stejně jako v oblasti CC mid posterior (propojující asociační oblasti parietální kůry), se nepotvrdila naše hypotéza o úbytku vláken u pacientů s Alzheimerovou nemocí.

11 Obrazová dokumentace

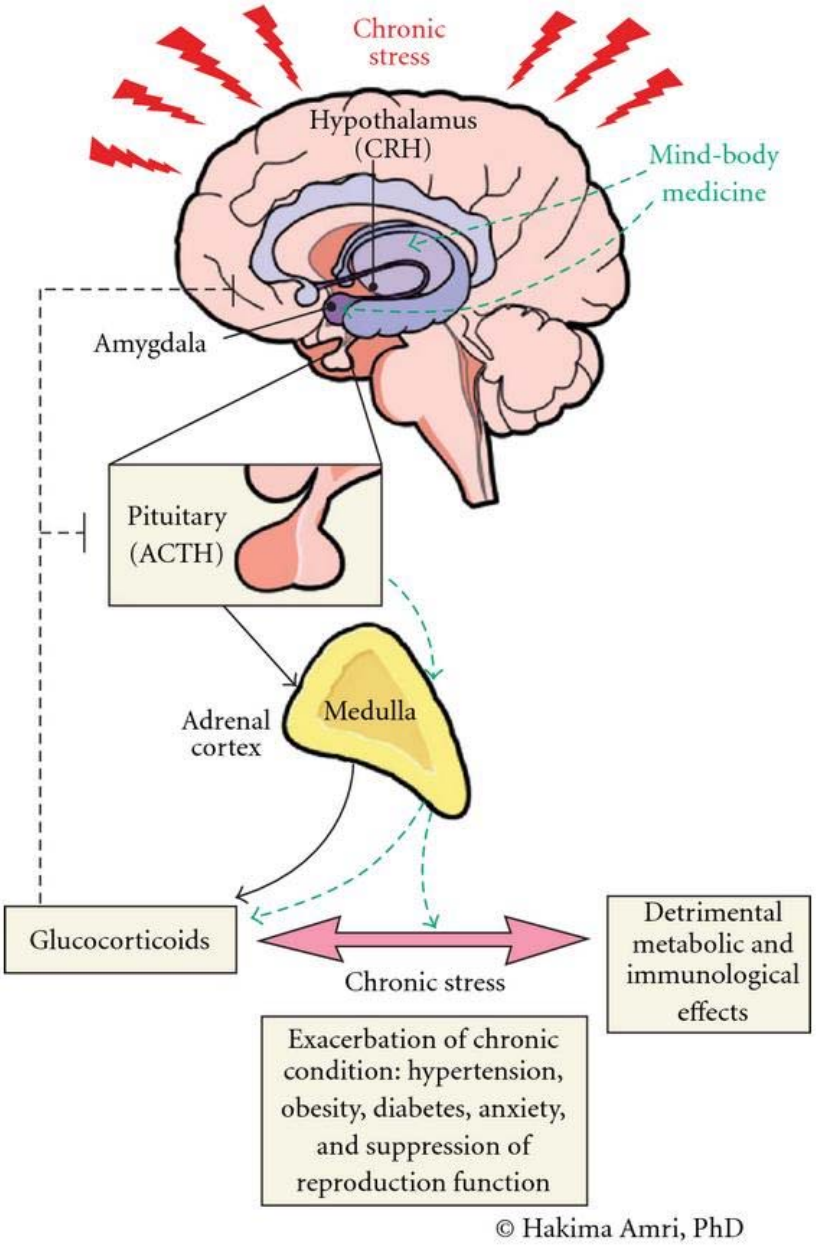

Obr. 1 Vliv chronického stresu na CNS (Amri, 2012)

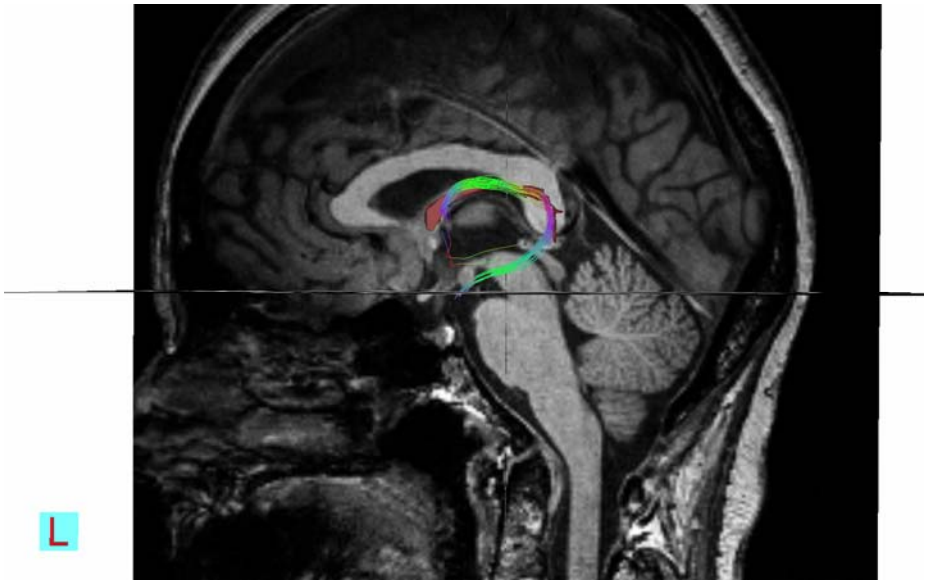

Obr 2 Traktografické zobrazení vláken fornixu v sagitální rovině.

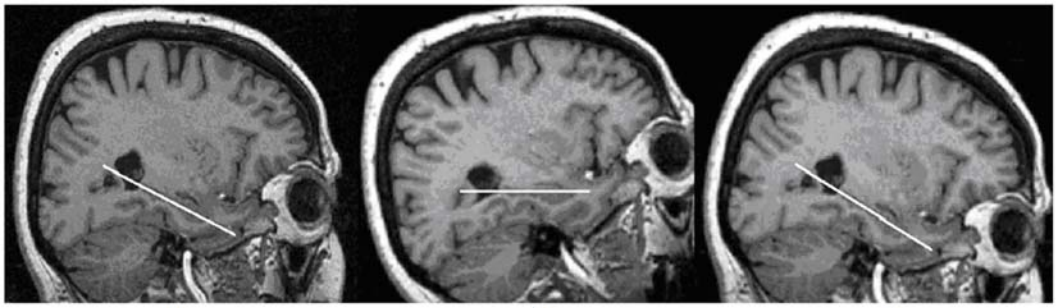

Obr. 3 Poloha dlouhé osy hipokampu (předo-zadní) v nativním snímku (A), reorientace do hipo-osy (B) a reorientace do CA-CP osy (C) (podle Mrzílková a kol., 2014)

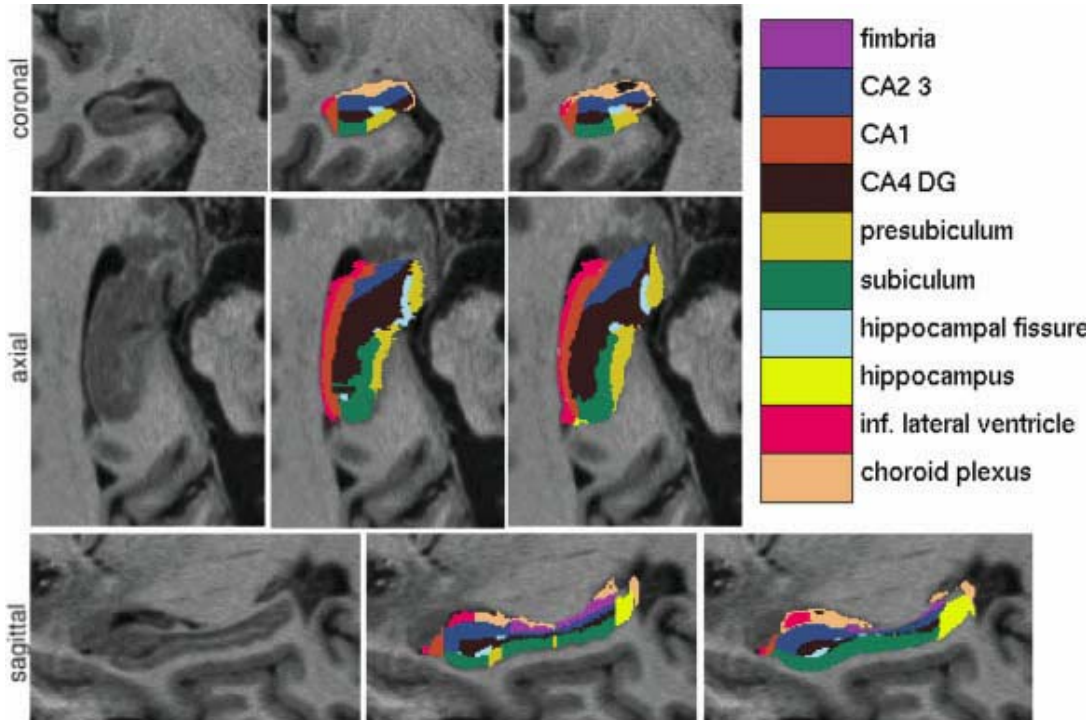

Obr. 4 Příklad automatické segmentace podčástí hipokampu na FreeSurfer (podle Leemput a kol., 2009)

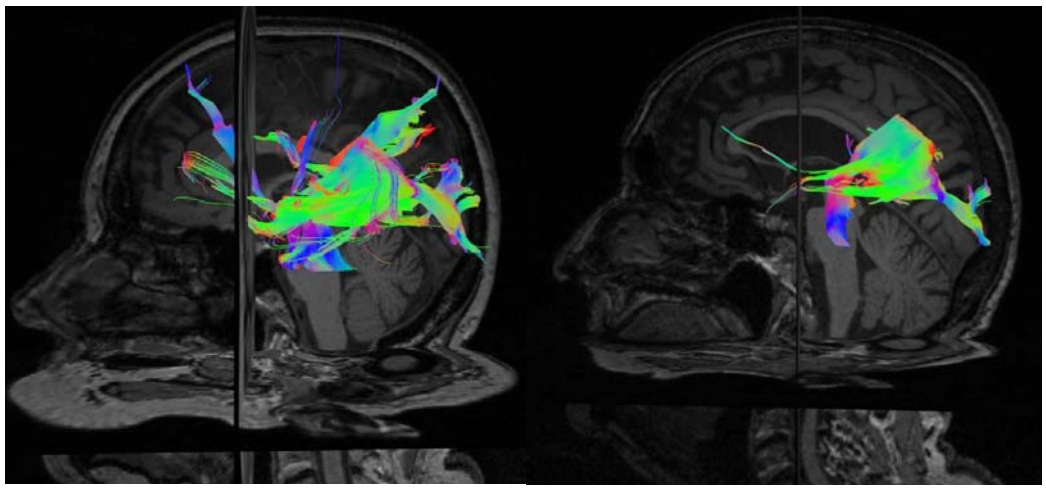

Obr. 5 Traktografie corpus callosum – CC posterior, porovnání počtu a zapojení vláken. Vlevo kontrola, vpravo AD pacient.

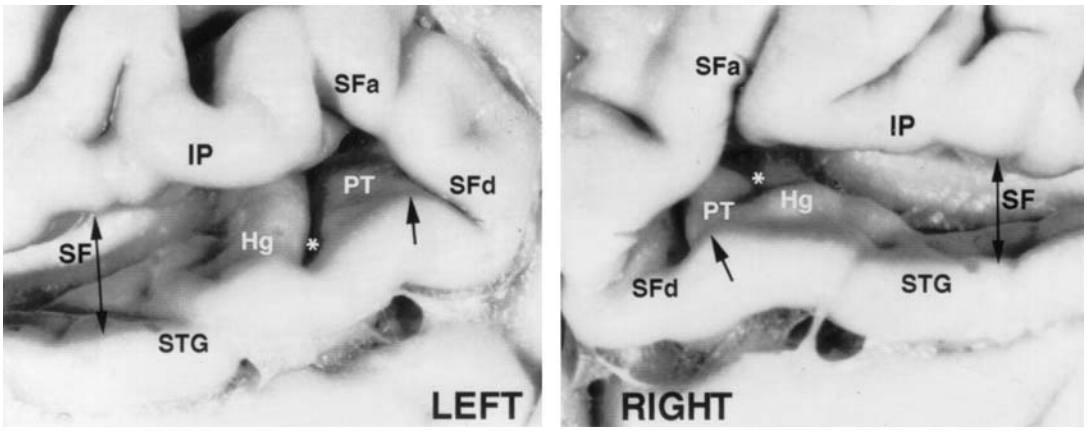

Obr. 6 Rozdíl v makroskopickém uspořádání planum temporale vlevo a vpravo u šimpanze (Gannon a kol., 1998)

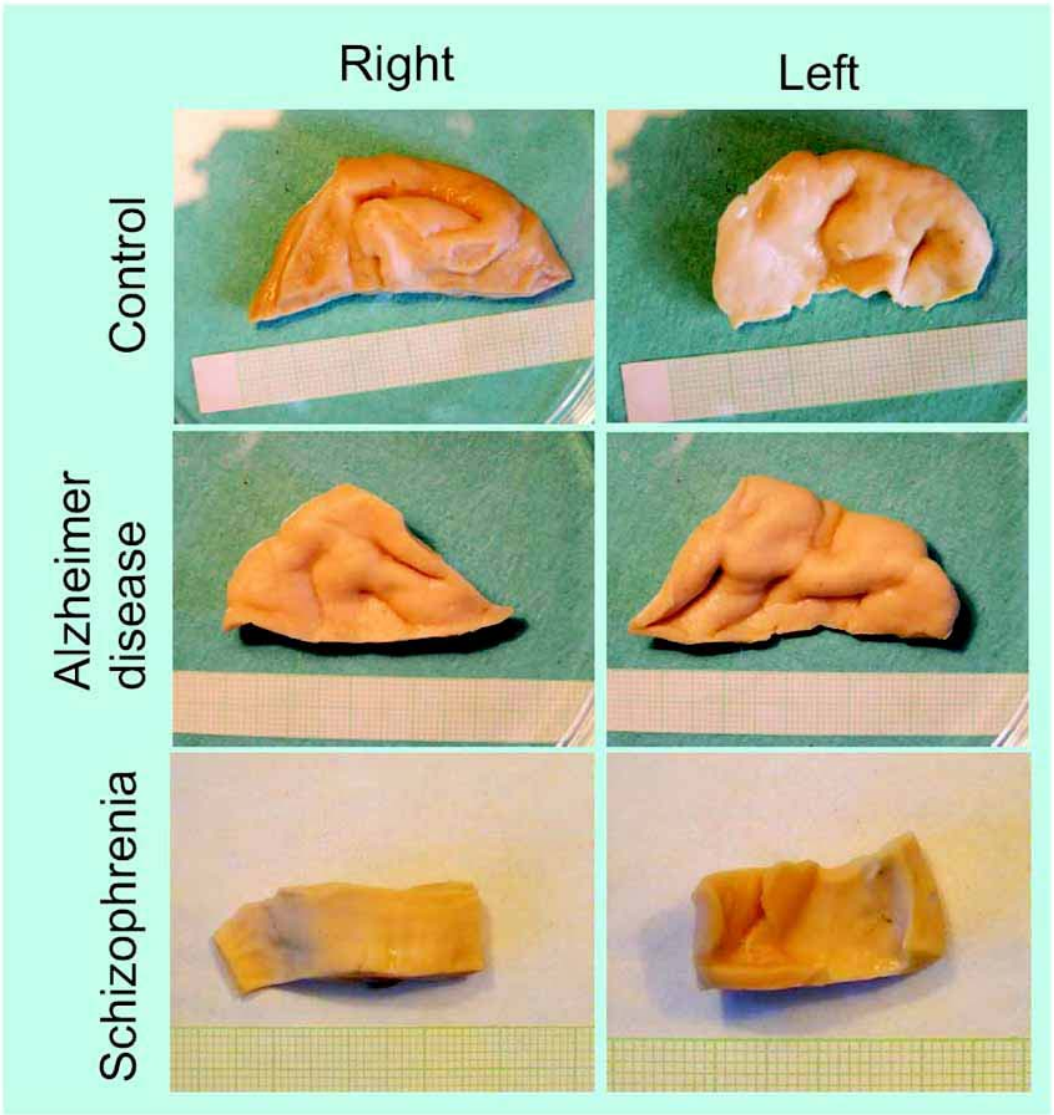

Obr. 7 Rozdíl ve velikosti a tvaru planum temporale u kontrol, pacientů s Alzheimerovou nemocí a se schizofrenií (Zach a kol., 2006)

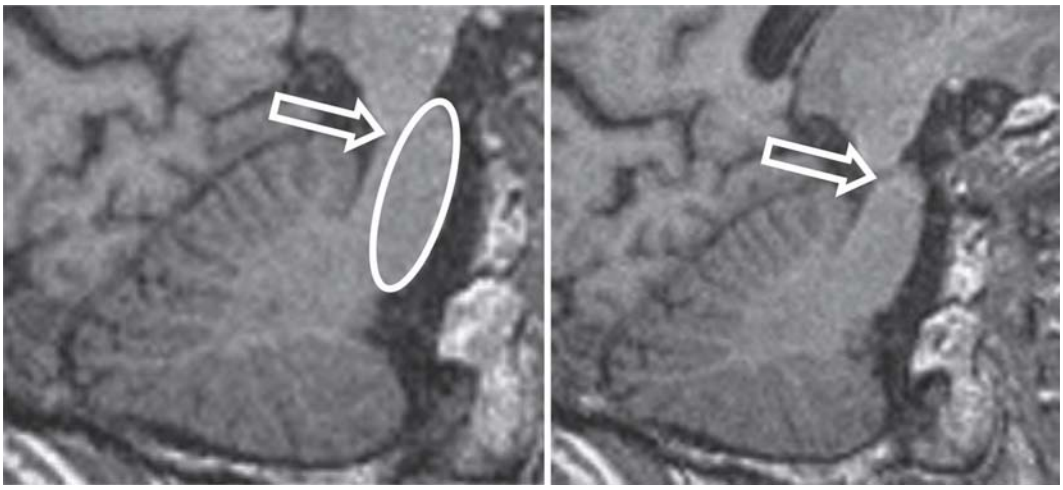

Obr. 8 Příklad ohraničení dorzální a laterální hranice pontu. Vlevo – šipka ukazuje velmi dobře viditelný přechod (mezi pons dorsálně a tegmentum) na snímku v blízkosti střední čáry, zobrazený jako kontrastní šedobílá linie ve tvaru eplipsoidu, která laterálně postupně vymizí. Vpravo – šipka ukazuje na prostor mezi crura cerebri a pedunculi cerebelli, kde již přechod pons – tegmentum není patrný. Oba snímky jsou v sagitální orientaci (Mrzílková a kol., 2012).

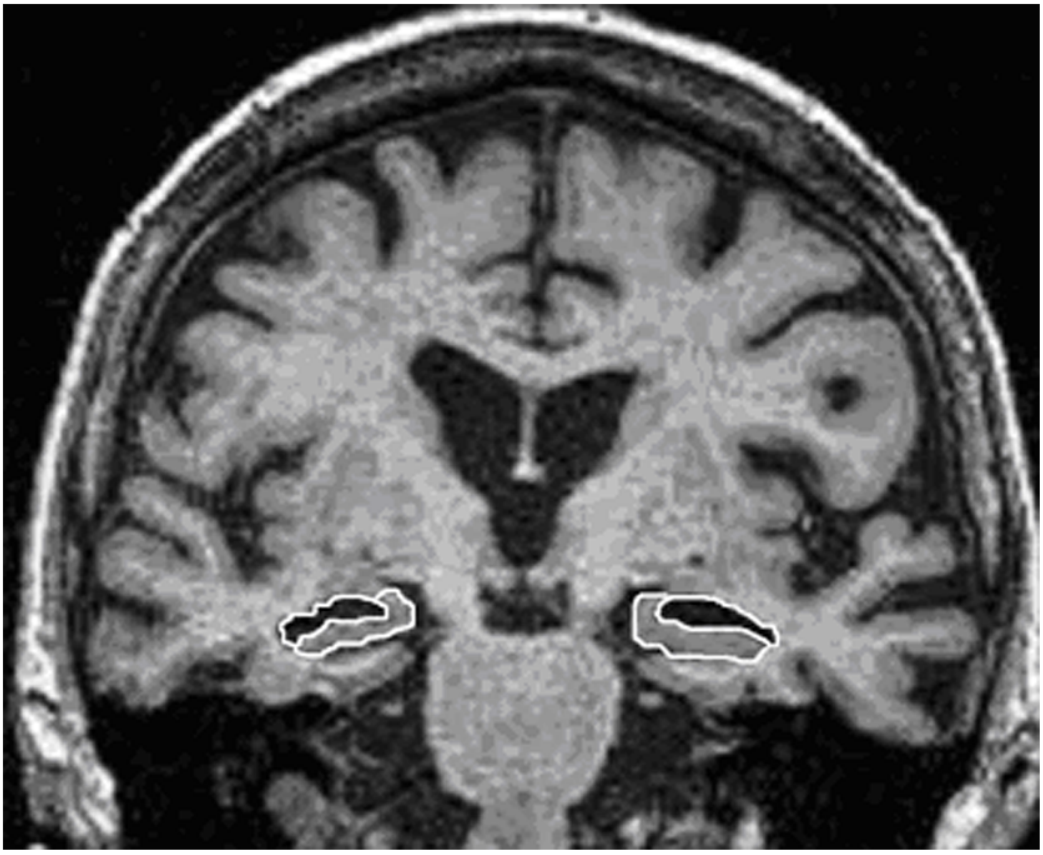

Obr. 9 Ukázka ohraničení hipokampu a spánkového rohu postranní komory vlevo a vpravo (Mrzílková a kol., 2014)

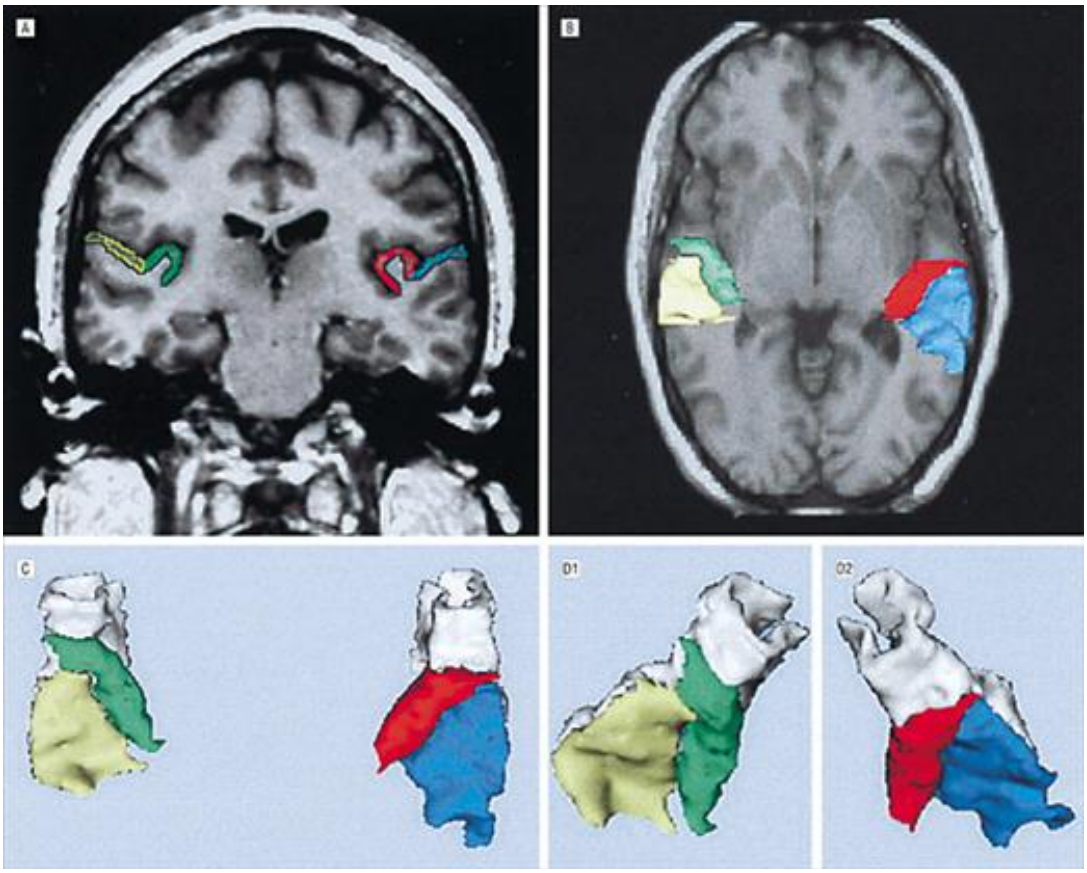

Obr. 10 Rozdíl ve velikosti planum temorale vpravo a vlevo u pacientů se schizofrenií (Hirayasu a kol., 2000)

12 Použitá literatura

ADLER, D. H.; LIU, A. Y.; PLUTA, J.; KADIVAR, S.; OROZCO, S.; WANG, H.; GEE, J. C.; AVANTS, B. B. a P. A. YUSHKEVICH. Reconstruction of the human hippocampus in 3D from histology and high-resolution ex-vivo MRI. *Proceedings / IEEE International Symposium on Biomedical Imaging*. 2012, **2012**, 294–297. ISSN 1945-7928.

BEASLEY, C. L.; CHANA, G.; HONAVAR, M.; LANDAU, S.; EVERALL, I. P. a D. COTTER. Evidence for altered neuronal organisation within the planum temporale in major psychiatric disorders. *Schizophrenia Research*. 2005, **73**(1), 69–78. ISSN 0920-9964.

BUREŠ, J.; BERMUDEZ-RATTONI, F. a T. YAMAMOTO. *Conditioned taste aversion. Memory of a special kind*. Oxford: Oxford University, 1998. ISBN 978-0-19-852347-5.

DE JONG, L. W.; VAN DER HIELE, K.; VEER, I. M.; HOUWING, J. J.; WESTENDORP, R. G.; BOLLEN, E. L.; DE BRUIN, P. W.; MIDDELKOOP, H. A.; VAN BUCHEM, M. A. a J. VAN DER GROND. Strongly reduced volumes of putamen and thalamus in Alzheimer's disease: an MRI study. *Brain*. 2008, **131**(Pt 12), 3277-3285. ISSN 0006-8950. DOI: 10.1093/brain/awn278.

DUBOIS, B.; FELDMAN, H. H.; JACOVA, C.; DEKOSKY, S. T.; BARBERGER-GATEAU, P.; CUMMINGS, J.; DELACOURTE, A.; GALASKO, D.; GAUTHIER, S.; JICHA, G.; MEGURO, K.; O'BRIEN J.; PASQUIER, F.; ROBERT, P.; ROSSOR, M.; SALLOWAY, S.; STERN, Y.; VISSER, P. J. a P. SCHELTENS. Research criteria for the diagnosis of Alzheimer's disease: revising the NINCDS-ADRDA criteria. *Lancet Neurology*. 2007, **6**(8), 734–746. ISSN 1474-4422.

COLLOBY, S. J.; O'BRIEN, J. T. a J. P. TAYLOR. Patterns of cerebellar volume loss in dementia with Lewy bodies and Alzheimer′s disease: A VBM-

DARTEL study. *Psychiatry Research*. 2014, **223**(3), 187-191. ISSN 0165-1781. DOI: 10.1016/j.pscychresns.2014.06.006.

DOSTÁLOVÁ, I.; BARTÁK, V.; PAPEŽOVÁ, H. a J. NEDVÍDKOVÁ. The effect of short-term exercise on plasma leptin levels in patients with anorexia nervosa. *Metabolism*. 2007, **56**(4), 497–503. ISSN 0026-0495.

GALABURDA, A. M.; CORSIGLIA, J.; ROSEN, G. D. a G. F. SHERMAN. Planum temporale asymmetry, reappraisal since Geschwind and Levitsky. *Neuropsychologia*. 1987, **25**(6), 853-868. ISSN 0028-3932. DOI:10.1016/0028-3932(87)90091-1.

GANNON, P. J.; HOLLOWAY, R. L.; BROADFIELD, D. C. a A. R. BRAUN. Asymmetry of chimpanzee planum temporale: humanlike pattern of Wernicke's brain language area homolog. *Science*. 1998, **279**(5348), 220-222. ISSN 0036-8075.

GESCHWIND, N. a W. LEWITSKY. Human brain: left-right asymmetries in temporal speech regions. *Science*. 1968, **161**(3837), 186-187. ISSN 0036-8075.

HARASTY, J. A.; HALLIDAY, G. M.; KRIL, J. J. AND C. CODE. Specific temporoparietal gyral atrophy reflects the pattern of language dissolution in Alzheimer's disease. *Brain*. 1999, **122**(Pt 4), 675-686. ISSN 0006-8950.

HICKOK, G. a K. SABERI. Redefining the functional organization of the planum temporale region: space, objects, and sensory-motor integration. In: POEPPEL, D. OVERATH, T.; POPPER, A. a R. R. FAY, eds. *The human auditory cortex.* Vol. 43. New York: Springer, 2012. Springer Handbook of Auditory.

HIRAYASU, Y.; McCARLEY, R. W.; SALISBURY, D. F.; TANAKA, S.; KWON, J. S.; FRUMIN, M.; SNYDERMAN, D.; YURGELUN-TODD, D.; KIKINIS, R.; JOLESZ, F. A. a M. E. SHENTON. Planum temporale and Heschl gyrus volume reduction in schizophrenia - A magnetic resonance imaging study of first- episode patients. *Archives of General Psychiatry*. 2000, **57**(7), 692-699. ISSN 0003-990X.

HUTSLER, J. J. The specialized structure of human language cortex: pyramidal cell size asymmetries within auditory and language-associated regions of the temporal lobes. *Brain and Language*. 2003, **86**(2), 226–242. ISSN 0093-934X.

INSAUSTI, R.; RINCÓN, M.; DÍAZ-LÓPEZ, E.; ARTACHO-PÉRULA, E.; MANSILLA, F.; FLORENSA, F.; GONZÁLEZ-MORENO, C.; ÁLVAREZ-LINERA, J.; GARCÍA, S.; PERAITA, H.; PAIS, E. a A. M. INSAUSTI. FreeSurfer automatic brain segmentation adaptation to medial temporal lobe structures: volumetric assessment and diagnosis of mild cognitive impairment. In: Ferrández IM, eds. New challenges on bioinspired applications. 4th international work-conference on the interplay between natural and artificial computation. In: FERRÁNDEZ, J. M.; ÁLVAREZ SÁNCHEZ, J. R.; DE LA PAZ, F. a F. J. TOLEDO, eds. *New Challenges on Bioinspired Applications. Proceedings, Part II*. Berlin: Springer, 2011, s. 112-119. ISBN 978-3-642-21325-0. Lecture Notes in Computer Science 6687.

ISHIZUKA, N. Laminar organization of the pyramidal cell layer of the subiculum in the rat. *Journal of Comparative Neurology*. 2001, **435**(1), 89-110. ISSN 0021-9967.

JOËLS, M. Functional actions of corticosteroids in the hippocampus. *European Journal of Pharmacology*. 2008, **583**(2-3), 312-321. ISSN 0014-2999. DOI: 10.1016/j.ejphar.2007.11.064.

KOLB, B.; SUTHERLAND, R. J.; NONNEMAN, A. J. a I. Q. WHISHAW. Asymmetry in the cerebral hemisphere of the rat, mouse, rabbit, and cat: the right hemisphere is larger. *Experimental Neurology*. 1982, **78**(2), 348-359. ISSN 0014-4886.

KRIŠTOFIKOVÁ, Z.; ŠŤASTNÝ, F.; BUBENÍKOVÁ, V.; DRUGA, R.; KLASCHKA, J. a F. ŠPANIEL. Age- and sex-dependent laterality of rat hippocampal cholinergic system in relation to animal models of neurodevelopmental and neurodegenerative disorders. *Neurochemical Research*. 2004, **29**(4), 671-680. ISSN 0364-3190.

LANDFIELD, P. W. Modulation of brain aging correlates by long-term alterations of adrenal steroids and neurally-active peptides. *Progress in Brain Research*. 1987, **72**, 279–300. ISSN 0079-6123.

LUFT, A. R.; SKALEJ, M.; SCHULZ, J. B.; WELTE, D.; KOLB, R.; BURK, K.; KLOCKGETHER, T. a K. VOIGHT. Patterns of age-related shrinkage in cerebellum and brainstem observed in vivo using three-dimensional MRI volumetry. *Cerebral Cortex*. 1999, **9**(7), 712–721. ISSN 1047-3211.

MAGARINOS, A. M. a B. S. McEWEN. Stress-induced atrophy of apical dendrites of hippocampal CA3c neurons: comparison of stressors. *Neuroscience*. 1995, **69**(1), 83–88. ISSN 0306-4522.

MCKHANN, G.; DRACHMAN, D.; FOLSTEIN, M.; KATZMAN, R.; PRICE, D. a E. M. STADLAN. Clinical diagnosis of Alzheimer's disease: report of the NINCDS-ADRDA Work Group under the auspices of Department of Health and Human Services Task Force on Alzheimer's Disease. *Neurology*. 1984, **34**(7), 939–944. ISSN 0028-3878.

MILLER, D. H. Biomarkers and surrgate outcome in neurodenerative disease: lessons from multiple sclerosis. *NeuroRx*. 2004, **1**(2), 284-294. ISSN 1545-5343.

MRZÍLKOVÁ, J.; ZACH, P.; BARTOŠ, A.; TINTĚRA, J. a D. ŘÍPOVÁ. Volumetric analysis of the pons, cerebellum and hippocampi in patients with Alzheimer's disease. *Dementia and Geriatric Cognitive Disorders*. 2012, **34**(3-4), 224-234. ISSN 1420-8008. DOI: 10.1159/000343445.

PAPEŽOVÁ, Hana; YAMAMOTOVÁ, Anna; UHER, Rudolf. Elevated Pain Threshold in Eating Disorders: Physiological and Psychological Factors. *Journal of Psychiatric Research*. 2005, **39**(4), 431-438. ISSN 0022-3956. DOI: 10.1016/j.jpsychires.2004.10.006 .

PAPEZ, J. W. A proposed mechanism of emotion. 1937. *Journal of Neuropsychiatry and Clinical Neuroscience*. 1995, **7**(1), 103-12. ISSN 0895-0172.

PARKER, K. L. a W. E. RAINEY. The adrenal glands. In: GRIFFIN, J. E. a S. R. OJEDA, eds. *Textbook of Endocrine Physiology*. New York: Oxford University Press, 2004, s. 319-348. ISBN 978-0-19-977425-8.

PHILIPPI, N.; NOBLET, V.; BOTZUNG, A.; DESPRÉS, O.; RENARD, F.; SFIKAS, G.; CRETIN, B.; KREMER, S.; MANNING, L. a F. BLANC. MRI-based volumetry correlates of autobiographical memory in Alzheimer's disease. *PLoS One*. 2012, **7**(10), e46200. ISSN 1932-6203. DOI: 10.1371/journal.pone.0046200.

PIEVANI, M.; BOCCHETTA, M.; BOCCARDI, M.; CAVEDO, E.; BONETTI, M.; THOMPSON, P. M. a G. B. FRISONI. Striatal morphology in early-onset and late-onset Alzheimer's disease: a preliminary study. *Neurobiology of Aging*. 2013, **34**(7), 1728-1739. ISSN 0197-4580. DOI: 10.1016/j.neurobiolaging.2013.01.016.

SAHIN, B.; ASLAN, H.; UNAL, B.; CANAN, S.; BILGIC, S.; KAPLAN, S. a L. TUMKAYA. Brain volumes of the lamb, rat and bird do not show hemispheric asymmetry: a stereological study. *Image Analysis & Stereology*. 2001, **20**(1), 9-13. ISSN 1580-3139. DOI: 10.5566/ias.v20.p9-13.

SAPOLSKY, R. M.; KREY, L. C. a B. S. McEWEN. Prolonged glucocorticoid exposure reduces hippocampal neuron number: implications for aging. *Journal of Neuroscience*. 1985, **5**(5), 1222–1227. ISSN 0270-6474.

SHAPLESKE, J.; ROSSELL, S. L.; WOODRUFF, P. W. R a A. S. DAVID. The planum temporale: a systematic, quantitative review of its structural, functional and clinical significance. *Brain research. Brain Research Reviews*. 1999, **29**(1), 26–49.

SHEN, L.; SAYKIN, A. J.; KIM, S.; FIRPI, H. A.; WEST, J. D.; RISACHER, S. L.; MCDONALD, B. C.; MCHUGH, T. L.; WISHART, H. A. a L. A. FLASHMAN. Comparison of manual and automated determination of hippocampal volumes in MCI and early AD. *Brain Imaging and Behavior*. 2010, **4**(1), 86-95. ISSN 1931-7557. DOI: 10.1007/s11682-010-9088-x.

SCHELTENS, P.; LEYS, D.; BARKHOF, F.; HUGLO, D.; WEINSTEIN, H. C.; VERMERSCH, P.; KUIPER, M.; STEINLING, M.; WOLTERS, E. C. a J. VALK. Atrophy of medial temporal lobes on MRI in ‘‘probable’’ Alzheimer’s disease and normal ageing: diagnostic value and neuropsychological correlates. *Journal of Neurology, Neurosurgery, and Psychiatry*. 1992, **55**(10), 967–972. ISSN 0022-3050.

SCHUBERT, M. I.; KALISCH, R.; SOTIROPOULOS, I.; CATANIA, C.; SOUSA, N.; ALMEIDA, O. F. a D. P. AUER. Effects of altered corticosteroid milieu on rat hippocampal neurochemistry and structure – an in vivo magnetic resonance spectroscopy and imaging study. *Journal of Psychiatric Research*. 2008, **42**(11), 902-912. ISSN 0022-3956.

SOUSA, N.; MADEIRA, M. D. a M. M. PAULA-BARBOSA. Corticosterone replacement restores normal morphological features to the hippocampal dendrites, axons and synapses of adrenalectomized rats. *Journal of Neurocytology*. 1999, **28**(7), 541-558. ISSN 0300-4864.

TATA, D. A.; MARCIANO, V. A. a B. J. ANDERSON. Synapse loss from chronically elevated glucocorticoids: relationship to neuropil volume and cell number in hippocampal area CA3. *Journal of Comparative Neurology*. 2006, **498**(3), 363–374. ISSN 0021-9967.

TEIPEL, S. J.; EWERS, M.; WOLF, S.; JESSEN, F.; KOLSCH, H.; ARLT, S.; LUCKHAUS, C.; SCHONKNECHT, P.; SCHMIDTKE, K.; HEUSER, I.; FROLICH, L.; ENDE, G.; PANTEL, J.; WILTFANG, J.; RAKEBRANDT, F.; PETERS, O.; BORN, C.; KORNHUBER, J. a H. HAMPEL. Multicentre variability of MRI-based medial temporal lobe volumetry in Alzheimer’s disease. *Psychiatry Research*. 2010, **182**(3), 244–250. ISSN 0165-1781. DOI: 10.1016/j.pscychresns.2010.03.003.

TENK, C. M.; KAVALIERS, M. a K. P. OSSENKOPP. The effects of acute corticosterone on lithium chloride-induced conditioned place aversion and locomotor activity in rats. *Life Sciences*. 2006, **79**(11), 1069–1080. ISSN 0024-3205.

TOGA, A. W. a P. M. THOMPSON. Mapping Brain Asymmetry. *Nature Reviews. Neuroscience*. 2003, **4**(1): 37-48. ISSN 1471-003X.

VAN LEEMPUT K.; BAKKOUR A.; BENNER T.; WIGGINS K.; WALD LL.; AUGUSTINACK J.; DICKERSON BC.; GOLLAND P.; FISCHL B. Automated Segmentation of Hippocampal Subfields from Ultra-High Resolution In Vivo MRI. *Hippocampus*. 2009, **19**(6), 549-557. ISSN 1050-9631. DOI: 10.1002/hipo.20615.

WANG, P. N.; CHOU, K. H.; CHANG, N. J.; LIN, K. N.; CHEN, W. T.; LAN, G. Y.; LIN, C. P. a J. F. Callosal degeneration topographically correlated with cognitive function in amnestic mild cognitive impairment and Alzheimer's disease dementia. *Human Brain Mapping*. 2014, **35**(4), ISSN 1065-9471. 1529-1543. DOI: 10.1002/hbm.22271.

WATANABE, Y.; GOULD, E.; CAMERON, H. A.; DANIELS, D. C. a B. S. McEWEN. Phenytoin prevents stress- and corticosterone-induced atrophy of CA3 pyramidal neurons. *Hippocampus*. 1992a, **2**(4), 431–435. ISSN 1050-9631.

WITELSON, S. F. Hand and sex differences in the isthmus and genu of the human corpus callosum. A postmortem morphological study. *Brain*. 1989, **112**(Pt 3), 799-835. ISSN 0006-8950.

WITTER, M. P. Connections of the subiculum of the rat: topography in relation to columnar and laminar organization. *Behavioural Brain Research*. 2006, **174**(2), 251-264. ISSN 0166-4328.

WOOLLEY, C. S.; GOULD, E. a B. S. MCEWEN. Exposure to excess glucocorticoids alters dendritic morphology of adult hippocampal pyramidal neurons. *Brain Research*. 1990, **531**(1–2), 225–231. ISSN 0006-8993.

ZACH, P.; KŘIVÁNEK, J. a K. VALEŠ. Serotonin and dopamine in the parabrachial nucleus of rats during conditioned taste aversion learning. *Behavioural Brain Research*. 2006, **170**(2), 271-276. ISSN 0166-4328. DOI: 10.1016/j.bbr.2006.03.001.

13 Přehled publikací autora

13.1 Publikace autora, vztahující se k tématu

Kapitola v knize:

ZACH, P.; KRIŠTOFIKOVÁ, Z.; **MRZÍLKOVÁ, J**.; MAJER, E.; SELINGER, P.; ŠPANIEL, F.; ŘÍPOVÁ, D.; KUTOVÁ, M. a J. KENNEY. Planum temporale analysis via a new volumetric method in autoptic brains of demented and psychotic patients. In: LAHIRI, Debomoy K.. *Advances in Alzheimer's Research*. Bussum: Bentham Science Publishers Ltd., 2014, s. 395-413. ISBN 978-1-60805-852-5. DOI: 10.2174/978160805852511402016.

Původní práce v časopisech s IF:

1. ZACH, P.; KRIŠTOFIKOVÁ, Z.; **MRZÍLKOVÁ, J**.; MAJER, E.; SELINGER, P.; ŠPANIEL, F.; ŘÍPOVÁ, D. a J. KENNEY. Planum Temporale Analysis Via a New Volumetric Method in Autoptic Brains of Demented and Psychotic Patients. *Current Alzheimer Research*. 2009, **6**(1), 69-76. ISSN 1567-2050. **IF: 4.971/2009**.

2. ZACH, P.; **MRZÍLKOVÁ J**.; ŘEZÁČOVÁ, L.; STUCHLÍK A. a K. VALEŠ. Delayed effects of elevated corticosterone level on volume of hippocampal formation in laboratory rat. *Physiological Research*. 2010, **59**(6), 985-996. ISSN 0862-8408. **IF: 1.646/2010**.

3. ZACH, P.; **MRZÍLKOVÁ, J.**; STUCHLÍK, A.; VALEŠ, K. a L. ŘEZÁČOVÁ. Delayed effect of chronic administration of corticoids on the taste aversion learning. *Neuroendocrinology Letters*. 2011, **32**(1), 90-95. ISSN 0172-780X. **IF: 1.296/2011**.

4. **MRZÍLKOVÁ, J.**; KOUTELA, A.; KUTOVÁ, M.; PATZELT, M.; IBRAHIM, I.; AL-KAYSSI, D.; BARTOŠ, A.; ŘÍPOVÁ, D.; ČERMÁKOVÁ, P. a P. ZACH. Hippocampal spatial position evaluation on MRI for research and clinical practice. *PLoS One*. 2014, **9**(12), e115174; 1-15. ISSN 1932-6203. DOI: 10.1371/journal.pone.0115174. **IF: 3.534/2013**.

5. **MRZÍLKOVÁ, J.**; ZACH, P.; BARTOŠ, A.; TINTĚRA, J. a D. ŘÍPOVÁ. Volumetric Analysis of the Pons, Cerebellum and Hippocampi in Patients with Alzheimer's Disease. *Dementia and Geriatric Cognitive Disorders*. 2012, **34**(3-4), 224-234. ISSN 1420-8008. DOI: 10.1159/000343445. **IF: 2.787/2012**.

Článek v časopise bez IF:

1. KUTOVÁ, M.; **MRZÍLKOVÁ, J.**; KIRDAJOVÁ, D.; ŘÍPOVÁ, D. a P. ZACH. Simple Method for Evaluation of Planum Temporale Pyramidal Neurons Shrinkage in Postmortem Tissue of Alzheimer's Disease Patients. *BioMed Research International*. 2014, **2014**(Article ID 607171), 1-6. ISSN 2314-6133. DOI: 10.1155/2014/607171.

2. ZACH, P.; BARTOŠ, A.; TINTĚRA, J.; **MRZÍLKOVÁ, J.** a D. ŘÍPOVÁ. Medial Temporal Atrophy (MTA) on magnetic resonance images in patients with Alzheimer disease. In: *9th Congress of the European Association of Clinical Anatomy*. Bologna: Medimond, 2007, s. 91-93. ISBN 978-88-7587-425-4.

3. ZACH, P.; **MRZÍLKOVÁ, J.** a K. VALEŠ. Role glutamátu v neurodegenerativních změnách v hipokampu způsobených stresem. *Kontakt*. 2010, **12**(1), 22-25. ISSN 1212-4117.

13.2 Ostatní publikace autora

Původní práce v časopisech s IF

1. DUDÁK, J.; ŽEMLIČKA, J.; KREJČÍ, F.; POLANSKÝ, Š.; JAKUBEK, J.; **MRZÍLKOVÁ, J.**; PATZELT, M. a J. TRNKA. X-ray micro-CT scanner for small animal imaging based on Timepix detector technology. *Nuclear Instruments & Methods in Physics Research Section A - Accelerators Spectrometers Detectors and Associated Equipment*. 2015, **774**(11), 81-86. ISSN 0168-9002. DOI: 10.1016/j.nima.2014.10.076. **IF: 1.316/2013**.

Práce v časopisech bez IF

1. ZACH, P.; **MRZÍLKOVÁ, J.** a S. KUČOVÁ. Praktická instrukce pro dlouhodobou stabilizaci pozornosti - základ práce se stresem. *Kontakt*. 2009, **11**(1), 81-84. ISSN 1212-4117.

2. ZACH, P.; **MRZÍLKOVÁ, J.** a S. KUČOVÁ. Srovnání popisu buddhistických osmi vědomí se strukturou mozku u člověka. *Kontakt*. 2009, **11**(1), 85-89. ISSN 1212-4117.

3. ZACH, P. a J. MRZÍLKOVÁ. Technika nácviku vědomé pozornosti ve zdraví i nemoci. *Kontakt*. 2008, **10**(1), 209-213. ISSN 1212-4117.

Účast na grantových a výzkumných projektech:

Grant IGA NR/9180: Role glutamátu v neurodegenerativních změnách hipokampu způsobených stresem. Hlavní řešitel: FgÚ AV ČR, spoluřešitel: 3. LF UK Praha. Období řešení: 2007 - 2009.

Grant GAUK 2011 č. 296211. Volumetrické změny v hippocampus, cerebellum a pons u pacientů s Alzheimerovou demencí. Období řešení 2011.

Grant PRVOUK P34. Psychoneurofarmakologický výzkum. Období řešení 2012 – současnost.

14 Plné znění významnějších prací autora, vztahujících se k tématu

ZACH, P.; KRIŠTOFIKOVÁ, Z.; **MRZÍLKOVÁ, J**.; MAJER, E.; SELINGER, P.; ŠPANIEL, F.; ŘÍPOVÁ, D. a J. KENNEY. Planum Temporale Analysis Via a New Volumetric Method in Autoptic Brains of Demented and Psychotic Patients. *Current Alzheimer Research*. 2009, **6**(1), 69-76. ISSN 1567-2050. **IF: 4.971/2009**.

Abstract: Investigations of alterations in brain asymmetry often focus on the planum temporale of patients with schizophrenia. Data also suggest changes in laterality of demented patients associated with a more marked impairment of the left hemisphere. Our study was performed on autoptic brain tissue of 84 patients, out of which there were 25 non-demented non-psychotic controls, 50 demented patients (34 Alzheimer's disease, 9 multi - infarct dementia and 7 mixed-type dementia patients) and 9 people with schizophrenia. The plana temporalia were evaluated via a new volumetric method using dental resin matter. Areas, cortical thickness and volumes of the right and left planum temporale were evaluated without normalization to brain weight in 60 patients and with normalization in 24 people. In controls, a mild right/left laterality of areas, cortical thickness and volumes was found. Moreover, in control women the areas of the left planum temporale were smaller than those observed in control men. The shifts to left/right laterality of areas and volumes were found in all demented groups. In the more numerous Alzheimer's group, the change in laterality of an area was associated with a mild decrease on the right and a mild increase on the left side. In contrast, marked but only bilateral area shrinkage as well as reduced cortical thickness and brain volumes were observed in schizophrenic patients.

Planum Temporale Analysis *Via* a New Volumetric Method in Autoptic Brains of Demented and Psychotic Patients

Petr Zach[1,2,*], Zdena Krištofiková[3], Jana Mrzílková[2], Emerich Majer[4], Pavel Selinger[5], Filip Španiel[3], Daniela Řípová[3] and Jana Kenney[6]

[1]*Department of Preclinical Studies, Faculty of Health and Social Studies, South Bohemian University, Czech Republic,* [2]*Institute of Anatomy, 3rd Faculty of Medicine, Charles University, Czech Republic,* [3]*Prague Psychiatric Centre, Czech Republic,* [4]*Psychiatric Hospital Bohnice, Czech Republic,* [5]*Faculty Hospital Bulovka, Czech Republic,* [6]*Czech Academy of Science, Czech Republic*

Abstract: Investigations of alterations in brain asymmetry often focus on the *planum temporale* of patients with schizophrenia. Data also suggest changes in laterality of demented patients associated with a more marked impairment of the left hemisphere. Our study was performed on autoptic brain tissue of 84 patients, out of which there were 25 non-demented non-psychotic controls, 50 demented patients (34 Alzheimer disease, 9 multi - infarct dementia and 7 mixed-type dementia patients) and 9 people with schizophrenia. The *plana temporalia* were evaluated *via* a new volumetric method using dental resin matter. Areas, cortical thickness and volumes of the right and left *planum temporale* were evaluated without normalization to brain weight in 60 patients and with normalization in 24 people. In controls, a mild right/left laterality of areas, cortical thickness and volumes was found. Moreover, in control women the areas of the left planum temporale were smaller than those observed in control men. The shifts to left/right laterality of areas and volumes were found in all demented groups. In the more numerous Alzheimer group, the change in laterality of an area was associated with a mild decrease on the right and a mild increase on the left side. In contrast, marked but only bilateral area shrinkage as well as reduced cortical thickness and brain volumes were observed in schizophrenic patients.

Keywords: Planum temporale, volumetry, brain laterality, dementia, schizophrenia.

INTRODUCTION

The *planum temporale* (PT) is an area of the temporal lobe located on the superior surface of the *superior temporal gyrus*. The anterior portion of the PT is a part of the unimodal auditory association cortex (part of BA22) that surrounds the Heschl´s gyrus, whereas the posterior portion adjacent to the *temporoparietal* junction (other portions of BA22 and a part of BA39-40) is partially coextensive with the Wernicke's area, consisting of heteromodal association cortex [1, 2]. Cytoarchitecture has been studied to help describe the borders of the PT, but distribution of auditory association cortex is not altogether confluent with it. Although there is still a debate concerning the exact delineation of the PT, Pfeifer´s definition [3, 4] adapted by von Economo and Horn [5] is preferred at the present time.

Firstly, assessments of the PT area were carried out from photographs of *post-mortem* brains and studies using magnetic resonance and computer tomography followed. In the past, *post-mortem* studies concentrated only on measurement of the length of the PT and this tendency was also seen in magnetic resonance studies. Later studies have measured the PT volume taking into account cortical depth.

*Address correspondence to this author at the Department of Preclinical Studies, Faculty of Health and Social Studies, South Bohemian University, Czech Republic; E-mail: zach.petr@post.cz

The PT area in the healthy human brain appears to be predominantly left/right (L/R) lateralized [6, 7]. The lateralization in a normal population lies along a continuum. This continuum (normal distribution) is skewed to the L in the normal population, with a few brains strongly asymmetrical towards the R [8]. Despite difficulties with an exact relationship between handedness on the PT size, there is a general agreement that R-handers demonstrate a significant leftward asymmetry of the PT in comparison to L-handed subjects, whose *plana temporalia* are usually either symmetrical or tend towards rightward asymmetry [9-11]. Little systematic anatomical research has been done into the effect of sex on structural differences in the PT. One such study reported that females show more frequent reversals of PT asymmetry (i.e., R>L) [12]. Another study supported this finding [13]. One study shows R/L asymmetry of the temporal region also in healthy males [14].

Functional neuroimaging studies indicate that the PT has a predominantly language related function. One study demonstrated that the L PT becomes activated equally to tones and words during passive listening and even greater activation was observed during active listening [15]. A further study reports that the PT shows greater activation bilaterally during a tone task compared with a semantic decision task [16], although another study has shown significant activation in the PT, particularly in the R hemisphere, when listening to a variety of acoustic stimuli [17]. Patients with a variety of lesions near or including the PT have been shown to exhibit

1567-2050/09 $55.00+.00

a number of associated auditory discrimination and speech comprehension deficits [18-20].

Data suggest atrophy of the medial and lateral parts of the temporal lobe in patients with Alzheimer disease (AD) when compared to the age-matched controls [21]. Moreover, the changes in temporal-parietal cortices appear to be lateralized. Namely, a spreading wave of grey matter loss occurs in both hemispheres, however, L-hemisphere regions are affected earlier and more severely [22, 23]. Nevertheless, another study performed on the *post-mortem* brain tissue reported either bilateral reduction of the PT volume in AD patients when compared to the controls or no gender-dependent differences in both groups [24]. In contrast to AD, laterality of the PT has not been evaluated yet in patients with multi-infarct dementia (MID).

Investigation of PT size or asymmetry differences in schizophrenic (SCHIZ) patients when compared with controls has yielded contradictory results. In the first-episode of disease, bilateral volumetric deficits but no differences in PT asymmetry were observed in patients when compared to the controls [25] but another study reported the marked reduction only in the L PT volume [26]. In chronic SCHIZ patients, reversed asymmetry (R/L) of the PT e.g., [27-30], bilateral reduction [31] or no changes when compared to the controls [for review, see [8, 23] were observed.

As mentioned above, the PT structure has a curved rather than planar surface. Besides, its anatomical borders have not been unequivocally determined. A vast majority of recent studies dealing with the PT were done only by magnetic resonance or computer tomography and there does not seem to be any recent purely anatomical study that would focus on measuring the area and volume of the PT in autoptic human brains. Thus the aims of the present study are as follows: 1) to create reliable anatomical methodology for measurement of the PT area and volume in autoptic human brains, and 2) to evaluate alterations in laterality of demented or psychotic patients compared to non-demented non-psychotic controls.

As for the anatomical terminology, the term *planum temporale* (temporal plane) has been part of the anatomical nomenclature since 1895. But the further terms concerning this area are not incorporated in the *Terminologia Anatomica* (TA, 1998), which is the last revision of the anatomical nomenclature and is followed in this article [38].

MATERIALS AND METHODS

Histological Analysis of the Brains and Diagnosis

In total, 84 human brains with *post-mortem* delays shorter than 24 hours were analyzed. Beside the PT, five other brain areas from both hemispheres were dissected and used for histological analysis. These include three neocortical areas (*gyrus frontalis medius, gyrus temporalis superior et medius* and *lobus parietalis inferior*), one area of hippocampus (*cornu Ammoni et gyrus parahippocampalis*) and one of cerebellum (*lobulus semilunaris inferior*). We used the same histology examination methods and diagnostic criteria as in our previous study [32]. Briefly, the clinical diagnosis of AD was confirmed *via* a silver stain technique based upon the distribution of numerous senile plaques and neurofibrillary tangles. The criteria were consistent with those used in the classification of Mirra [33]. Subsequently, the samples were divided into five groups: non-demented non-psychotic controls (patients without marked signs of dementia or psychosis, number of senile plaques and tangles corresponding to normal aging), AD (clinically diagnosed dementia, number of senile plaques and tangles in given areas of the cortex and hippocampus higher than would be expected for age), MID (clinically diagnosed dementia, vascular changes, neuropathologic lesions and gliosis, number of senile plaques and tangles corresponding to normal aging), MIX (clinically diagnosed dementia, changes due to the AD and MID simultaneously) and SCHIZ (clinically diagnosed schizophrenia, number of senile plaques and tangles corresponding to normal aging). Information concerning handedness of our patients was not available to us.

PT Delineation and Dissection

Literature offers more than one working definition of the PT area anatomical delineation. We have selected the most widely accepted anatomical definition according to two studies of Pfeifer [3, 4] and von Economo and Horn [5]. Briefly, anterior border of the PT is defined as the transverse sulcus located dorsally to the transverse Heschl´s gyrus, where the transverse sulcus originates from the *retroinsular* region. The situation, where two Heschl´s gyri are on the R side and one Heschl´s gyrus is on the L side, is considered normal anatomy. Sometimes the Heschl´s gyrus is divided into anterior and posterior sections by an additional ´transverse sulcus´, called the sulcus intermedius of Beck arising from the lateral border. If, however, there is a second or a third transverse sulcus arising separately from the *retroinsular* region, then there should be by definition two or more Heschl´s gyri. The posterior boundary of the PT is complicated by asymmetries in the temporal lobe and the lateral sulcus (formerly Sylvian fissure). As most others investigators we have used an arbitrary cut-off point, where the horizontal lateral sulcus either terminates or bifurcates into the posterior descending *ramus* and/or posterior ascending *ramus*. The lateral border has been uniformly defined as coincident with the *superolateral* margin of the *superior temporal gyrus*. Since the PT resembles an isosceles triangle with its apex pointing medially, the medial border is theoretically located where the anterior border heading *posteromedially* meets the posterior border heading *anteromedially* behind the insula.

PT areas cuts from L and R hemisphere were carefully dissected with sharp knife and placed into 8% paraformaldehyde solution.

Volumetric Analysis of the PT

60 out of the 84 analysed human brains were used for determination of areas, cortical thickness and volumes of the PT and were not normalized to brain weight. The remaining 24 brains were used for determination of areas normalized to brain weights and of alterations in cytoarchitecture (data not shown, the experiments are still in progress). The group totally included 25 non-demented non-psychotic controls, 50 demented patients (34 AD, 9 MID and 7 MIX) and 9 psychotic patients with different clinical subsets of SCHIZ.

Dental Resin Impression of the PT Area

We washed the PT samples in water and placed them on glass Petri dishes. We covered by means of a small brush the whole surface of the samples with a liquid phase of condensation curing polysiloxane impression material (STOMAF LEX CRÈME (SC)), a substance conventionally used in dental medicine. We made sure that liquid phase penetrated into all irregularities on the PT surfaces. The SC polymerized and formed a thin impression layer on the samples (mask), which we then carefully removed *via* forceps and put back on Petri dishes. This way created masks of the PT surfaces were noted for irregular 3D shape. Using scissors, we have cut masks in order to obtain several pieces with almost ideal 2D surface. All 2D pieces from one PT were placed between two glass slides normally used in microscopy. Images of these slides were acquired by means of digital camera Olympus 5050 attached to standard PC.

The PT Cortical Width Measurement

The PT brain samples were washed by distilled water and placed again on Petri dishes. Then five 4-5 mm thick slices were carefully obtained using a sharp knife from the following parts of every PT sample: transition to the lateral sulcus, transition to *gyrus temporalis superior*, transition to the posterior part of the PT, where tissue continues to ascending or descending *rami*, the second Heschl´s gyrus, if present and the center of the area dorsal to the second Heschl´s gyrus. Knife cuts were done perpendicularly to the PT cortex in selected parts, so that slices on the cut sides would have reliably exposed cortical width and *subcortical* white matter for further examination. Slices were placed on antireflection white paper and photographed with digital camera (Olympus C-5050, light for photographing was obtained from Intralux 6000-1) into standard PC. The photographed pictures were then processed using software Image J.31. Cortical thickness in the samples was measured manually using mouse pointer.

Computer Measurement of the PT Dental Resin Impressions

Slides with 2D SC masks together with a millimeter scale were photographed with a digital camera (Olympus C-5050) on tripod. We exported the pictures from the digital camera to the software Image J.31 program in a TIFF format and set the measurement scale. Then we delineated the PT SC masks images with a mouse pointer and the software computed the PT area in mm^2. Cortical thickness and PT area data were applied to calculate the volume of the PT.

Statistical Analysis

Lateralization index of the PT was obtained as (L-R)/(L+R). To evaluate the experimental data, BMDP statistical software was used [34]. For global analysis, ANOVA with repeated measures (program 2V) and one-way ANOVA (program 7D) were applied. Student´s t-test (pooled variance) was calculated with respect to controls (* $p < 0.05$, ** $p < 0.01$, *** $p < 0.001$) or to AD (+ $p< 0.05$, ++ $p < 0.01$). Data in charts are presented as mean values ± S.D.

RESULTS

We obtained totally 25 brains of non-demented non-psychotic control patients, 15 of whom were men (Tables **1** and **3**). Non-psychiatric (n = 22, especially people with carcinoma) as well as neurological/psychiatric patients (Parkinsonism, n = 2 and oligophrenia, n = 1) were included in the study. We observed a mild R/L laterality of the areas (Tables **2, 4, 5** and **6**) and of cortical thickness or volumes (Table **2**). In control women, L sides of PT area were generally smaller when compared to control men, however, global tests did not indicate statistically significant differences (Table **5**).

There was totally 34 people in the AD group, who were further classified according to plaque density (sparse, n = 3, moderate, n = 9 and frequent, n = 22). 14 of the patients were men (Tables **1** and **3**). In most cases, the plaque density did not differ between hemispheres, although in a few patients it was higher in the L than R hemisphere. The group with pure MID consisted totally of 9 people (5 men and 4 women) and the MIX group only of 7 people (5 men and 2 women) with sparse or moderate plaque density (Table **1**). Mild shifts to L/R laterality of the PT areas (Tables **2, 4** and **6**) and volumes (Table **2**) were observed in all demented groups but statistically significant changes supported by global tests were found especially in the more numerous AD group. The shifts were associated with a moderate shrinkage in the R and a mild increase in the L sides of PT area (Table **6**). In addition, a pronounced reduction of cortical thickness in the L side of the PT was found in the MIX group (Table **2**). Normalization of areas to brain weight did not significantly influence the differences between the AD and the control groups (see results of ANOVA with repeated measures, Table **4**).

SCHIZ group consisted of 9 patients, 5 of whom were men (Table **1**). Clinical diagnoses indicated residual (n = 4), chronic (n = 3) and paranoid (n = 2) phase of the disease. In patients with SCHIZ, marked but only bilateral alterations in areas, cortical thickness and volumes of the PT were found when compared to controls (Table **2**). Beside these, we observed shape abnormalities of the PT (Fig. **1**).

DISCUSSION

New Volumetric Method

The SC substance, when in liquid phase, is capable of replicating the surface pattern of the PT, including fissures, twists and other irregularities, and after polymerization it creates an ideal rubber mask of the surface. Then, with a little skill, it is possible to flatten the whole imprint, or to separate the problematic parts that stick out with scissors. Then, the irregularities and non-linear shape of the PT surface became easy to evaluate, in contrast to more complicated methods of former *post-mortem* brain analyses e.g., [24]. We believe that SC could be potentially used for imprints of not only the PT area, but also of other cortical surface regions that are difficult to measure. When histological analysis of the brain tissue is performed, both area and volumes can be evaluated.

Table 1. Characteristics of Patiens, Where Brain Tissue, the Areas, Cortical Heights and Volumes of the PT were Determined Without Normalization

Groups	n	Sex (M/F)	Age (years)	Cause of Death
controls	16	11/5	68.0 ± 13.3	6xM, 2xCI, BP, A, MI, TC, BI, HC, P, U
AD	19	10/9	79.9 ± 7.9***	13xCI, 2xBP, U, MI, ChP, EXS
MID	9	5/4	80.6 ± 3.6**	8xCI, BP
MIX	7	5/2	79.7 ± 6.6**	6xCI, BP
SCHIZ	9	5/4	68.7 ± 10.5	4xBP, 3xCI, 2xPE
	60		ANOVA: p = 0.0007	

Sex: M – men, F - women

Causes of death: M – malignancy, CI - cardiac insufficiency, BP - bronchopneumonia, A – alcoholism, MI - myocardial infarct, TC - tumorous cachexia, BI - brain infarct, HC - hepatocirrhosis, P - peritonitis, U - uremia, ChP - cholecyst perforation, EXS - exsanguination, PE – pulmonary embolism

Student´s t-test was calculated with respect to controls (**p < 0.01, *** p < 0.001)

Table 2. Alterations in the Areas, Cortical Heights and Volumes of the PT Without Normalization (Patients of Table 1)

Groups	R	L	L-R/L+R
i) area	**mm^2**	**mm^2**	
controls	1216.9 ± 396.6	1182.6 ± 487.9	-0.034 ± 0.183
AD	1044.1 ± 240.5	1195.2 ± 274.8	+0.067 ± 0.117*
MID	962.0 ± 472.5	1084.4 ± 403.4	+0.082 ± 0.111*
MIX	1031.0 ± 333.6	1223.1 ± 430.1	+0.086 ± 0.102
SCHIZ	690.2 ± 335.1***$^{+}$	719.1 ± 288.1**$^{++}$	+0.034 ± 0.129
ANOVA:	p = 0.0161	p = 0.0297	p = 0.1523
ii) cortical height	**mm**	**mm**	
controls	3.154 ± 0.372	3.030 ± 0.334	-0.019 ± 0.082
AD	2.875 ± 0.511	2.777 ± 0.364	-0.014 ± 0.077
MID	2.810 ± 0.533	2.943 ± 0.519	+0.024 ± 0.068
MIX	2.795 ± 0.364	2.404 ± 0.299***$^{+}$	-0.075 ± 0.052
SCHIZ	2.622 ± 0.714*	2.545 ± 0.441**	-0.005 ± 0.107
ANOVA:	p = 0.1305	p = 0.0033	p = 0.1958
iii) volume	**mm^3**	**mm^3**	
controls	3850.6 ± 1381.6	3591.8 ± 1530.7	-0.052 ± 0.209
AD	2979.9 ± 800.4*	3293.0 ± 763.2	+0.053 ± 0.130
MID	2854.4 ± 1884.7	3252.4 ± 1532.4	+0.105 ± 0.153*
MIX	2946.7 ± 1144.1	2993.7 ± 1195.6	+0.012 ± 0.085
SCHIZ	1676.0 ± 653.5 ***$^{++}$	1801.8 ± 730.8 ***$^{++}$	+0.029 ± 0.174
ANOVA:	p = 0.0023	p = 0.0118	p = 0.1792

ANOVA with repeated measures i) for area: groups - F(4,55) = 3.44, p = 0.0141, laterality – F(1,55) = 5.31, p = 0.0250, interaction – F(4,55) = 1.30, p = 0.2820, ii) for for cortical height: groups – F(4,55) = 3.56, p = 0.0119, laterality – F(1,55) = 2.70, p = 0.1062, interaction – F(4,55) = 1.15, p = 0.3439 and iii) for volume: groups – F(4,55) = 4.92, p = 0.0018, laterality – F(1,55) = 0.76, p = 0.3871, interaction – F(4,55) = 0.87, p = 0.4865

Student´s t-test was calculated with respect to controls (* p< 0.05, **p < 0.01, *** p < 0.001) or to patients with AD (+ p< 0.05, ++ p < 0.01)

Table 3. Characteristics of Patients in which Brain Tissue the Areas of the PT were Normalized to Brain Weight

Groups	n	Sex (M/F)	Age (years)	Brain Weight (g)	Cause of Death
controls	9	4/5	76.1 ± 15.7	1103.3 ± 102.7	5xCI, 2xA, BP, H
AD	15	4/11	77.9 ± 7.9	1157.3 ± 178.7	12xCI, 3xBP
	24	8/16	ANOVA: p = 0.7178	ANOVA: p = 0.4189	

Sex: M – men, F - women
Causes of death: CI – cardiac insufficiencia, A – asphyxia, BP – bronchopneumonia, H – hepatocirrhosis

Table 4. The Areas of the PT Without Normalization to Brain Weight when Compared to the Normalized (Patients of Table 3)

	i) without normalization			ii) normalized	
Groups	R mm^2	L mm^2	L-R/L+R	R mm^2/g	L mm^2/g
controls	936.9±106.5	873.4±226.0	-0.045±0.112	0.853±0.104	0.790±0.177
AD	952.6±225.8	1026.7±309.6	+0.030±0.157	0.827±0.170	0.901±0.296
ANOVA	p = 0.8473	p = 0.2108	p = 0.2284	p = 0.6778	p = 0.3232

ANOVA with repeated meaures:
i) for areas without normalization: groups – F(1,22) = 1.05, p = 0.3164, laterality – F(1,22) = 0.01, p = 0.9291, interaction – F(1,22) = 1.34, p = 0.2594
ii) for normalized areas: groups – F(1,22) = 0.34, p = 0.5665, laterality – F(1,22) = 0.01, p = 0.9186, interaction – F(1,22) = 1.70, p = 0.2062

Table 5. The Areas of the PT Without Normalization Of All Controls

Sex	n	R mm^2	L mm^2	L-R/L+R
M	15	1186.1 ± 391.4	1198.6 ± 483.2	-0.013 ± 0.177
F	10	1011.0 ± 252.3	880.4 ± 269.4*	-0.075 ± 0.126
	25	ANOVA: p = 0.2246	ANOVA: p = 0.0718	ANOVA: p = 0.3523

Sex: M – men, F - women
ANOVA with repeated measures: sex – F(1,23) = 3.17, p = 0.0881, laterality – F(1,23) = 0.72, p = 0.4063, interaction – F(1,23) = 1.05, p = 0.3163
Student's t-test was calculated with respect to controls (*p<0.05).

Table 6. The Areas of the PT Without Normalization of All Controls and All Patients with AD

Groups	n Sex (M/F)	R mm^2	L mm^2	L-R/L+R
controls	25 15/10	1116.1 ± 347.7	1071.3 ± 434.4	-0.038 ± 0.158
AD	34 14/20	1003.7 ± 235.2	1120.9 ± 298.4	+0.051 ± 0.135*
	59 29/30	ANOVA: p = 0.1440	ANOVA: p = 0.6055	ANOVA: p = 0.0246

Sex: M – men, F - women
ANOVA with repeated measures: groups – F(1,57) = 0.17, p = 0.6811, laterality – F(1,57) = 0.80, p = 0.3752, interaction – F(1,57) = 4.00, p = 0.0504
Student's t-test was calculated with respect to controls (*p<0.05).

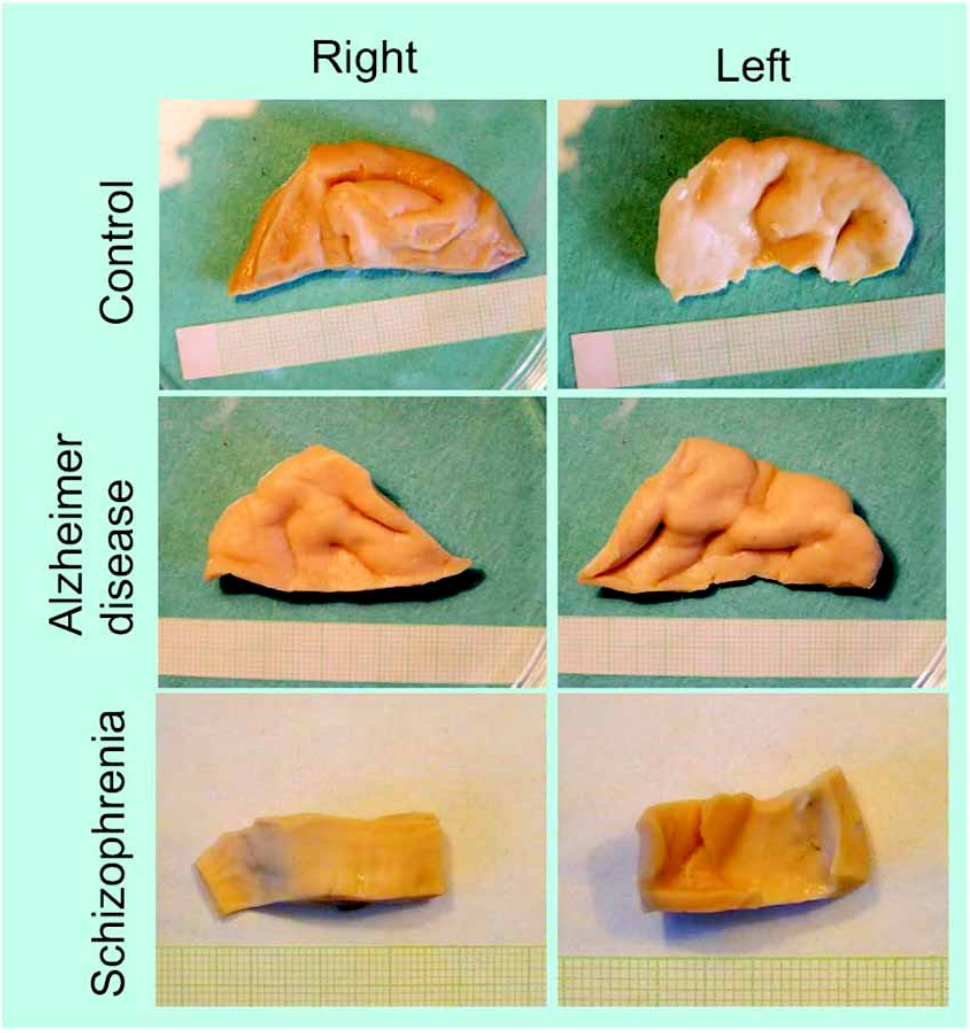

Fig. (1). The right and left PT of controls or of Alzheimer disease and schizophrenic patients. Typical examples of shape of the right and left PT of controls, Alzheimer diesease and schizophrenic patients (from above down, attached is millimeter scale).

When compared to highly expensive imaging techniques, further advantages of the method are as follows. In volumetric studies, delineation methodologies used in the imaging techniques (magnetic resonance, computer tomography) fit basically into the two categories. Firstly, there is manual delineation of structures of interest, based on direct recognition by investigator eye. The second approach is voxel-based volumetry. Delineation of structures of interest is done automatically by computer. Distinguishing mark is there grey scale of pixels (voxels) ranging from white to dark. There are many structures, where this grey scale gradient serves well, since these structures have more or less sharp anatomical boundaries with contrast white-dark pixel (voxel) transitions. Among these structures belongs e.g. the hippocampus. On the other hand, many cortical areas of the human brain are anatomically defined within context of neuronal cytoarchitecture (for example subdivisions of the medial frontal cortex or parietal cortex). When delineating these structures *via* imaging techniques, we have to approximate selected regions, often taking into the account well visible surrounding structures or areas. Our volumetric method can be a good substitute in the cases when imaging techniques have problems with exact delineation of rather cytoarchitectonically defined parts of brain cortex.

Although we did not observe marked alterations between our data without and with normalization to brain weight (Table **4**), we recommend using it to eliminate possible sex- or age-dependent differences. However, area or volume of the brain at the level of the *commissura anterius* could be used to normalization, too.

Controls

We have found the mild R/L laterality in area, cortical thickness and volume of the PT (i.e., negative indexes of laterality on average, see Tables **2, 4, 5** and **6**) in the non-demented non-psychotic controls. The results are not in a good accord with many data in literature reporting L/R asymmetry e.g., [6, 7], however, they can be supported by another studies e.g., [14]. Discrepancies can be associated e.g. with differences in PT delineation derived from various definitions of the PT borders. It results sometimes in incorporation of adjacent areas (*gyrus temporalis superior*, *posterior ascending ramus* and *posterior descending ramus*).

Moreover, even if area delineation is comparable, there are still differences in morphological settings of the PT as obvious from naked eye observations of the PT and sometimes only approximation of PT borders is possible. And finally, we suppose that differences between R and L sides of the PT are too small on average to correctly evaluate laterality of healthy controls in relation to their low number in our study.

Although global statistical analysis did not support pronounced sex-dependent differences in the controls, borderline results of ANOVA with repeated measures and significant result of pair-wise t-test did not exclude it (Table **5**). It seems that R area of the PT is bigger than L area in women which could be associated with enhanced reversal asymmetry in women when compared to men. The result is in a good accord in literature [12].

Demented Groups

We have observed generally shifts to L/R laterality in area, cortical height of volume of the PT in all demented groups, however, global statistical analysis supported it only in the case of AD (Tables **2** and **6**). A more detailed analysis of the PT area revealed the mild decrease in the R side but the mild increase in the L side in AD group when compared to the controls (Table **6**). As our experiments evaluating changes in PT cytoarchitecture are not yet terminated, we can only speculate about the reasons. Firstly, the R side of the PT could be more damaged by neurodegenerative processes in AD especially *via* atrophy. This finding is however in contradiction with works reporting a more pronounced damage of the dominant, i.e. L hemisphere, in the majority of cases [23]. Secondly, the L side of the PT could be more afflicted through processes of inflammation and *gliosis* leading among others to increased area and volume [35]. And finally, both sides of the PT could be impaired but antagonistic changes should occur in the R and L hemisphere. Histological analysis did not reveal marked laterality in the plaque densities in the hippocampal or cortical areas, nevertheless, the L hemisphere was impaired in a higher degree in same cases (data not shown).

Schizophrenia

We have found the reduction in the PT area, cortical thickness and volume in patients with SCHIZ (Table **2**) in accordance with most previously published studies [8, 23]. However, bilateral decreases were not followed by significant changes in laterality, in contrast to some studies e.g., [27-30]. Nevertheless, our results can be supported by the others e.g., [31].

Our most prominent findings in SCHIZ patients, i.e. the striking shape abnormalities of the PT on both sides were observed when compared to the controls or to patients with AD (the typical examples are shown in Fig. **1**). Sometimes the abnormalities were different in the L and R PT within one brain. Moreover, it was often extremely difficult to estimate borders of these PT areas by application of anatomical delineation mentioned above, since the superior part of the temporal lobe was of almost rectangular shape, often without Heschl´s gyri and/or visible transition to the lateral sulcus. Therefore, a question arises whether estimation of the PT area in patients with SCHIZ can be reliable.

PT as a Marker of Handedness

Although the left hemisphere is dominant for language in the majority of people (approximately 96% of R- and 73% of L-handers show L-hemisphere language localization), the dominant hemisphere or handedness should be determined to correctly evaluate brain laterality e.g. at biochemical level. In human autoptic tissue, the relevant information is often not accessible, data however suggest that volumetric asymmetry of the PT could be used as a possible marker since the degree of its laterality is higher in R- than in L-handers for review, see [23].

We used our new method to evaluate laterality of mitochondrial enzyme 17β-hydroxysteroid dehydrogenase type 10 [36] or of nitric oxide mediator system [37] in the hippocampus of people with AD, MID and SCHIZ. However, no marked correlation was found on the controls. The negative result suggests that there is no simple relationship between e.g. asymmetry of endothelial nitric oxide synthase and handedness or more universally either between laterality at biochemical/volumetric level or between laterality of various brain regions. Nevertheless, it is important to point out that the number of our control samples was too small to reveal subtle links. On the other hand, the volumetric asymmetry of the PT sensitively reflected alterations due to pathological processes [36, 37].

CONCLUSION

Our new volumetric method using SC dental resin matter is relatively simple and cheap when compared to imaging techniques. It is also sufficiently precise but cannot be used in experiments *in vivo*. Beside confirming the alterations in the PT of SCHIZ patients previously described in the literature, our results demonstrate for the first time changes in laterality of the PT in demented patients, statistically significant especially in the AD group. Causes leading to these changes will be evaluated in our future research. Information about the degree of PT lateralization could be used as a supplementary source of data in situations where information concerning handedness is missing, such as in already dead subjects.

ACKNOWLEDGEMENT

We would like to express gratitude for the excellent help of our laboratory technician Ludmila Horáková. The research was performed under the MŠMT project 1M0517 and the MZČR project MZ0PCP2005 of the Czech Republic.

ABBREVIATIONS

AD = Clinically diagnosed dementia, number of senile plaques and tangles in given areas of the cortex and hippocampus higher than would be expected for age

L = Left

MID = Clinically diagnosed dementia, vascular changes, neuropathologic lesions and gliosis, number of senile plaques and tangles corresponding to normal aging

MIX = Clinically diagnosed dementia, changes due to the AD and MID simultaneously

PT = Planum temporale

R = Right

SC = Stomaflex creme (polysiloxane substance)

SCHIZ = Clinically diagnosed schizophrenia, number of senile plaques and tangles corresponding to normal aging

REFERENCES

[1] Pearlson GD. Superior temporal gyrus and planum temporale in schizophrenia: A selective review. Prog NeuroPsychopharmacol 21: 1203-1229 (1997).

[2] Mesulam MM. Behavioral neuroanatomy. Principles of Behavioral and Cognitive Neurology. Oxford University, New York, p. 1-120 (2000).

[3] Pfeifer RA. Mylogenetisch - anatomische untersuchungen uber das corticale ende untersuchungen end der heorleitung. Acad Wiss Berlin, p. 37 (1920).

[4] Pfeifer RA. In: 'Pathologie der Hoerstrahlung und der corticalen Hoesphare. Handbuch der Neurologie'. (Bumke O and Foerster O Ed:), Springer Verlag Berlin', p. 523-626 (1936).

[5] Von Economo C and Horn L. Uber windungsrelief mabe und Rindenarchitektonic der supratemporal flache, ihre individuellen und seitenunterschiede. Neuropsychiatrie 30: 678-757 (1930).

[6] Geschwind N and Lewitsky W. Human brain: left – right asymmetries in temporal speech regions. Science 161: 186-187 (1968).

[7] Galaburda AM, Corsiglia J, Rosen GD and Sherman GF. Planum temporale asymmetry, reappraisal since Geschwind and Levitsky. Neuropsychology 25: 853-868 (1987).

[8] Shapleske J, Rossell SL, Woodruff PWR and David AS. The planum temporale: a systematic, quantitative review of its structural, functional and clinical significance. Brain Res Rev 29: 26-49 (1999).

[9] Steinmetz H, Volkmann J, Jancke L and Freund HJ. Anatomical left-right asymmetry of language related temporal cortex is different in left handers and right handers. Ann Neurol 29: 315-319 (1991).

[10] Foundas AL, Leonard CM, Gilmore R, Fennell E and Heilman KM. Planum temporale asymmetry and language dominance. Neuropsychology 32: 1225-1231 (1994).

[11] Habib M and Robichon F. Neuroanatomical correlates of hemispheric specialization. Rev Neuropsychol 12: 87-127 (2002).

[12] Wada J, Clarke R and Hamm A. Cerebral hemispheric asymmetry in humans. Cortical speech zones in 100 adult and 100 infant brains. Arch Neurol 32: 239-246 (1975).

[13] Witelson SF and Kigar DL. Sylvian fissure morphology and asymmetry in men and woman – bilateral differences in relation to handedness in men. J Comp Neurol 323: 326-340 (1992).

[14] Bilder RM, Wu H, Bogerts B, Degreef G, Ashtari M, Alvir JM, *et al*. Absence of regional hemispheric volume asymmetries in first – episode schizophrenia. Am J Psychiatry 151: 1437-1447 (1994).

[15] Binder JR, Frost JA, Hammeke TA, Rao SM and Cox RW. Function of the left planum temporale in auditory and linguistic processing. Brain 119: 1239-1247 (1996).

[16] Binder JR. Neuroanatomy of language processing studied with functional magnetic resonance. Clin Neurosci 4: 87-94 (1997).

[17] Johnsrude IS, Paus T, Zatorre RJ, Perry DW, Ward GP and Evans AC. The location of auditory activation foci relative to Heschl´s gyri. Neuroimage 5: 177-201 (1997).

[18] Praamstra P, Hagoort P, Maassen B and Crul T. Word deafness and auditory cortical function – A case history and hypothesis. Brain 114: 1197-1225 (1991).

[19] Caplan D, Gow D and Makris N. Analysis of lesions by MRI in stroke patients with acoustic – phonetic processing deficits. Neurology 45: 293-298 (1995).

[20] Alsop DC, Detre JA, D'Esposito M, Howard RS, Maldjian JA, Grossman M, *et al*. Functional activation during an auditory comprehension task in patients with temporal lobe lesions. Neuroimage 4: 55-59 (1996).

[21] Visser PJ, Verhey FRJ, Hofman PAM, Scheltens P and Jolles J. Medial temporal lobe atrophy predicts Alzheimer's disease in patients with minor cognitive impairment. J Neurol Neurosur Psychiatry 72: 491-497 (2002).

[22] Thompson PM, Mega MS, Woods RP, Zoumalan CI, Lindshield CJ, Blanton RE, *et al*. Cortical change in Alzheimer´s disease detected with a disease-specific population- based brain atlas. Cereb Cortex 11: 1-16 (2001).

[23] Toga AW and Thompson PM. Mapping Brain Asymmetry. Nat Rev Neurosci 4: 37-48 (2003).

[24] Harasty JA, Halliday GM, Kril JJ and Code C. Specific temporoparietal gyral atrophy reflects the pattern of language dissolution in Alzheimer's disease. Brain 122: 675-86 (1999).

[25] Steen RG, Mull C, McClure R and Lieberman JA. Brain volume in first-episode schizophrenia - systematic review and meta-analysis of magnetic resonance imaging studies. Brit J Psychiatry 188: 510-518 (2006).

[26] Hirayasu Y, McCarley RW, Salisbury DF, Tanaka S, Kwon JS, Frumin M, *et al*. Planum temporale and Heschl gyrus volume reduction in schizophrenia - A magnetic resonance imaging study of first- episode patients. Arch Gen Psychiatry 57: 692-699 (2000).

[27] Falkai P, Bogerts B, Schneider T, Greve B, Pfeiffer U, Pilz K, *et al*. Disturbed planum temporale asymmetry in schizophrenia. A quantitative post-mortem study. Schizophr Res 14: 161-76 (1995).

[28] Petty RG, Barta PE, Pearlson GD, McGilchrist IK, Lewis RW, Tien AY, *et al*. Reversal of asymmetry of the planum temporale in schizophrenia. Am J Psychiatry 152: 715-721 (1995).

[29] Sommer I, Ramsey N, Kahn R, Aleman A and Bouma A. Handedness, language lateralization and anatomical asymmetry in schizophrenia: Meta-analysis. Brit J Psychiatry 178: 344-351 (2001).

[30] Kawasaki Y, Suzuki M, Takahashi T, Nohara S, McGuire PK, Seto H, *et al*. Anomalous cerebral asymmetry in patients with schizophrenia demonstrated by voxel- based morphometry. Biol Psychiatry 15: 793-800 (2008).

[31] Mosnik DM, Tranel AP, Oleary DS and Andreasen NC. Left-hemisphere language dominance in schizophrenic-patients and normal controls-a study of anatomical and functional asymmetries. Schizophr Res 15: 30-31 (1995).

[32] Zach P, Kristofikova Z, Majer E and Selinger P. Alterations in the planum temporale in patients with Alzheimer disease estimated via a new volumetric method. In 'New Trends in Alzheimer and Parkinson Related Disorders' (Fisher A, Hanin I, Memo M, Stocchi F Eds:), Medimond, Bologna, p. 171-176 (2005).

[33] Mirra SS, Heyman A, McKeel D, Sumi SM, Crain BJ, Brownlee LM, *et al*. The consortium to establish a registry for Alzheimer´s disease (CERAD). 2. standardization of the neuropathologic assessment of Alzheimer´s disease. Neurology 4: 479-486 (1991).

[34] Dixon WJ. BMDP Statistical Software Manual. University of California Press, Berkeley, pp. 1-220 (1990).

[35] Miller DH. Biomarkers and surrogate outcomes in neurodegenerative disease: Lessons from multiple sclerosis. NeuroRx 1: 284-294 (2004).

[36] Hovorkova P, Kristofikova Z, Horinek A, Ripova D, Majer E, Zach P, *et al*. Lateralization of 17beta-hydroxysteroid dehydrogenase type 10 in hippocampi of demented and psychotic patients. Dement Geriatr Cogn Disord 26: 193-198 (2008).

[37] Kristofikova Z, Kozmikova I, Hovorkova P, Ricny J, Zach P, Majer E, *et al*. Lateralization of hippocampal nitric oxide mediator system in people with Alzheimer disease, multi-infarct dementia and schizophrenia. Neurochem Int 53: 118-125 (2008).

[38] Kachlik D, Baca V, Bozdechova I, Cech P and Musil V. Anatomical Terminology and Nomenclature: Past, Presence and Highlights. Surg Radiol Anat 30: 459-466 (2008).

Received: April 06, 2008 Revised: September 02, 2008 Accepted: September 03, 2008

ZACH, P.; **MRZÍLKOVÁ J**.; ŘEZÁČOVÁ, L.; STUCHLÍK A. a K. VALEŠ. Delayed effects of elevated corticosterone level on volume of hippocampal formation in laboratory rat. *Physiological Research*. 2010, **59**(6), 985-996. ISSN 0862-8408. **IF: 1.646/2010**.

Abstract: We studied delayed effects of elevated plasma levels of corticosterone (Cort) on volumetry, neuronal quantity, and gross marks of neurodegeneration in the hippocampal formation of Long-Evans rats. Animals were exposed to increased CORT levels for three weeks via implanted subcutaneous pellets. Volumetry, neuronal quantification and gross marks of degeneration were measured seven weeks after the termination of CORT treatment. We observed significant differences in volumes and especially in laterality of hippocampal subfields between control and CORT-treated animals. We found that the left hippocampus was substantially larger than the right hippocampus in the corticosterone-treated group, but not in the control group. In the control group, on the other hand, right hippocampal volume was markedly higher than all other measured volumes (hippocampal left control, hippocampal left CORT-treated and hippocampal right CORT-treated). Left hippocampal volume did not differ between the groups.

Physiol. Res. 59: 985-996, 2010

Delayed Effects of Elevated Corticosterone Level on Volume of Hippocampal Formation in Laboratory Rat

P. ZACH[1,3], J. MRZÍLKOVÁ[1], L. ŘEZÁČOVÁ[2], A. STUCHLÍK[2], K. VALEŠ[2]

[1]Institute of Anatomy, Third Faculty of Medicine, Charles University, Prague, Czech Republic, [2]Institute of Physiology, Academy of Sciences of the Czech Republic, Prague, Czech Republic, [3]Department of Preclinical Studies, University of South Bohemia, České Budějovice, Czech Republic

Received October 7, 2009
Accepted April 1, 2010
On-line June 9, 2010

Summary

We studied delayed effects of elevated plasma levels of corticosterone (Cort) on volumetry, neuronal quantity, and gross marks of neurodegeneration in the hippocampal formation of Long-Evans rats. Animals were exposed to increased CORT levels for three weeks via implanted subcutaneous pellets. Volumetry, neuronal quantification and gross marks of degeneration were measured seven weeks after the termination of CORT treatment. We observed significant differences in volumes and especially in laterality of hippocampal subfields between control and CORT-treated animals. We found that the left hippocampus was substantially larger than the right hippocampus in the corticosterone-treated group, but not in the control group. In the control group, on the other hand, right hippocampal volume was markedly higher than all other measured volumes (hippocampal left control, hippocampal left CORT-treated and hippocampal right CORT-treated). Left hippocampal volume did not differ between the groups.

Key words

Corticosterone • Hippocampus • Lateralization • Volumetry • Long Evans rat

Corresponding author

P. Zach, Institute of Anatomy, Third Faculty of Medicine, Charles University, Ruská 87, 110 00 Prague 10, Czech Republic. Fax: +420 267102508. E-mail: zach.petr@post.cz

Introduction

Neurotoxicity of corticoids is a subject of ongoing debate. Animal models show that the exposure to high and/or long-term doses of corticoids or intensive stress leads to structural and behavioral changes and often to hippocampal neuronal death. Patients suffering from diseases connected with high levels of corticoids at onset (e.g. post traumatic stress disorder) or during the course of the illness (affective disorders, Alzheimer´s dementia and also consummatory disorders such as anorexia nervosa or bulimia), show important shrinkage of the hippocampus and deficits in short-term memory tests in comparison with healthy controls (Brunner *et al*. 2005, Gluck *et al*. 2005, Alfarez *et al*. 2006). Different effects on neuronal and/or glial morphology in the hippocampus were observed after acute or chronic administration of corticoids to rats. Significant reductions in the volume of the dentate gyrus and the CA3 subfield were observed in rats acutely exposed to higher doses of corticoids, without neuronal loss (Sousa *et al*. 1998). Repeated stress is seen to exert similar effects as corticoids on dendritic remodeling in CA3. A key feature of prolonged stress is the alteration in dendritic spine number and morphology in the hippocampal formation. These changes could be the neurobiological substrate of stress-induced changes in behavior and reactivity.

Despite intensive investigations, the neurobiological mechanisms of the effects of stress and corticoids on the molecular level remain poorly understood (for review see Joëls 2008, McEwen 2008). Generally, most of the studies in animals and humans report a negative correlation between corticoid levels and hippocampal volume (Sousa *et al*. 1998, Tessner *et al*. 2007), although some studies in humans support

otherwise conflicting view (MacLullich *et al*. 2005). Similarly, several studies found significant neuronal death within hippocampal subfields (Sapolsky 1985, Tata *et al*. 2006), whereas others did not (Sousa *et al*. 1998). Laterality changes in brain structure are another important aspect of stress. Hippocampal theory of cerebral lateralization posits that neuroanatomical, neurophysiological, and neurochemical asymmetries exist in the hippocampus. Besides, there are several models showing how this hippocampal asymmetry can be experimentally induced *in vivo*. Well documented are for example experience-dependent modifications (neonatal novelty exposure or long-term potentiation) or effects of neuromodulators (Tang 2003). The effects of corticoids on the laterality of various brain structures, particulary the hippocampus, remain poorly understood. Therefore, we examined if long-term exposure to corticoids asymmetrically affected hippocampal structure. The main goals of our study were: (1) Does exogenous corticosterone treatment have a lasting effect on hippocampal structure weeks later? (2) Does this corticosterone treatment affect the hippocampus in an asymmetric manner? We expected the changes in neuronal quantity, volumes of hippocampal subfields and hemispheres and in laterality.

Methods

Subjects

The experiments were performed on 3-month-old male hooded rats of the Long-Evans strain. A total of 20 animals were used in the study. Ten animals received the corticosterone treatment and 10 animals served as a control group. The animals were obtained from the breeding colony of the Institute of Physiology AS CR (Prague) and housed in a room with a constant temperature (20-22 °C) and 12 h/12 h light/dark cycle with the lights on at 7 AM. All animal procedures complied with the Animal Protection Law of the Czech Republic and the European Communities Council directive 86/609/ECC.

Corticosterone administration

Subcutaneous corticosterone pellets were implanted in the regio interscapularis. Each pellet contained 200 mg of corticosterone released over 21 days (pellets purchased from Innovative Research of America Ltd.). Control animals received pellets containing cholesterol (Innovative Research of America Ltd.) All animals were regularly weighed first 1 week before the onset of the experiment and then regularly each week. Animals were killed in the seventh week after the peak corticosterone application (for details see Fig. 1). In order to minimize the activation of complex anti-stress systems of an organism (both humoral and cellular), we did not use animal stress model. Exogenous corticosterone treatment is pharmacologically important in animal stress model as well as in medicine.

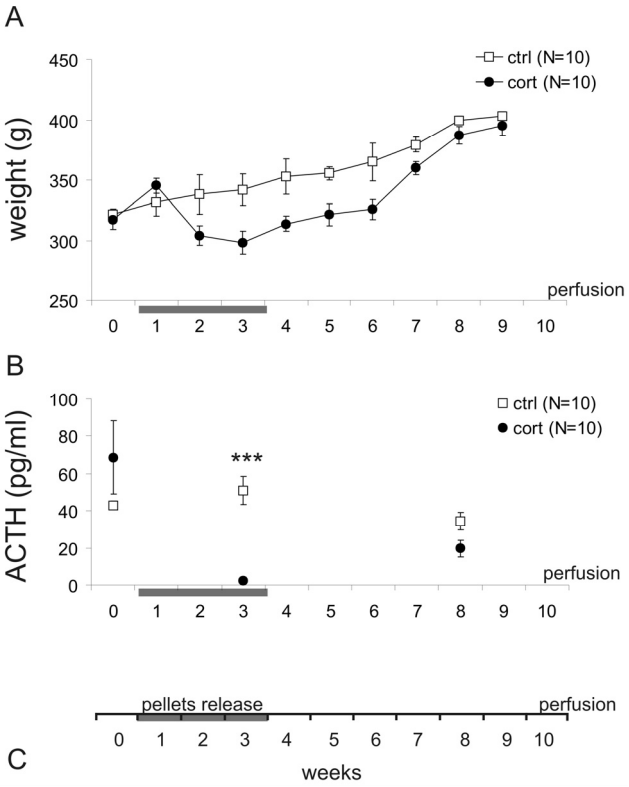

Fig. 1. A. Weight of the animals in the course of the experiment. Control group (ctrl) and corticosterone-treated group (cort). **B.** Plasmatic levels of the ACTH. *** – significant difference between groups for (p<0.001). Data presented as means values ± S.E.M. **C.** Time schedule of experiment.

The ACTH determination

Repeated blood samples were collected from the tail vein no longer than 90 s after handling the rat one week prior to onset of experiment, in the third week during corticosterone application, and finally in the fifth week after corticosterone application (for details see Fig. 1). Samples were collected in a separate sterile room at 9:00 in the morning. The blood was put into a test tube with EDTA. The collected blood was centrifuged at 3000 rpm for 15 min and the plasma was then immediately frozen and stored in –80 °C freezer. ACTH level was determined using a „sandwich type“ immuno-

radiometric assay (Immunotech, France). The procedure of sample analysis has been described in detail previously (Šimůnková *et al.* 2008).

Neurohistology

Animals were deeply anesthetized with pentobarbital (30 mg/kg i.p., Sigma) and perfused with 10 % saline-buffered paraformaldehyde solution and stored overnight in 10 % paraformaldehyde solution. The brains were removed and saturated in sacharose gradient solutions (10 %, 20 %, 30 %) for a total of 48 h, then quickly frozen on dry ice for 10 min, and stored in –20 °C. Whole series of 25 μm thick coronal sections (section thickness less than 20 μm should be avoided in case of stereology measurements due to shrinkage in z-axis – Keuker *et al.* 2001) were cut in cryostat Leica CM1850. The sections were stained with cresyl violet and mounted on histological glass slides with DPX mount (Sigma). Anatomical boundaries of the hippocampal formation and its subparts were distinguished under light microscope according to The Rat Brain Atlas (Paxinos and Watson 1998). Granular layer of the dentate gyrus and pyramidal layers in CA1-CA3 and subiculum were analyzed. Polymorphic layer (or hilus) was not included, so that only one layer from each subfields was selected. Pyramidal cell layer of subiculum was excluded from neuronal counts. Borders of dentate gyrus, CA1 and CA3 subfield and subiculum were recognized according to neuronal shape of granular/pyramidal cell layer. Borders of CA2 in Nissl stain are generally more difficult to estimate, so that stereological measurement of CA2 subfield are usually included into CA3 subfield. Since we worked with coronal brain sections, it was easier to distinguish borders between subfields. We used two markers for CA2 delineation: i) CA2-CA1 transition on the inner side of pyramidal cells is visible as a zone where CA3-like dark stained pyramidal neurons of CA2 become less stained and they are relatively smaller compared to CA1 subfield, ii) neuronal bodies in CA3 are more intensively stained than in CA2 pyramidal cells. Although not-so-well visible, stratum lucidum in non-primates terminating at the apical dendrites corresponds to narrowing of pyramidal cell layer. The mossy fibers do not extend into CA2, roughly delineating CA2-CA3 transition, but that is not readily visible using Nissl stain (Paxinos and Watson 1998). There is also higher density of granule cells close to CA2-CA3 transition, whose small nuclei are darkly stained and well visible.

Neuron number estimation

Neuronal quantity was estimated using the optical fractionator method, as described earlier (Gundersen *et al.* 1988a,b, West *et al.* 1991). A systematic random sampling strategy and fractionator with an optical dissector were deployed. Every tenth section and beginning at a random starting position, visual fields were sampled by step-size movements of 150 μm in the x- and y- axis for all hippocampal formation subdivisions. Step size movements in x and y axis were measured as previously described (Kaplan *et al.* 2001, Adiguzel *et al.* 2003). This technique uses two dial indicators (KBN instruments, Czech Republic) attached to the microscope stage. One of them measures the length of the stage movements along the x direction and the other in the y direction. Cells were counted in every frame using the optical dissector with a fixed height of 10 μm for granule cells of the dentate gyrus and for CA1-CA3 pyramidal cells at a final magnification of x2520. Dissector height and section thickness (including simple calibration method) was measured according to Korkmaz and Tumkaya (1997). This technique uses projection of rotation of the fine focus knob of the microscope onto enlarged circular scale. Section thickness was measured prior to counting at random part of each section and overall varied between 16-21 μm. Shrinkage of the tissue in the z-axis then varied between 4-9 μm. The areas of the counting frames at level of the tissue, were 125 μm^2 for the dentate gyrus, 280 μm^2 for the CA1 subfield, 100 μm^2 for the CA2 subfield and 320 μm^2 for the CA3 subfield. Neurons were differentiated from other cells on the basis of nuclear size (larger in neurons than in glial cells), a prominent nucleolus, and the shape of their perikarya attributable to dendritic emergence. Gross marks of neuronal degeneration were considered utilizing the following signs: swelling of the cytoplasm, pyknosis of the nucleus and loss of Nissl tigroid substance (Peinado *et al.* 1997). We did not select special sampling procedure for counting degenerated neurons. Numbers of degenerated neurons were counted together with neuronal quantity at times, when normal neurons appeared within counting frames. In this way, degenerated neurons were included in normal neuronal quantity. Light microscope (Leica DMLB; Leica Microsystems, Inc., Wetzlar, Germany) attached to standard PC with monitor and Leica adapter was used.

Hippocampal formation volume

The volumes of the granular cell layer of the dentate gyrus and pyramidal neurons within CA1 - CA3 subfields and subiculum (without presubiculum and parasubiculum) were estimated on the basis of the Cavalieri principle (Gundersen *et al.* 1988b). The sampling procedures for selecting the sections were the same as used by Gundersen and Jensen (1987). Starting at a random position, every fifth section was subject to sampling. An average of 18 sections were analyzed par each hippocampal subfield. The areas of all hippocampal subfields were estimated by the point-counting test point system (lattice) on a monitor connected to a light microscope with a final magnification of x110. The distance between points at the tissue level was 150 μm for granular cell layer of the dentate gyrus and pyramidal layers of the CA1-CA3 subfields and 300 μm for subiculum. Total volumes of hippocampal formation subfields were subsequently calculated from the numbers of points and distances of sampled sections.

Brain volume

Light microscope images of whole brain sections (without olfactory bulbs, pineal and pituitary gland, optic chiasma and cerebellum – brain stem was cut immediately above colliculi superiores) were transferred to the standard PC where areas of sections were manually delineated and computed with Image J freeware PC program. In the case of missing or damaged sections (less than 8 sections in average for all brains) data was matematically calculated as average area values from preceding and following sections.

Data analysis and statistics

Normalized hippocampal volume was calculated as percentage of the volume of hippocampal formation from the volume of the whole hemisphere. Normalized hippocampal volumes were calculated separately for right (R) and left (L) hemispheres. Lateralization index was calculated as (R-L)/(R+L)*100. A repeated measures two-way ANOVA with lateralization (right, left) as the within-subject factor and group (control and corticosterone) as the between-subject factor compared the volumetry of the different subregions of the hippocampus. Newman-Keuls test was used for *post-hoc* analysis of significant main effects and interactions. For statistical analysis of the laterality index, independent samples t-tests were used to examine group differences. One-sample t-tests were used to examine whether the laterality index differed within each group. Significance was accepted at the 5 % level of probability. We did not use three-way ANOVA for analysis of various hippocampal subregions as a within-subject factor, because we did not compare hippocampal subregions between themselves. The statistical analyses were computed using program Statistica v.5.5 (Statsoft, CR).

Neuron number estimation

Section sampling fraction (ssf) was 1/10, since each tenth section was used for analysis. Total neuronal quantity (N) for left and right hippocampal subfields (dentate gyrus, CA1-CA3) were calculated according to formula by West *et al.* (1991):

$$N(total) = (\sum Q^{-}) * (1/ssf) * (1/asf) * (t/h)$$

$\sum Q^{-}$ is the total quantity of neurons counted in the dissectors on the sampled sections, *ssf* is the section sampling fraction, *asf* is areal sampling fraction, *t* is the mean thickness of the sections (μm) and *h* is the optical dissector height (μm).

CE (coefficient of error) was calculated separately for each hippocampal formation subfield and left and right side and CV, coefficient of variation was estimated as CV = S.D./mean (Table 2), as described by West *et al.* (1991). For overview of stereology parameters used in the study see Table 3.

Results

Neuron number estimation (Table 1)

No changes were observed in the dentate gyrus.

CA1 subfield

We found higher neuronal quantity on the right CA1 in the controls, but not in the CORT group. The two-way ANOVA found significant main effects of group ($F_{1,18}$=5.4, $p<0.05$) and lateralization ($F_{1,18}$=115.7, $p<0.001$) and a significant interaction between group and lateralization ($F_{1,18}$=157.7, $p<0.001$). *Post-hoc* analysis revealed: a) higher neuronal quantity on the right CA1 in the controls ($p<0.001$) and b) higher neuronal quantity on the right CA1 in the controls compared to the right CA1 in the corticosterone-treated rats ($p<0.05$). Independent samples t-test confirmed the difference in lateralization difference between groups ($p<0.001$). One-sample t-test confirmed rightward laterality in the control group ($p<0.001$).

Table 1. Neuronal quantity (x10^3) and neuronal degeneration in control group (ctrl) and corticosterone-treated group (cort).

	DG L	DG R	CA1 L	CA1 R	CA2 L	CA2 R	CA3 L	CA3 R
Neuronal quantity ctrl	484.4±9.8	483.5±9.9	160.2±6.7	169.8±7.2	48.9±3.1	47.9±3.5	95.3±6.1	94.8±5.5
Neuronal quantity cort	482.8±9.5	481.5±9.2	158.2±6.8	157.5±6.9	47.5±2.4	49.2±3.2	97.5±5.8	101.1±6.2
Neuronal degener. ctrl	4.9±0.6	5.5±0.7	3.4±0.6	4.9±0.4	2.3±0.2	4.1±0.71	8.1±0.5	7.2±0.6
Neuronal degener. cort	5.1±0.5	7±0.8	4.4±0.3	5.5±0.4	2.4±0.4	3±0.5	8.6±0.6	10.9±0.7
CE (mean)	0.05	0.05	0.06	0.05	0.05	0.05	0.05	0.06
CV	0.02	0.02	0.04	0.06	0.05	0.06	0.05	0.06

DG – dentate gyrus, L – left, R – right. CE is the intra-animal and between subfields estimated coefficient of error, see Table 2. CV was calculated as S.D./mean. Neuronal quantity data are presented in thousands. Neuronal quantity and neuronal degeneration data are presented as means ± S.E.M. *Neuronal quantity*. In the right control group CA1 was found significantly higher number of neurons compared to left one (R ctrl > L ctrl ($p<0.001$)) and in rigth control group CA1 was found significantly higher number of neurons compared to right corticosterone-treated group CA1 (R ctrl > R cort ($p<0.05$)). In left control group CA2 was found significantly higher number of neurons compared to right one (L ctrl > R ctrl ($p<0.01$)) and in right corticosterone treated group CA2 was found significantly higher number of neurons compared to left one (R cort > L cort ($p<0.001$)). *Neuronal degeneration.* In the right corticosterone-treated group CA3 was found significantly higher number of neurons compared to left one (CA3 – R cort > L cort ($p<0.05$)) and in the right corticosterone-treated group CA3 was found significantly higher number of neurons compared to right control group (R cort > R ctrl ($p<0.01$)).

CA2 subfield

The control group displayed leftward laterality while the corticosterone-treated group showed opposite (rightward) laterality. We found higher neuronal quantity on the left CA2 in the controls compared to the left CA2 in the CORT group. Also, lower neuronal quantity was found on the right CA2 in the controls compared to the right CA2 in the CORT group. The two-way ANOVA found a significant interaction between group and lateralization ($F_{1,18}=31.9$, $p<0.001$). *Post-hoc* analysis revealed: a) higher neuronal quantity on the left CA2 in the control group ($p<0.01$) and b) higher neuronal quantity on the right CA2 in the CORT group ($p<0.001$). Independent samples t-test showed lateralization difference between groups ($p<0.001$). One-sample t-test showed leftward lateralization in the control group ($p<0.001$) and rightward lateralization in the CORT group ($p<0.05$).

CA3 subfield

The two-way ANOVA found no significant effect of laterality, group or interaction. Only one-sample t-test detected rightward lateralization in the CORT group ($p<0.001$).

Degenerated neuron number estimation (Table 1)

No significant changes were observed in the dentate gyrus or CA2 subfield.

CA1 subfield

The two-way ANOVA found a significant effect of lateralization ($F_{1,18}=16.9$, $p<0.05$). One-sample t-test detected rightward laterality in the control group ($p<0.05$).

CA3 subfield

The corticosterone-treated group had more degenerated neurons compared to the control group on both sides. The two-way ANOVA found a significant main effect of group ($F_{1,18}=9.6$, $p<0.01$) and a significant interaction between group and lateralization ($F_{1,18}=5.6$, $p<0.05$). *Post-hoc* analysis revealed a) more degenerated neurons on the right CA3 in the CORT group ($p<0.05$), and b) more degenerated neurons on the right CA3 in the CORT group compared to the right CA3 in the control group ($p<0.01$). Moreover, independent samples t-test revealed lateralization difference between the groups ($p<0.05$).

Volume estimation (Figs 2 and 3)

Dentate gyrus and the CA1-CA3 subfield

The CORT group showed smaller volumes of the dentate gyrus (Fig. 4a) and the CA1-CA3 subfields

Table 2. Example of CE calculation for neuronal numbers in the right CA1 subfield in control animal no.2.

Section No.	Q^-	Q^-xQ^- *(A)*	$Q^-xQ^-_{+1}$ *(B)*	$Q^-xQ^-_{+2}$ *(C)*
2	3	9	18	36
3	6	36	72	48
4	12	144	96	108
5	8	64	72	32
6	9	81	36	54
7	4	16	24	44
8	6	36	66	60
9	11	121	110	88
10	10	100	80	60
11	8	64	48	56
12	6	36	42	54
13	7	49	63	28
14	9	81	36	27
15	4	16	12	32
16	3	9	24	27
17	8	64	72	96
18	9	81	108	36
19	12	144	48	96
20	4	16	32	24
21	8	64	48	32
22	6	36	24	30
23	4	16	20	
24	5	25		
	$(\sum^{Q-})$=162	*A*=1299	*B*=1071	*C*=1068
$CE(\sum^{Q-})=0.05$				

The CE was calculated separately for each structure (left and right) and animal according to this formula:

$$CE(\sum^{Q-}) = \frac{\sqrt{(3A + C - 4B)/10}}{\sum Q^-}$$

$\sum Q^-$ is the sum of the number of neurons counted in the sections used in the analysis, A is the sum of the squares of the number of neurons counted in each section, B is the sum of Q^- of section times Q^- from the next section and C is the sum of Q^- of section times Q^- from the second next section.

(Fig. 4b) compared to the control group on both sides. The two-way ANOVA found a significant main effect of lateralization ($F_{1,18}$=5.3, $p<0.05$ and $F_{1,18}$=8.11, $p<0.01$) and a significant interaction between group and lateralization ($F_{1,18}$=7.53, $p<0.05$ and $F_{1,18}$=10.4, $p<0.01$) in the dentate gyrus and the CA1-CA3 subfields, respectively. *Post-hoc* analysis revealed higher dentate gyrus volume on the right in the control group ($p<0.01$), as well as higher CA1-CA3 subfields volume on the right in the control group ($p<0.0001$). Independent samples t-test revealed lateralization difference between the groups in the dentate gyrus ($p<0.05$) and in the CA1-CA3 subfields ($p<0.01$). One sample t-test found rightward laterality in the dentate gyrus ($p<0.001$) and in the CA1-CA3 subfield ($p<0.001$) in the control group.

Subiculum (Fig. 4c)

We found higher volume of the right subiculum in the control group compared to the left subiculum in the control group and opposite for the CORT group – volume of the right subiculum smaller compared to the left subiculum. The two-way ANOVA found a significant main effect of group ($F_{1,18}$=7.13, $p<0.05$) and significant interaction between group and lateralization ($F_{1,18}$=38.8, $p<0.001$). *Post-hoc* analysis revealed: a) higher volume of the right subiculum compared to the left one in the control group ($p<0.01$), b) higher volume of the left subiculum compared to the right one in the CORT group ($p<0.001$), and c) higher volume of the right subiculum in the CORT group compared to the volume of the right subiculum in the control group ($p<0.001$). Independent

Table 3. Overview of the stereological parameters used in the study. Table illustrates in details method of measurement.

Neuronal quantity measurement	Granule cells of the DG	Pyramidal layer of the CA1	Pyramidal layer of the CA2	Pyramidal layer of the CA3	Pyramidal layer of the SUB
h	10 μ	10 μ	10 μ	10 μ	-
t	18 μ	19 μ	18 μ	17 μ	18 μ
ssf	1/10	1/10	1/10	1/10	-
asf	125 μ^2	280 μ^2	100 μ^2	320 μ^2	-
Volume measurement	Granule cells of DG	Pyramidal layer of the CA1-CA3	Pyramidal layer of the SUB		
Interpoint distance	150 μ	150 μ	300 μ		
ssf	1/5	1/5	1/5		

h - optical dissector heigh, t - mean section thickness, ssf - section sampling fraction, asf - area sampling fraction, DG - dentate gyrus, SUB - subiculum.

samples t-test revealed lateralization difference between the groups ($p<0.001$) and one sample t-test showed rightward lateralization in the control group ($p<0.001$) and leftward lateralization in the CORT group ($p<0.01$).

Hemispheres

Left hemispheres were larger in both groups. Right hemisphere was smaller in the CORT group than in the control group and the left hemisphere was smaller in the control group than in the CORT group. The two-way ANOVA found a significant effect of lateralization ($F_{1,18}=9$, $p<0.01$). *Post-hoc* test revealed larger left hemisphere compared to the right hemisphere in the CORT group ($p<0.05$). Independent samples t-test revealed lateralization difference between the groups ($p<0.05$) and one sample t-test showed leftward lateralization in the CORT group ($p<0.05$).

Hippocampal formation as a whole

Control group showed leftward volume lateralization and the CORT showed the opposite – rightward volume lateralization. Lower volume on the right was observed in the CORT group compared to the control group. The two-way ANOVA showed significant group effect ($F_{1,18}=15.8$, $p<0.001$) and significant interaction between group and lateralization ($F_{1,18}=48$, $p<0.01$). *Post-hoc* test revealed: a) volume of the right hippocampal formation was higher than the left one in the control group ($p<0.001$), b) volume of the left hippocampal formation was smaller than the right one in the CORT group ($p<0.001$), c) volume of the right hippocampal formation in the control group was higher compared to the right one in the CORT group ($p<0.001$), and d) volume of the left hippocampal formation in the CORT group was higher compared to the left hippocampal formation in the control group ($p<0.001$). Independent samples t-test revealed lateralization difference between the groups ($p<0.01$) and one sample t-test showed leftward lateralization in the CORT group ($p<0.001$) and rightward lateralization in the control group ($p<0.01$).

Normalized hippocampal formation

The results were similar to volumes of hippocampal formation as a whole. Control group had higher volume of the right hippocampal formation and CORT group had higher volume of the left hippocampal formation. We also found volume decrease on the right side in the CORT group compared to the right side in the control group. The two-way ANOVA found a significant effect of group ($F_{1,18}=57.1$, $p<0.001$), lateralization ($F_{1,18}=31.7$, $p<0.001$) and significant interaction between group and lateralization ($F_{1,18}=107.4$, $p<0.001$). *Post-hoc* test revealed: a) higher volume of the right hippocampal formation compared to the left one in the control group ($p<0.001$), b) higher volume of the left hippocampal formation compared to the right one in the CORT group ($p<0.001$), c) higher volume of the right hippocampal formation in the control group compared to the right hippocampal formation in the CORT group ($p<0.01$), and d) higher volume of the left hippocampal formation in the CORT group compared to the left hippocampal formation

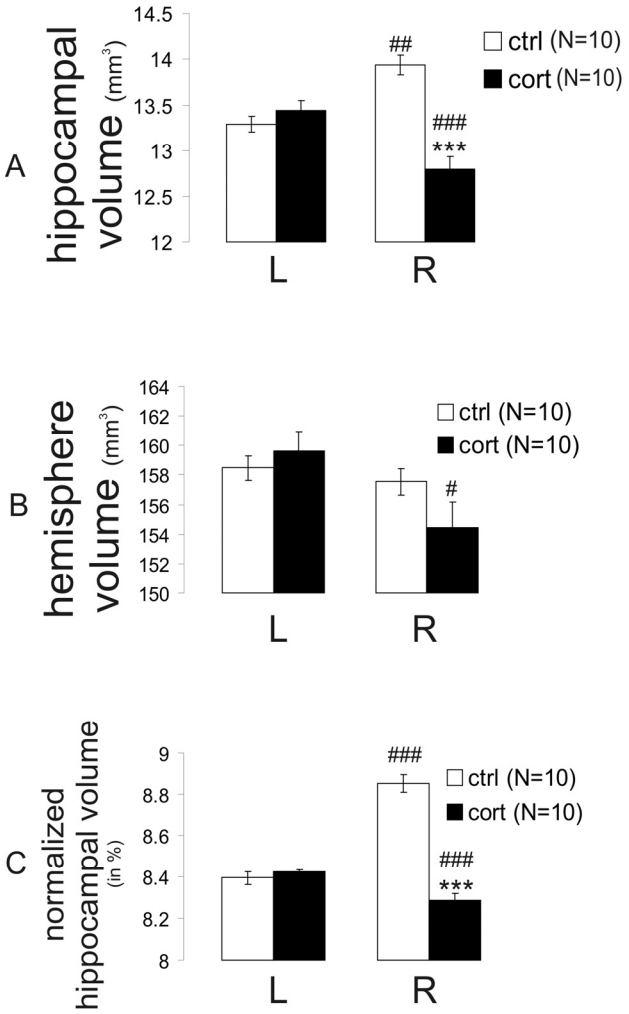

Fig. 2. Overview of volume measurement of hippocampal formation **(A)**, hemispheres **(B)** and normalized hippocampal formation **(C)** in mm^3 in control group and corticosterone-treated group. We found rightward laterality in hippocampal formation in control group as well as in normalized hippocampal formation of control group. Volume differences were not found in control group. In corticosterone-treated group we found rightward volume decrease of both non-normalized and normalized hippocampal formation. Interestingly, we also found mild but significant decrease of right hemisphere volume in the corticosterone-treated group. "*" means significant difference between groups and "#" between L and R in the same group for * $p<0.05$, ** $p<0.01$, *** $p<0.001$. Data are presented as means values ± S.E.M. Control group (ctrl) and corticosterone-treated group (cort), left (L) and right (R).

in the control group ($p<0.001$). Independent samples t-test revealed lateralization difference between the groups ($p<0.001$), one sample t-test showed leftward lateralization in the CORT group ($p<0.01$) and rightward lateralization in the control group ($p<0.001$).

Animal body weight

The groups had similar weight one week before corticosterone application (Fig. 1). Weight of the control

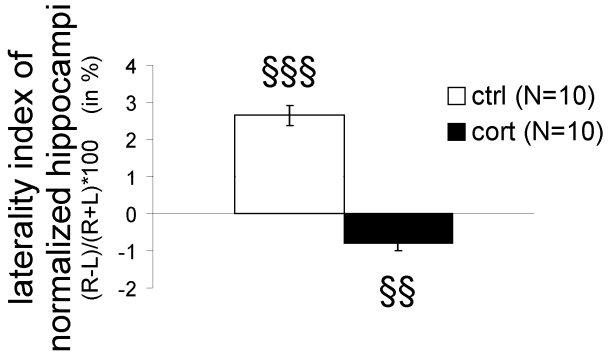

Fig. 3. Laterality index of normalized hippocampi. We found laterality index in control group significantly above zero – right hippocampal formation volume is significantly higher compared to left one. Also laterality index in corticosterone-treated group below zero – significant decrease of the right hippocampal formation. It shows that corticosterone treatment affected mostly dominant - right hippocampal formation. Laterality index was calculated as (R-L)/(R+L)*100 in %. R – right and L – left."§" means significantly different value relative to 0. Data are presented as means values ± S.E.M. Control group (ctrl) and corticosterone-treated group (cort).

group slightly increased every week until the end of experiment. The CORT group initially showed increase in the weight (in the first week of corticosterone application), followed by sudden weight drop (in the second week of corticosterone application) compared to the control group. Then the CORT group weight increased similarly to the control group, but remained lower. The ANOVA showed time effect ($F_{9,162}=39.1$, $p<0.001$) and interaction between group and time (weeks) ($F_{9,162}=4.1$, $p<0.001$).

ACTH determination

Unexpectedly, plasma level of the ACTH in the control group was slightly lower ($p<0.05$) compared to the CORT group. In the third week, plasma level of the ACTH in the CORT group was significantly lower ($p<0.001$) compared to the control group (Fig. 1). In the seventh week, plasma level of the ACTH in the CORT group was still lower compared to the control group. The ANOVA showed time effect ($F_{2,26}=7.8$, $p<0.01$) effect and interaction between groups and time (weeks) ($F_{2,26}=12.6$, $p<0.001$).

Discussion

We studied delayed effects of elevated levels of corticosterone on volumetry, neuronal quantity and gross marks of neurodegeneration in the hippocampal formation of Long-Evans rats. Animals were exposed to corticosterone treatment for three weeks by means of

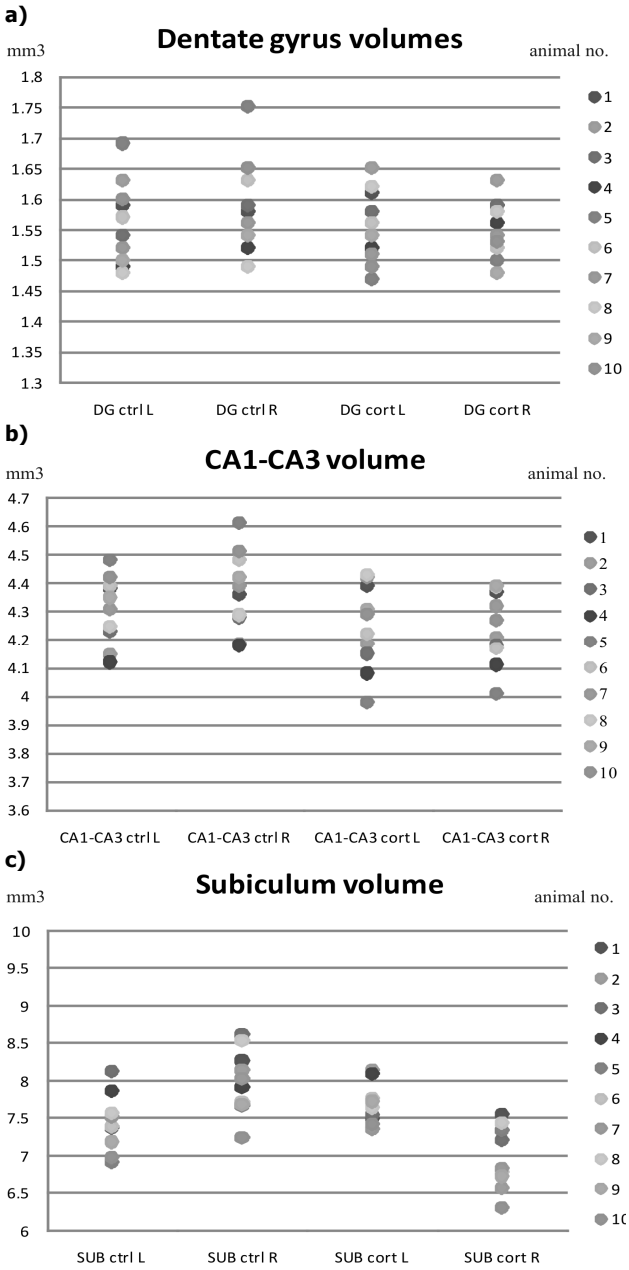

Fig. 4. Volume distribution without normalization in **a)** dentate gyrus (DG), **b)** CA1-CA3 and **c)** subiculum (SUB) on the left (L), right (R), between control group (ctrl) and corticosterone treated group (cort). Data are presented in mm^3 for individual animals. Figure 4a shows right hippocampal formation volume significantly higher compared to left one in control group ($p<0.01$). Figure 4b shows right hippocampal formation volume significantly higher compared to left one in control group ($p<0.001$) but in corticosterone treated group absence of right hippocampal volume dominance. Figure 4c shows right hippocampal formation volume significantly higher compared to left one in control group ($p<0.01$), left hippocampal formation volume significantly higher compared to right one in corticosterone treated group ($p<0.001$) and right hippocampal formation in control group significantly higher compared to right hippocampal formation in corticosterone treated group ($p<0.001$).

subcutaneous pellets (control group received cholesterol pellets). Neuronal quantification, gross marks of degeneration and volume were estimated seven weeks after the termination of corticosterone treatment.

We observed a decrease in plasma ACTH during the corticosterone treatment (Fig. 1) This could be explained by direct inhibition of the ACTH release by corticosterone in the adenohypophysis and indirect inhibition of the ACTH release *via* CRH regulation (Parker and Rainey 2004). Since we focused on the effects that develop over time rather than the acute effects, we did not perform stereological assessment at peak ACTH suppression. Changes that may have occurred in the period between the maximum ACTH reduction (week three) and the stereological experiments (week ten) could include: drop in the corticosterone plasma level, restoration of normal HPA axis function and neuronal and glial reparative processes.

The right hippocampal formation was significantly larger compared to the left one in the control group even when the volumes were normalized. However, we have found no significant volume differences between left and right hemispheres in the control group.

Larger left hemisphere compared to the right one was found in the study of Sahin *et al*. (2001), although it was more significant compared to our results (Fig. 2). Another study on male Long-Evans rats showed the opposite – right hemisphere was larger than the left one, measured by brain weight or surface dimensions. Detailed analysis showed difference in the thickness of neocortex (right thicker than left), although measurement of cross-section area of hemispheres, hippocampi, cerebellum, thalamus and brain stem did not show reliable differences (Kolb *et al*. 1982).

The most interesting result of this study is the decrease in absolute volume of the right hippocampal formation in the corticosterone-treated group. Since normalization of the hippocampal formation volume did not show the effect either on this decrease or on leftward asymmetry, volume decrease of the right hemisphere could be explained by hippocampal volume decrease as well. It is well known that brief and transient early life stimulation increases the right hippocampal volumetric dominance at mid-adulthood in Long-Evans rats (Verstynen *et al*. 2001). Accordingly, novelty-induced increases in short- and long-term potentiation, two relatively longer-lasting forms of synaptic plasticity, were found only in the right hippocampus (Tang *et al*. 2008). Moreover, the sensitivity of synaptic plasticity in the right hippocampus to corticosterone treatment measured on long-term

potentiation *in vitro* was significantly increased after neonatal novelty exposure compared to controls (Tang and Zou 2002). This is in a good agreement with our results, where volume of only right hippocampal formation was affected by corticosterone treatment. Although stress generally reduces hippocampal formation volume, novel contribution of our study is that reduction of hippocampal formation volume occurs only on the right side. We hypothesize that if neonatal novelty exposure increases asymmetrically volume of the right hippocampal formation, corticosterone treatment does the opposite – asymmetrically decreases the volume of the right hippocampal formation, mostly in the subiculum and less in the dentate gyrus and the CA1-CA3 subfield (Fig. 2). Decrease of the right hippocampal formation volume in the corticosterone-treated group may be due to decreased quantity of neurons. However, significant reduction in the quantity of neurons in dentate gyrus and CA3 hippocampal subfield was only found in rats exposed to glucocorticoids in the neonatal period, not in the adulthood (Sousa *et al*. 1998). Similarly, our data show only little (CA1 and CA2 subfield) or no changes (dentate gyrus and CA3) in the neuronal quantity (Table 1). Unfortunately, we did not include subiculum in neuronal quantity measurement due to the following reasons. Although subicular pyramidal cells are morphologically uniform in their shape, there are controversies concerning their laminar and/or columnar organization with distinct sublamination present (Ishizuka 2001). The cell packing in the pyramidal layer of the subiculum is looser than that seen in area CA1 and electrophysiologically, there is unique division into bursting and regular spiking cells compared to other hippocampal subfields (for review see Witter 2006). Nevertheless, since volumetric changes of subiculum were the most important in our study, we recommend to measure their neuronal quantity in the future.

We used different systems for hippocampal subfield volume estimation and hemispheric volume estimation. We have selected unbiased point lattice system for volumetry of hippocampal subfields with high accuracy of estimation (West *et al.* 1991). We measured hemisphere volume with more biased manual structural delineation method, similar to that described by Verstynen *et al.* (2001). Interestingly, volume normalization of hippocampal subfields to hemisphere volumes showed no significant effect. CE and CV were estimated only for neuronal quantity but not for numbers of degenerated neurons.

In the second part of the experiment we examined, whether hippocampal volumetric changes could be the result of ongoing degeneration processes. That is why in addition to volumetry, we also measured neuronal quantity and gross marks of neuronal degeneration, but we did not observe any significant differences between the corticosterone-treated group and controls. We have calculated CE (coefficient of error) only for neuronal quantity measurements and not for neuronal degeneration.

Neither neuronal quantity nor neurodegeneration data explain the decrease in right hippocampal formation volume in corticosterone-treated group. Neuronal degeneration plays a role only in specific short-time interval and therefore observed volume changes cannot be attributed to presently ongoing degenerative processes, since these would have already been terminated. We observed no significant changes in numbers of degenerated neurons, because these neurons were already destroyed by immune system, or other reparation processes.

Alterations of circulating corticosterone levels lead to changes in neuronal microstructure, gross marks of neuronal degeneration, and disruption of cognitive functions (Schubert *et al.* 2008). However, most of these changes are reversible and later it is difficult to detect them on the morphological level as time progresses (Sousa *et al*. 1999, Joëls 2008).

Permanent volume decrease of right hippocampal formation in corticosterone-treated group could be expained by neuroplasticity (cell cytoplasm volume decrease, loss of synapses etc.). Mechanism of corticosterone-mediated decrease of only the right hippocampal formation could be found on the molecular level. Several studies confirm asymmetrical distribution of hippocampal neuronal receptors or enzyme systems. Synaptic distribution of N-methyl-D-aspartate (NMDA) receptor GluR epsilon2 (NR2B) subunits in the adult mouse hippocampus shows asymmetry between left and right hippocampus and between apical and basal dendrites of single neurons (Kawakami *et al*. 2003). Functional lateralization of the high-affinity choline uptake (HACU) system was found in the hippocampus of Wistar rats. Markedly increased HACU activity was found in left hippocampal formation compared to the right one of adult male, but not female, rats (Krištofíková *et al*. 2004).

We do not know whether a decrease of the right hippocampal formation in corticosterone-treated group is specific for the rat, or even only for Long-Evans strain. On the other hand, it is not possible to rule out the hypothesis that it is a more general phenomenon of delayed corticosterone effect on the brain. Unfortunately,

most studies known to us do not include laterality estimations. Sometimes it is not clear, whether the reported volumes are only from one hemisphere or from both hemispheres summed together.

Conclusions

Taken together, animals received corticosterone for three weeks by means of subcutaneous pellets. Volumetry, neuronal quantity and marks of neuronal degeneration were estimated seven weeks after the termination of corticosterone treatment. The first main finding of our study is significant volume laterality of the hippocampal formation in the Long-Evans rats. In the control group right hippocampal volume was markedly higher than all other measured volumes (hippocampal left control, hippocampal left corticosterone-treated and hippocampal right corticosterone-treated). Left hippocampal volume did not differ between the groups. The second main finding of our study is delayed permanent effect of corticosterone on the dominant hippocampal formation. We observed significant differences in volumes and especially in laterality of hippocampal subfields between control and corticosterone-treated animals. Many studies describe corticosterone effect on volumetry of hippocampal formation. The results are very often not consistent. The lateralization effect of corticosterone treatment in most of the studies is neglected. Major contribution of our study is in its focus on the lateralization of the hippocampal formation under corticosterone treatment.

Conflict of Interest

There is no conflict of interest.

Acknowledgements

This work was supported by grants IGA MH NR/9180-3 and by AV0Z 50110509. We thank Michaela Fialová and Věra Šenková for technical assistance and Vanessa Doulames for language review.

References

ADIGUZEL E, DUZCAN SE, AKDOGAN I, TUFAN AC: A simple low-cost method for two dimensional microscopic measuring and stepping on the microscopic plate. *Neuroanatomy* **2**: 6-8, 2003.

ALFAREZ DN, WIEGERT O, KRUGERS HJ: Stress, corticosteroid hormones and hippocampal synaptic function. *CNS Neurol Disord Drug Targets* **5**: 521-529, 2006.

BRUNNER R, SCHAEFER D, HESS K, PARZER P, RESCH F, SCHWAB S: Effect of corticosteroids on short-term and long-term memory. *Neurology* **64**: 335-337, 2005.

GLUCK MA, MYERS C, MEETER M: Cortico-hippocampal interaction and adaptive stimulus representation: a neurocomputational theory of associative learning and memory. *Neural Netw* **18**: 1265-1279, 2005.

GUNDERSEN HJG, JENSEN EB: The efficiency of systematic sampling in stereology and its prediction. *J Microsc* **147**: 229-263, 1987.

GUNDERSEN HJG, BENDTSEN TF, KORBO L, MARCUSSEN N, MILLER A, NIELSEN K, NYENGAARD JR, PAKKENBERG B, SØRENSEN FB, VESTBY A, WEST MJ: Some new, simple and efficient stereological methods and their use in pathological research and diagnosis. *APMIS* **96**: 379-394, 1988a.

GUNDERSEN HJG, BAGGER P, BENDTSEN TF, EVANS SM, KORBO L, MARCUSSEN N, MILLER A, NIELSEN K, NYENGAARD JR, PAKKENBERG B, SØRENSEN FB, VESTERBY A, WEST MJ: The new stereological tools: disector, fractionator, nucleator and point sampled intercepts and their use in pathological research and diagnosis. *APMIS* **96**: 857-881, 1988b.

ISHIZUKA N: Laminar organization of the pyramidal cell layer of the subiculum in the rat. *J Comp Neurol* **435**: 89-110, 2001.

JOËLS M: Functional actions of corticosteroids in the hippocampus. *Eur J Pharmacol* **583**: 312-321, 2008.

KAPLAN S, CANAN S, ASLAN H, UNAL B, SAHIN B: A simple technique to measure the movements of the microscope stage along the x and y axes for stereological methods. *J Microsc* **203**: 321-325, 2001.

KAWAKAMI R, SHINOHARA Y, KATO Y, SUGIYAMA H, SHIGEMOTO R, ITO I: Asymmetrical allocation of NMDA receptor epsilon2 subunits in hippocampal circuitry. *Science* **300**: 990-994, 2003.

KEUKER JIH, VOLLMANN-HONSDORF GK, FUCHS E: How to use the optical fractionator: an example based on the estimation of neurons in the hippocampal CA1 and CA3 regions of tree shrews. *Brain Res Protocol* **7**: 211-221, 2001.

KOLB B, SUTHERLAND RJ, NONNEMAN AJ, WHISHAW IQ: Asymmetry in the cerebral hemisphere of the rat, mouse, rabbit, and cat: the right hemisphere is larger. *Exp Neurol* **78**: 348-359, 1982.

KORKMAZ A, TUMKAYA L: Estimation of the section thickness and optical dissector height with a simple calibration method. *J Microsc* **187**: 104-109.

KRIŠTOFÍKOVÁ Z, ŠŤASTNÝ F, BUBENÍKOVÁ V, DRUGA R, KLASCHKA J, ŠPANIEL F: Age-and sex-dependent laterality of rat hippocampal cholinergic system in relation to animal models of neurodevelopmental and neurodegenerative disorders. *Neurochem Res* **29**: 671-680, 2004.

MACLULLICH AM, DARY IJ, STARR JM, FERGUSON KJ, WARDLAW JM, SECKL JR: Plasma cortisol levels, brain volumes, and cognition in healthy elderly men. *Psychoneuroendocrinology* **30**: 505-515, 2005.

MCEWEN BS: Central effects of stress hormones in health and disease: Understanding the protective and damaging effects of stress and stress mediators. *Eur J Pharmacol* **583**: 174-185, 2008.

PARKER KL, RAINEY WE: The adrenal glands. *In: Textbook of Endocrine Physiology.* JE GRIFFIN, SR OJEDA (eds), Oxford University Press, New York, 2004, pp 324-326.

PAXINOS G, WATSON C: *The Rat Brain in Stereotaxic Coordinates*. Academic Press, London, 1998.

PEINADO MA, QUESADA A, PEDROSA JA, MARTINEZ M, ESTEBAN FJ, DEL MORAL ML, PEINADO JM: Light microscopic quantification of morphological changes during aging in neurons and glia of the rat parietal cortex. *Anat Rec* **247**: 420-425, 1977.

SAHIN B, ASLAN H, UNAL B, CANAN S, BILGIC S, KAPLAN S, TUMKAYA L: Brain volumes of the lamb, rat and bird do not show hemispheric asymmetry: a stereological study. *Image Anal Stereol* **20**: 9-13, 2001.

SAPOLSKY RM: A mechanism for glucocorticoid toxicity in the hippocampus – increased neuronal vulnerability to metabolic inzulte. *J Neurosci* **5**: 1228-1232, 1985.

SCHUBERT MI, KALISCH R, SOTIROPOULOS I, CATANIA C, SOUSA N, ALMEIDA OF, AUER DP: Effects of altered corticosteroid milieu on rat hippocampal neurochemistry and structure – an in vivo magnetic resonance spectroscopy and imaging study. *J Psychiatr Res* **42**: 902-912, 2008.

ŠIMŮNKOVÁ K, STÁRKA M, HILL L, KŘÍŽ R, HAMPL K, VONDRA K: Comparison of total and salivary cortisol in a low-dose ACTH (Synacthen) test: influence of three-month oral contraceptives administration to healthy women. *Physiol Res* **57** (Suppl 1): S193-S199, 2008.

SOUSA N, MADEIRA MD, PAULA-BARBOSA MM: Effects of corticosterone treatment and rehabilitation on the hippocampal formation of neonatal and adult rats. An unbiased stereological study. *Brain Res* **794**: 199-210, 1998.

SOUSA N, MADEIRA MD, PAULA-BARBOSA MM: Corticosterone replacement restores normal morphological features to the hippocampal dendrites, axons and synapses of adrenalectomized rats. *J Neurocytol* **28**: 541-558, 1999.

TANG AC: A hippocampal theory of cerebral lateralization. In: *The Asymmetrical Brain*. K HUGDAHL, RJ DAVIDSON (eds), A Bradford Book, MIT, Cambridge, Massachusetts, 2003, pp 37-69.

TANG AC, ZOU B: Neonatal exposure to novelty enhanced long-term potentiation in CA1 region of the rat hippocampus. *Hippocampus* **13**: 398-404, 2002.

TANG AC, BENDE Z, REEB BC, CONNOR JA: An epigenetic induction of a right-shift in hippocampal asymmetry: selectivity for short- and long-term potentiation but not post-tetanic potentiation. *Hippocampus* **18**: 5-10, 2008.

TATA DA, MARCIANO VA, ANDERSON BJ: Synapse loss from chronically elevated glucocorticoids: relationship to neuropil volume and cell number in hippocampal area CA3. *J Comp Neurol* **498**: 363-374, 2006.

TESSNER KD, WALKER EF, DHRUV SH, HOCHMAN K, HAMANN S: The relation of cortisol levels with hippocampus volumes under baseline and challenge conditions. *Brain Res* **1179**: 70-78, 2007.

VERSTYNEN T, TIERNEY R, URBANSKI T, TANG A: Neonatal novelty exposure modulates hippocampal volumetric asymmetry in the rat. *Neuroreport* **12**: 3019-3022, 2001.

WEST MJ, SLOMIANKA L, GUNDERSEN HJ: Unbiased stereological estimation of the total number of neurons in the subdivisions of the rat hippocampus using the optical fractionator. *Anat Rec* **231**: 482-497, 1991.

WITTER MP: Connections of the subiculum of the rat: topography in relation to columnar and laminar organization. *Behav Brain Res* **174**: 251-264, 2006.

ZACH, P.; **MRZÍLKOVÁ, J.**; STUCHLÍK, A.; VALEŠ, K. a L. ŘEZÁČOVÁ. Delayed effect of chronic administration of corticoids on the taste aversion learning. *Neuroendocrinology Letters*. 2011, **32**(1), 90-95. ISSN 0172-780X. **IF: 1.296/2011**.

Abstract: Long term permanent changes of eating behavior and concomitant structural changes in the CNS are matter of debade in literature. Often there is not enough distinction beween acute and chronic exposure to corticoids in evaluating its effect on behavior and/or brain structural changes. For behavioral evaluation we used well established conditioned taste aversion (CTA) paradigm and coronal Nissl-stained brain sections for evaluation of neuroanatomical changes. The CTA is part of complex adaptive behavioral processes controling food intake. It is well established methodological tool for study of biological substrates of learning and memory.

ORIGINAL ARTICLE

Delayed effect of chronic administration of corticoids on the taste aversion learning

Petr ZACH [2,3], Jana MRZILKOVA [2], Ales STUCHLIK [1], Karel VALES [1], Lenka REZACOVA [1]

1 Institute of Physiology, Academy of Sciences, Czech Republic
2 Institute of Anatomy, 3rd Faculty of Medicine, Charles University, Prague, Czech Republic
3 Social and Health Faculty, South-Bohemian University, Ceske Budejovice, Czech Republic

Correspondence to: Petr Zach, MD., PhD.
Institute of Anatomy, 3rd Faculty of Medicine, Charles University
Ruska 87, Prague 10, Czech Republic.
TEL: +420 267102511; FAX: +420 267102508; E-MAIL: zach.petr@post.cz

Submitted: 2010-11-25 *Accepted: 2011-01-05* *Published online: 2011-02-25*

Key words: **conditioned taste aversion; corticosterone; eating disorders; eating behavior; neuronal structural changes; corticoids; memory**

Neuroendocrinol Lett 2011; **32**(1):90–95 **PMID:** 21407164 NEL320111A12

Abstract

BACKGROUND: Long term permanent changes of eating behavior and concomitant structural changes in the CNS are matter of debade in literature. Often there is not enough distinction beween acute and chronic exposure to corticoids in evaluating its effect on behavior and/or brain structural changes. For behavioral evaluation we used well established conditioned taste aversion (CTA) paradigm and coronal Nissl-stained brain sections for evaluation of neuroanatomical changes. The CTA is part of complex adaptive behavioral processes controling food intake. It is well established methodological tool for study of biological substrates of learning and memory.

AIM: Our hypothesis was that long term changes in laboratory rat behavior induced by exogenous corticosterone are not accompanyied by neurohistological changes in the rat brain, previously described in literature.

RESULTS: Firstly, our results support CTA paradigm as promising tool for testing chronic influence of stress hormones on eating behavior and memory. The results support fact that previous long term elevated corticosterone levels disrupt normal eating behavior and it could also lead to structural changes, which could be biological substrates of behavioral changes. The fact we have not found significant morphological changes in brain strengthen the notion of possible subcellular impairment taking place instead of simple neuronal loss.

INTRODUCTION

Neurotoxicity of corticoids belongs to actually debated problems. Animal models shows, that exposition to high and/or long-term functioning doses of corticoids or intensive stress leads to structural and behavioral changes and often to hippocampal neuronal death. Also patients suffering from diseases connected with high levels of corticoids at the onset of disease (post traumatic stress disorder) or during illness course (afective disorders, Alzheimer´s dementia and also group of eating disorders, such as anorexia nervosa or bulimia (Gluck, 2006), showed statistically important shrinkage of hippocampus and worse results in tests focused on short term memory evaluation in comparison with control groups (Alfarez *et al.* 2006; Brunner *et al.* 2005).

In the literature often appears to be discrepancies in description of categories of corticoids administration as for the timing. There exists at least following possibilities concerning timing of corticoids administration to the laboratory rat: acute effect and chronic effect (Skórzewska *et al.* 2006). Acute effect of corticoids manifests primarily on non-genomic level of changes, on the contraty chronic effect of corticoids administration targets primarily genomic level, which include also onset of permanent degeneration changes (de Vries *et al.* 2002). In the acute administration there is vital dosing of the corticoids. Corticoids in a given range dose are inevitable for learning and memory formation (Payne & Nadel 2004).

Chronic corticoids administration to artificially high levels induces apical dendritic retraction and debranching (20%) in rat CA3c pyramidal neurons (Watanabe *et al.* 1992b; Woolley *et al.* 1990), while longer durations of corticoids administration result in more substantial hippocampal damage, such as neuronal death, gliosis, and atrophied perikarya in principal layers, most notably in the CA3c region (Sapolsky *et al.* 1985). Repeated stress exerts similar effects as corticoids on dendritic remodeling in CA3. One key feature of prolonged stress is the alteration in dendritic spine number and morphology in the hippocampal formation. These changes could be neurobiological substrate for behavioral changes and stress induced reactivity.

The aim of our experimental work was to find out whether long term behavioral changes induced by chronic corticosterone treatment are followed by significant gross neurohistological changes in the selected structures – hippocampus, amygdala, prefrontal cortex and parabrachial nucleus of the brain stem.

MATERIALS AND METHODS

Characteristics of experimental animals

The experiments were performed in 3-month-old male hooded rats of the Long-Evans strain. In total 21 animals were used in the study. The animals were obtained from the breeding colony of the Institute and housed in a room with constant temperature (20–22 °C) and 12 h/12 h light/dark cycle with the light switched on at 7 AM. While standard food was freely available, access to water was limited as described later. The experiments were performed in agreement with the Animal Protection Law of the Czech Republic and corresponded fully to the European Communities Council recommendations for the use of laboratory animals (directive 86/609/ECC).

Corticosterone administration

Corticosterone was administered by means of subcutaneous pellets. Pellets were inserted in the regio interscapularis. Each pellet contained 200 mg of corticosterone, release time 28 days (pellets purchased from Innovative Research of America Ltd.). Control animals received equivalent pellets containing cholesterole (pellets purchased from Innovative Research of America Ltd.)

CTA procedure

Water-deprived rats were trained for 2 days to drink their daily supply of water during a 15-min interval in the drinking box ($40 \times 30 \times 20\,cm^3$). It was equipped with an array of ten calibrated pipettes (2 ml each) arranged along the shorter wall of the box. Rats were placed into the drinking box individually and the fluid consumed from all ten pipettes was measured for each animal. On day 3, the rats were offered 0.1% solution of sodium saccharin in all pipettes. Thirty minutes after drinking the rats received i.p. injection of lithium chloride (LiCl; 0.15 M; 2% b.w.). On day 4 the animals were again offered water in the drinking box for 15 min. For the retrieval test on day 5, the pipettes were alternately filled with water and saccharin solution and the individual preference scores for each rat were expressed as the percentage of saccharin intake from the total fluid consumption.

Time schedule of experiment

First, to the animals were implanted subcutaneous pellets containing corticosterone (resp. cholesterole in control group). Animals were allowed spontaneous activity during this phase. Substances from pellets were released for 28 days, (Figure 1). Following three weeks were animals left without any behavioral manipulations. Next week followed behavioral procedure in order to reveal delayed effect of corticosterone on CTA formation. The animals were for last two weeks again left without any behavioral manipulations. Animals were enabled spontaneous activity during this phase. At this point were animals ready for histological analysis.

Histology

Animals were perfused with 4% paraformaldehyde under deep pentobarbital anesthesia. Brains were removed from the skull and embedded in paraplast. Serial sections (in coronal plane) of whole brains were performed (20 μ) on table microtome (Leica). All brain sections were then mounted on microscope slides and

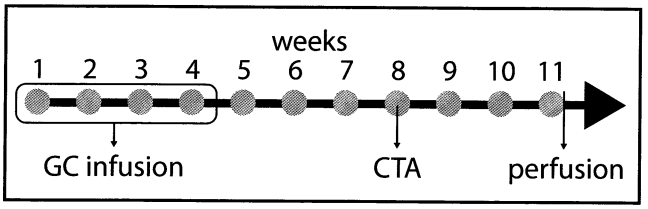

Fig. 1. Time schedule of experiment. The animals were implanted with subcutaneous pellets containing corticosterone (GC infusion) (resp. cholesterole in control group). Substances from pellets were released for 28 days. Following three weeks were animals left without any behavioral manipulations. Next week followed behavioral procedure in order to reveal delayed effect of corticosterone on CTA formation.

stained according to Nissl. Brain sections were then viewed on Leica light microscope attached to the standard PC computer with Leica IM 1000 stereology/database software (Leica Microsystems, GmbH, Wetzlar, Germany).

Neurohistology and stereology

Brain regions (prefrontal cortex (PFC) – it´s infralimbic, prelimbic and cingulate portion, CA3 of hippocampus, central nucleus of the amygdala and ncl. parabrachialis – its medial and lateral groups of subnuclei) were distinguished using Paxinos atlas of the rat brain (Paxinos & Watson 2005). We have started always with the cell numbers measurement in the middle of the selected structure of the interest of the rat brain (except for PFC) (West *et al.* 1991). Since all crossections were obtained in the frontal plane, optimal shape of the structure was approximated as ovoid (except for PFC, where we have selected lateral part of PFC according to Paxinos atlas without estimating ovoid shape). All stereology procedures were performed according to (Cerqueira *et al.* 2005). Average cell numbers were estimated using the optical fractionator method, as described previously (West *et al.* 1991). Briefly, for analysis were selected always 5 sections depending on the region being analyzed. Beginning at the central area of the structure of interest (except for PFC), a grid of virtual three-dimensional boxes (30x30x15 μm) that were equally spaced were used and neurons were counted whenever their nucleus came into focus within the counting box. Neurons were differentiated from other cells on the basis of nuclear size (larger in neurons than in glial cells), a prominent nucleolus, and the shape of their perikarya attributable to dendritic emergence (Peinado *et al.* 1997).

Neuron number estimation and statistics

Section sampling fraction and total neuronal quantity of hippocampus, amygdala, PFC and PBN were calculated according to formula by (West *et al.* 1991). CE (coefficient of error) was calculated separately for each structure and CV, coefficient of variation was estimated as CV=SD/mean as described in (West *et al.* 1991).

A repeated measures two-way ANOVA (lateralization – right, left) as the within-subject factor and group (control and corticosterone) as the between-subject factor compared neuronal numbers in the right and left hippocampus, amygdala, PFC and PBN. Newman-Keuls test was used for posthoc analysis of significant main effects and interactions. For statistical analysis of the laterality differences, independent samples t-tests were used to examine group differences.

RESULTS

Behavioral results

Twenty one male rats were randomly assigned to two groups. First group was implanted with corticosterone pellets (n=9). Second group was control (n=12). All groups did not differ in total amount of liquid consumption as shown on Figure 2. This was confirmed by two-way ANOVA with repeated measures ($F_{1,19}$=0.66, p>0.05). The mean saccharin preference scores during the retrieval test performed on day 5 are shown on Figure 3. T-test (two-sample assuming unequal variances) indicated significance between groups (t_{17}=2.94,

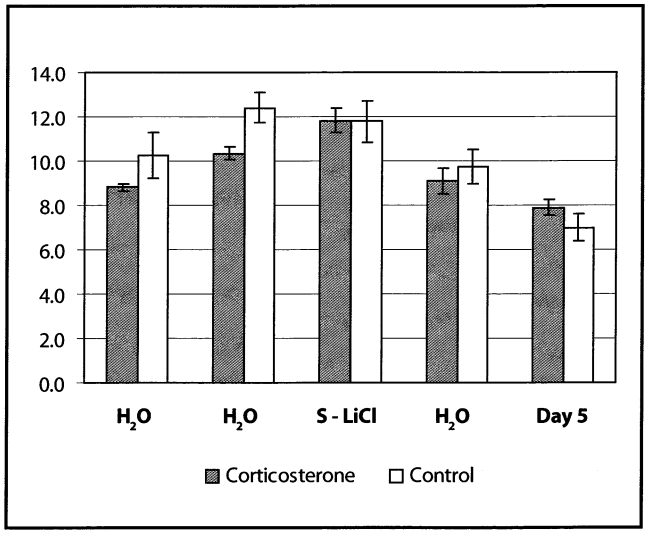

Fig. 2. Liquid consumption during experiment. The groups did not differ in total amount of liquid consumption. Each column represents the mean (±SEM) of total amount of fluid consumption in each days. Y-axis data are in ml. On the X-axis - 1st and 2nd day rats received only water, on day 3 received 0.1% solution of sodium saccharin with LiCl, 0.15 M; 2% b.w.

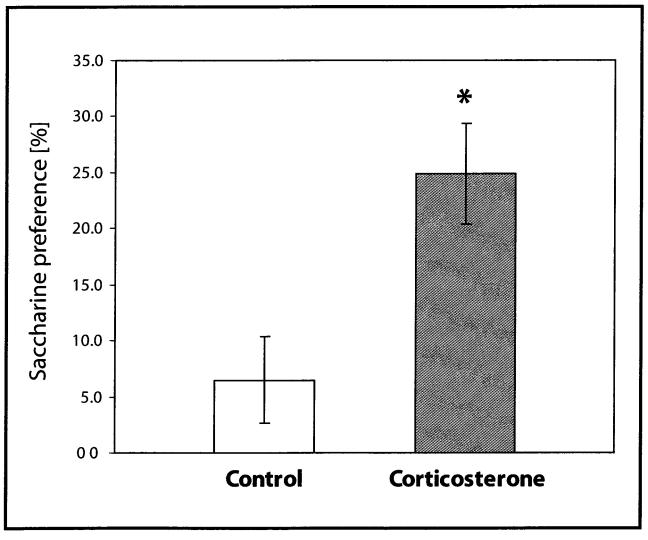

Fig. 3. The delayed effect of previous chronic corticosterone administration on CTA. Data show that corticosterone group differed from control group. Each column represents the mean (±SEM) percentage of saccharine intake from total fluid intake during the retrieval test. Y-axis shows saccharine preference in %. X-axis shows two groups – control and corticosterone.

$p<0.01$). These findings show delayed effect of previous chronic corticosterone administration on CTA.

Neurohistology and stereology results

In the PFC in the layers II and III there was not significant reduction of the numbers of neurons of experimental animals compared to controls. In experimental group there were only rare neurons with clear marks of degeneration (pyknosis and swelling of cytoplasm). In all subsets of neurons within CA3 field (CA3a-c) there were also solitary neurons with clear marks of degeneration compared to control group. In the central nucleus of the amygdala (in the central region, containing more densely packed cells) we have observed no neurons with clear marks of degeneration in the experimental animals compared to controls. In the lateral part of parabrachial nucleus there was small reduction (less than 2% neurons totally) of the numbers of neurons of experimental animals compared to controls and there was no difference in the numbers of neurons in the medial part of the parabrachial nucleus of experimental animals compared to controls. It is necessary to mention, that due to relatively small numbers of neurons in the parabrachial nucleus, approx. hundreds of neurons (Petrovicky & Kolesarova 1989) even small changes in the total number could be potentially functionally important.

In the first three structures (PFC, hippocampus, central nucleus of amygdalar complex) there are only rare cases of neuronal degeneration in the experimental group compared to control group. On the contrary in the parabrachial nucleus there are couple of neurons with marks of neuronal degeneration compared to control group. Summary of these results are in Table 1. We have not found significant effect of laterality on neuronal numbers in all structures.

DISSCUSION

Our results document impairment of CTA formation due to previous chronic administration of corticosterone (Figure 3). These results point to long term changes of animal inability to adequatly react on different cognitive tasks, which could be associated with structural changes of the brain.

Conditioned taste aversion is well established behavioral paradigm of learning and memory and represents good tool for studying neuronal plasticity (advantages of this paradigm are mainly well described anatomical structures and physiological cellular mechanisms and easy and precise measurability) (Bureš 1998). Taste aversion is integral part of eating behavior. It is biologically important phenomenon because survival of all organisms depends on their capabilities efficiently acquire and use food and avoid poisoned one. Eating behavior and long term weight regulation and food intake is arranged by complex interactions of CNS and peripheral organs (leptin, glucocorticoid, insulin, hormones of GIT) (Dostálová *et al.* 2007; Zach *et al.* 2006; Papežová *et al.* 2005). Regulation is maintained primarily by hypothalamus, prefrontal cortex, amygdala, striatum and midbrain.

Influence of stress and corticosterone on the learning and memory is in the center of scientific discussions because it participates in a number of neuropsychiatric disorders (from the point of this work especially in eating disorders). Morphological studies have shown that prolonged exposure to stress or to excess glucocorticoids results in time-dependent neuronal damage, ranging from an initial and reversible atrophy of dendritic processes (Woolley *et al.* 1990; Watanabe *et al.* 1992a; Magariños *et al.* 1995) to the irreversible loss (Landfield 1987; Sapolsky *et al.* 1985) of hippocampal pyramidal cells. This stress- or glucocorticoid-induced structural damage appears to coincide with learning and memory deficits.

CTA formation enhancement by acute corticosterone administration was shown previously (Tenk *et al.* 2006). Nevertheless, there are marked differences between acute and delayed effects of corticoids exposure on the cognitive abilities. Acute administration of corticoids has been shown to facilitate the acquisition of conditioned taste aversions to a novel-flavoured solution paired with the visceral illness inducing toxin, lithium chloride (Kent *et al.* 2002).

On the contrary design of our experiment was setup to monitor long term permanent changes of eating behavior and concomitant structural changes in the CNS. It is intensively discussed in literature, that previous elevated levels of corticoids or stress events lead to delayed changes in the eating behavior and probably participate in the pathophysiology of eating disorder (Papežová *et al.* 2005).

Tab. 1. Neurohistological changes in the brain structures 4 weeks after corticosterone application termination.
We have not found significant changes in numbers of Nissl stained neurons in any of selected brain region of animals who received corticosterone, except for nc. parabrachialis compared to controls, where was . Number of severely damaged neurons observed by Nissl staining has not exceeded 5 of them in all selected brain regions in animals, who received corticosterone.

	Ctrl NN	Exp NN	Ctrl ND	Exp ND
PFC	no significant difference		rare	
Hipp	no significant difference		rare	
Amyg	no significant difference		none	
PBN				
lateral	slightly lower in Exp		rare	
medial	no significant difference		none	

PFC – prefrontal cortex, Hipp – hippocampus, Amyg – amygdala, PBN – parabrachial nucleus, NN – neuronal numbers, ND – neuronal damage, Ctrl – control animals, Exp – experimental animals.

Cerebral atrophy accompanying eating disorders is early detectable. Structural morphometry of the brain has shown that volume of either white and gray matter in case of acute anorexia is severely reduced. But white matter has tendency return to normal after successful realimentation, while gray matter deficit remains. This could be partially explained by permanent loss of neurons and/or glial cells, caused for example by cortisol elevation. Alternative explanation could be: loss of neurons is not effect of anorexia, but its cause and it reflects abnormal neural system development. Our results support the fact, that previously long term elevated corticosterone levels disrupt normal eating behavior.

Previous stress event plays a role in subsequent onset of eating disorders in animals as well as in humans. Most famous are examples of pig eating disorders, described as wasting pig syndrome (WPG) and thin sow syndrome (TSS), which are connected with stress in critical period of weaning and in lactation period in adult female pigs manifesting as growth slowdown and bodily weight loss and finally loss of fertility and death. Similar situation is described for humans by Schmidt *et al.* (1997) where there is always preceding stressing life event to onset of anorexia and bulimia.

We have not found significant increase/decrease in neuronal numbers and gross neuronal degeneration in PFC, amydala nor hippocampus using Nissl staining protocol in experimental animals. These findings are in a good accord with study (Tata *et al.* 2006) where mainly ultrastructural changes are described in corticoid treated animals, although previous studies (Sapolsky *et al.* 1985), (Woolley *et al.* 1990) were able to show even gross changes in neuronal bodies and dendrites. Partly this could be due to different methodologies used.

Minor loss of neurons in lateral part of the parabrachial nucleus (not exceeding 2% neurons totally) needs further verification by means of immunohistochemistry to prove it more securely. Damage of parabrachial complex neurons nucleoli could be anticipated due to its prominent position in CTA reaction neuroanatomical circuitry.

Our results show only minor damage of CNS structures participating in taste aversion formation, but significant behavioral changes. Our study offers insight into time delayed situation, where neurodegenerative and neuroreparative processes take place. We can speculate that permanent changes in the CNS are way too subtle for gross morphological methods of detection. Another explanation is that atrophy or neuronal loss after acute stress or acute corticoids application (Sapolsky *et al.* 1985) is later almost completely reversed by reparative processes.

Our results show that longer term exposure to glucocorticoids lead later to impaired ability to form taste aversion. Contemporary findings of morphological impairment of brain structures are relatively not consistent. Meanwhile some authors describe moderate atrophy or hippocampal neuronal loss (Woolley *et al.* 1990), other studies do not confirm that (Tata *et al.* 2006). Similarly, our results show only moderate permanent changes. It is possible to conclude that even significant behavioral impairment may not be accompanied by gross neuronal changes. Our model offers possibility for further study of more precise mechanisms of corticoids effect on memory and eating behavior.

ACKNOWLEDGEMENT

We thank M. Fialova and L. Horakova for laboratory work. This study was supported by grants IGA MH NR/9180-3, MEYS CR, project 1M0517 and grant AV0Z50110509 from AV CR.

REFERENCES

1 Bureš J, Bermúdez-Rattoni F, Yamamoto T (1998). *Conditioned taste aversion. Memory of a special kind.* Oxford: Oxford University Press.
2 Alfarez DN, Wiegert O, Krugers HJ (2006). Stress, corticosteroid hormones and hippocampal synaptic function. CNS & Neurological Disorders - Drug Targets. **5**: 521–529. Review.
3 Brunner R, Schaefer D, Hess K, Parzer P, Resch F, Schwab S (2005). Effect of corticosteroids on short-term and long-term memory. Neurology. **64**(2): 335–7.
4 Cerqueira JJ, Pêgo JM, Taipa R, Bessa JM, Almeida OF, Sousa N (2005). Morphological correlates of corticosteroid-induced changes in prefrontal cortex-dependent behaviors. J Neurosci. **25**(34): 7792–800.
5 de Vries WB, van der Leij FR, Bakker JM, Kamphuis PJ, van Oosterhout MF, Schipper ME, Smid GB, Bartelds B, van Bel F (2002). Alterations in adult rat heart after neonatal dexamethasone therapy. Pediatr Res. **52**(6): 900–6.
6 Dostálová I, Barták V, Papežová H, Nedvídková J (2007). The effect of short-term exercise on plasma leptin levels in patients with anorexia nervosa. Metabolism. **56**(4): 497–503.
7 Gluck ME (2006). Stress response and binge eating disorder. Appetite. **46**(1): 26–30. Review.
8 Kent WD, Cross-Mellor SK, Kavaliers M, Ossenkopp KP (2002). Acute effects of corticosterone on LiCl-induced rapid gustatory conditioning in rats: a microstructural analysis of licking patterns. Behav Brain Res. **136**(1): 143–50.
9 Landfield PW (1987). Modulation of brain aging correlates by long-term alterations of adrenal steroids and neurally-active peptides. Prog Brain Res. **72**: 279–300. Review.
10 Magariños AM, McEwen BS (1995). Stress-induced atrophy of apical dendrites of hippocampal CA3c neurons: comparison of stressors. Neuroscience. **69**(1): 83–8.
11 Papezová H, Yamamotová A, Uher R (2005). Elevated pain threshold in eating disorders: physiological and psychological factors. J Psychiatr Res. **39**(4): 431–8. Epub 2005 Jan 20.
12 Paxinos G, Watson Ch (2005). *The Rat Brain in Stereotaxic Coordinates - The New Coronal Set.* Fifth Edition, New York: Elsevier.
13 Payne JD, Nadel L (2004). Sleep, dreams, and memory consolidation: the role of the stress hormone cortisol. Learn Mem. **11**(6): 671–8. Review.
14 Peinado MA, Quesada A, Pedrosa JA, Martinez M, Esteban FJ, Del Moral ML, Peinado JM (1997). Light microscopic quantification of morphological changes during aging in neurons and glia of the rat parietal cortex. Anat Rec. **247**(3): 420–5.
15 Petrovický P, Kolesárová D (1989). Parabrachial nuclear complex. A comparative study of its cytoarchitectonics in birds and some mammals including man. J Hirnforsch. **30**(5): 539–50.
16 Sapolsky RM, Krey LC, McEwen BS (1985). Prolonged glucocorticoid exposure reduces hippocampal neuron number: implications for aging. J Neurosci. **5**(5): 1222–7.

17 Schmidt PJ, Rubinow DR (1997). Neuroregulatory role of gonadal steroids in humans. Psychopharmacol Bull. **33**(2): 219–20.
18 Skórzewska A, Bidziński A, Lehner M, Turzyńska D, Wisłowska-Stanek A, Sobolewska A, Szyndler J, Maciejak P, Taracha E, Płaźnik A (2006). The effects of acute and chronic administration of corticosterone on rat behavior in two models of fear responses, plasma corticosterone concentration, and c-Fos expression in the brain structures. Pharmacol Biochem Behav. **85**(3): 522–34. Epub 2006 Nov 14.
19 Tata DA, Marciano VA, Anderson BJ (2006). Synapse loss from chronically elevated glucocorticoids: relationship to neuropil volume and cell number in hippocampal area CA3. J Comp Neurol. **498**(3): 363–74.
20 Tenk CM, Kavaliers M, Ossenkopp KP (2006). The effects of acute corticosterone on lithium chloride-induced conditioned place aversion and locomotor activity in rats. Life Sci. **79**(11): 1069–80.
21 Watanabe Y, Gould E, Cameron HA, Daniels DC, McEwen BS (1992a). Phenytoin prevents stress- and corticosterone-induced atrophy of CA3 pyramidal neurons. Hippocampus. **2**(4): 431–5.
22 Watanabe Y, Gould E, McEwen BS (1992b). Stress induces atrophy of apical dendrites of hippocampal CA3 pyramidal neurons. Brain Res. **588**(2): 341–5.
23 West MJ, Slomianka L, Gundersen HJ (1991). Unbiased stereological estimation of the total number of neurons in the subdivisions of the rat hippocampus using the optical fractionator. Anat Rec. **231**(4): 482–97.
24 Woolley CS, Gould E, McEwen BS (1990). Exposure to excess glucocorticoids alters dendritic morphology of adult hippocampal pyramidal neurons. Brain Res. **531**(1–2): 225–31.
25 Zach P, Krivanek J, Vales K (2007). Serotonin and dopamine in the parabrachial nucleus of rats during conditioned taste aversion learning. Behav Brain Res. **170**(2): 271–6.

MRZÍLKOVÁ, J.; ZACH, P.; BARTOŠ, A.; TINTĚRA, J. a D. ŘÍPOVÁ. Volumetric Analysis of the Pons, Cerebellum and Hippocampi in Patients with Alzheimer's Disease. *Dementia and Geriatric Cognitive Disorders*. 2012, **34**(3-4), 224-234. ISSN 1420-8008. DOI: 10.1159/000343445. **IF: 2.787/2012**.

Abstract: Our goal was to find out whether a decrease in hippocampal volume in Alzheimer's disease measured via magnetic resonance imaging is accompanied by a similar volume decrease in the pons and cerebellum. We also tried to evaluate whether there are any accompanying hippocampal, pontine and cerebellar asymmetries between the left and right side. We performed a manual volumetric magnetic resonance analysis of the pons, cerebellum and hippocampi in 29 healthy controls and 26 patients with Alzheimer's disease, divided into two groups according to the Mini-Mental State Examination score. We confirmed a known decrease in hippocampal volume in Alzheimer's disease patients but found that there is no similar volume decrease in the pons or cerebellum that could serve as a radiologic diagnostic tool in Alzheimer's disease diagnosis. Also, there was no statistically significant right-left asymmetry in all three measured structures. Only hippocampal volume and not pontine and cerebellar volumes could serve as a magnetic resonance diagnostic tool in Alzheimer's disease.

Original Research Article

Dementia and Geriatric Cognitive Disorders

Dement Geriatr Cogn Disord 2012;34:224–234
DOI: 10.1159/000343445

Accepted: September 3, 2012
Published online: November 1, 2012

Volumetric Analysis of the Pons, Cerebellum and Hippocampi in Patients with Alzheimer's Disease

Jana Mrzilková[a] Petr Zach[a] Aleš Bartoš[c,d] Jiří Tintěra[b] Daniela Řípová[c]

[a]Institute of Anatomy, Third Faculty of Medicine, Charles University, [b]Institute for Clinical and Experimental Medicine, [c]AD Center, Prague Psychiatric Center, and [d]Charles University in Prague, Third Faculty of Medicine, University Hospital Královské Vinohrady, Department of Neurology, Prague, Czech Republic

Key Words
Hippocampus · Cerebellum · Pons · Alzheimer's disease · Volumetry · Asymmetry

Abstract
Background/Aims: Our goal was to find out whether a decrease in hippocampal volume in Alzheimer's disease measured via magnetic resonance imaging is accompanied by a similar volume decrease in the pons and cerebellum. We also tried to evaluate whether there are any accompanying hippocampal, pontine and cerebellar asymmetries between the left and right side. ***Methods:*** We performed a manual volumetric magnetic resonance analysis of the pons, cerebellum and hippocampi in 29 healthy controls and 26 patients with Alzheimer's disease, divided into two groups according to the Mini-Mental State Examination score. ***Results:*** We confirmed a known decrease in hippocampal volume in Alzheimer's disease patients but found that there is no similar volume decrease in the pons or cerebellum that could serve as a radiologic diagnostic tool in Alzheimer's disease diagnosis. Also, there was no statistically significant right-left asymmetry in all three measured structures. ***Conclusion:*** Only hippocampal volume and not pontine and cerebellar volumes could serve as a magnetic resonance diagnostic tool in Alzheimer's disease.

Introduction

Volumetric changes of the hippocampi play an important role in the diagnostic evaluation of Alzheimer's disease (AD) [1]. A decrease in volume of the right or left (or both) hippocampi in patients with AD was measured on magnetic resonance imaging (MRI) and described in numerous studies, for example in Scher et al. [2]. In addition to the hippocampi, a reduction in cerebellar volume was also observed in patients with AD [3] and in patients with cerebellar atrophy via the semiautomated volumetry method [4]. Observed changes were correlated with an overall volumetric decrease in molecular and granular layers of the cerebellum and a decrease in the total count of Purkinje cells as opposed to healthy controls. On the

KARGER

Fax +41 61 306 12 34
E-Mail karger@karger.ch
www.karger.com

1420–8008/12/0344–0224$38.00/0

Accessible online at:
www.karger.com/dem

Jana Mrzilkova, MD
Ruska 87
CZ–110 00 Prague 10 (Czech Republic)
E-Mail mrzilkova.jana@seznam.cz

other hand, volumetric changes of brain stem structures (pons) in patients with AD are not well known, probably due to difficulty with anatomical borders with these structures on MRI. As an example, thioflavin-S-stained sections of the brain stem revealed impairment of reticular nuclei, colliculi superiores et inferiores and many other brain stem neurons [5]. Nevertheless, a novel hypothesis was suggested for the pathogenesis of AD, i.e. that a degeneration of adrenergic neurons in the locus coeruleus and/or of serotonergic neurons in the raphe nuclei leads to impairment in metabolic and functional interactions between neurons and astrocytes (in the cerebral cortex and hippocampus as well as in nucleus basalis magnocellularis) [6]. At the same time, brain stem volume (including the mesencephalon, pons and oblongata) does not significantly change during the ageing process [7]. In our previous study, we measured cortical thickness and volume of the planum temporale, a structure in the supratemporal plane of the temporal lobe, and found mild right/left laterality of both measures in controls and left/right shift in patients with AD [8].

The aim of our present study was:

(a) to evaluate volumetric changes of the hippocampus, pons and cerebellum with and without normalization to the brain and skull in patients with AD,

(b) to find whether eventual volume changes are lateralized to the left or right sides and

(c) whether a hippocampal volume decrease is accompanied by similar cerebellar and/or pontine volume changes in patients with AD when compared to a control group.

Materials and Methods

Diagnosis of AD

This study utilized 26 patients with confirmed AD diagnosis based on NINCDS-ADRDA criteria [9]. All patients with AD and 29 healthy seniors underwent MRI of the brain. Both groups were tested with the following neuropsychological tests: Mini-Mental State Examination (MMSE), Mattis Dementia Rating Scale, Trail Making Test version A and B, Disability Assessment in Dementia, 7-Minute Screen, verbal fluency tests and Edinburgh Handedness Inventory. According to the revised version of research criteria for the diagnosis of AD [10], we added medial temporal lobe atrophy score [11], separately for the left and right hemisphere (table 1).

Personal Characteristics of the Control Group and the AD Patients

The control group consisted of 29 cognitively normal elderly controls who were either recruited from the Third Age University of the Charles University at Prague, Czech Republic (educational courses for seniors) or among healthy volunteers visiting the AD Center at Prague. All of them reached 55 years of age, had Czech as their native language, and no self-reported memory impairments. Exclusion criteria included a history of psychiatric treatment, the use of psychoactive medications (e.g. antidepressants, neuroleptics, anxiolytics, or hypnotics), a history of episodes of unconsciousness lasting longer than 5 min, seizures, any serious brain damage (stroke, trauma, neuro-infection, operation, tumor), and drug/alcohol abuse. Normal cognitive functions were determined using the MMSE, the 7-Minute Screen and verbal fluency tests (1-min version: 3 phonemic, with the initial letters of NKP, and 3 semantic, using fruits, animals, and shopping items) [12].

For both groups, the following data were collected: detailed anamnesis, mapping potential comorbidities (hypertension, diabetes, cardiovascular diseases, hyperlipidemia, smoking, kidney/liver diseases, psychiatric illnesses, ictus, epilepsy and neurological diseases), medical treatment (antidepressants, antipsychotics, anxiolytics, hypnotics, nootropics, cognitive treatment and others) and basic demographic data (living standards, years of education, highest education). All patients were subjected to an EEG to exclude abnormal signal presence. Patients with AD were monitored for several years and annually underwent all examinations. All participants signed an informed consent. The research was approved by the Ethics Committee of the University Hospital Kralovske Vinohrady, Prague, Czech Republic.

MRI Specifications

Three-dimensional MR images were acquired on a 1.5-tesla scanner Siemens Vision 1.5T by magnetization-prepared rapid gradient echo sequence in the sagittal plane, software version VB33G, scanning sequence IR, voxel size 1 × 1 × 1 mm, number of layers 160, TE 7 ms, TR 2,130 ms, matrix 258 × 258 and folding angle 10°. All scans were performed at the Institute of Clinical and Experimental Medicine (IKEM), Prague, Czech Republic.

Computer Analysis

MR images were exported as multiple file data formats to a standard PC. All MR images of the brain were then converted into DICOM stack files by MRIcro freeware. MR images of the brains from the stack files were then analyzed on Image J freeware (http://rsbweb.nih.gov/ij/) on a standard PC in frontal and sagittal planes. Areas (in cm^2) of hippocampal, cerebellar and pontine images (structures of interest) were manually delineated independently by two experienced neuroanatomists. Volumes of the structures of interest were then calculated by summing up all the areas together in Excel program.

Anatomical Boundaries of Structures of Interest

All patients were scanned in the horizontal position while lying on their backs. Their head was oriented fronto-occipitally to the vertical line; we assumed that the pons or cerebellum is positioned rotation symmetrically to the brain stem, especially to the sylvian canal of the mesencephalon, which we used as midline border between the left and right halves of these structures. In the sagittal plane, a whole stack always had 160 MR images.

Pons

The pons was viewed in sagittal sections, mostly without pedunculi cerebellares and considered rotationally symmetrical, similarly as in Raz et al. [13]. Areas of the pons were delineated

Table 1. MTA score

		1	2	3	4	5	6	7	8	9	10	11	12	13	14	15	16	17	18	19	20	21	22	23	24	25	26	27	28	29
AD	R	1	3	2	1	3	1	2	2	1	4	3	2	3	1	2	3	2	0	1	3	3	4	3	3	4	3			
	L	1	3	3	2	4	2	2	3	1	3	2	2	4	1	3	4	2	1	2	1	3	4	2	2	3	3			
Ctrl	R	1	1	1	1	1	0	0	0	0	1	0	0	0	0	1	0	0	0	0	1	1	0	2	0	0	1	1	1	1
	L	1	1	1	1	2	0	0	0	0	1	0	0	0	1	1	1	0	1	2	2	1	0	4	0	0	0	1	0	1

MTA score for controls (Ctrl) and patients with AD and for the right (R) and left (L) hemisphere. Shown are all 26 controls and 29 AD.

manually on each image containing pons segments. All measured pontine areas were then summed up to obtain the total volume of the pons. First, we located the image where the sylvian canal of the brain stem had the largest diameter. This image served as a reference to determine the border between the right and left halves of the pons. The number of images containing the pons differed amongst investigated brains between 15 and 21 images. There were always more images containing the right half of the pons compared to the left half. The lateral border of the pons is usually described in the literature as trigeminofacial line (line connecting the emergence of the nervus trigeminus and nervus facialis from the brain stem); however, this delineation is not usable in the sagittal view on MR images. Therefore, we came up with our own definition of the lateral border based on observations from postmortem brains in the anatomy dissecting room. On MR images, the last image laterally from the midpoint was estimated as the one prior to the point where the trunk of the brain stem becomes visually split into the upper and lower masses – cranially crura cerebri and caudally cerebellar pedunculi. We checked the position of this image on the paraformaldehyde-fixed postmortem brains and found that it is located approximately 2 cm rostrally from the pontomesencephalic junction (along the substantia perforata posterior and oculomotor nerve emergence).

The ventral border of the pons is clearly visible, bordered by the sulcus bulbopontinus caudally and the pontomesencephalic junction rostrally.

The dorsal border is mostly seen as gray/white line, separating the pons dorsally from the bottom of the fourth ventricle, especially in the first 5–8 images from the midline. On other, more lateral images, this line cannot be found so we came up with another approximation. This was done by an ovoid-shaped curve that copies the ventrally extending visible part of the pons (pontine white matter irradiates into brain stem without gross structural shape changes) (fig. 1).

Hippocampus

Anatomical boundaries of the hippocampus were set in the coronal projection: (1) the anterior border level: at which the head of the hippocampus first appears below the amygdalar complex; (2) the posterior border level: where the superior and inferior colliculi are jointly visualized; (3) the medial border transition: between the subiculum and parahippocampal gyrus, and (4) the lateral border: temporal horn of the lateral ventricle.

Cerebellum

Cerebellar hemispheres were measured in the sagittal projection. The measurement starting point (from the midline) was set similarly as in the pons – the image with the widest diameter being the sylvian canal of the mesencephalon. Depending on the brain shape and size, the number of measured images within one hemisphere was 48–67. We included in our measurements all folia, vermis, paravermal parts and lateral hemispheres of the cerebellum. We delineated the external outline of the mentioned structures without any attempt to parcellate separate lobuli and subtract volumes of the empty spaces in between them. The only exceptions were fissura prima, fissura posterolateralis, and spaces separating vermis from hemispheres. At the point where the brain stem gives rise to the velum medullare superius et inferius, connecting with the vermis of the cerebellum and paravermal parts, we delineated a border with a straight line, so that the pedunculi cerebellares were not included in the measurements. Volumes of the left and right cerebellar hemispheres were also measured separately.

Measurements and Mathematics

Volumes of the left and right hippocampi were measured in the coronal projection. Volumes of the left and right halves of the pons and left and right halves of the cerebellum were measured in the sagittal projection. The starting section for measurements in the sagittal projection was the sylvian canal in its widest lumen (this was considered a midpoint between the left and right halves of these structures). For volume normalization purposes, areas (in cm^2) of the brain and the skull were also measured at the level of the commissura anterior. Anatomical delineation of the brain consisted of the manual tracing of all gyri on coronal projections between the cingulate gyrus (just above the callosal body) and parahippocampal gyrus disappearing into the temporal horn of the lateral ventricle. The area of the skull at the level of the commissura anterior was measured by delineating the periost of the calva's concavity till the fissura lateralis cerebri (sylvian fissure) on the left and right side was reached. Ends of these delineation points were then joined together by a straight line.

Absolute volumes of the left and right hippocampus, and left and right halves of the pons and cerebellum were then mathematically normalized to both the brain and skull area [unpubl. data]. Volumes normalized to the brain area were calculated as volume of the hippocampus (pons, cerebellum) divided by area of the brain and multiplied by 100. Similarly, volumes normalized to the skull were calculated as volume of the hippocampus (pons, cere-

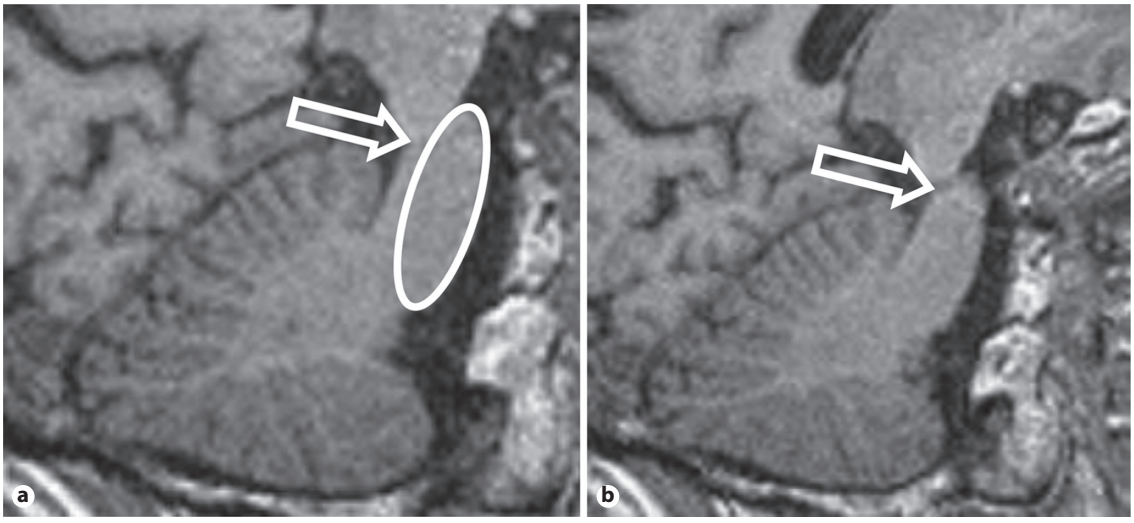

Fig. 1. Examples of delineation of dorsal and lateral borders of the pons. **a** The arrow points to the spot where on the next image would be a gap (this image was not measured). The ellipsoid delineates the area of the measured pons and shows the approximation that we made in delineating the dorsal border – with the bottom of the fourth brain ventricle. Image No. 69 from the MR image stack. **b** The arrow pointing to the gap between crura cerebri and cerebellar pedunculi. This is the image, where the pontine area was not measured (last measurement was made on the previous image). This image demonstrates our approximation of the lateral border of the pons. Image No. 68 from the MR image stack. Both images are viewed in the sagittal projection.

bellum) divided by area of the skull and multiplied by 100 [unpubl. data]. In order to express structural asymmetry, the laterality index between left and right sides was calculated as (L – R)/(L + R).

Statistics

Patients with AD were divided into two groups based on the MMSE score (15 patients with an MMSE score ≥18 and 11 patients with an MMSE score <18) to correlate volumes with milder or more severe neuropsychological impairment. A 2-way ANOVA with repeated measures was selected to determine significant interactions between groups (control group and AD group). Within-subject factors were right-left side (lateralization) and structures of interest (hippocampus, pons and cerebellum). For significant main effects and interactions (post hoc analysis), the Newman-Keuls test was utilized. Whenever post hoc analysis reached significance, a paired t test was used to compare the lateralization effect between the right and left sides of the structure, separately for both the control and AD group. The laterality index for the cerebellum, pons and hippocampus (based on absolute volumes, without normalization to the brain) was evaluated by t test for independent samples and separated by groups (control and AD). Significance was accepted at the 5% level of probability. Finally, real usefulness of the findings was tested with ROC curve analysis to see whether areas may discriminate between control and AD group with appropriate sensitivity and specificity. ROC curve analysis was performed for each structure (hippocampus, pons and cerebellum), separately for both the right and left sides. Briefly, controls were assigned with the number 0 and AD patients were assigned with the number 1. Using an online ROC analysis Web-based calculator, we selected data format 5 (fig. 2).

All statistics was done on Statistica v.6 software and ROC curve analysis using an online program (http://www.rad.jhmi.edu/jeng/javarad/roc/JROCFITi.html).

Results

The study included a total of 55 patients (29 healthy controls and 26 patients with AD). Since the AD group was composed of patients with a wide range of dementia severity, from mild to severe (table 2), we compared brain volumes at different stages of severity. Therefore, the AD group volume results were calculated separately for AD patients with an MMSE score <18 (11 patients) and for AD patients with an MMSE score ≥18 (15 patients) (table 3).

Hippocampus

A significant volume decrease of both left and right hippocampi (normalized to the brain area at the commissura anterior) was present in the AD group compared to the control group in both groups of AD patients, i.e. those with an MMSE score ≥18 ($p = 0.006$) and those with an MMSE score <18 ($p = 0.02$) (fig. 3a, b). Although

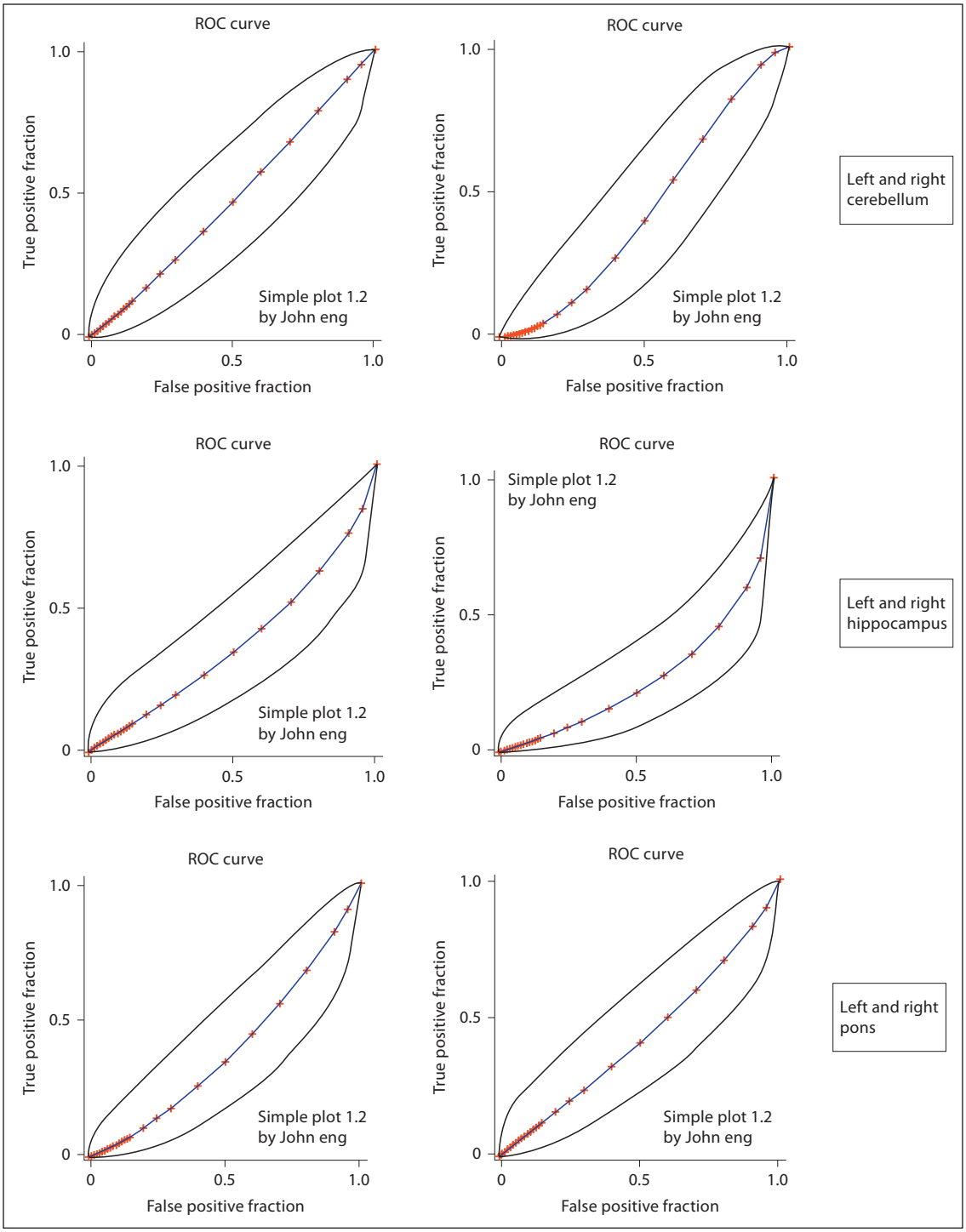

Color version available online

Fig. 2. ROC curve analysis. Volumes of the structures in AD patients were compared to volumes in the control patients, separately for the right and left side. ROC curve was generated in the free online ROC curve calculator (http://www.rad.jhmi.edu/jeng/javarad/roc/JROCFITi.html). Data were inserted into data table in format 5. None of the volume measurements belonged to the true positive fraction area above the diagonal line, but at the same time none of the volumes fit into the false-positive fraction below the diagonal line.

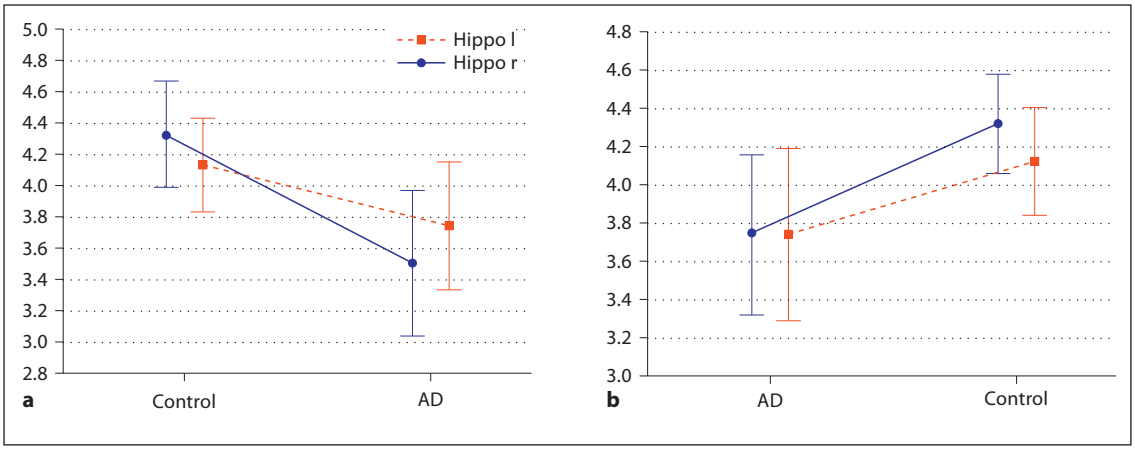

Fig. 3. **a**, **b** Normalized hippocampal volumes in control and AD groups. Data are presented in cm^3 ± 0.95 confidence intervals. **a** AD group had an MMSE score ≥18. Figures are least squares means. Wilks' lamba = 0.80806, F(2, 40) = 4.7507, p = 0.1409. Effective hypothesis decomposition; vertical bars denote 0.95 confidence intervals. **b** AD group had an MMSE score <18. Figures are least squares means. Wilks' lamba = 0.86556, F(2, 36) = 2.7958, p = 0.7436. Effective hypothesis decomposition; vertical bars denote 0.95 confidence intervals. Hippo r = Right hippocampus; Hippo l = left hippocampus.

Table 2. Clinical and personal characteristics of healthy controls and patients with AD

	Control group	AD group
Number of subjects	26	29
Age, years	70 M/66 F (60–79)	74 M/77 F (57–81)
Female sex, %	80	62
Education, years	12 M/13 F (12–19) mostly high school with national exam	13 M/12 F (8–20) mostly high school w/o national exam
Right handedness, %	n.a. M/100 F (only one subject 40)	n.a. M/100 F (all right handers)
AD duration, years	n.a.	2.9 M/3 F (0–6)
MMSE score	29.3 M/29.5 F (26–30)	16.5 M/19 F (2–26)
MDRS score	141 M/141 F (133–144)	90 M/98 F (8–129)
TMT A, s	37 M/38.5 F (19–76)	n.a.
TMT B, s	90 M/88 F (38–177)	n.a.
DAD, %	100 M/100 F (n.a.)	62 M/64 F (7–80)

Values are presented in the following format: average (minimum-maximum). MDRS = Mattis Dementia Rating Scale; TMT A, B = Trail Making Test version A, B; DAD = Disability Assessment in Dementia = percentage of daily activities maintenance; n.a. = not suitable, or not available; M = male; F = female.

Table 3. Volumes of the hippocampus, cerebellum and pons in AD patients (MMSE score <18 and MMSE score ≥18) and controls without normalization

	Controls (n = 29)	AD group (n = 15) (MMSE score ≥18)	AD group (n = 11) (MMSE score <18)
Hippo r, cm^3	2.21±0.44	1.83±0.5	1.84±0.35
Hippo l, cm^3	2.11±0.39	1.84±0.5	1.78±0.41
CRBL r, cm^3	64.5±6	62.5±4.9	58.1±4.2
CRBL l, cm^3	63.7±4.9	61.1±4.9	59.1±5.5
Pons r, cm^3	4.3±0.9	3.7±0.8	4±0.9
Pons l, cm^3	4.1±0.7	3.5±0.7	3.7±0.8
CA skull, cm^2	69.1±5.3	67.2±5.5	68.2±8.5
CA brain, cm^2	51.1±4.1	47.1±3.5	47.7±4.9

Hippo r = Right hippocampus; Hippo l = left hippocampus; CRBL r = right cerebellum; CRBL l = left cerebellum; Pons r = right pons; Pons l = left pons; CA skull = area of the skull at coronal section at the level of commissura anterior; CA brain = area of the brain at coronal section at the level of commissura anterior. Values are presented in cm^3 ± SD.

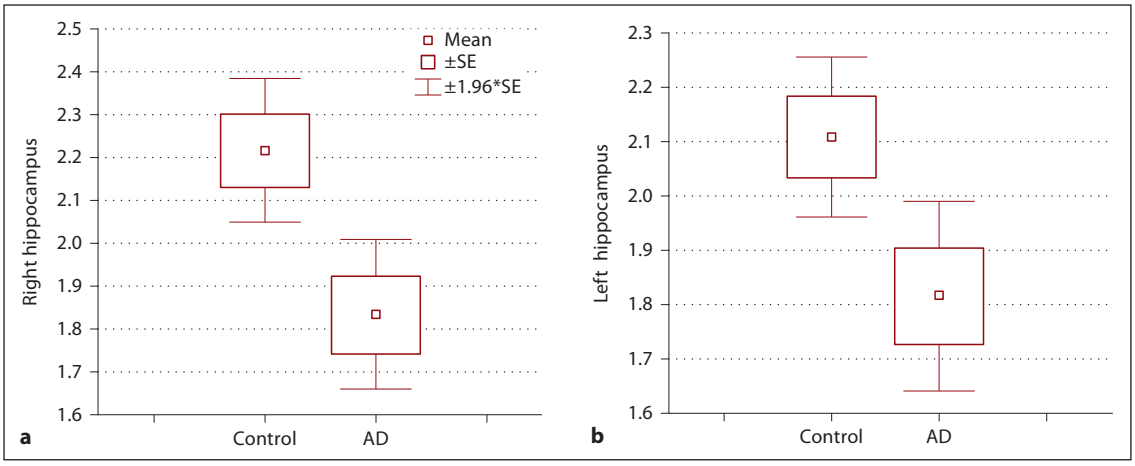

Fig. 4. Box-and-whisker plot. Volumes of the right (**a**) and left hippocampus (**b**) in the control and AD group, without normalization to the brain volume. Data are presented in cm^3 ± SE.

this volume decrease was present in both right and left hippocampi, it was more pronounced on the right side (fig. 4a).

The normalization of brain or skull volumes did not lead to different results compared to absolute hippocampal volumes, both in terms of asymmetry as well as the lesser volume of the AD group compared to the control group. We found right > left asymmetry in both the control and AD group ($p = 0.26$) (fig. 5), which was decreased in the AD group because of the right hippocampal volume decrease in the AD group (fig. 4a, b).

Pons

We did not find a significant difference in volumes between the AD and control group (either absolute, with and without normalization to the brain or skull), although slight differences were present (fig. 6a, b). Volumes of the AD group with an MMSE score <18 were almost equal to the control group ($p = 0.87$), while volumes of the AD group with an MMSE score ≥18 were lower compared to the control group ($p = 0.12$) for both left and right sides. A slight right > left asymmetry was not significant either in the control or the AD group, although in the control group the right-left interval was smaller ($p = 0.9$) compared to the AD group (fig. 7).

Cerebellum

Similar as in the pons, we did not find a significant difference in volumes between the AD and control groups (either absolute, with and without normalization to the brain or skull). In the case of the AD group with an MMSE score <18, both right and left sides were smaller compared to the control group with more pronounced differences on the right compared to the left side ($p = 0.38$) (fig. 8b). On the contrary, in the case of the AD group with an MMSE score ≥18, the right side

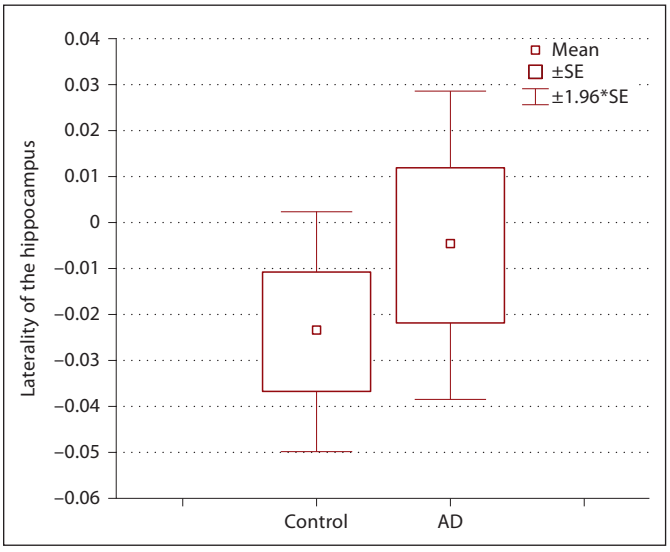

Fig. 5. Box-and-whisker plot of the laterality of the hippocampus. Hippocampal asymmetry in the control and whole AD group without MMSE dichotomy ($p = 0.38$). Data were calculated as $(L - P)/(L + P)$.

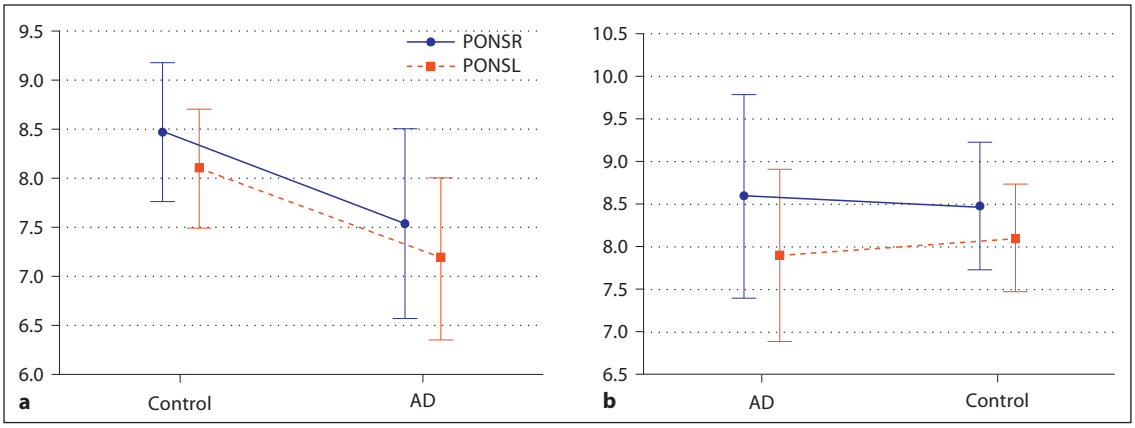

Fig. 6. **a**, **b** Normalized pontine volumes in control and AD groups. Data are presented in $cm^3 \pm 0.95$ confidence intervals. **a** AD group had an MMSE score ≥18 (p = 0.12). Figures are least squares means. Wilks' lamba = 0.92183, F(2, 40) = 1.6960, p = 0.19634. Effective hypothesis decomposition; vertical bars denote 0.95 confidence intervals. **b** AD group had an MMSE score <18 (p = 0.87). Figures are least squares means. Wilks' lamba = 0.98855, F(2, 36) = 2.0849, p = 0.81278. Effective hypothesis decomposition; vertical bars denote 0.95 confidence intervals. PONSR = Right pons; PONSL = left pons.

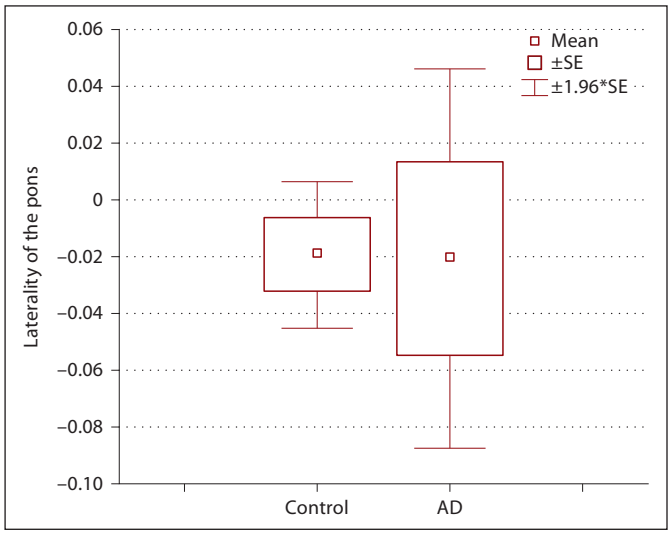

Fig. 7. Box-and-whisker plot of the laterality of the pons. Pontine asymmetry in the control and whole AD group without MMSE dichotomy (p = 0.9). Data were calculated as (L – P)/(L + P).

was almost equal to the controls and the left side was slightly larger compared to the control group (p = 0.96) (fig. 8a). Analysis revealed nonsignificant right > left asymmetry for both AD and control groups (p = 0.9) (fig. 9).

Discussion

In the whole AD group with or without MMSE dichotomy), we found a bilateral hippocampal decrease in the AD group compared to the control group, although we did not evaluate gender differences, due to the lack of equal numbers of male and female patients in both the control and AD group. We did not find a significant lateralization in any measured structures in both the AD and control groups, with the exception of the hippocampus (right > left asymmetry in both the control and AD group). Normalization to the brain and skull area had only a limited effect on the outcome of the above-mentioned results, mostly in the pons. Interestingly, a volume decrease of the right hippocampus in the AD group compared to the control group was set at $p < 0.01$ either with or without normalization to the brain and skull, which we think denotes great significance. Volume decreases in the left hippocampus in the AD group were only significant when compared to the control group without normalization but with normalization to the brain. We did not find significant cerebellar or pontine volume reduction in the AD group compared to the control group. This could be explained by the relative stability of brain stem volume during the ageing process [7]. On the other hand, at the level of the midbrain, auditory asymmetries are frequently reported [14], but their propagation into the pons is not known. When viewing

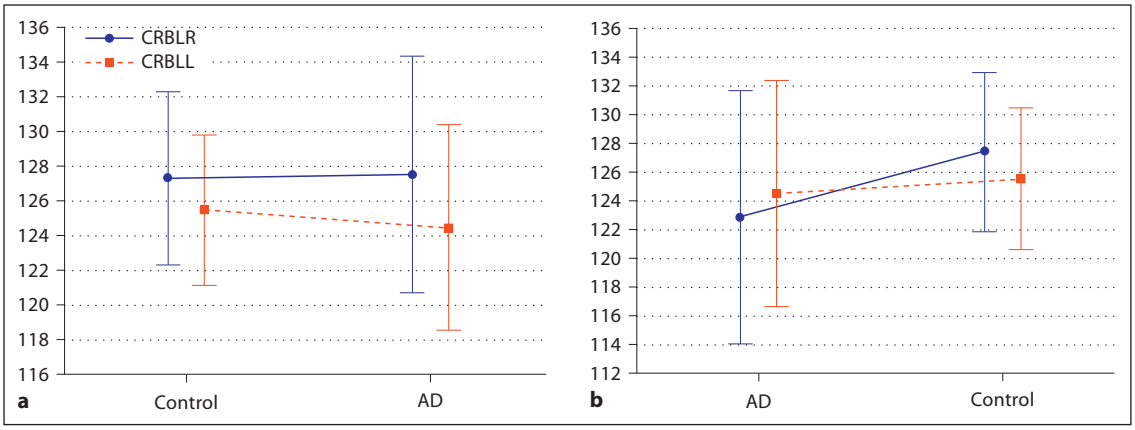

Fig. 8. **a**, **b** Normalized cerebellar volumes in the control and AD groups. Data are presented in cm^3 ± 0.95 confidence intervals. **a** AD group had an MMSE score ≥18 (p = 0.96). Figures are least squares means. Wilks' lamba = 0.99615, F(2, 40) = 0.07732, p = 0.92573. Effective hypothesis decomposition; vertical bars denote 0.95 confidence intervals. **b** AD group had an MMSE score <18 (p = 0.38). Figures are least squares means. Wilks' lamba = 0.97360, F(2, 36) = 0.48816, p = 0.61776. Effective hypothesis decomposition; vertical bars denote 0.95 confidence intervals. CRBLR = Right cerebellum; CRBLL = left cerebellum.

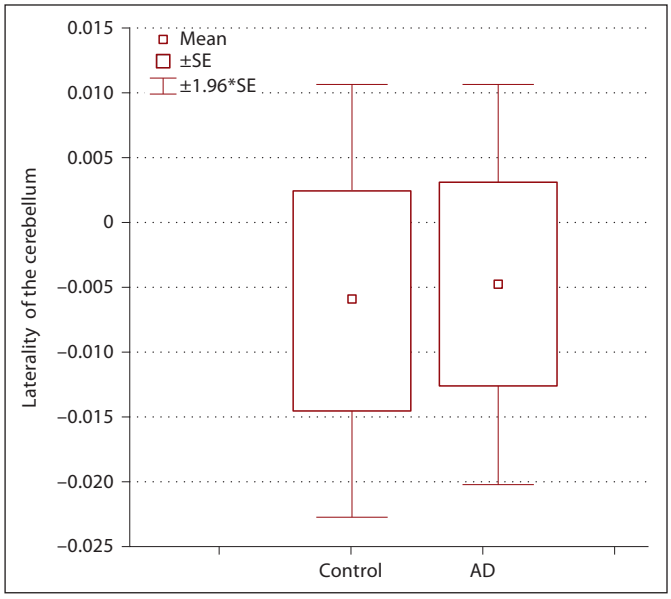

Fig. 9. Box-and-whisker plot of the laterality of the cerebellum. Cerebellar asymmetry in the control and whole AD group without MMSE dichotomy (p = 0.9). Data were calculated as (L – P)/(L + P).

MRI scans, we found, even with the naked eye, that brain stem is not straight in the sagittal projection, but tends to turn slightly to the left or right, especially in older patients. If this is the case, then the pons cannot be in such cases regarded as rotational symmetrical at all. To evaluate the influence of brain stem 'scoliosis' on the left-right volume lateralization, we selected 6 patients from the AD group with clear turn bias of the brain stem and measured pontine lateralization separately. Although we found greater rightward laterality in those 6 selected patients, t tests revealed no significant difference compared to the whole AD group [unpubl. results].

Methodologically, we faced the problem of how to delineate the dorsal and lateral part of the pons. Firstly, we decided not to use the commonly accepted trigeminofacial line for the lateral border, delineating laterally the transition from the pons to cerebellar pedunculi, because in the sagittal projection this line is not visible on the MRI scans. Secondly, the transition between the pons dorsally and the tegmentum is visible very well as a gray/white line, but only on images close to the midline. On further images, this transition disappears. Therefore, in these images we approximated the dorsal border via an ellipsoid curve, copying the shape of the present ventral pontine outline. Furthermore, it would be more appropriate to say that we measured an approximated volume of the pontine mass, not the pons as a whole structure. We believe that this pontine shrinkage is still valuable information for neurological evaluation.

We used old criteria for the AD diagnosis evaluation [9], although we implemented the medial temporal lobe atrophy score as a modern biomarker of AD evaluation.

We did not use cerebrospinal fluid markers of AD, since at the time of collection of our patient group, it was not regularly performed (since 2001). Although we acknowledge new modern AD diagnostic criteria [10, 15, 16], there is also controversy concerning their accuracy, especially in pre-AD settings [17].

Surprisingly, selecting AD patients with an MMSE score <18 did not yield significantly different results, compared to the volumes and lateralization of the AD group with MMSE scores >18 . We expected that the AD group with an MMSE score <18 would have greater differences in volumes and laterality, due to severity of neuropsychological impairment. A possible explanation could be the relatively low number of patients in the AD group with an MMSE score <18 (n = 11).

From an overall perspective, the brain undergoes general volume shrinkage over the course of AD pathology [18]. We failed to confirm that hippocampal shrinkage on the MRI scans would be accompanied (or maybe started) by similar volume decreases of the brain stem structures (pons) and cerebellum. This is not to say that changes in the brain stem observed by other methods (immunohistochemistry and molecular biology) may not prove the onset of AD from there. In accord with the literature, we confirmed a significant volume decrease of only the right hippocampus in the AD group (the whole AD group, as well as AD group with an MMSE score <18).

For further studies, it appears reliable to perform manual volumetric hippocampal analysis in multicenter MRI acquisition as a biomarker of AD versus mild cognitive impairment [19].

Acknowledgement

This study was supported by grant IGA no. NT 13183 from the Czech Ministry of Health, grant agency GA UK no. 296211 of the Czech Republic and grant P 304/12/G069 from the Grant Agency of the Czech Republic and the Research Project Charles University in Prague, PRVOUK 34.

References

1 van de Pol LA, Hensel A, van der Flier WM, Visser PJ, Pijnenburg YA, Barkhof F, Gertz HJ, Scheltens P: Hippocampal atrophy on MRI in frontotemporal lobar degeneration and Alzheimer's disease. J Neurol Neurosurg Psychiatry 2006;77:439–442.

2 Scher AI, Xu Y, Korf ES, White LR, Scheltens P, Toga AW, Thompson PM, Hartley SW, Witter MP, Valentino DJ, Launer LJ: Hippocampal shape analysis in Alzheimer's disease: a population-based study. Neuroimage 2007;36:8–18.

3 Wegiel J, Wisniewski HM, Dziewiatkowski J, Badmajew E, Tarnawski M, Reisberg B, Mlodzik B, De Leon MJ, Miller DC: Cerebellar atrophy in Alzheimer's disease –clinicopathological correlations. Brain Res 1999;818:41–50.

4 Hayashi N, Sanada S, Suzuki M, Matsuura Y, Kawahara K, Tsujii H, Yamamoto T, Matsui O: Semiautomated volumetry of the cerebrum, cerebellum-brain stem, and temporal lobe on brain magnetic resonance images. Radiat Med 2008;26:104–114.

5 Parvizi J, Van Hoesen GW, Damasio A: The selective vulnerability of brainstem nuclei to Alzheimer's disease. Ann Neurol 2001;49:53–66.

6 Hertz L: Is Alzheimer's disease an anterograde degeneration, originating in the brainstem, and disrupting metabolic and functional interactions between neurons and glial cells? Brain Res Brain Res Rev 1989;14:335–353.

7 Luft AR, Skalej M, Schulz JB, Welte D, Kolb R, Bürk K, Klockgether T, Voight K: Patterns of age-related shrinkage in cerebellum and brainstem observed in vivo using three-dimensional MRI volumetry. Cereb Cortex 1999;9:712–721.

8 Zach P, Kristofiková Z, Mrzílková J, Majer E, Selinger P, Spaniel F, Řípová D, Kenney J: Planum temporale analysis via a new volumetric method in autoptic brains of demented and psychotic patients. Curr Alzheimer Res 2009;6:69–76.

9 McKhann G, Drachman D, Folstein M, Katzman R, Price D, Stadlan EM: Clinical diagnosis of Alzheimer's disease: report of the NINCDS-ADRDA Work Group under the auspices of Department of Health and Human Services Task Force on Alzheimer's Disease. Neurology 1984;34:939–944.

10 Dubois B, Feldman HH, Jacova C, Dekosky ST, Barberger-Gateau P, Cummings J, Delacourte A, Galasko D, Gauthier S, Jicha G, Meguro K, O'brien J, Pasquier F, Robert P, Rossor M, Salloway S, Stern Y, Visser PJ, Scheltens P: Research criteria for the diagnosis of Alzheimer's disease: revising the NINCDS-ADRDA criteria. Lancet Neurol 2007;6:734–746.

11 Scheltens PH, Leys D, Barkhof F, Huglo D, Weinstein HC, Vermersch P, Kuiper M, Steinling M, Wolters ECH, Valk J: Atrophy of medial temporal lobes on MRI in 'probable' Alzheimer's disease and normal ageing: diagnostic value and neuropsychological correlates. J Neurol Neurosurg Psychiatry 1992;55:967–972.

12 Budson AE, Solomon PR: Memory Loss: A Practical Guide for Clinicians. Philadelphia, Elsevier Saunders, 2011.

13 Raz N, Torres IJ, Spencer WD, White K, Acker JD: Age-related regional differences in cerebellar vermis observed in vivo. Arch Neurol 1992;149:412–416.

14 Schönwiesner M, Krumbholz K, Rübsamen R, Fink GR, von Cramon DY: Hemispheric asymmetry for auditory processing in the human auditory brain stem, thalamus, and cortex. Cereb Cortex 2007;17:492–499.

15 McKhann GM, Knopman DS, Chertkow H, Hyman BT, Jack CR Jr, Kawas CH, Klunk WE, Koroshetz WJ, Manly JJ, Mayeux R, Mohs RC, Morris JC, Rossor MN, Scheltens P, Carrillo MC, Thies B, Weintraub S, Phelps CH: The diagnosis of dementia due to Alzheimer's disease: recommendations from the National Institute on Aging-Alzheimer's Association workgroups on diagnostic guidelines for Alzheimer's disease. Alzheimers Dement 2011;7:263–269.

16 Jack CR Jr, Albert MS, Knopman DS, McKhann GM, Sperling RA, Carrillo MC, Thies B, Phelps CH: Introduction to the recommendations from the National Institute on Aging-Alzheimer's Association workgroups on diagnostic guidelines for Alzheimer's disease. Alzheimers Dement 2011;7:257–262.

17 Oksengard AR, Cavallin L, Axelsson R, Andersson C, Nägga K, Winblad B, Eriksdotter-Jönhagen M, Wahlund LO: Lack of accuracy for the proposed 'Dubois criteria' in Alzheimer's disease: a validation study from the Swedish brain power initiative. Dement Geriatr Cogn Disord 2010;30:374–380.

18 Hua X, Leow AD, Lee S, Klunder AD, Toga AW, Lepore N, Chou YY, Brun C, Chiang MC, Barysheva M, Jack CR, Bernstein MA, Britson PJ, Ward CP, Whitwell JL, Borowski B, Fleisher AS, Fox NC, Boye RG, Barnes J, Harvey D, Kornak J, Schuff N, Boreta L, Alexander GE, Weiner MW, Thompson PM: 3D characterization of brain atrophy in Alzheimer's disease and mild cognitive impairment using tensor-based morphometry. Neuroimage 2008;41:19–34.

19 Teipel SJ, Ewers M, Wolf S, Jessen F, Kölsch H, Arlt S, Luckhaus C, Schönknecht P, Schmidtke K, Heuser I, Frölich L, Ende G, Pantel J, Wiltfang J, Rakebrandt F, Peters O, Born C, Kornhuber J, Hampel H: Multicentre variability of MRI-based medial temporal lobe volumetry in Alzheimer's disease. Psychiatry Res 2010;182:244–250.

KUTOVÁ, M.; **MRZÍLKOVÁ, J.**; KIRDAJOVÁ, D.; ŘÍPOVÁ, D. a P. ZACH. Simple Method for Evaluation of Planum Temporale Pyramidal Neurons Shrinkage in Postmortem Tissue of Alzheimer's Disease Patients. *BioMed Research International*. 2014, **2014**(Article ID 607171), 1-6. ISSN 2314-6133. DOI: 10.1155/2014/607171.

Abstract: We measured the length of the pyramidal neurons in the cortical layer III in four subregions of the planum temporale (transitions into superior temporal gyrus, Heschl's gyrus, insular cortex, and Sylvian fissure) in control group and Alzheimer's disease patients. Our hypothesis was that overall length of the pyramidal neurons would be smaller in the Alzheimer disease group compared to controls and also there would be right-left asymmetry in both the control and Alzheimer's disease groups. We found pyramidal neuron length asymmetry only in controls--in the transition into the Sylvian fissure--and the rest of the subregions in the control group and Alzheimer's disease patients did not show size difference. However, control-Alzheimer disease group pyramidal neuron length comparison revealed (a) no length difference in superior temporal gyrus transition area, (b) reversal of asymmetry in the insular transition area with left insular transition significantly shorter in the Alzheimer's disease group compared to the control group, (c) both right and left Heschl's gyrus transitions significantly shorter in the Alzheimer's disease group compared to the control group, and (d) right Sylvian fissure transition significantly shorter in the Alzheimer's disease group compared to the control group. This neuronal length measurement method could supplement already existing neuropathological criteria for postmortem Alzheimer's disease diagnostics.

Hindawi Publishing Corporation
BioMed Research International
Volume 2014, Article ID 607171, 6 pages
http://dx.doi.org/10.1155/2014/607171

Research Article

Simple Method for Evaluation of Planum Temporale Pyramidal Neurons Shrinkage in Postmortem Tissue of Alzheimer Disease Patients

Martina Kutová,[1] Jana Mrzílková,[1] Denisa Kirdajová,[1] Daniela Řípová,[2] and Petr Zach[1]

[1] *Institute of Anatomy, Third Medical Faculty, Charles University at Prague, Ruská 87, Prague 10, 100 00 Praha, Czech Republic*
[2] *Prague Psychiatric Center, Ústavní 91, Prague 8, 181 03 Praha, Czech Republic*

Correspondence should be addressed to Martina Kutová; martinakutova@volny.cz

Received 18 October 2013; Revised 17 December 2013; Accepted 4 January 2014; Published 11 February 2014

Academic Editor: Milos Petrovic

We measured the length of the pyramidal neurons in the cortical layer III in four subregions of the planum temporale (transitions into superior temporal gyrus, Heschl's gyrus, insular cortex, and Sylvian fissure) in control group and Alzheimer disease patients. Our hypothesis was that overall length of the pyramidal neurons would be smaller in the Alzheimer disease group compared to controls and also there would be right-left asymmetry in both the control and Alzheimer disease groups. We found pyramidal neuron length asymmetry only in controls—in the transition into the Sylvian fissure—and the rest of the subregions in the control group and Alzheimer disease patients did not show size difference. However, control-Alzheimer disease group pyramidal neuron length comparison revealed (a) no length difference in superior temporal gyrus transition area, (b) reversal of asymmetry in the insular transition area with left insular transition significantly shorter in the Alzheimer disease group compared to the control group, (c) both right and left Heschl's gyrus transitions significantly shorter in the Alzheimer disease group compared to the control group, and (d) right Sylvian fissure transition significantly shorter in the Alzheimer disease group compared to the control group. This neuronal length measurement method could supplement already existing neuropathological criteria for postmortem Alzheimer disease diagnostics.

1. Introduction

Neurodegeneration in Alzheimer disease (AD) affects structures of the temporal lobe (MTA) and in particular the supratemporal plane of the temporal lobe—planum temporale (PT) (for review see [1]). PT is mostly a heteromodal auditory association region whose asymmetry is established by 31 weeks of gestation. Functionally, it is involved in auditory and spatial objects processing, auditory-motor integration, music pitch and tune recognition, and sound localization functions [2], and its structural and functional organization was recently revised. Neuroanatomical and neurophysiological evidence suggest subdivision of the PT into anterior and posterior parts. The anterior part belongs to the auditory cortex proper supporting spatially related but not spatially specific functions like stream segregation. The posterior part is not part of the auditory cortex and it supports sensory-motor integration of the vocal tract actions [3]. At the gross anatomy level, the PT exhibits leftward asymmetry (approx. in 60% of the population) of its length and/or area. In clinical populations was observed reversal of this asymmetry in dyslexia and a loss of asymmetry combined with an increase in right PT size in schizophrenia [4]. Anatomical changes of the PT in dementia were not extensively studied. Microanatomical changes were found in the cortex of the PT in patients with AD in the form of minicolumn thinning, although this finding was not well correlated with decline in cognitive functions [5]. Age associated minicolumn thinning in normally aged people was found in the medial temporal gyrus and temporal lobe association cortex but not in Heschl's gyrus [6]. Our previous anatomical study of PT in AD revealed overall volume and cortical width decrease in AD compared to controls together with rightward asymmetry reversal in AD [7]. We were interested in whether this gross anatomical finding could be correlated with the histological level. If so, PT could be another brain region (besides

the hippocampus, prefrontal cortex, gyrus collateralis, locus coeruleus of the brain stem, and cerebellum) that is included in neuropathological examinations in postmortem AD diagnostics.

In our present study, we measured shrinkage of layer III pyramidal neurons in four different parts of the PT (transition to superior temporal gyrus, transition to Heschl's gyri, and transition into insula and posterior part of Sylvian fissure) on the left and right side. Cytoarchitectonically, the first three parts are classified as auditory parakoniocortices (internal: PaAi, external: PaAe, and caudodorsal: PaA) with prominent granularity in layer IV and sparse layer V. The fourth part is nonauditory temporal-parietal area—Tpt—occupying the posterior side of the PT with a weak layer IV and prominent layer V. The reasons for selecting layer III pyramidal neurons for shrinkage measurement were anatomical abnormalities of the PT were observed particularly in the upper cortical layers I–III of the Tpt part of PT in the left hemisphere in schizophrenics [8], axons of layer III pyramidal neurons do not project outside the cortex and their apical dendrites are most prominent, and finally relative homogeneity in the presence of layer III pyramidal neurons across the PT compared to other layers.

We expected more prominent pyramidal neuron size loss in AD compared to controls and also a change towards rightward asymmetry in AD compared to controls.

2. Materials and Methods

This study uses the same brain PT tissue samples that were conserved from our past anatomical study on a new volumetric method of AD postmortem diagnosis. Clinical diagnosis of AD as well as postmortem verification on autoptic tissue, demographic data, method of extraction of PT samples from postmortem brains, brain tissue fixation, control patient characterization, and other data were fully described in our previous study [7]. Out of 84 formerly studied postmortem brains, we selected 10 AD PT and 7 control PT (age and sex matched, similar severity of neuropathological findings in the case of AD).

Out of each PT embedded in paraplast four samples were cut at the following anatomical localizations: (1) at the lateral border as the superolateral margin of the superior temporal gyrus (STG), (2) at the medial border of the PT at the point of transition into the insular cortex (I), (3) at the ventral border at the point of transition into one of the Heschl's gyri (HG), and (4) at the dorsal border at the point where the Sylvian fissure terminates or bifurcates into posterior descending ramus (SR) (Figure 1) (for more detailed regional description see [1]). All samples were cut on a standard rotary microtome Leica (30 μm slice thickness) with the knife positioned vertically to the cortical surface. Slices were mounted on poly-lysine coated glass slides and stained according to standard Nissl cresylviolet staining. Pyramidal neurons from layer III of the cortex (where most disorganization was previously reported [6]) were studied on a Leica DMLB microscope with 10x magnification and images were digitally captured. Digital images were transferred onto a standard PC and opened in freeware image analysis program

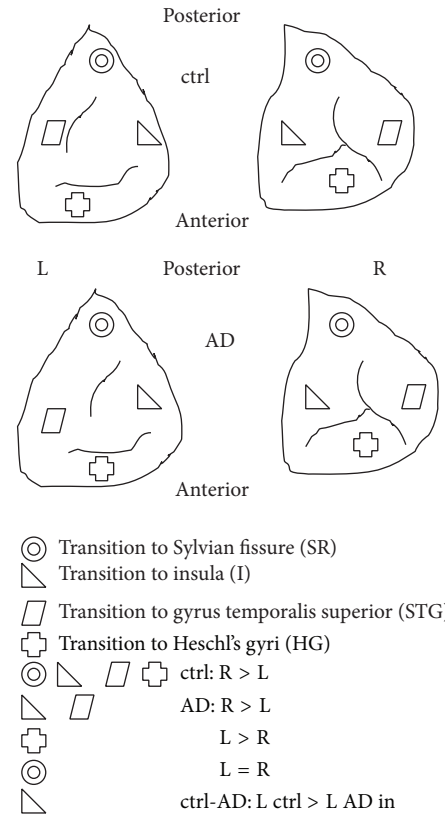

Figure 1: Example of the PT sample from ctrl and AD group (above view, left and right control and AD). Four symbols indicate four positions within the PT where brain tissue was collected and where pyramidal neurons in the cortical layer 3 were measured (STG, HG, I, and SR). Ctrl = control group, AD = Alzheimer disease group, L = left, and R = right. Equations in the lower half of the picture show asymmetries within ctrl, AD, and between ctrl and AD.

Image J 1.47 (http://rsb.info.nih.gov/ij/download.html) with implemented stereological tools. Image J was first calibrated using a calibration slide micrometer (OptixCam, USA). Length of the pyramidal neurons was measured manually by PC mouse pointer after software magnification of the images. Briefly, a thin line was drawn by mouse from the apical dendrite towards the midst of the base of the pyramidal neuron where basilary dendrites were emerging. Measured data in micrometers were stored in the Excel database. All length measurements were done blind to the status of the AD or controls using double blind labeling system of the glass slides.

Measured neurons were selected according to their pyramidal shape and horizontal position. Their length was estimated by our modification of the nucleator method [9]. Instead of measuring the length of 3 isotropic random lines from a nucleolus to the cell periphery, we measured a straight line connecting the apical dendrite with the point on the opposing cell membrane in between two emerging basilary dendrites. Criteria for inclusion of pyramidal neuron into measurement were position in the cortical layer III, triangular shape of the cell body and clearly visible whole cytoplasmic

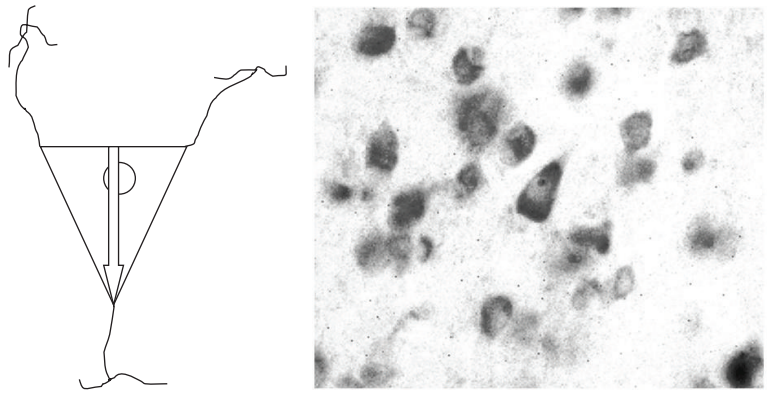

(a) (b)

Figure 2: Shape of selected pyramidal neurons of the PT cortical layer III from STG, HG, I, and SR subregions. (a) Base of the arrow represents the starting and tip of the arrow represents the terminating point of the length of the cell body measurement. Tip of the arrow is pointing to the apical dendrite. Only neurons having at the same time visible apical dendrite, both basilary dendrites emerging from the cell body and full contour of the cytoplasm membrane with nucleus inside, were selected into measurement. The ratio of the size of cell, basilary dendrites, and apical dendrite is only for illustration in this picture. (b) Typical pyramidal neuron selected for measurement (in the middle), Nissl stained section, 30 μm thickness, magnification 400x.

membrane and clearly visible apical dendrite leaving the cell body and at the opposite side of two or more emerging basilary dendrites. This way we believe we avoided anisotropy in the shape and orientation of the sampled neurons as mentioned in [9]. Such criteria should guarantee horizontal position of the pyramidal neurons relatively to the camera view (see Figure 2). Always five randomly selected neurons were measured in all of the samples (STG, I, HG, SR) on the left (L) and right (R) sides so we measured 680 neurons in total.

The data were exported from Excel into Statistica 10 software. ANOVA with repeated measures was selected for control-AD group differences and Newman-Keuls post hoc analysis for statistical significance [10]. t-test for dependent samples was used to evaluate R/L asymmetries within control and AD group. Statistical significance was accepted at $P = 0.05$.

3. Results

In all subregions (STG, I, HG, SR), length of pyramidal neurons was higher in the control group compared to the AD group. Dependent t-test showed that within the control group, there was R > L length for all subregions except for I (L > R) (Figure 4). Within the AD group, there was R > L for STG, reversal of asymmetry (L > R) for HG, decrease of L > R asymmetry (but still L > R) for I, and R = L for SR. Comparison of control-AD group by ANOVA with repeated measures yielded mixed results: no significance in STG, L AD < L control in I, both L and R AD < control in HG and R AD < R control in SR (Figure 3). In terms of within groups asymmetry, we found significance only in the SR of the control group (R > L).

3.1. STG. R > L in both control (w/o significance) and AD groups (w/o significance). No significant difference exists between control and AD groups on both sides.

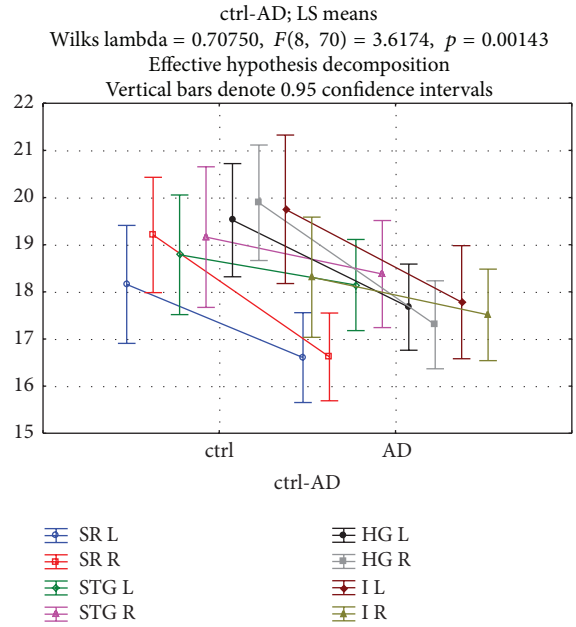

Figure 3: Lenght of pyramidal neurons in cortical layer 3 of the PT subregions in control and AD groups for R and L sides. Length of the cell bodies is in μm. Abbreviations: R: right, L: left, STG: PT transition to superior temporal gyrus, HG: PT transition to Heschl's gyri, I: PT transition to insula and SR: PT transition to Sylvian fissure, ctrl: control group, and AD: Alzheimer disease group.

3.2. I. L > R in control (w/o significance) and AD groups (almost equal, $P = 0.78$). L is significantly shorter in AD compared to control group ($P = 0.04$).

3.3. HG. R > L in the control group (w/o significance) and L > R in the AD group (w/o significance). Both R and L are significantly shorter in the AD group compared to control group (R; $P = 0.001$, L; $P = 0.01$).

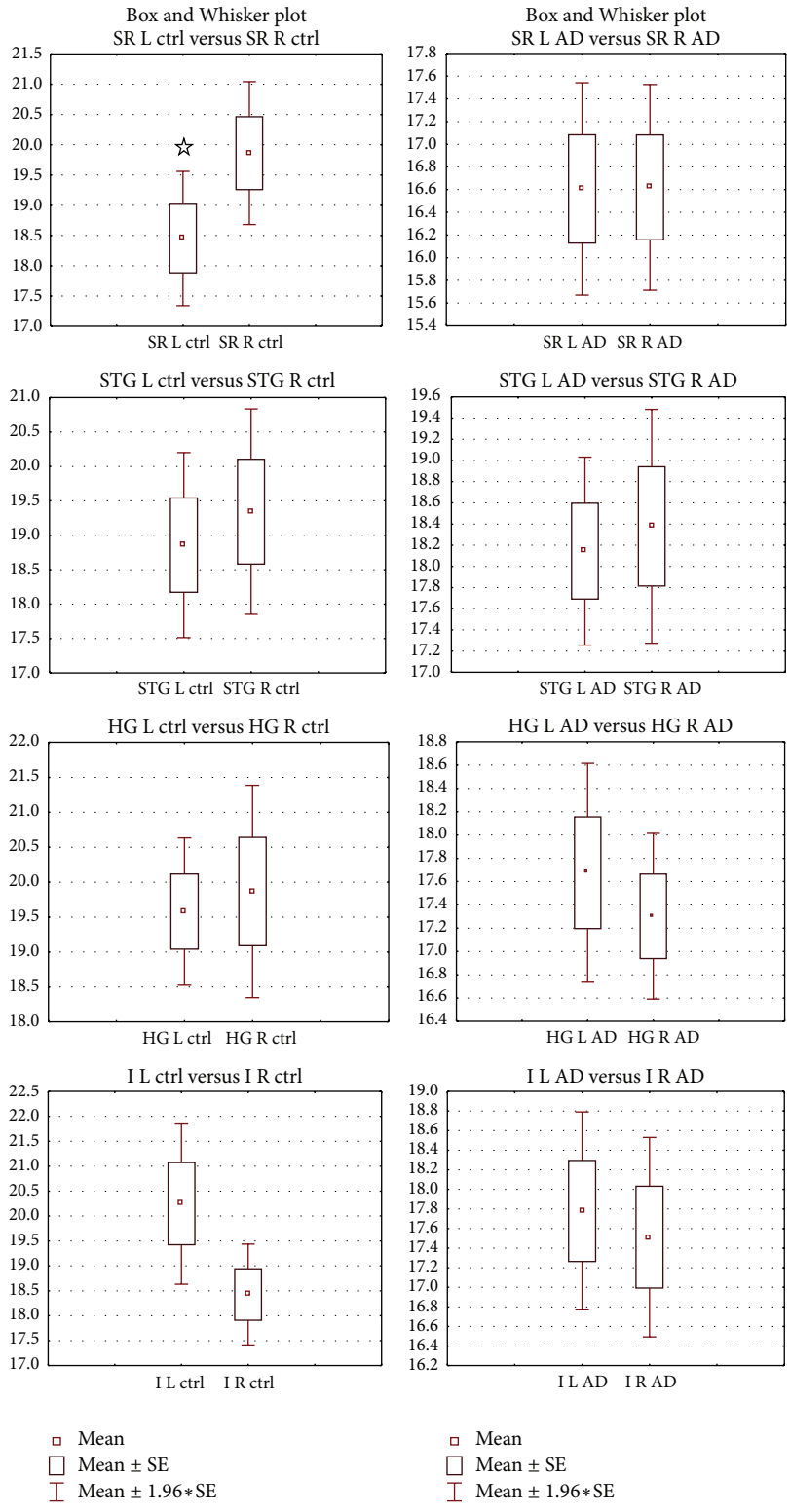

Figure 4: Left-right asymmetries in the length of the layer III pyramidal neurons in the PT of the control (left) and AD (right) groups. Y-axis data are in μm. Data are presented as means ± SE. Abbreviations: SR: transition to Sylvian fissure, STG: transition to gyrus temporalis superior, HG: transition to Heschl's gyri, I: transition to insula, L: left side, and R: right side. Significance between left and right side estimated by dependent samples t-test at $P < 0.05$ is marked by ☆.

3.4. SR. R > L in the control group ($P = 0.04$) and R = L in the AD group ($P = 0.98$). R is significantly shorter in AD compared to control group ($P = 0.003$).

4. Discussion

We measured length of PT cortical layer III pyramidal neurons in 7 controls and 10 AD patients on postmortem brain tissue. As mentioned in our previous study [7], PT tissue samples of AD patients and controls were embedded in paraplast in 2009, so we expected unavoidable tissue shrinkage. We presume similar tissue shrinkage due to the same paraplast embedding protocol for all samples. Also, all paraplast embedded PT tissue samples were stored in the same dry boxes at room temperature until sectioning. Interestingly, although we did not sort out pyramidal neurons according to their cell body size, our results ranged typically from 15 to 22 μm regardless of AD or control groups. If there would be a significant difference in shrinkage between samples, then the neurons would exhibit greater size variability. This is the reason we did not calculate tissue shrinkage corrections [11].

Our findings show that only one subregion of PT, SR, had larger cell bodies (R > L) and only in the control group. This part of the PT is a nonauditory cortex involved in sensorymotor integration of vocal tract actions [3]. In the AD group in all subregions, we did not find significant R/L asymmetry. One region (I) showed that L > R, and one region (SR) is almost equal to R = L. This is in contrast with a study reporting that L > R in controls (cells in the auditory or speech areas—but only magnopyramidal cells accounting for 10% of the cells sorted for binomial analysis for hemisphere lateralization out of great size variability of total pyramidal neurons were measured [12]). Our observation of the lack of R/L asymmetry in the AD group could be seen as a decrease of rightward dominance that is normally present in controls. Similarly, well-known rightward decrease in hippocampal volume in AD leads to call-down of normally present asymmetry in controls [13]. Therefore, the posterior part of the PT can be another area specifically lesioned by AD, in addition to the gyrus collateralis, entorhinal cortex, hippocampus, and brain stem. Due to participation of Tpt in the vocal processing streams, its decreased size layer III pyramidal neurons could contribute to vocalization problems in patients with AD in combination with declarative memory impairment. This would however be valid only for population with rightward lateralized auditory and speech centers since we did not find a decrease in neuronal size on the left side. Reduced neuronal size in layer III of the PT was also observed in bipolar disorder [14] but not in schizophrenia and major depressive disorder, and significance was lost when adjusted for six layerwise comparisons. Also reduction of somal volume of the layer III pyramidal neurons of the temporal association cortex was described in schizophrenia [15], so our finding may not be limited to the extent of the PT but rather with overlaps to neighbouring regions. Our observed reversal of asymmetry in the HG region (R > L to L > R) is opposite to reversals of PT asymmetry observed in schizophrenia (R > L) [1].

Layer III: external pyramidal layer of the cortex predominantly contains small- and medium-sized pyramidal neurons and also nonpyramidal cells. Pyramidal cells are principal targets of interhemispheric corticocortical afferents and also a primary source of corticocortical efferents. Rightward lateralized decrease of their size in AD may not be restricted only to the layer III, and that could be a topic of further studies.

5. Conclusion

We present neurohistological methodology of measuring length changes in layer III pyramidal neurons in the PT (especially in its subparts of I, SR, and HG) in patients with progressed Alzheimer disease. The data from our previous study [7] showed right/left laterality in the cortical thickness, area and volume of the PT in controls, and change into left/right laterality in the AD group. In the present study, we found similar right/left laterality in the control group and a decrease, disappearance, or reversal of this asymmetry in the AD group. Therefore, gross changes in the PT in AD may be at least partially attributed to neurohistological changes in the layer III pyramidal neurons. We suggest that this method of pyramidal neuron length measurement could be used in addition to existing clinical neuropathological evaluations of AD in hospitals.

Conflict of Interests

The authors declare that there is no conflict of interests regarding the publication of this paper.

Acknowledgments

This study was supported by the research project GACR Grant no. P304/12/G069 of the Czech republic and Charles University Grant PRVOUK P34 of the Czech republic. The authors thank Elizabeth Zakszewsky for language check.

References

[1] J. Shapleske, S. L. Rossell, P. W. R. Woodruff, and A. S. David, "The planum temporale: a systematic, quantitative review of its structural, functional and clinical significance," *Brain Research Reviews*, vol. 29, no. 1, pp. 26–49, 1999.

[2] J. Ahveninen, N. Kopco, and I. P. Jääskeläinen, "Psychophysics and neuronal bases of sound localization in humans," *Hearing Research*, vol. 307, no. 1, pp. 86–97, 2014.

[3] G. Hickok and K. Saberi, "Redefining the functional organization of the planum temporale region: space, objects, and sensory-motor integration," in *The Human Auditory Cortex*, D. Poeppel et al., Ed., vol. 43 of *Springer Handbook of Auditory Research*, 2012.

[4] J. T. Ratnanather, C. B. Poynton, D. V. Pisano et al., "Morphometry of superior temporal gyrus and planum temporale in schizophrenia and psychotic bipolar disorder," *Schizophrenia Research*, vol. 150, no. 2-3, pp. 476–483, 2013.

[5] S. A. Chance, L. Clover, H. Cousijn, L. Currah, R. Pettingill, and M. M. Esiri, "Microanatomical correlates of cognitive ability

and decline: normal ageing, MCI, and Alzheimer's disease," *Cerebral Cortex*, vol. 21, no. 8, pp. 1870–1878, 2011.

[6] S. A. Chance, M. F. Casanova, A. E. Switala, T. J. Crow, and M. M. Esiri, "Minicolumn thinning in temporal lobe association cortex but not primary auditory cortex in normal human ageing," *Acta Neuropathologica*, vol. 111, no. 5, pp. 459–464, 2006.

[7] P. Zach, Z. Krištofiková, J. Mrzílková et al., "Planum temporale analysis via a new volumetric method in autoptic brains of demented and psychotic patients," *Current Alzheimer Research*, vol. 6, no. 1, pp. 69–76, 2009.

[8] J. F. Smiley, G. Rosoklija, B. Mancevski, J. J. Mann, A. J. Dwork, and D. C. Javitt, "Altered volume and hemispheric asymmetry of the superficial cortical layers in the schizophrenia planum temporale," *European Journal of Neuroscience*, vol. 30, no. 3, pp. 449–463, 2009.

[9] H. J. G. Gunderson, "The nucleator," *Journal of Microscopy*, vol. 151, no. 1, pp. 3–21, 1988.

[10] D. Freedman, R. Pisani, and R. Purves, *Statistics*, W.W. Norton & Company, 4th edition, 2007.

[11] M. J. West, "Tissue shrinkage and stereological studies," *Cold Spring Harb Protoc*, vol. 3, 2013, Adapted from Basic Stereology for Biologists and Neuroscientists by M. J. West, CSHL Press, Cold Spring Harbor, NY, USA, 2012.

[12] J. J. Hutsler, "The specialized structure of human language cortex: pyramidal cell size asymmetries within auditory and language-associated regions of the temporal lobes," *Brain and Language*, vol. 86, no. 2, pp. 226–242, 2003.

[13] J. Mrzilková, P. Zach, A. Bartoš, J. Tintera, and D. Řípová, "Volumetric analysis of the pons, cerebellum and hippocampi in patients with Alzheimer's disease," *Dementia and Geriatric Cognitive Disorders*, vol. 34, no. 3-4, pp. 224–234, 2012.

[14] C. L. Beasley, G. Chana, M. Honavar, S. Landau, I. P. Everall, and D. Cotter, "Evidence for altered neuronal organisation within the planum temporale in major psychiatric disorders," *Schizophrenia Research*, vol. 73, no. 1, pp. 69–78, 2005.

[15] R. A. Sweet, J. N. Pierri, S. Auh, A. R. Sampson, and D. A. Lewis, "Reduced pyramidal cell somal volume in auditory association cortex of subjects with schizophrenia," *Neuropsychopharmacology*, vol. 28, no. 3, pp. 599–609, 2003.

MRZÍLKOVÁ, J.; KOUTELA, A.; KUTOVÁ, M.; PATZELT, M.; IBRAHIM, I.; AL-KAYSSI, D.; BARTOŠ, A.; ŘÍPOVÁ, D.; ČERMÁKOVÁ, P. a P. ZACH. Hippocampal spatial position evaluation on MRI for research and clinical practice. *PLoS One*. 2014, **9**(12), e115174; 1-15. ISSN 1932-6203. DOI: 10.1371/journal.pone.0115174. **IF: 3.534/2013**.

Abstract: In clinical practice as well as in many volumetric studies we use different reorientations of the brain position towards x and y axis on the magnetic resonance imaging (MRI) scans. In order to find out whether it has an overall effect on the resulting 2D data, manual hippocampal area measurements and rotation variability of the brain (in two reoriented axes) and the skull were performed in 23 Alzheimer's disease patients and 31 healthy controls. After the MRI scanning, native brain scans (nat) were reoriented into the two different artificial planes (anterior commissure-posterior commissure axis (AC-PC) and hippocampal horizontal long axis (hipp)). Hippocampal area and temporal horn of the lateral ventricle was measured manually using freeware Image J program. We found that 1) hippocampal area of nat images is larger compared to hipp images, area of the nat images is equal to the AC-PC images and area of the hipp images is smaller compared to AC-PC images, 2) hippocampal area together with the area of the temporal horn for nat images is larger compared to hipp images, area of the hipp images is smaller compared to the AC-PC images and area of the nat images is smaller compared to the AC-PC images. The conclusion is that the measured area of the hippocampus in the native MRI is almost the same as the area of MRI reoriented only into the AC-PC axis. Therefore, when performing 2D area studies of the hippocampus or in the clinical practice we recommend usage of not-reoriented MRI images or to reorient them into the AC-PC axis. Surprising finding was that rotation of both AC-PC and hipp line towards x-axis among patients varies up to 35° and the same is true for the skull rotation so that it is not only a matter of the brain position.

PLOS ONE

RESEARCH ARTICLE

Hippocampal Spatial Position Evaluation on MRI for Research and Clinical Practice

Jana Mrzílkova[1], Antonella Koutela[1], Martina Kutová[1], Matěj Patzelt[1], Ibrahim Ibrahim[6], Dina Al-Kayssi[1], Aleš Bartoš[2,3], Daniela Řípová[2], Pavla Čermáková[4,5], Petr Zach[1]*

1. Institute of Anatomy, Third Faculty of Medicine, Charles University, Ruská 87, 100 00 Prague 10, Czech Republic, **2.** AD Center, Prague Psychiatric Center, Ustavni 91, 181 03 Prague 8 – Bohnice, Czech Republic, **3.** Charles University in Prague, Third Faculty of Medicine, Teaching Hospital Královské Vinohrady, Department of Neurology, Šrobárova 50, 100 34 Prague 10, Czech Republic, **4.** Alzheimer Disease Research Center, Department of Neurobiology, Care Sciences and Society, Karolinska Institutet, 141 86 Stockholm, Sweden, **5.** International Clinical Research Center and St.Anne's University Hospital, Pekařská 53, 656 91 Brno, Czech Republic, **6.** Department of Radiodiagnostic and Interventional Radiology, Institute for Clinical and Experimental Medicine, Vídeňská 1958/9, 140 21, Prague 4, Czech Republic

*zach.petr@post.cz

Citation: Mrzílkova J, Koutela A, Kutová M, Patzelt M, Ibrahim I, et al. (2014) Hippocampal Spatial Position Evaluation on MRI for Research and Clinical Practice. PLoS ONE 9(12): e115174. doi:10.1371/journal.pone.0115174

Editor: Xia Wu, Beijing Normal University, China

Received: March 6, 2014

Accepted: November 19, 2014

Published: December 12, 2014

Data Availability: The authors confirm that all data underlying the findings are fully available without restriction. All relevant data are within the paper and the Supporting Information file.

Funding: The study was supported by grant P 304/12/G069 from the Grant Agency of the Czech Republic and the Research Project Charles University in Prague, PRVOUK 34, project 260045/SVV/2014 of the Czech Republic and GAUK 1894214. The funders had no role in study design, data collection and analysis, decision to publish, or preparation of the manuscript.

Competing Interests: The authors have declared that no competing interests exist.

Abstract

In clinical practice as well as in many volumetric studies we use different reorientations of the brain position towards x and y axis on the magnetic resonance imaging (MRI) scans. In order to find out whether it has an overall effect on the resulting 2D data, manual hippocampal area measurements and rotation variability of the brain (in two reoriented axes) and the skull were performed in 23 Alzheimer's disease patients and 31 healthy controls. After the MRI scanning, *native brain scans* (nat) were reoriented into the two different artificial planes (*anterior commissure – posterior commissure* axis (AC-PC) and *hippocampal horizontal long axis* (hipp)). Hippocampal area and temporal horn of the lateral ventricle was measured manually using freeware Image J program. We found that 1) hippocampal area of nat images is larger compared to hipp images, area of the nat images is equal to the AC-PC images and area of the hipp images is smaller compared to AC-PC images, 2) hippocampal area together with the area of the temporal horn for nat images is larger compared to hipp images, area of the hipp images is smaller compared to the AC-PC images and area of the nat images is smaller compared to the AC-PC images. The conclusion is that the measured area of the hippocampus in the native MRI is almost the same as the area of MRI reoriented only into the AC-PC axis. Therefore, when performing 2D area studies of the hippocampus or in the clinical practice we recommend usage of not-reoriented MRI images or to reorient them into the AC-PC axis. Surprising finding was that rotation of both AC-PC and hipp line towards x-axis among patients varies up to 35˚

and the same is true for the skull rotation so that it is not only a matter of the brain position.

Introduction

Visualization of the medial temporal structures, especially the hippocampus, plays an important role in the clinical evaluation of the Alzheimer's disease (AD) [1, 2]. There are numerous methods of hippocampal atrophy classification using magnetic resonance imaging (MRI) [3]. Most of them utilize frontal sections of the hippocampus. In order to evaluate hippocampal atrophy in neurological practice, we often look at the transition from the hippocampal *alveus* into the hippocampal body which we call optimal section. At this section we can observe the area of both hippocampus as well as temporal horn of the lateral ventricle in its prime (other more frontal or dorsal sections does not fully cover structure). From our experience the severity of the hippocampal atrophy can be best scored there. However, the absolute position of the brain structures commonly used for evaluation, such as anterior and posterior commissure and the hippocampus may vary for example due to cellular changes accompanying aging process [4].

1.1 Head and brain stabilization and possible bias during MRI scanning

During MRI scanning of the brain the patient's head is stabilized in default position without any movements. Nevertheless, the real position of the head may differ from one case to another. It may happen so due to a simple rotation of the head or neck in the sagittal plane. If we rule out head instability during MRI scanning, among other factors could be the amount of the musculature and the adipose tissue, difference in the shape of the skull (i.e. *dolichocephaly* etc.) or the presence of *lordosis/kyphosis* of the cervical/thoracic vertebras. But according to the radiologists' reports, even the most precise instructions followed by the patient's cooperation may not guarantee the same position of the head during MRI data acquisition, which may lead to a source of variability in MRI studies [5, 6]. Interestingly, previous research investigating a similar problem in the functional magnetic resonance imaging (fMRI) studies found that head-repositioning did not decrease the reproducibility of the results [7]. We were interested in finding out whether the position of the head plays an important role in manual area measurements and volumetric software processing. When considering other brain MRI studies focused on 2D or 3D analysis it is not clear whether researchers have taken repositioning into account or not. In some articles, the authors reoriented native MRI scans into the standard orientation relative to *anterior* and *posterior commissure* line (AC-PC) [8–11]. In another study [12] the MRI images were adapted from a midsagittal sections to the

brainstem axis. However, in several other articles it is not specified whether the head was reoriented into the midsagittal axis or not [13, 14]. In order to evaluate the influence of the head rotation in the sagittal plane on the hippocampal area measurement, we introduced one more axis – the hippocampal long axis. We compared it with the commonly used AC-PC axis and native scan (images w/o any reorientations – as they are after MRI scanning).

We aimed to investigate how much the view of the hippocampus differs in native and optimal section compared to various axial reorientations that are commonly used in research and clinical practice. We were also interested in finding out whether the position of the head can limit the reliability of the MRI evaluations. Therefore, our goals were firstly to evaluate the rotation of the head in sagittal axis by comparing hippocampal area measurement of native images to the standardized AC-PC axis reoriented images and to the hippocampal long axis reoriented images. Secondly, to evaluate our hypothesis that area measurements in the hippocampal long axis reorientation of MRI images would yield similar results compared to the native images and be thus more useful for clinicians, in comparison with the AC-PC axis reorientation. Thirdly, to find out how much variability during MRI scanning is there in the skull rotation.

Material and Methods

2.1 Study population

This study utilized 23 patients (average age 76 ± 6 years, 8 males and 15 females) with confirmed AD diagnosis based on the NINCDS-ADRDA criteria [15]. All patients with AD and 31 healthy seniors underwent MRI of the brain. Both groups were tested with the following neuropsychological tests: Mini-Mental State Examination (MMSE), Mattis Dementia Rating Scale, Trail Making Test version A and B, Disability Assessment in Dementia, 7-Minute Screen, verbal fluency tests and Edinburgh Handedness Inventory. According to the revised version of research criteria for the diagnosis of AD [16], we added medial temporal lobe atrophy score [12], separately for the left and right hemisphere. The control group consisted of 31 cognitively normal elderly persons (average age 82 ± 8 years, 7 males and 24 females), who were either recruited from the Third Age University of the Charles University at Prague, Czech Republic (educational courses for seniors) or among healthy volunteers visiting the AD Center at Prague. All of them reached 55 years of age, had Czech as their native language and no self-reported memory impairments. Exclusion criteria included the history of psychiatric treatment, the use of psychoactive medications (e.g. antidepressants, neuroleptics, anxiolytics, or hypnotics), the history of unconsciousness lasting longer than 5 min, seizures, any serious brain damage (stroke, trauma, neuro-infection, operation, tumor), and drug/alcohol abuse. Normal cognitive functions were determined using the MMSE, the 7-Minute Screen and verbal fluency tests (1-min version: 3 phonemic, with the initial letters of NKP, and 3 semantic, using fruits, animal, and shopping items). For both groups, the following data were collected: detailed anamnesis,

mapping potential comorbidities (hypertension, diabetes, cardiovascular diseases, hyperlipidemia, smoking, kidney and liver diseases, psychiatric illnesses, ictus, epilepsy and neurological diseases), medical treatment (antidepressants, anti-psychotics, anxiolytics, hypnotics, nootropics, cognitive treatment and others) and basic demographic data (living standards, years of education, highest education). Patients with AD were followed for several years and the healthy seniors underwent neuropsychological testing bi-annually. All participants signed an informed consent. The research was approved by the Ethics Committee of the University Hospital Kralovske Vinohrady, Prague, Czech Republic.

2.2 MRI specifications

Three-dimensional MRI images were acquired on the scanner Siemens Trio 3 T, TQ-engine gradient system, and 18 RF channels. Acquisition parameters for the volume analysis were: 192 sagittal layers, 3D sequence MP-RAGE, resolution $0{,}85 \times 0{,}85 \times 0{,}85$ mm, (FOV 326 mm, matrix 384×384), TE 4,73 ms, TR 2000 ms, TI 800 ms, declination angle 10°, bandwidth 130 Hz/pixel, acquisition time 10:50 min.

2.3 Area measurement and computer analysis

The MRI images were exported as a multiple data format files into a standard computer. The MRI images of the brains were then converted into the stack of files by the MRIcro freeware and analyzed on Image J freeware. The areas of the hippocampi in (mm^2) and hippocampus with temporal horn of the lateral ventricle (both at the level of the transition of *alveus* into the hippocampal body) were manually delineated independently by two experienced neuroanatomists. Hippocampal areas solely and collectively with the temporal horn of the lateral ventricle areas were measured in the three different rotational scan stacks of the MRI. Firstly, we measured areas in the ''native'' (nat) unaltered MRI scan stacks (Fig. 1a) as we obtained it from the MRI scanner. Secondly, we measured areas in the MRI scan stacks that were rotated using the MRIcro program so that the hippocampal long axis in the sagittal projection was parallel to the x-axis (hipp). Finally, the MRI scan stacks once again were rotated using the MRIcro program so that the sagittal projection line connecting the AC-PC was parallel to the x – axis (AC-PC). The areas of the hippocampi and hippocampus together with temporal horn of the lateral ventricle were calculated separately and adjusted to the areas of the brain and skull at the frontal cross-section at the level of *anterior commissure*; to exclude the impact of the brain and the skull size. The areas were adjusted according to formula (area of the hippocampus/area of the brain (skull) * 100. We did not observe statistically significant differences between adjusted and non-adjusted areas (unpublished results) so that we used in the calculations data w/o brain or skull adjustment.

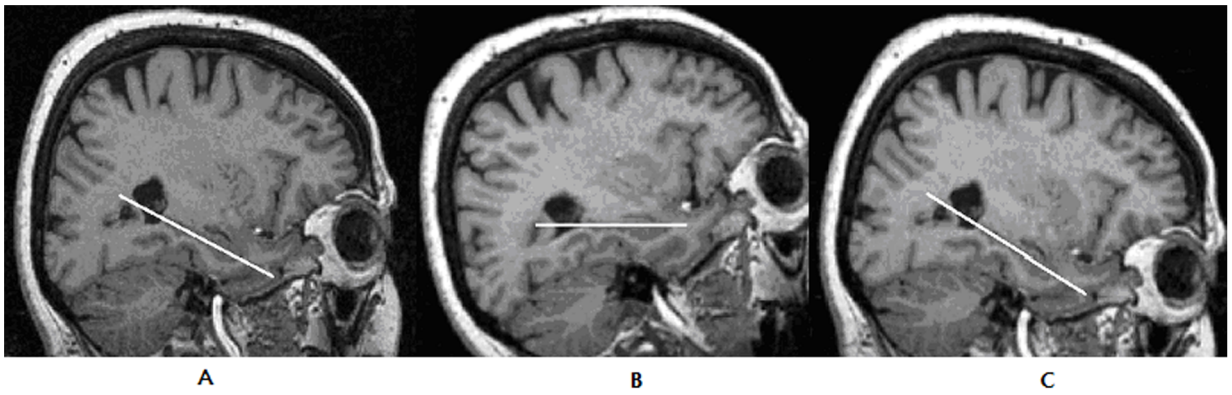

Fig. 1. a,b,c Examples of the sagittal view of the right hippocampus on the MRI in one native and two reoriented axis. MRI sections were selected according to the best visibility of the of the hippocampus on the sagittal sections (its long or dorsoventral axis), a) position of the hippocampus on the ''native'' MRI scan, b) reorientation of the ''native'' MRI scan into the hipo-axis axis (where long axis of the hippocampus is parallel to the horizontal axis), c) reorientation of the ''native'' MRI scan into the CA-CP. White lines represent long axis of the hippocampus.

doi:10.1371/journal.pone.0115174.g001

2.4 Anatomical delineation of the hippocampus and temporal horn of the lateral ventricle

We measured only the area of the hippocampus proper – without *subiculum* and *parahippocampal gyrus*. However, these measurements did include *dentate gyrus* due to its close position to the hippocampus on the frontal section (Fig. 2). This method is in line with a large amount of studies that use a similar protocol for hipppocampal delineation, for example [17]. The inferior border of the measured area was a clearly visible line between hippocampus and the grey matter of parahippocampal gyrus medially and directly caudally white matter of the *subiculum*. The caudo-medial border was set as cerebrospinal fluid (CSF) filled space between hippocampus and crura cerebri on both sides and cranio-medial border as the point where fornix (included in the measurement) inserts on the roof of the temporal horn of the lateral ventricle via *stria medullaris*. The lateral border of the measured area was a clearly visible round shape of the hippocampus with dark black color of the cerebrospinal fluid in the temporal horn of the lateral ventricle.

2.5 Rotation of the AC-PC and hipp axes of the brain

In case of AC-PC axis we measured together controls and AD patients (w/o left or right side dichotomy since AC-PC axis is midline structure without laterality) because there are no data in the literature about its impairment in the AD compared to healthy controls. On the other hand the measurement of the hipp axis rotation was performed separately in controls and AD patients (with left and right side dichotomy) due to its well known atrophy in AD compared to the controls. We opened brain scan files in MRIcro program in mid - sagittal projection and we rotated the brain so that AC-PC line was parallel to the x – axis (Fig. 1c). As next step we scrolled from the mid – sagittal projection laterally till

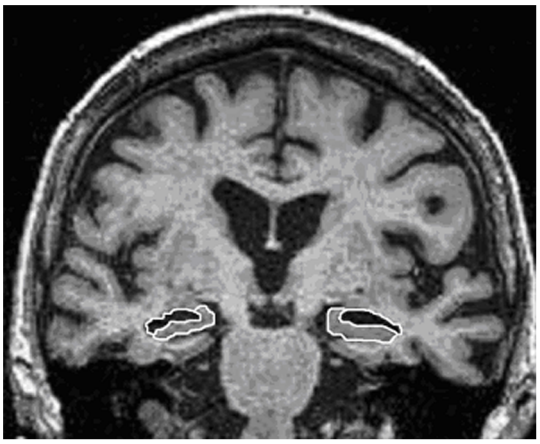

Fig. 2. Example of manual anatomical delineation of the hippocampus (white line with grey area inside) and temporal horn of the lateral ventricle (white line with black area inside) on the left and right side. Coronal sections of the MRI are located at the transition from the *alveus* of the hippocampus into the hippocampal body.

doi:10.1371/journal.pone.0115174.g002

we reached long axis of the hippocampus (Fig. 1b). At this point we got the rotation angle between long axis of the hippocampus and AC-PC line previously set parallel to x axis. This was done separately for the right and left sides.

2.6 Rotation of the skull (Frankfurt auriculo-orbital plane)

We evaluated the anterior-posterior rotation of the head by Frankfurt plane [18] which is the most reliable anthropological measure defining position of the human skull. We measured the angle between a line connecting the upper margin of *meatus acusticus externus* with the inferior margin of the orbita on the maxilla (at the level of equator of the eyeball) and x-axis in the MRIcro program.

Statistics

3.1 Hippocampal area analysis

Statistical analysis was performed for all variables (nat, hipp and AC-PC) by the non-parametrical Friedman Analysis of Variance (ANOVA) and then each two variables together by parametrical paired t-test. In case of statistical significance we continued with Wilcoxon paired test for each grouping (hipp vs nat, AC-PC vs nat and AC-PC vs hipp). For the evaluation of the Friedman's test we did normalization by Kendall's coefficient of concordance W (0 – no agreement to 1 – complete agreement).

3.2 Relationship between nat, hipp and AC-PC brain rotations

Rotation of AC-PC axis vs nat axis was evaluated by the histogram (Fig. 3). Rotations of the left and right hipp axes vs nat axis (separately for controls and

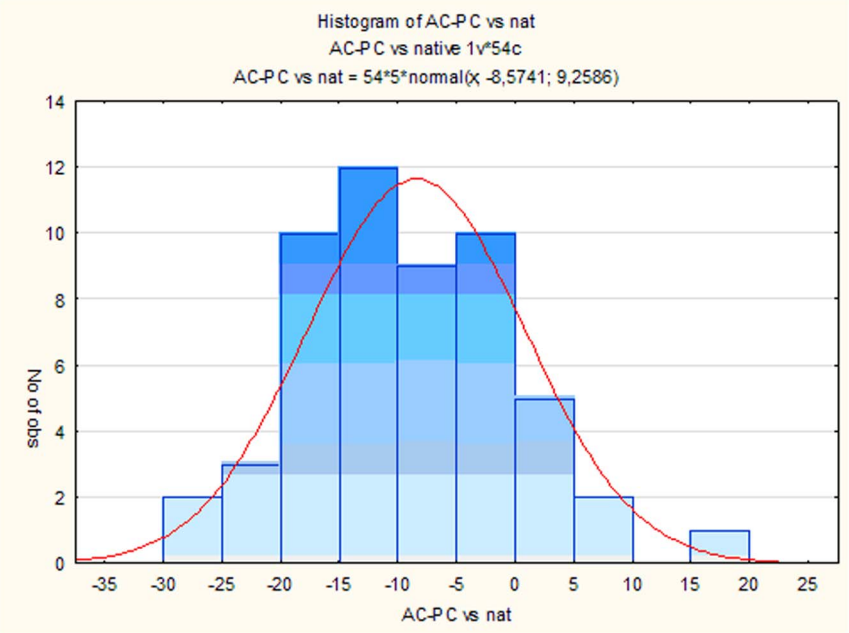

Fig. 3. Brain rotation variability of AC-PC vs nat on MRI. The extent of the brain rotation in AC-PC vs nat is shown in decimal degrees on x-axis (– counter clockwise and + clockwise rotation) ($p<0.05$).

doi:10.1371/journal.pone.0115174.g003

AD patients groups) (Fig. 4) and rotations of the AC-PC axis vs hipp axis was evaluated by parametrical paired t-test.

3.3 Relationship between skull rotation and AC-PC brain rotation

The Frankfurt plane variability for the whole group was evaluated by the histogram (Fig. 5). Similarity as in the case of skull and brain rotation (for the whole group) statistics was evaluated by dependent paired t-test (Frankfurt plane vs AC-PC axis) (Fig. 6).

Results

The area of the hippocampal cross-section was measured in 54 subjects (31 controls and 23 AD patients of heterogeneous age category) in three types of brain rotation (nat, hipp and AC-PC) so that for each brain rotation (3x) we accounted 216 area measurements (2×108 - left and right together). Hipp axis rotation variability was measured separately on the left and on the right in controls ($n=31$) and AD patients ($n=23$). Nat and AC-PC axes rotation variability were calculated as one group (w/o sidedness and grouping effects).

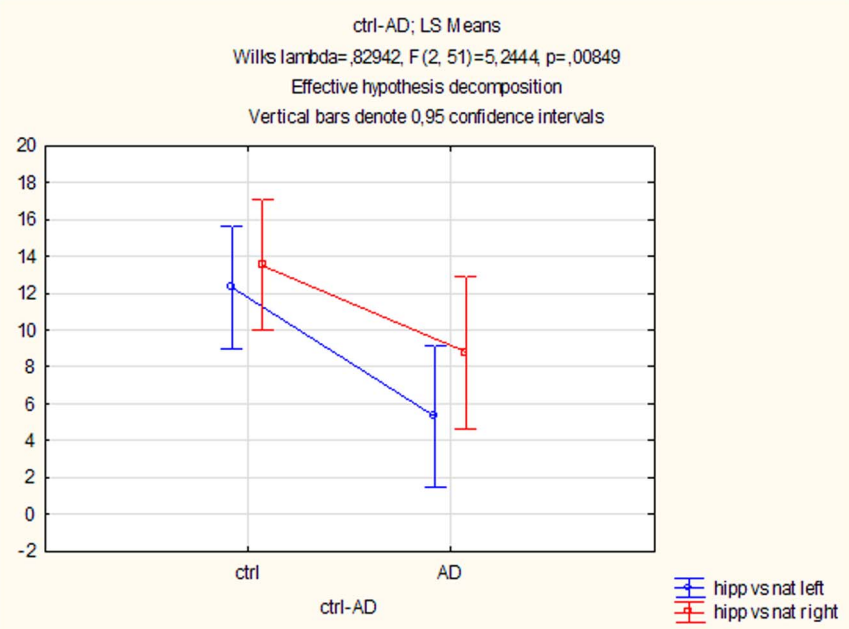

Fig. 4. Brain rotation variability of hipp vs nat on MRI. Data showing difference between left and right hipp axes (in the left and right hemisphere). There is a significant difference between left hipp axis rotation in the AD patients compared to the controls (p=0.008). The right hipp axis rotation in the AD patients compared to the controls are not significant (p=0.08). ANOVA F (2, 51) =2.54.

doi:10.1371/journal.pone.0115174.g004

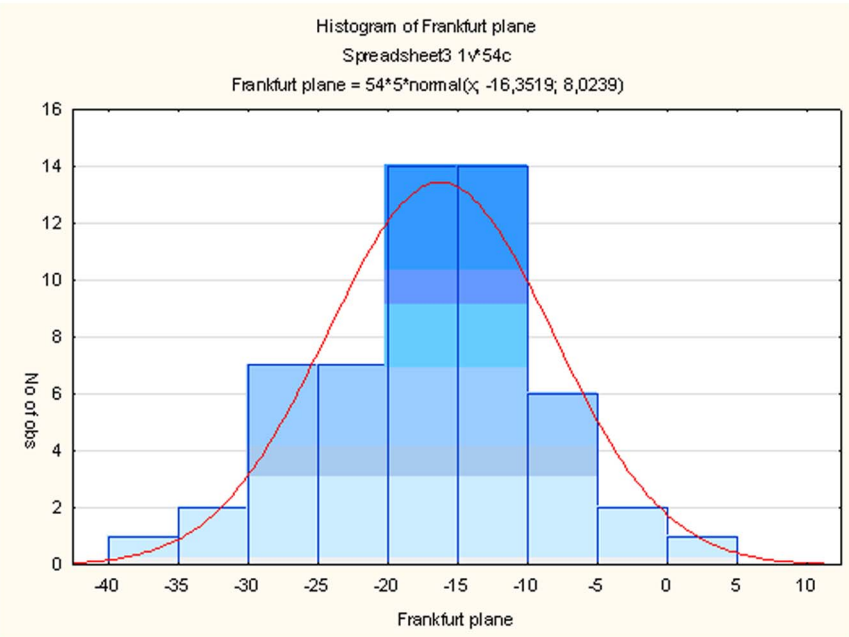

Fig. 5. Skull rotation variability in MRI. Skull dorsal and ventral skull rotation expressed as Frankfurt plane angles in decimal degree on x-axis (- counter clockwise rotation or dorsal and + clockwise rotation or ventral).

doi:10.1371/journal.pone.0115174.g005

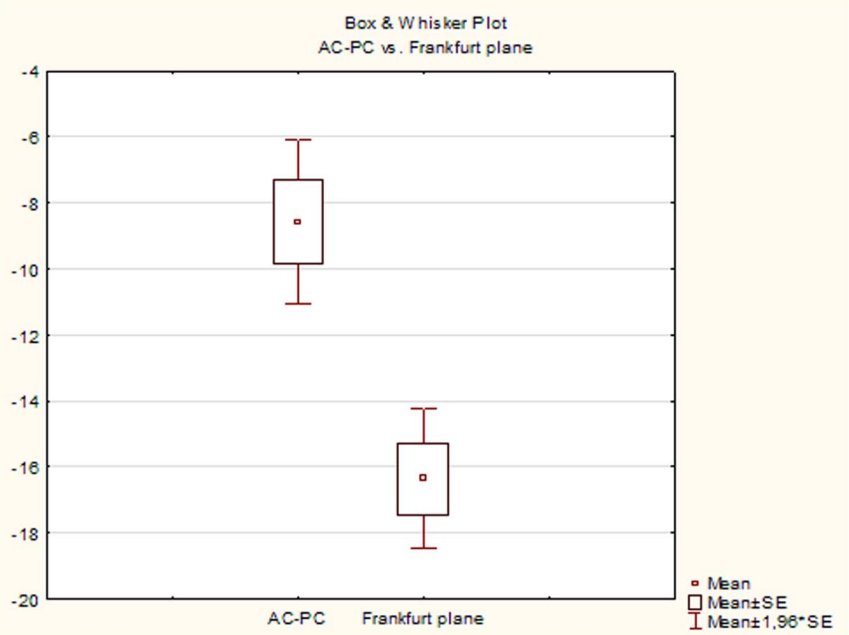

Fig. 6. Relationship between brain and skull rotation. The brain rotation in AC-PC axis and the skull rotation (Frankfurt plane) exhibit a similar degree of variability (- counter clockwise or dorsal). AC-PC axis, Mean =-8.57˚, SE=9.2˚. Frankfurt (auriculo-orbital) plane, Mean =−16.3˚, SE=8.02˚.

doi:10.1371/journal.pone.0115174.g006

4.1 Effect of brain rotations on the extent of hippocampal cross section area

There was no significant difference between the measured area of hippocampus in nat compared to AC-PC ($p=0.82$, $W=0.17$). On the other hand, the area of the hippocampus in nat was larger than the area in hipp ($p<0.05$, $W=0.17$). The area of the hippocampus in hipp was smaller compared to the area in AC-PC ($p<0.05$, $W=0.17$) (Fig. 7).

4.2 Effect of brain rotation variability on the extent of the area of hippocampus and ventricle

We found a significant difference between nat compared to hipp ($p<0.05$, $W=0.27$) as well as between hipp compared to AC-PC ($p<0.05$, $W=0.27$). This is on the contrary to the hippocampal area measurement only, where we found also a significant difference between nat compared to AC-PC ($p<0.05$, $W=0.27$) (Fig. 8).

4.3 Relationship between nat, hipp and AC-PC brain rotations and skull rotation

The degree of the AC-PC axis rotation vs nat varies from −27˚ to +16˚ (Fig. 3). On the contrary we found that both the left and right hipp axes are rotated largely

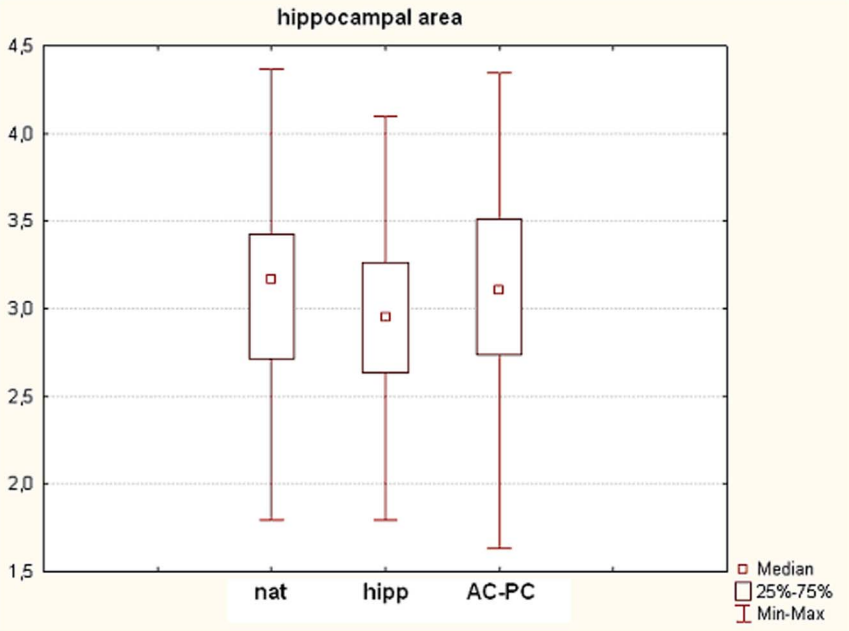

Fig. 7. Effects of the brains rotations on the area measurements of the hippocampus on the MRI. Three groups are presented on the x-axis – nat (as the unaltered MRI scans were exported for 2D area analysis), hipp (x-axis is parallel to the long axis of the hippocampus) and AC-PC (x axis is parallel to the line connecting *anterior* and *posterior commissure*). On the y-axis, 2D area values of the hippocampi in mm^2 are presented. Results are presented as median $\pm$ min-max.

doi:10.1371/journal.pone.0115174.g007

ventrally (+) and fewer dorsally (−). We also found that the left hipp axis in controls is rotated significantly more ventrally than the left hipp axis in AD patients ($p=0.008$). Similarly, although without statistical significance, the right hipp axes in controls compared to AD group are also rotated more ventrally (Fig. 4).

We found that skull was rotated almost exclusively dorsally (−), only in one case ventrally (+) (Fig. 5). Comparison of the brain rotation in AC-PC axis vs skull rotation showed similar degree of variability (AC-PC, Mean −8.57°, SE 9.2° and Frankfurt plane, Mean −16.3°, SE 8.02°) (Fig. 6).

Discussion

We evaluated effects of the rotation of the head in the sagittal plane on the manual 2D area measurements of the hippocampus that could lead to incongruent results between MRI evaluations where the manual delineation of the structures is deployed. After all we did not find any significant statistical differences in the areas of the hippocampus (AC-PC vs nat), measured on the regular coronal plane images (in the transition of the *alveus* into the body of the hippocampus). This contrasts with a simple observations made by the naked eye, where the shape of the hippocampus and temporal horn of the lateral ventricle seems different in all

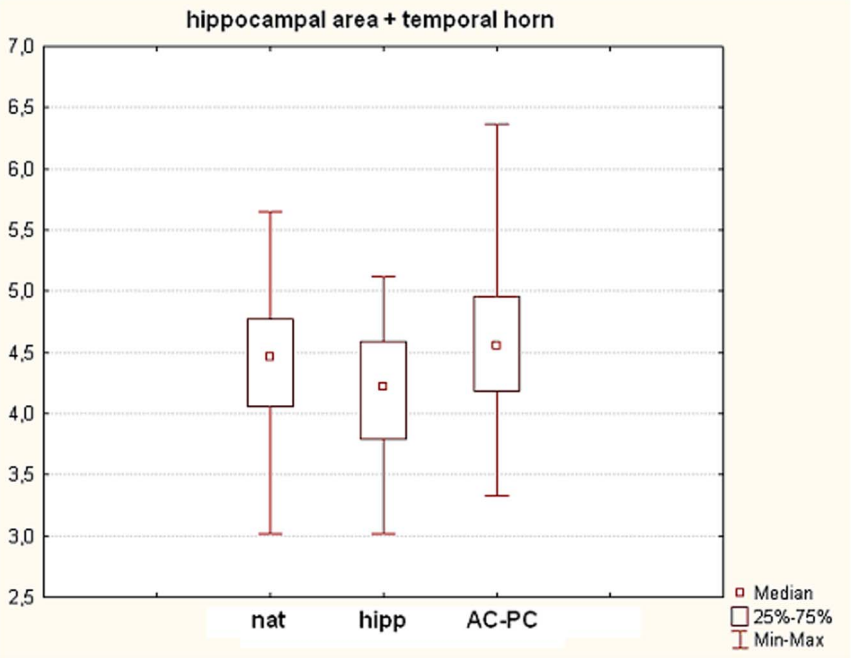

Fig. 8. Effects of the brain rotation variability on the extent of the cross-section area of hippocampus and ventricle on the MRI. On the x-axis, three groups are presented – nat (as the unaltered MRI scans were exported for the 2D area analysis), hipp (x-axis is parallel to the long axis of the hippocampus) and AC-PC (x-axis is parallel to the line connecting *anterior* and *posterior commissure*). On the y-axis, 2D area values of the hippocampi in mm^2 are presented. Results are presented as median $\pm$ min-max.

doi:10.1371/journal.pone.0115174.g008

the three brain rotations. Besides this, neither the hippocampus nor temporal horn of lateral ventricle is rotationally symmetrical in all the geometrical projections (frontal, sagittal, horizontal). Also, we found distinct, yet not significant differences between the areas of the hippocampus compared to the hippocampus with temporal horn of lateral ventricle. This could be possibly explained by effect of the higher total area; leading to the higher impact on the overall brain position. Furthermore, we included into the measurements together the controls, AD patients, different age categories and left-right hemispheres since our interest was in the effect of the regional geometry on the areas (which is often the case in most of MRI volumetric studies). Taken these differences in categorization into account, AD patients have generally larger volumes of the temporal horn of the lateral ventricle compared to healthy controls [12]; therefore more patients with this diagnosis could have larger areas and thus possibly leading to the different results. We did not try to measure volumes of the whole hippocampus and/or whole volume of the temporal horn of lateral ventricle, since the effect of the brain rotations would manifest in terms of absolute values and this way it would be eventually nullified. Assessing our eventual experimental limitations, we worked with magnetic resonance images from the same institute and the same magnetic resonance scanner. This could add to the causes biases, since different setups and protocols in different radiology/MRI departments may

lead to incongruent results. Moreover, we did not measure the effects of the lateral head/brain rotation, whose effect may have similar impact on the area measurement as the sagittal rotation.

If we stop thinking of the previously discussed rotations of the head or brain during MRI processing, further rotations could be conceived for different good reasons (i.e. change of the angle of the coronal plane of the MRI stack, to see better borders of the hippocampus, etc.) within the stereological software itself. We are not certain, whether it is possible to calculate how much we can afford to rotate the brain within the stereological software, while not changing 2D area results significantly. In another words, it is still unknown how large is the interval within which we can afford to manipulate the rotation of the brain, while still getting undistorted area results. Once this information is known, then we can rely more on inter reliability of different studies on the volumes of hippocampus, regardless of different view angles. This would be another interesting topic to be further studied. In addition to the previously discussed biases, our research was performed using only one MRI scanner, and it would be impossible to conclude that similar results could be obtained by the MRI scanners worldwide. Therefore it is necessary to perform similar measurements on different MRI scanners to find out whether these differences exist.

Unexpected finding was high inter – individual variability in the brain and skull rotations in the MRI (up to 35°). Both AC-PC vs nat as well as hipp vs nat and skull rotations showed similar trend. This finding was very surprising. In case of the skull rotation we used reliable method for its evaluation (Frankfurt plane is considered to be the most reliable skull anthropological measure) so that it would be easy to explain this phenomenon by a wrong head fixation protocol during the MRI processing. But our results from hipp vs nat rotation showed significant decrease in the dorsal brain rotation (or just its temporal lobe) in AD patients, especially on the left side. This finding is consistent with the overall hippocampal volume decrease in AD but it is showing more. It appears that hippocampal volume shrinkage may have specific effect on the position of the brain inside the skull, especially in the *middle cerebral fossa* where the temporal lobe resides. It is a matter of dispute what exactly accounts for the variability of the brain position inside the skull or if this could be attributed to the differences in the skull position or also to geometrically specific tissue shrinkage. If this is the case then any normalization of the brain positions are questionable because of the great variability in the tissue torsion, elongation and eventually not yet recognized patterns of the brain internal geometry variations. We did not find any suitable reference in the current literature describing similar anatomical features.

Conclusions

In order to quantify the effect of 3 different brain positions (native position and position according to hippocampal long axis or AC-PC axis) on the hippocampal area measurement, we rotated the brain manually in the MRIcro program prior to

the area measurements of the hippocampus alone and hippocampus with the temporal horn of the lateral ventricle. We found differences of the brain/head position in the sagittal plane in the native MRI stacks (unavoidable rotations of the head during MRI data acquisition). Also we found significant effect of the 1st artificial rotation (hipp axis) on the manual volumetric area measurements of the hippocampus and significant effect of the 2nd artificial rotation (hipp vs nat and AC-PC vs nat) of the hippocampus with temporal horn of the lateral ventricle in the frontal plane. In other words, reorientation of native MRI images into AC-PC axis does not make any significant difference on the measurements of the hippocampal area. However, this does not say other MRI scanners would produce the same results. We recommend performing similar measurements on several different MRI scanners for comparison. Regardless of this we presume, that inevitable head rotation of the patient (due to for example the size of the posterior neck muscles) does not have significant impact on the measurements of areas of the medial temporal structures. For the routine area measurements we can use ''native'' images and the reorientation of images into the standardized AC-PC axis is not crucial in the research or clinical practice. The head may be flexed dorsally or ventrally due to the volume of the neck muscles or adipous tissue on the back or due to different shape of the skull (dolichocephaly, microcephaly, etc.) and maybe for plenty other reasons. The brain may suffer inconsitent atrophy of the temporal lobe or the frontal lobe or cerebellum (although in the cerebellum we did not observe significant atrophical changes [2]. Also the amount and volume of the CSF in the interventricul or subarachnoid space may contribute to change in the shape or volume. Furthermore, insertion of the dura mater on the periost inside the skull may differ significantly and this may affect the volume of the subdural or epidural space. This may cause for example ventral or dorsal torsion of the frontal lobe (sometimes reffered to as Yakovlevian torsion), which would lead to the higher AC-PC rotation angle compared to the hipp rotation angle or viceversa. In the case of the temporal lobe atrophy there would be increased rotation angle between AC-PC vs hippo due to the descensus of the whole temporal lobe together with hippocampus into the *middle cerebral fossa*. Taken together we came to the conclusion, that it is hardly possible to account for all possible effects and so it is questionable if any normalizations and brain subparts delineations in volumetric studies are valid as presented in the literature. Nevertheless, we found that the area of the hippocampus in the optimal section in native is statistically comparable to the area of the hippocampus reoriented into the AC-PC, which is according to literature taken as standard procedure. For clinicians this reorientation is a relatively complicated and time consuming process, therefore we see the advantage of our results for simplification of the clinical practice.

Supporting Information

S1 Data. Table of raw data used in the calculations.
doi:10.1371/journal.pone.0115174.s001 (XLS)

Author Contributions

Conceived and designed the experiments: JM PZ. Performed the experiments: MK AB II. Analyzed the data: JM DR MP AK. Contributed reagents/materials/analysis tools: DAK PZ PC. Wrote the paper: PZ.

References

1. **Scher AI, Xu Y, Korf ES, White LR, Scheltens P, et al.** (2007) Hippocampal shape analysis in Alzheimer's disease: a population-based study. Neuroimage 36: 8–18.
2. **Mrzilkova J, Zach P, Bartos A, Tintera J, Ripova D** (2012) Volumetric analysis of the pons, cerebellum and hippocampi in patients with Alzheimer's disease. Dement Geriatr Cogn Disord 34: 224–234.
3. **Westman E, Cavallin L, Muehlboeck JS, Zhang Y, Mecocci P, et al.** (2011) Sensitivity and specificity of medial temporal lobe visual ratings and multivariate regional MRI classification in Alzheimer's disease. PLoS One 6: e22506.
4. **Cerbai F, Lana D, Nosi D, Petkova-Kirova P, Zecchi S, et al.** (2012) The neuron-astrocyte-microglia triad in normal brain ageing and in a model of neuroinflammation in the rat hippocampus. PLoS One 7: e45250.
5. **McGonigle DJ, Howseman AM, Athwal BS, Friston KJ, Frackowiak RS, et al.** (2000) Variability in fMRI: an examination of intersession differences. Neuroimage 11: 708–734.
6. **Raemaekers M, du Plessis S, Ramsey NF, Weusten JM, Vink M** (2012) Test-retest variability underlying fMRI measurements. Neuroimage 60: 717–727.
7. **Soltysik DA, Thomasson D, Rajan S, Gonzalez-Castillo J, DiCamillo P, et al.** (2011) Head-repositioning does not reduce the reproducibility of fMRI activation in a block-design motor task. Neuroimage 56: 1329–1337.
8. **Oksengard AR, Cavallin L, Axelsson R, Andersson C, Nagga K, et al.** (2010) Lack of accuracy for the proposed 'Dubois criteria' in Alzheimer's disease: a validation study from the Swedish brain power initiative. Dement Geriatr Cogn Disord 30: 374–380.
9. **Maller JJ, Reglade-Meslin C, Anstey KJ, Sachdev P** (2006) Sex and symmetry differences in hippocampal volumetrics: before and beyond the opening of the crus of the fornix. Hippocampus 16: 80–90.
10. **Bozoki AC, Korolev IO, Davis NC, Hoisington LA, Berger KL** (2012) Disruption of limbic white matter pathways in mild cognitive impairment and Alzheimer's disease: a DTI/FDG-PET study. Hum Brain Mapp 33: 1792–1802.
11. **Hayashi T, Wada A, Uchida N, Kitagaki H** (2009) Enlargement of the hippocampal angle: a new index of Alzheimer disease. Magn Reson Med Sci 8: 33–38.
12. **Scheltens P, Leys D, Barkhof F, Huglo D, Weinstein HC, et al.** (1992) Atrophy of medial temporal lobes on MRI in ''probable'' Alzheimer's disease and normal ageing: diagnostic value and neuropsychological correlates. J Neurol Neurosurg Psychiatry 55: 967–972.
13. **Teipel SJ, Ewers M, Wolf S, Jessen F, Kolsch H, et al.** (2010) Multicentre variability of MRI-based medial temporal lobe volumetry in Alzheimer's disease. Psychiatry Res 182: 244–250.
14. **Fleisher AS, Sun S, Taylor C, Ward CP, Gamst AC, et al.** (2008) Volumetric MRI vs clinical predictors of Alzheimer disease in mild cognitive impairment. Neurology 70: 191–199.

15. **McKhann G, Drachman D, Folstein M, Katzman R, Price D, et al.** (1984) Clinical diagnosis of Alzheimer's disease: report of the NINCDS-ADRDA Work Group under the auspices of Department of Health and Human Services Task Force on Alzheimer's Disease. Neurology 34: 939–944.

16. **Dubois B, Feldman HH, Jacova C, Dekosky ST, Barberger-Gateau P, et al.** (2007) Research criteria for the diagnosis of Alzheimer's disease: revising the NINCDS-ADRDA criteria. Lancet Neurol 6: 734–746.

17. **Geuze E, Vermetten E, Bremner JD** (2005) MR-based in vivo hippocampal volumetrics: 1. Review of methodologies currently employed. Mol Psychiatry 10: 147–159.

18. **Finlay LM** (1980) Craniometry and cephalometry: a history prior to the advent of radiography. The Angle Orthodontist 50: 312–321.

ZACH, P.; ROBERTS, B. M.; BARTOŠ, A.; **MRZÍKOVÁ, J.**; KUTOVÁ, M.; IBRAHIM, I.; TINTĚRA, J.; KOUTELA A. a D. ŘÍPOVÁ. Laterality distribution in FreeSurfer automated volumetric brain analysis of patients with Alzheimer's disease (Czech population). *Journal of Neuroradiology*. ISSN 0150-9861. **In review.**

Abstract: We studied volumes and other parameters of lateralized and non-lateralized brain regions by FreeSurfer v5.2.0 and v5.3.0 automated segmentation software in patients with Alzheimer's disease (AD) and the normal elderly people. In many analysed structures eg. putamen, pallidum, cerebellar grey matter, number of the cortical holes we found non significant difference between AD group and control group. Only in some structures we found statistically significant differences between the control group and the AD group, eg. in overall brain cortical area, size of the fourth ventricle, volume of the cerebrospinal fluid, left inferior horn of the lateral ventricle, nucleus accumbens, amygdalar complex. Interestingly, righ-left asymmetries showed different results in case of AD group and control group. In AD group we found significant difference in the number of the cortical holes between left and right side and asymmetrical volumes in case of lateral ventricles and amygdalar complex. In control group we found significant difference in the cerebellar white matter and cerebellar cortex. Two robust findings of ours was 1) bilateral decrease of the volume of nucleus accumbens in AD group compared to control and 2) absence of asymmetrical volume increase of the temporal horn of the lateral ventricle – that suggests that lateralized volume increase of the lateral ventricles in the AD has to be attributed to either cornu frontale, pars centralis or cornu occipitale.

Introduction

FreeSurfer (FS) automated reconstruction of the brain structures (Van Leemput et al., 2009) seems to be a new promising tool in the diagnostics of the Alzheimer disease (AD). However, automatization of the brain structures bordering using different pre-made atlases (Talairach, Tournoux) may pose a problem of discrepancies between actual structures and approximated ones. In the literature there are reports of three cathegories concerning the validity of automated brain parcellations: a) the manual segmentation is to the present moment more precise compared to the automated one, b) both manual and automated segmentations are equivocal in their results and finally, c) automated segmentation is more advanced and precise compared to the manual one. In our study we tried to evaluate automated FS volume segmentation of AD patients compared to the normal elderly in terms of the most lateralized and non-lateralized structues of the brain that more or less have precise anatomical borders towards white matter. Rarely in the literature is mentioned lateralization of volume changes of structures in AD patients. Therefore we included detailed analysis of the asymmetrical nature of these changes both in AD group and control group. We also presumed to find more pronounced right-left asymmetry in most of the studied structures in the AD group compared to the controls.

Materials and methods

Diagnosis of AD

We evaluated 26 patients with diagnosis of probable AD based on NINCDS-ADRDA criteria (McKhann et al., 1984). All patients with AD and 27 normal seniors underwent MRI of the brain. Both groups were tested with the following neuropsychological tests: Mini-Mental State Examination (MMSE), Mattis Dementia Rating Scale, Trail Making Test version A and B, Disability Assessment in Dementia, 7-Minute Screen, verbal fluency tests and Edinburgh Handedness Inventory. According to the revised version of research criteria for the diagnosis of AD (Dubois et al., 2007), we added medial temporal lobe atrophy score (Scheltens et al., 1992), separately for the left and right hemisphere.

Personal Characteristics of the Control Group and the AD Patients

The control group consisted of 27 cognitively normal elderly controls who were either recruited from the Third Age University of the Charles University at Prague, Czech Republic (educational courses for seniors) or among healthy volunteers visiting the AD Center at Prague. All of them reached 55 years of age, had Czech as their native language, and no self-reported memory impairments. Exclusion criteria included a history of psychiatric treatment, the use of psychoactive medications (e.g. antidepressants, neuroleptics, anxiolytics, or hypnotics), a history of episodes of unconsciousness lasting longer than 5 min, seizures, any serious brain damage (stroke, trauma, neuro-infection, operation, tumor), and drug/alcohol abuse. Normal cognitive functions were determined using the MMSE, the 7-Minute Screen and verbal fluency tests (1-min version: 3 phonemic, with the initial letters of NKP, and 3 semantic, using fruits, animals, and shopping items) (Budson et al., 2011). For both groups, the following data were collected: detailed anamnesis, mapping potential comorbidities (hypertension, diabetes, cardiovascular diseases, hyperlipidemia, smoking, kidney/ liver diseases, psychiatric illnesses, ictus, epilepsy and neurological diseases), medical treatment (antidepressants, antipsychotics, anxiolytics, hypnotics, nootropics, cognitive treatment and others) and basic demographic data (living standards, years of education, highest education). Basic biography characteristics about patients are summarized in Table 2. The normal elderly and AD patients were followed up for several years and annually underwent some neuropsychological examinations. All participants signed an informed consent. The research was approved by the Ethics Committee of the University Hospital Kralovske Vinohrady, Prague, Czech Republic.

MRI Specifications

Three-dimensional MR images were acquired on a scanner Siemens Vision 1.5T by magnetization-prepared rapid gradient echo sequence in the sagittal plane, software version VB33G, voxel size 1 x 1 x 1 mm, number of slices 160, TE 7 ms, TR 2.130 ms, matrix 256 x 256 and flip angle 10°.

FreeSurfer (FS) analysis

Analysis was performed on single table PC (Debian Linux 3.2.46-1 x86_64 operating system) with two installed versions of FreeSurfer (freesurfer-Linux-

centos4_x86_64-stable-pub-v5.2.0 and v5.3.0 program, http://surfer.nmr.mgh.harvard.edu/). DICOM MR images from the scanner of the controls and the AD patients were converted into FS program *.mgz files by mri_convert command. Full images reconstruction (cortical and subcortical areas, brain stem, cerebrospinal fluid, ventricles, white matter) was done by recon –all command. Recon –all procedure failed in 2 control MRI – these were removed from analysis. Volume datasets for statistical analysis were taken from /stats directory (aseg.stats, lh aparc.stats, etc.) within FS program and exported into Statistica 10 software.

Statistics

ANOVA with repeated measured was used for left and right volumes in both controls and AD groups followed by Newman-Keuls post hoc analysis. For non-paired structures (brain stem volume, CSF volume, volume of the third and fourth ventricle) t-test for independent samples was used. Lateralization between left and right side for both the AD group and controls we evaluated by t-test for dependent samples. Statistical significance was accepted for the $p<0,05$*, $p<0,01$** and $p<0,001$*** levels.

Results

Volumetry and cortical defects

We evaluated lateralized and non-lateralized brain structures in 26 patients with AD and in 27 normal elderly people. Most of the lateralized brain structures showed expected volume decrease in the AD group compared to controls - number of cortical defects (cortical holes defined as incongruencies in the structure of the gray matter of different origin – vascular lesions, atrophic foci, lacunae etc.) (Fig. 1), volumes of the whole cerebral cortex (Fig. 2), lateral ventricle (Fig. 3), inferior horn of the lateral ventricle (Fig. 4), cerebellar white matter (Fig. 5), whole cerebellar cortex (Fig. 6), caudate nucleus (Fig. 7), putamen (Fig. 8), pallidum (Fig. 9), amygdalar complex (Fig. 10) and nc. accumbens (Fig. 11). For the non-lateralized brain structures we evaluated volumes of the third ventricle (Fig. 12), the fourth ventricle (Fig. 13), volume of the cerebrospinal fluid (Fig. 14) and the whole brain stem (Fig. 15).

Statistically significant volume decrease of selected structures in AD group compared to controls were found in the case of brain cortical area (both left and right hemispheres, $p<0,001$), lateral ventricles (left side, $p<0,001$ and right side, $p=0,002$), inferior horn of the lateral ventricle (left side, $p<0,001$), cerebellar white matter (right side $p=0,03$), caudate nucleus (right side, $p=0,02$), amygdalar complex (left side, $p<0,01$ and right side, $p=0,02$), nucleus accumbens (left side, $p<0,001$ and right side, $p=0,001$), lower volume of cerebrospinal fluid in ctrl compared to AD ($p=0,001$) and smaller volume of brain stem in AD compared to ctrl ($p=0,03$), see Table 2.

Left-right asymmetry within AD group and control group

For the AD group we found significant laterality between left and right side only in the case of number of the cortical holes (left > right, $p=0,02$, Fig. 16), volumes of the lateral ventricles (left > right, $p=0,01$, Fig. 17) and volumes of the amygdalar complex (right>left, $p=0,02$, Fig. 18).

For the control group we found significant laterality between left and right side only in the case of cerebellar white matter (right>left, $p<0,001$, Fig. 19) and cerebellar cortex (right>left, $p=0,02$, Fig. 20).

Discussion

We used FreeSurfer automated procedure for volumetric measurement of the major important structures of the human brain whose volume decrease is often used for AD evaluation. Our hypothesis was that we find volume decrease of generally all measured structures, especially smaller amygdalar complex but increased volume of the ventricles in AD patient compared to controls. As expected our results are in agreement with general concept of structural brain volume decrease in AD so far (de Jong et al., 2008; Philippi et al., 2012). In order to rule out artifacts of the mathematical processing we used two consecutive versions of the FS program – v5.2.0 and v5.3.0. and both runs gave exactly the same data results. After discussion with the creators of the FreeSurfer software (MGH/HST Athinoula A. Martinos Center for Biomedical Imaging) we came to conclusion that several of the brain regions anatomical borders needs to be improved in the software in order to give even more reliable results. An attempt for neurohistological collocalization of the hippocampal formation subfields with the high-resolution ex-vivo MRI already led

to significant improvement of its borders within FS environment (Adler et al., 2012). Nevertheless in the cases of the severe brain tissue impairment due to the AD atrophy borders of the brain structures may become undistinguishable. On the other hand, a comparison of the manual and automated segmentation of the temporal lobe structures in the AD, MCI and control groups focused mostly on the cortical areas (entorhinal, perirhinal and parahippocampal cortices plus hippocampal formation) showed close overlap in the bordering of the structures (Insausti et al., 2011). Similarly, comparison of manual and automated determination of hippocampal volumes in MCI and early AD showed that both methods derived highly correlated results with strong agreement. After controlling for the age, sex and intracranial volume in statistical group analysis, both the manual tracing and FreeSurfer methods yield similar patterns (Shen et al., 2010).

Structural volume loss between AD group and control was bilaterally significant in nucleus accumbens (similarly as in Pievani et al., 2013) and only slightly significant in nucleus caudatus on the right side. These two neighbouring structures have different function. Both belong to the basal nuclei but nucleus accumbens is part of reward system and nucleus caudatus belongs to motor regulation circuit.

Analysis of the volume structural lateralization showed difference between AD and control group. In case of the control group we found asymmetrical distribution only in the cerebellar white matter and cerebellar cortex. In case of the AD group we found asymmetrical distribution of number of the cortical holes between left and right side and asymmetrical volumes in case of lateral ventricles and amygdalar complex. Dissapearance of the cerebellar white matter and cortical volumes laterality in case of the AD group could be explained by rather assymetrical loss of the both volumes during disease progression (Colloby et al., 2014). Also in AD group we found higher volume of the left lateral ventricle compared to the right one. Analysis of the inferior horn of the lateral ventricle itself showed no such significant asymmetry, although non-significant higher volume of the left ventricle compared to the right one was present. This suggests that volume of the inferior horn of the lateral ventricle does not play crucial role in the asymmetry of the lateral ventricles in the AD. Other parts of the lateral ventricular system has to account for this asymmetry. We do not know presently which part would it be - cornu frontale, pars centralis of the lateral ventricle or cornu occipitale. As expected we found pronounced rightward asymmetry of the amygdalar complex in the AD group while

in the control group we did not observe any asymmetry of the amygdalar complex. We presume that this accompany similar distribution of volume loss and rightward asymmetry of hippocampal formation in AD patients (Mrzílková et al., 2012).

Conclusion

We observed left-right asymmetry in number of cortical holes, volume of the whole lateral ventricle and right-left asymmetry in volume of the amygdalar complex in AD group. Interestingly, this does not overlap at all with asymmetries in control group where we found right-left asymmetry in cerebellar cortex and cerebellar white matter. Another important finding was higly significant bilateral volume decrease of nucleus accumbens and amygdalar complex in the AD group compared to the control. We failed to observe increased right-left laterality of the volume loss in many structures in AD group compared to controls.

Literature

Van Leemput K, Bakkour A, Benner T, Wiggins G, Wald LL, Augustinack J, Dickerson BC, Golland P, Fischl B. Automated Segmentation of Hippocampal Subfields from Ultra-High Resolution In Vivo MRI. Hippocampus 2009; 19: 549-557.

McKhann G, Drachman D, Folstein M, Katzman R, Price D, Stadlan EM: Clinical diagnosis of Alzheimer's disease: report of the NINCDS-ADRDA Work Group under the auspices of Department of Health and Human Services Task Force on Alzheimer's Disease. Neurology 1984; 34: 939–944.

Dubois B, Feldman HH, Jacova C, Dekosky ST, Barberger-Gateau P, Cummings J, Delacourte A, Galasko D, Gauthier S, Jicha G, Meguro K, O'brien J, Pasquier F, Robert P, Rossor M, Salloway S, Stern Y, Visser PJ, Scheltens P: Research criteria for the diagnosis of Alzheimer's disease: revising the NINCDS-ADRDA criteria. Lancet Neurol 2007; 6:734–746.

Scheltens PH, Leys D, Barkhof F, Huglo D, Weinstein HC, Vermersch P, Kuiper M, Steinling M, Wolters ECH, Valk J: Atrophy of medial temporal lobes on MRI in

‘probable’ Alzheimer’s disease and normal ageing: diagnostic value and neuropsychological correlates. J Neurol Neurosurg Psychiatry 1992; 55: 967–972.

Budson AE, Solomon PR: Memory Loss: A Practical Guide for Clinicians. Philadelphia, Elsevier Saunders, 2011.

de Jong LW, van der Hiele K, Veer IM, Houwing JJ, Westendorp RG, Bollen EL, de Bruin PW, Middelkoop HA, van Buchem MA, van der Grond J. Strongly reduced volumes of putamen and thalamus in Alzheimer's disease: an MRI study. Brain 2008; 131: 3277-3285.

Philippi N, Noblet V, Botzung A, Després O, Renard F, Sfikas G, Cretin B, Kremer S, Manning L, Blanc F. MRI-based volumetry correlates of autobiographical memory in Alzheimer's disease. PLoS One 2012; 7: e46200.

Adler DH, Liu AY, Pluta J, Kadivar S, Orozco S, Wang H, Gee JC, Avants BB, Yushkevich PA. Reconstruction of the human hippocampus in 3D from histology and high-resolution ex-vivo MRI. Proc IEEE Int Symp Biomed Imaging 2012; 2012: 294–297.

Insausti R, Rincón M, Díaz-López E, Artacho-Pérula E, Mansilla F, Florensa F, González-Moreno C, Álvarez-Linera J, García S, Peraita H, Pais E, Insausti AM. FreeSurfer automatic brain segmentation adaptation to medial temporal lobe structures: volumetric assessment and diagnosis of mild cognitive impairment. In: Ferrández IM, eds. New challenges on bioinspired applications. 4th international work-conference on the interplay between natural and artificial computation, IWINAC 2011, Proceedings, Part II. Berlin: Springer. Lecture Notes in Computer Science 6687, 2011; 112-119.

Shen L, Saykin AJ, Kim S, Firpi HA, West JD, Risacher SL, McDonald BC, McHugh TL, Wishart HA, Flashman LA. Comparison of manual and automated determination of hippocampal volumes in MCI and early AD. Brain Imaging Behav 2010; 4:86-95.

Colloby SJ, O'Brien JT, Taylor JP. Patterns of cerebellar volume loss in dementia with Lewy bodies and Alzheimer′s disease: A VBM-DARTEL study. Psychiatry Res. 2014 Sep 30;223(3):187-91.

Mrzilková J, Zach P, Bartoš A, Tintěra J, Řípová D. Volumetric analysis of the pons, cerebellum and hippocampi in patients with Alzheimer's disease. Dement Geriatr Cogn Disord. 2012;34(3-4):224-34.

Pievani M, Bocchetta M, Boccardi M, Cavedo E, Bonetti M, Thompson PM, Frisoni GB. Striatal morphology in early-onset and late-onset Alzheimer's disease: a preliminary study. Neurobiol Aging. 2013 Jul;34(7):1728-39.

Tang AC, Zhou B: Neonatal exposure to novelty enhanced long-term potentiation in CA1 region of the rat hippocampus. Hippocampus 13: 398-404, 2002.

	Control group	AD group
Number of subjects	27	26
age (years)	70/66 (60-79)	74/77 (57-81)
females (%)	80	62
education (years)	12/13 (12-19) mostly University with graduation	13/12 (8-20) mostly University w/o graduation
Dominant right hander *	NA/100 (only one subject 40)	NA/100 (all right handers)
Illness duration (years)	NA	2.9/3 (0-6)
MMSE (body)	29.3/29.5 (26-30)	16.5/19 (2-26)
MDRS (body)	141/141 (133-144)	90/98 (8-129)
TMT A (sec)	37/38.5 (19-76)	NA
TMT B (sec)	90/88 (38-177)	NA
DAD (%)	100/100 (NA)	62/64 (7-80)

Table 1. Clinical and neuropsychological characteristics in control and AD group. Data are stated in the format of average/median (minimum-maximum). MMSE – Mini Mental State Examination, MDRS – Mattis Dementia Rating Scale, TMT A,B – Trail Making Test version A, B, DAD – Disability Assessment in Dementia – percentage of maintenance of the daily activities, na – not available or not found, * expressed in % according to Edinburgh Handedness Inventory.

Brain cortical area	Left hemisphere AD<ctrl p<0.001***	Right hemisphere AD<ctrl w/o significance
Lateral ventricle	Left side ctrl<AD p<0.001***	Right side ctrl<AD p=0.002***
Temporal horn of the lateral ventricle	Left side ctrl<AD p<0.001***	Right side ctrl<AD w/o significance
Cerebellar white matter	Left hemisphere AD<ctrl w/o significance	Right hemisphere AD<ctrl p=0.03*
Caudate nucleus	Left side AD<ctrl w/o significance	Right side AD<ctrl p=0.02*
Amygdalar complex	Left side AD<ctrl p<0.01**	Right side AD<ctrl p=0.02*
Nucleus accumbens	Left side AD<ctrl p<0.001***	Right side AD<ctrl p<0.001***
Cerebrospinal fluid	Volume in ctrl<AD p<0.001***	
Brain stem	Volume in AD<ctrl p<0.03**	

Table 2. Structures whose right or left side shows statistically significantly volume changes in AD group compared to control on FS. In table not included structures with non significant volume changes.

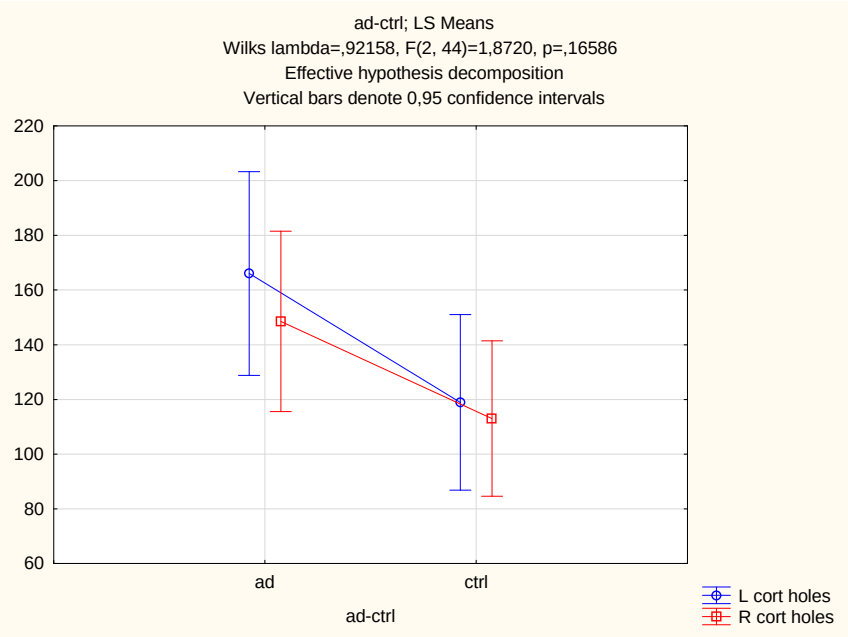

Fig. 1

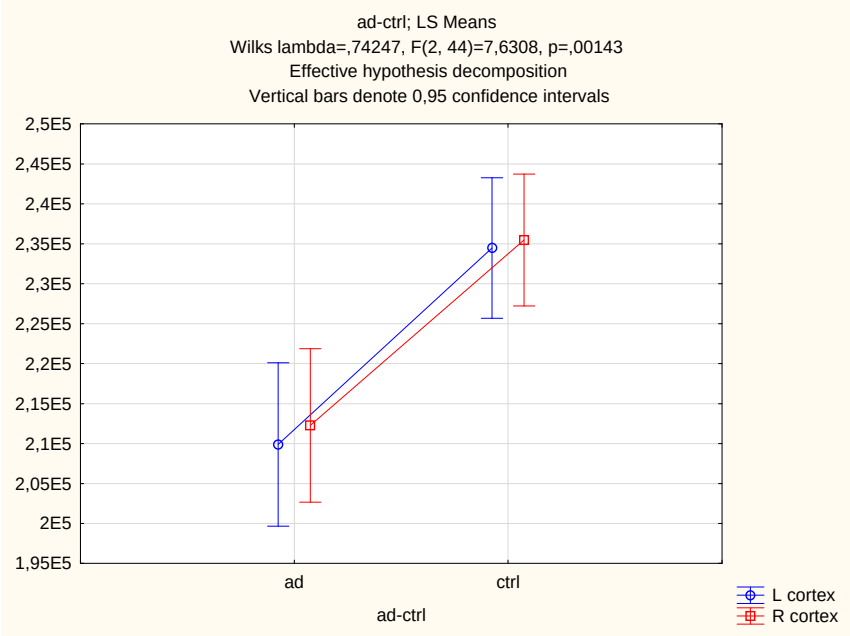

Fig. 2

Fig. 1 **Overall number of brain cortical holes** in ctrl vs AD. ANOVA w repeated measures F(2.44) p=0.16. Post hoc Newman-Keul p=0.06 (L), p=0.1 (R). Data on y axis are in absolute numbers.

Fig. 2 **Overall brain cortex area** in ctrl vs AD. ANOVA w repeated measures F(2.44) p= 0.001***. Post hoc Newman-Keul p<0.001*** (L), p<0.001* (R). Data on y-axis in mm^3.

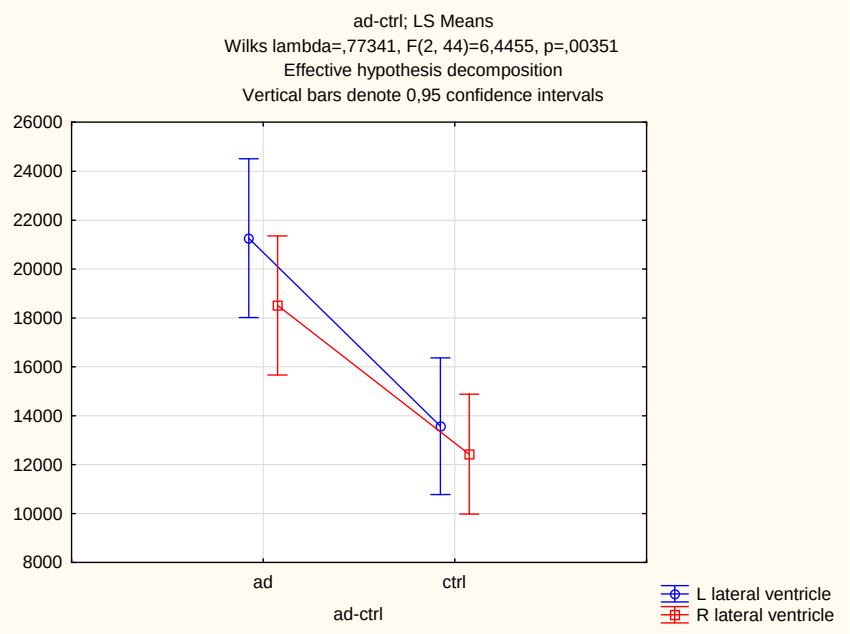

Fig. 3

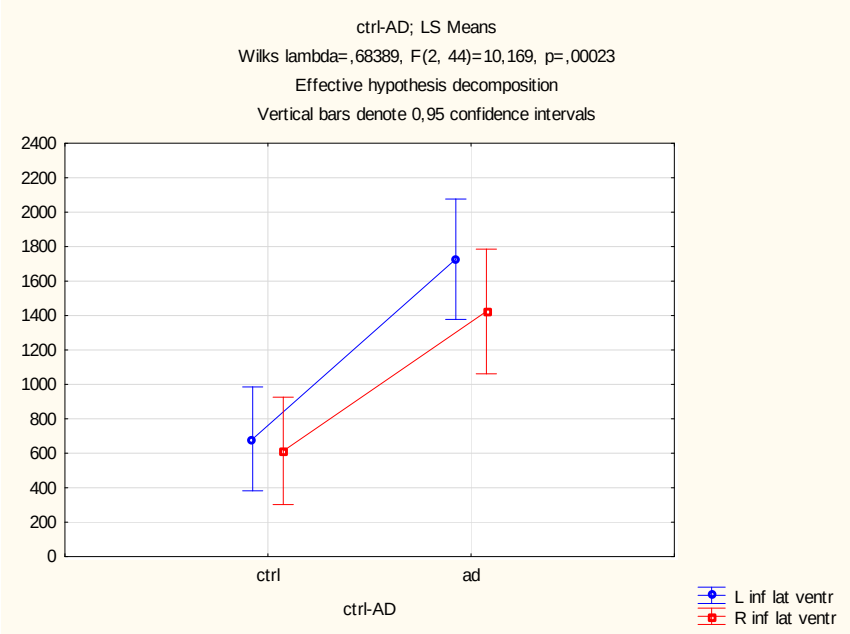

Fig. 4

Fig 3 **Volume of lateral ventricles** in ctrl vs AD. ANOVA w repeated measures F(2.44) p<0.001. Post hoc Newman-Keul p<0.001*** (L), p=0.002** (R). Data on y-axis in mm^3.	Fig 4 **Volume of inferior horn of the lateral ventricle** in ctrl vs AD. ANOVA w repeated measures F(2.44) p<0.001. Post hoc Newman Keul p<0.001 (L)*** and p<0.001 (R)***. Data on y-axis in mm^3.

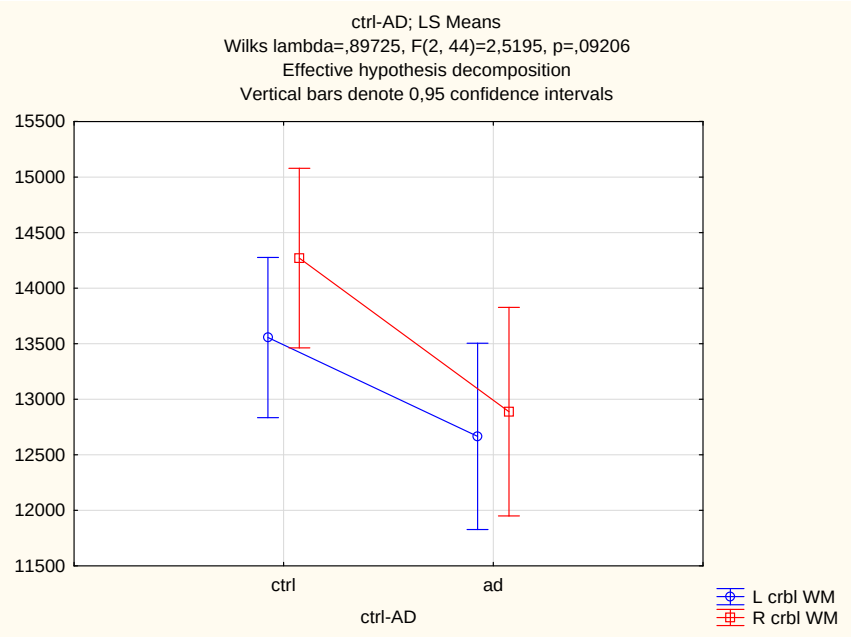

Fig. 5

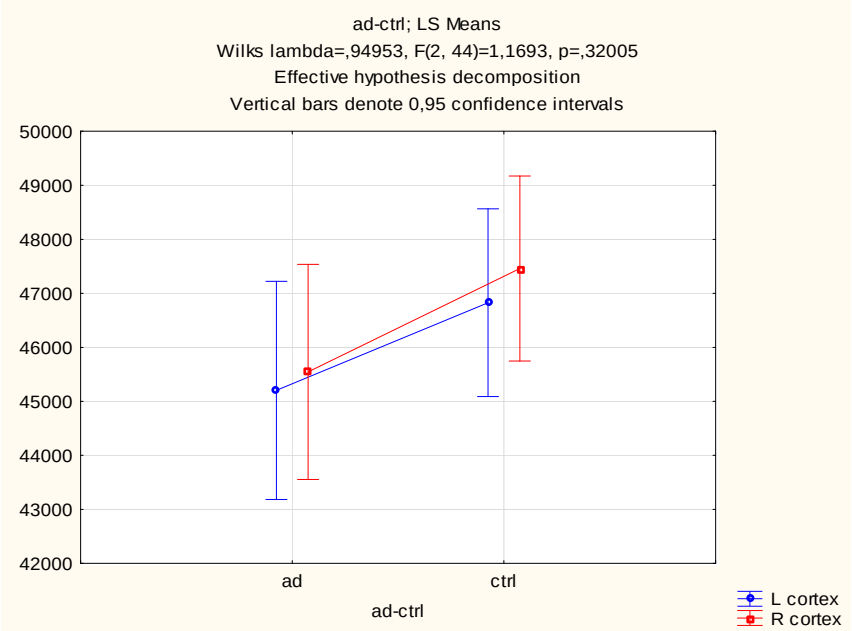

Fig. 6

Fig 5 Volume of **all cerebellar white matter** in ctrl vs AD. ANOVA w repeated measures F(2.44) p=0.09. Post hoc Newman Keul p=0.11 (L) and p=0.03 (R)*. Data on y-axis in mm^3.	Fig 6 Volume of **cerebellar cortical grey matter** in ctrl vs AD. ANOVA w repeated measures F(2. 44)=1.1693, p=.32005. Post hoc Newman Keul p=0.23 (L) and p=0.15 (R). Data on y-axis in mm^3.

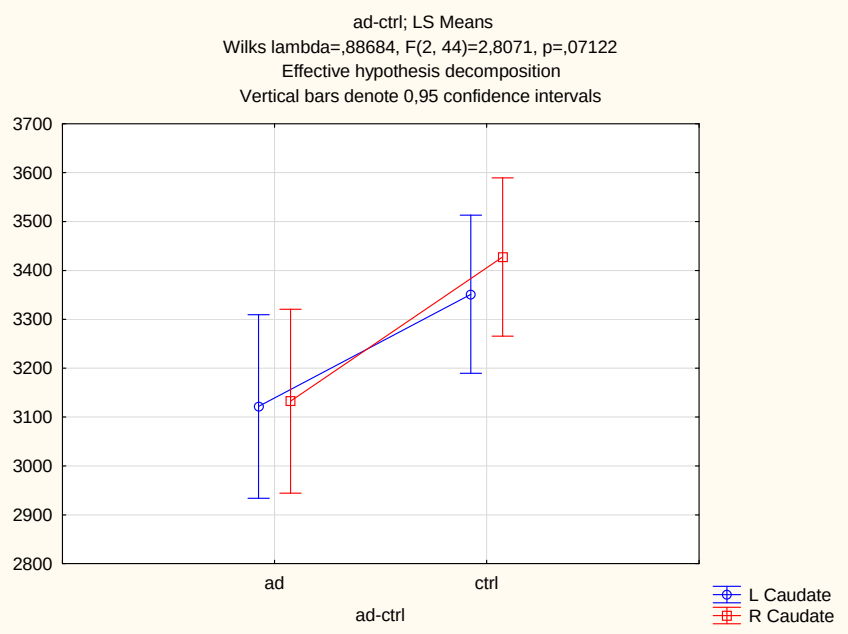

Fig. 7

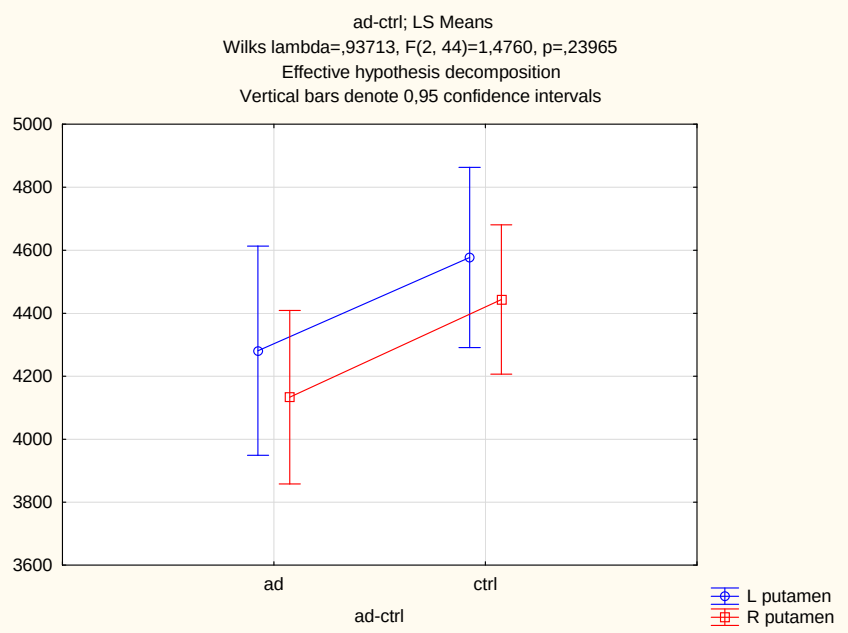

Fig. 8

Fig 7 Volume of **caudate nucleus** in ctrl vs AD. ANOVA w repeated measures F(2, 44)=2,8071, p=,07122. Post hoc Newman Keul p=0,07 (L) and p=0,02 (R)*. Data on y-axis in mm^3.	Fig 8 Volume of **putamen** in ctrl vs AD. ANOVA w repeated measures F(2, 44)=1,4760, p=,23965. Post hoc Newman Keul p=0,18 (L) and p=0,09 (R). Data on y-axis in mm3.

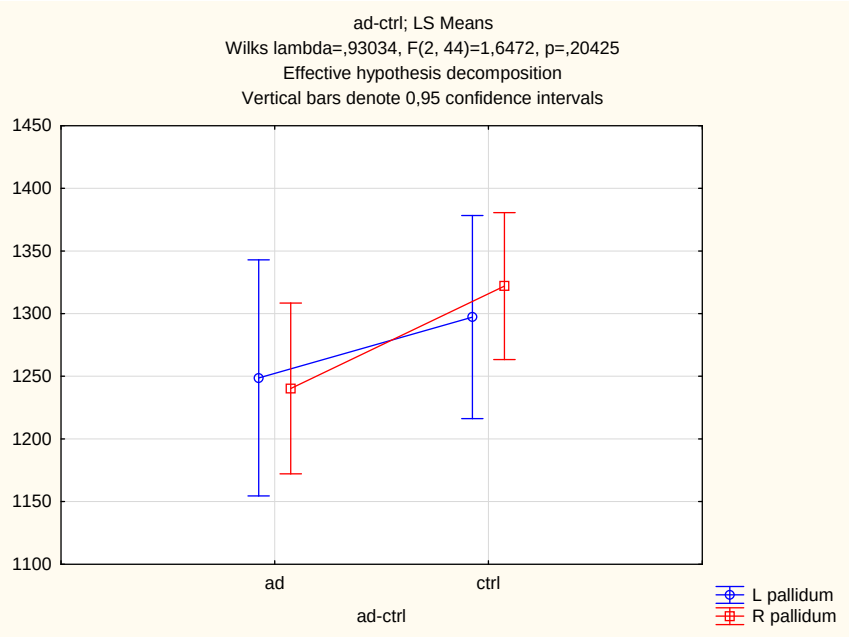

Fig. 9

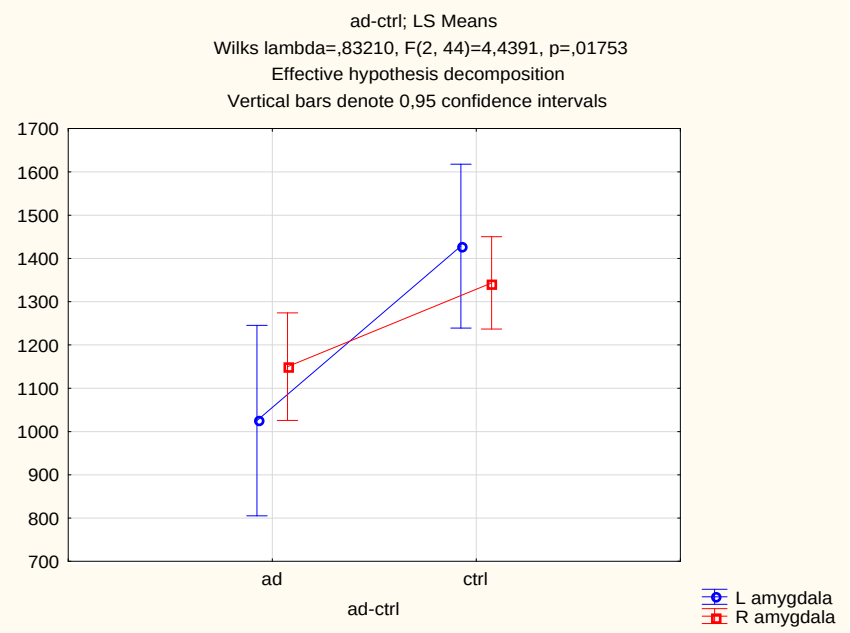

Fig. 10

Fig 9. Volume of **pallidum** in ctrl vs AD. ANOVA w repeated measures F(2. 44)=1.6472. p=0.20425. Post hoc Newman Keul p=0.43 (L) and p=0.07 (R). Data on y-axis in mm^3.	Fig 10. Volume of **amygdala** in ctrl vs AD. ANOVA w repeated measures F(2. 44)=4.4391. p=.01753. Post hoc Newman Keul p<0.01 (L)** and p=0.02 (R)*. Data on y-axis in mm^3.

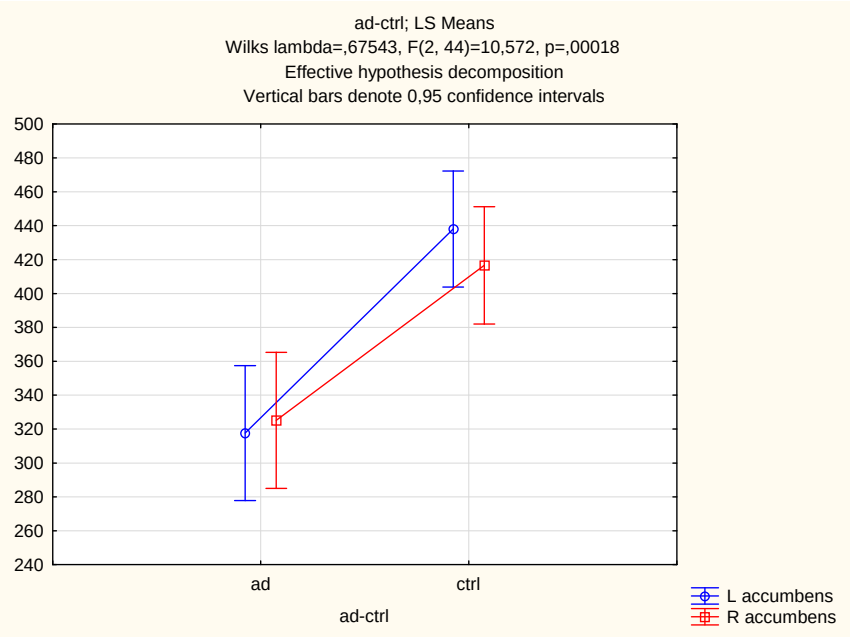

Fig. 11

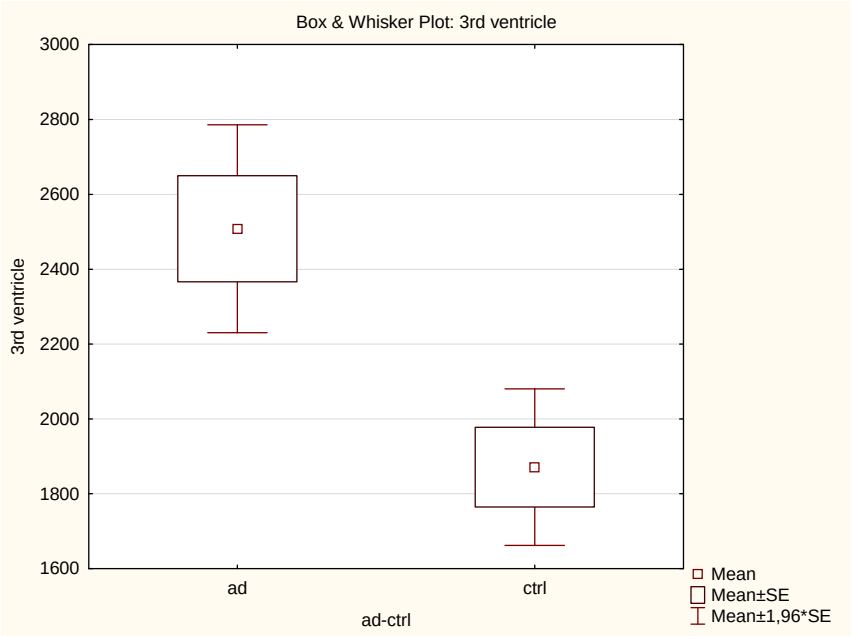

Fig. 12

Fig 11. Volume of **nc. accumbens** in ctrl vs AD. ANOVA w repeated measures F(2. 44)=10.572. p=.00018. Post hoc Newman Keul p<0.001 (L)*** and p=0.001 (R)***. Data on y-axis in mm^3.

Fig 12. Volume of the **3rd ventricle** in ctrl vs AD. T-test for independent samples by groups p<0.001*. Data on y-axis in mm3.

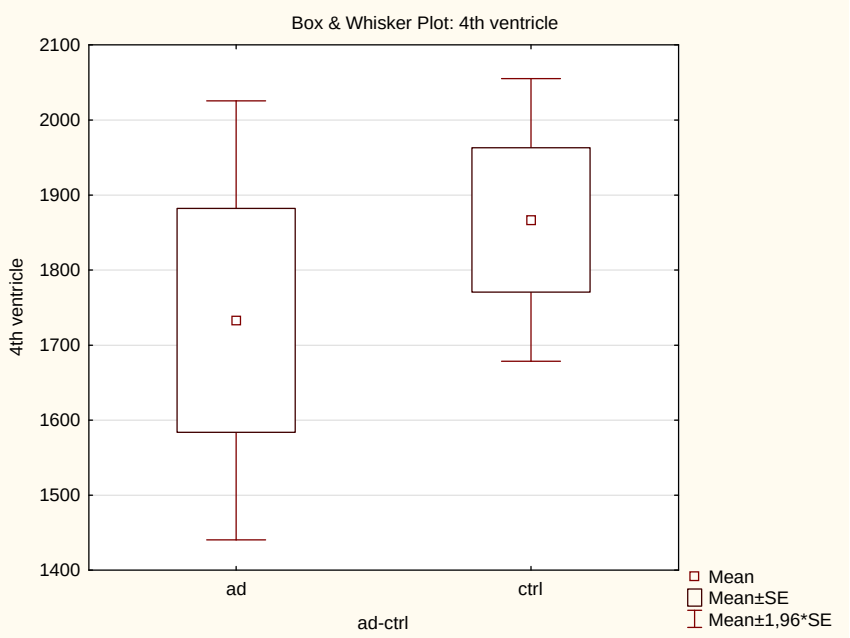

Fig. 13

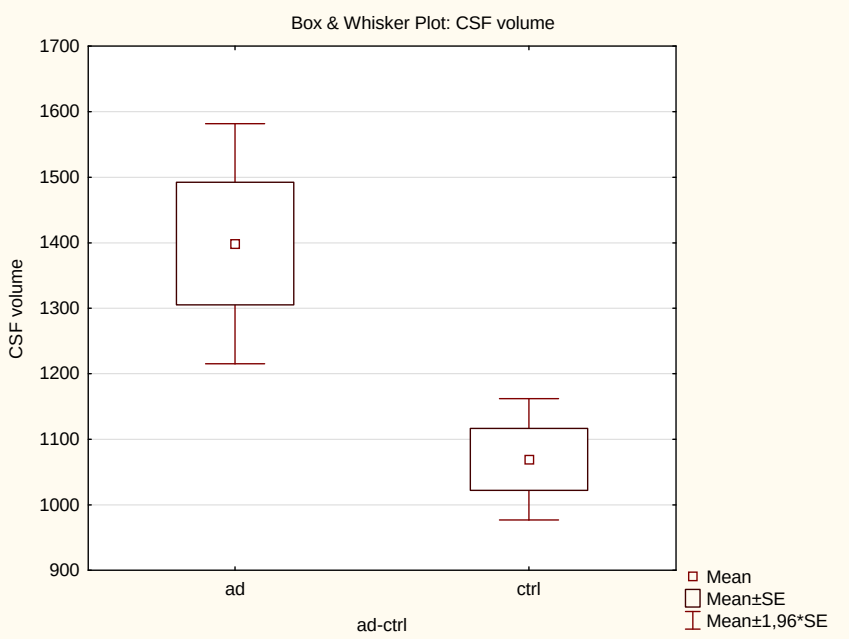

Fig. 14

Fig 13. Volume of the **4th ventricle** in ctrl vs AD. T-test for independent samples by groups p=0.4. Data on y-axis in mm^3.	Fig 14. Volume of the **CSF** in ctrl vs AD. T-test for independent samples by groups p=0.001***. Data on y-axis in mm^3.

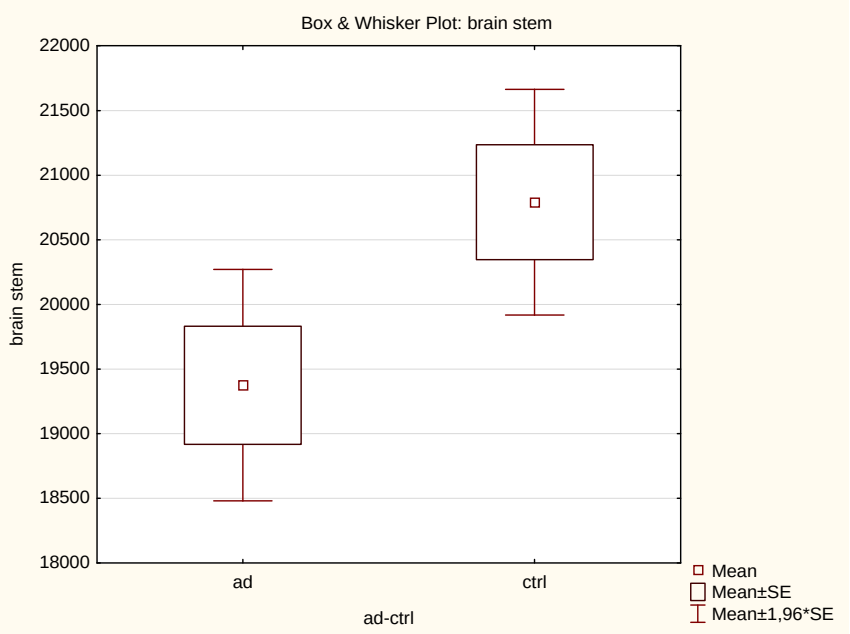

Fig. 15

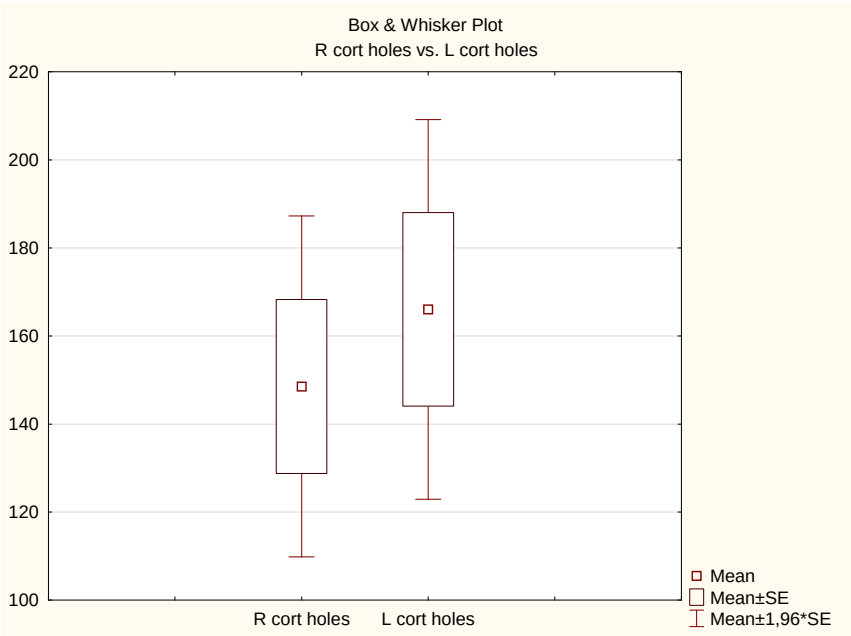

Fig. 16

Fig 15. Volume of the **brain stem** in ctrl vs AD. T-test for independent samples by groups p=0.03**. Data on y-axis in mm^3.	Fig 16. Laterality of **cortical holes** in AD group. T-test for dependent samples by groups p=0.02**. Data on y-axis in absolute numbers.

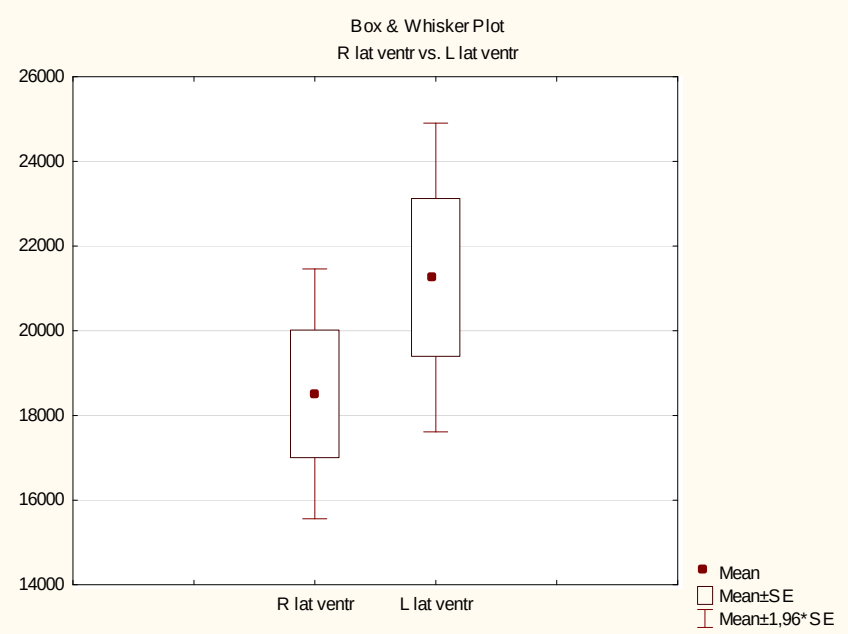

Fig. 17

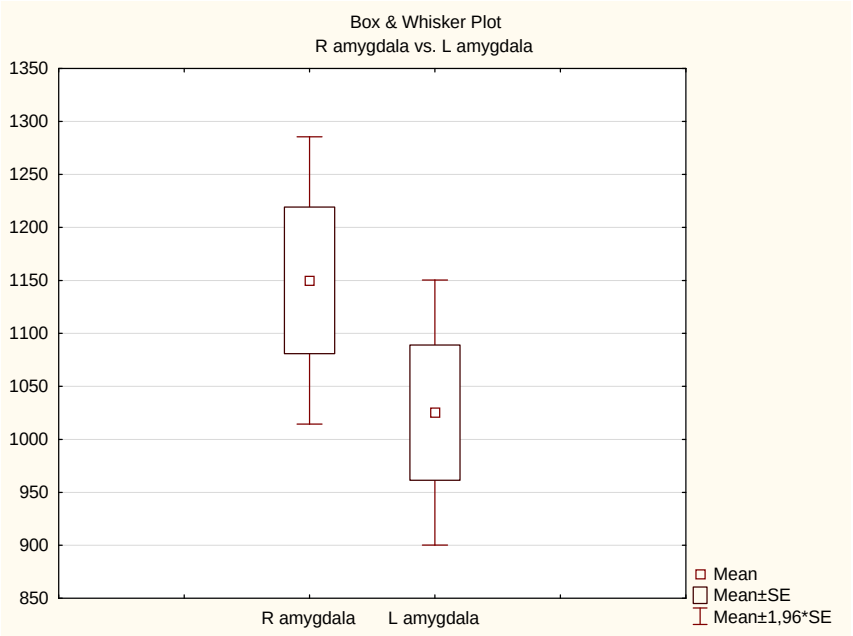

Fig. 18

Fig 17. Laterality of volume of the **lateral ventricle** in AD group. T-test for dependent samples by groups p=0.01**. Data on y-axis in mm^3.	Fig 18. Laterality of **amygdalar complex** in AD group. T-test for dependent samples by groups p=0.04**. Data on y-axis in mm^3.

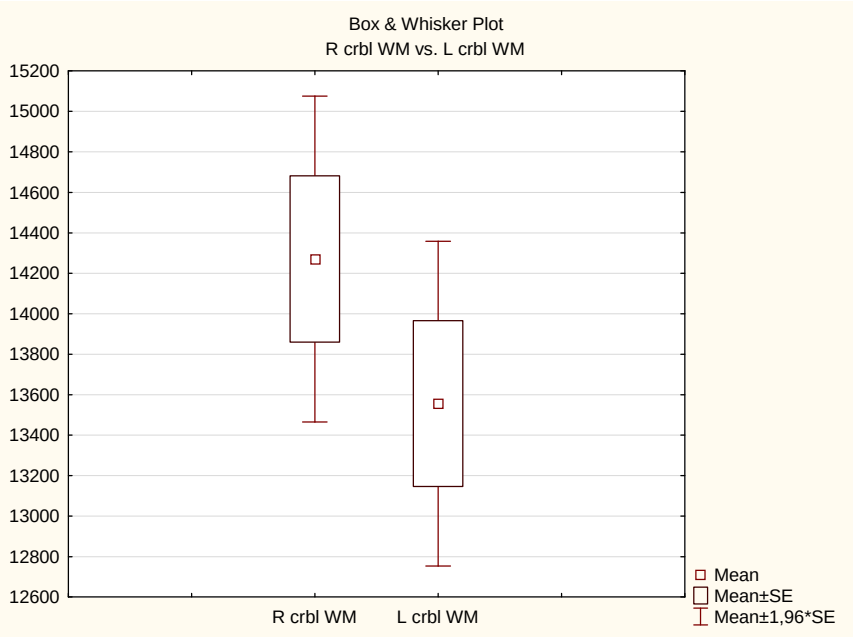

Fig. 19

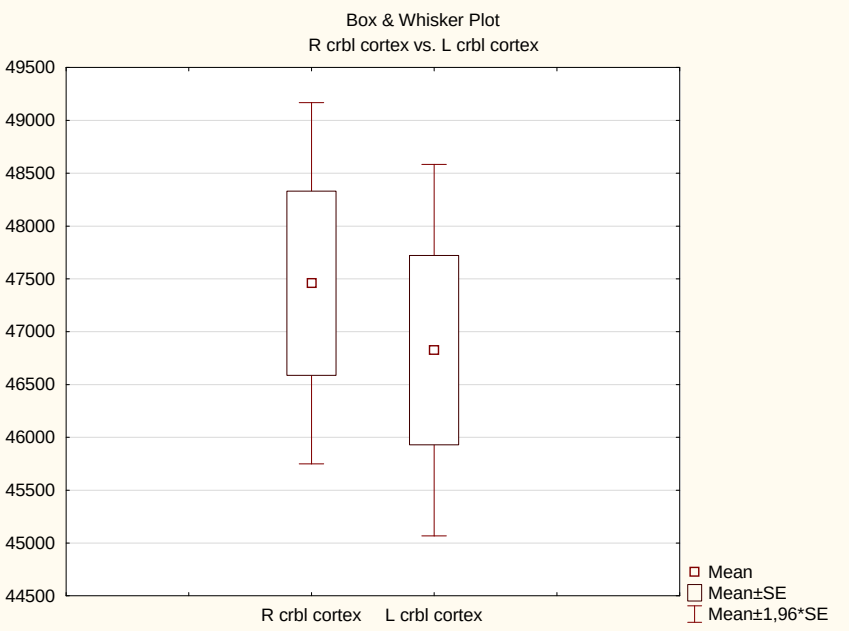

Fig. 20

Fig 19. Laterality of **cerebellar white matter** in ctrl group. T-test for dependent samples by groups p<0.001***. Data on y-axis in mm^3.	Fig 20. Laterality of **cerebellar cortex** in ctrl group. T-test for dependent samples by groups p=0.02*. Data on y-axis in mm^3.